Thèse de Doctorat de l'Université de Strasbourg

Ecole doctorale des Sciences de la Vie et de la Santé (ED414)
Spécialité: Immunologie

Présentée Par

Georgio KOURJIAN

Pour Obtenir le grade de

Docteur de l'Université de Strasbourg

Sujet de Thèse

Effect of HIV antiretroviral drugs on antigen processing and epitope presentation by MHC-I to cytotoxic T cells

Soutenue le 30 juin 2015 devant le jury composé de:

Docteur Arnaud MORIS	Rapporteur
Docteur Lisa CHAKRABARTI	Rapporteur
Docteur Christiane MOOG	Examinateur
Professeur Etienne WEISS	Co-directeur de thèse
Professeur Sylvie LE GALL	Co-directeur de thèse

Acknowledgment

This PhD work could not have been realized without the permanent and kind support of different people around me. Hereby, I would like to express my deepest thanks to them.

To my two co-mentors, Pr. Sylvie Le Gall and Pr. Etienne Weiss

I would like to thank Pr. Sylvie Le Gall for welcoming me in her lab and guiding me through my master and PhD thesis. We shared many fruitful discussions and brainstorming sessions over the last 4 years. Her outstanding ability, scientific and pedagogical, together with personal kindness and openness turned my work into truly one of a kind experience.

I would like to express my sincere gratitude to Pr. Etienne Weiss for trusting me and allowing me to do this long distance PhD. Without him I would not have been able to achieve this PhD. Thank you for always being supportive and for understanding the difficulties and complications that we faced with the long distance thesis.

To the members of my PhD committee

I would like to sincerely thank Pr. Arnaud Moris and Pr. Lisa Chakrabarti for the careful review of my manuscript and Pr. Christiane Moog for accepting to examine my PhD work and thesis defense. I am grateful to have you on my jury committee and to learn from your extensive knowledge and advice.

To all the Le Gall's lab past and present members

It was a pleasure to be part of this wonderful lab. Your help with lab experiments, scientific discussions, advice on data presentation as well as all the time together outside the lab made these past 4 years a very enjoyable experience for me. Thank you very much for that!

To the whole Ragon Institute

I would like to thank the flow and microscopy core as well as the processing lab for helping me with my experiments. I am also grateful for Pr. Daniel Kavanagh and Dr. Florencia Pereyra for their stimulating discussions and input on my projects. Thanks to Dr. Bruce Walker and all Ragon Institute members for making the institute a pleasant place to work.

To my family

My sincere thanks to my father and mother for their unconditional love and support. For the past 10 years that I spent away from you, you were always by my side spiritually and psychologically every step of the way giving me the power to continue and accomplish my goals. Without you none of this would have been possible!

Thanks to my brother for always being there when I needed him. I am truly proud to have a brother like you! Be sure that you can always count on your big brother.

I am sincerely grateful to my Aunt Marie and Uncle “Tonton” Vahe for taking care of me when I first arrived to France and supporting me in every possible way.

To Morgane and her/my family

Hokis, thank you for bringing joy to my life, for always supporting and helping me (even when I told you that I was tough and that I didn’t need any help!). Your presence with me brought comfort to my difficult moments and made happy moments more enjoyable. Thanks for being part of my life. I am proud of you Dr. Griesbeck!

Thanks to all Griesbeck/Langlaude/Husselstein family members for welcoming me in their family and considering me as their own son, brother and cousin.

TABLE OF CONTENTS

List of abbreviations

ADCC	Antibody-dependent cell-mediated cytotoxicity
AIDS	Acquired immunodeficiency syndrome
APC	Antigen presenting cell
ART	Antiretroviral therapy
ARV	Antiretroviral
BH	Bleomycin hydrolase
BMD	Bone mineral density
CMV	Cytomegalovirus
CTLs	Cytotoxic T lymphocytes
DC	Dendritic cell
dNTP	Deoxynucleoside triphosphate
DRIPs	Defective ribosomal products
EC	Elite controllers
EMEA	European Medicine Agency
ER	Endoplasmic reticulum
ERAP1	ER aminopeptidase associated with antigen processing 1
ERAP2	ER aminopeptidase associated with antigen processing 2
FDA	U S Food and Drug Administration
HAART	Highly active antiretroviral therapy
HDAC	Histone deacetylase
HIV	Human immunodeficiency virus
HLA	Human leukocyte antigen
iDC	Immature dendritic cell
IFN	Interferon
II	Integrase inhibitor
IL	Interleukin
IN	Integrase
KIR	Killer immunoglobulin-like receptors
LAP	Leucine aminopeptidase
LOD	Limit of detection
LTNP	Long- term nonprogressors
LTR	Long terminal repeats
mDC	Mature dendritic cell
MHC-I	Major histocompatibility complex class I
MHC-II	Major histocompatibility complex class II
MI	Myocardial infarction
Mϕ	Macrophage
NAbs	Neutralizing antibodies
NK	Natural killer
NNRTI	Non-nucleoside reverse transcriptase inhibitor
NOX2	NADPH oxidase 2
NRTI	Nucleoside/Nucleotide reverse transcriptase inhibitor

PBMC	Peripheral blood mononuclear cell
PI	Protease Inhibitor
PR	Protease
PSA	Puromycin-sensitive aminopeptidase
PYFU	Person-years follow-up
ROS	Reactive oxygen species
RT	Reverse transcriptase
SIV	Simian immunodeficiency virus
TAP	Transporter associated to antigen processing
TCR	T cell receptor
Th	T helper cell
Th1	T helper cell 1
Th2	T helper cell 2
TNF	Tumor-necrosis factor
TOP	Thimet oligopeptidase
TPPII	Tripeptidyl peptidase II
Tregs	Regulatory T cells
VL	Viral load
WHO	World health organization

List of figures

List of tables

Résumé de la thèse

Malgré l'absence de vaccin contre le VIH, des traitements antirétroviraux (ARV) adaptés permettent aux personnes séropositives pour le VIH de bloquer la réplication du VIH dans leur organisme et ainsi de garder un système immunitaire opérationnel. Les inhibiteurs de la protéase (IP) du VIH, constituent une classe thérapeutique d'antirétroviraux, ayant pour cible la protéase du VIH. La protéase du VIH est une enzyme qui participe à la maturation des protéines virales. Lorsque la protéase est bloquée, les nouveaux virus produits sont défectueux, et ne peuvent plus infecter de nouvelles cellules (Figure 1). Il a été mis en évidence que certains IP du VIH en plus de leur action sur la protéase du VIH ciblent le proteasome cellulaire, impliqué dans plusieurs mécanismes cellulaires importants y compris la machinerie de présentation antigénique par les CMH-I.

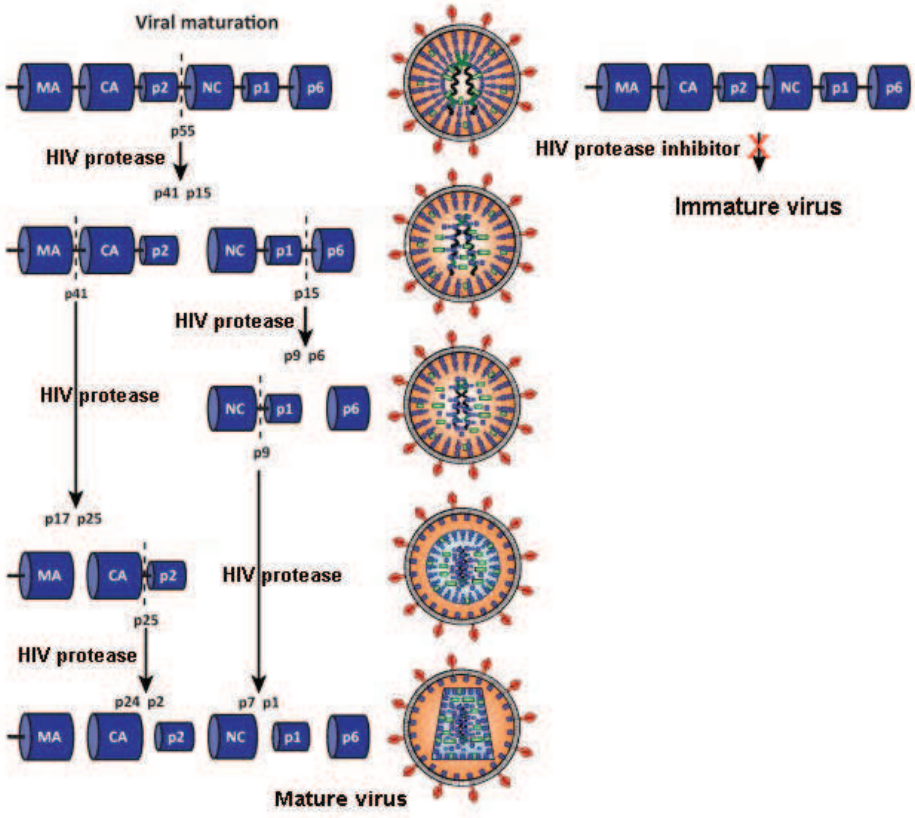

Figure 1: Mode d'action des inhibiteurs de la protease du VIH.

Les peptides présentés par les molécules CMH-I proviennent de la dégradation antigénique intracellulaire par le protéasome et par d'autres peptidases intracellulaires. Les peptides issus de ces dégradations cytoplasmiques sont transportés au réticulum endoplasmique (RE), raccourcis par les aminopeptidases du RE, chargés sur le CMH-I et présentés à la surface cellulaire. En plus de cette voie de présentation antigénique directe, les cellules présentatrices d'antigènes ont la capacité de phagocyter des antigènes extracellulaires, de les dégrader dans la voie endolysosomale par les cathepsines et de présenter les peptides antigéniques à la surface cellulaire après des étapes supplémentaires de dégradation cellulaire. (Figure 2) Malgré le rôle des protéasomes dans la machinerie de présentation antigénique, aucune étude n'a encore évalué l'effet de l'inhibition du protéasome par les IP du VIH sur l'apprêtement antigénique, ni l'effet sur la quantité et la nature des peptides présentés par les CMH-I à la surface cellulaire.

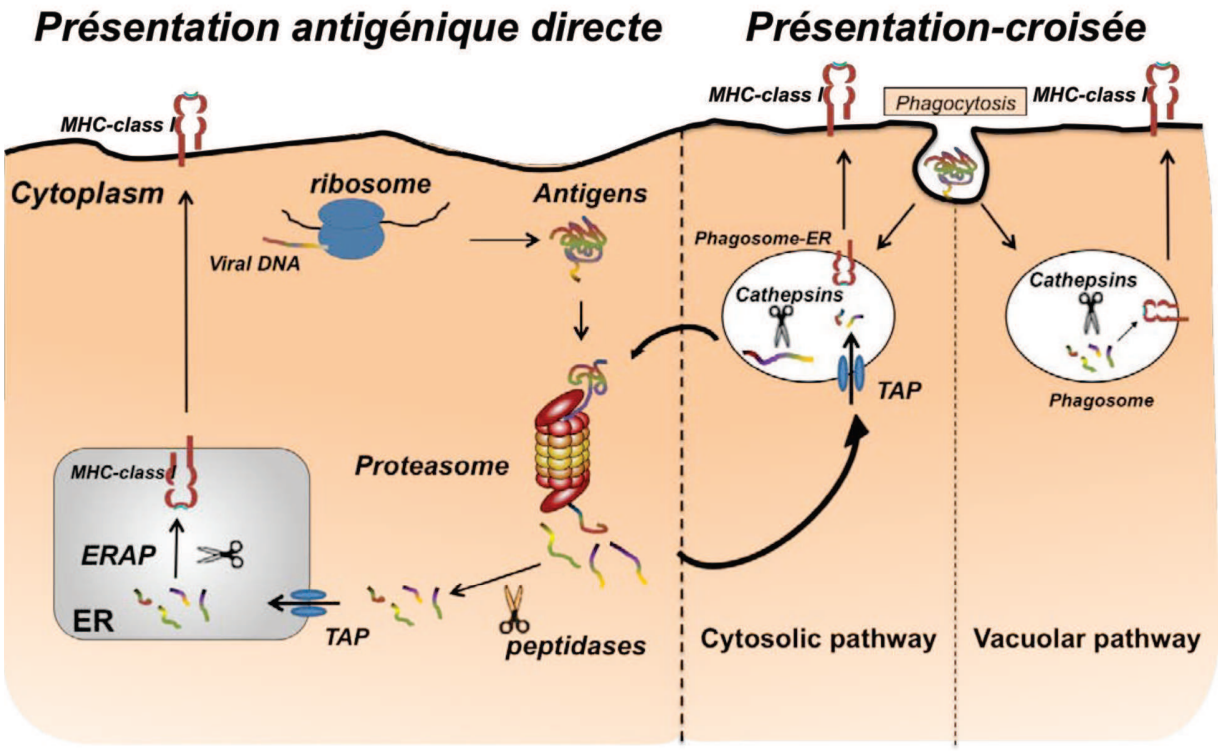

Figure 2: Présentation antigénique directe et coisée.

Mon travail de doctorat avait pour objectif d'étudier l'effet des IP du VIH sur le protéasome et les autres protéases cellulaires impliqués dans la voie d'apprêtement des antigènes directe ainsi que croisée et la conséquence des perturbations d'activité enzymatique induites par les IP du VIH sur la présentation des peptides à la surface cellulaire et la reconnaissance par les lymphocytes T cytotoxiques. L'effet des IP du VIH a été étudié d'abord sur la présentation antigénique directe puis sur la présentation-croisée.

I. Effet des IP du VIH sur la présentation antigénique directe

Les activités hydrolytiques du protéasome et des aminopeptidases ont été mesurées dans les cellules mononucléaires humaines du sang périphérique (PBMC) grâce à des substrats fluorescents spécifiques de chaque enzyme en présence ou en absence de sept IP du VIH différents. Les IP ritonavir, saquinavir, nelfinavir et Kaletra mais pas indinavir, atazanavir et darunavir inhibent les activités des protéasomes et des aminopeptidases (Figure 3).

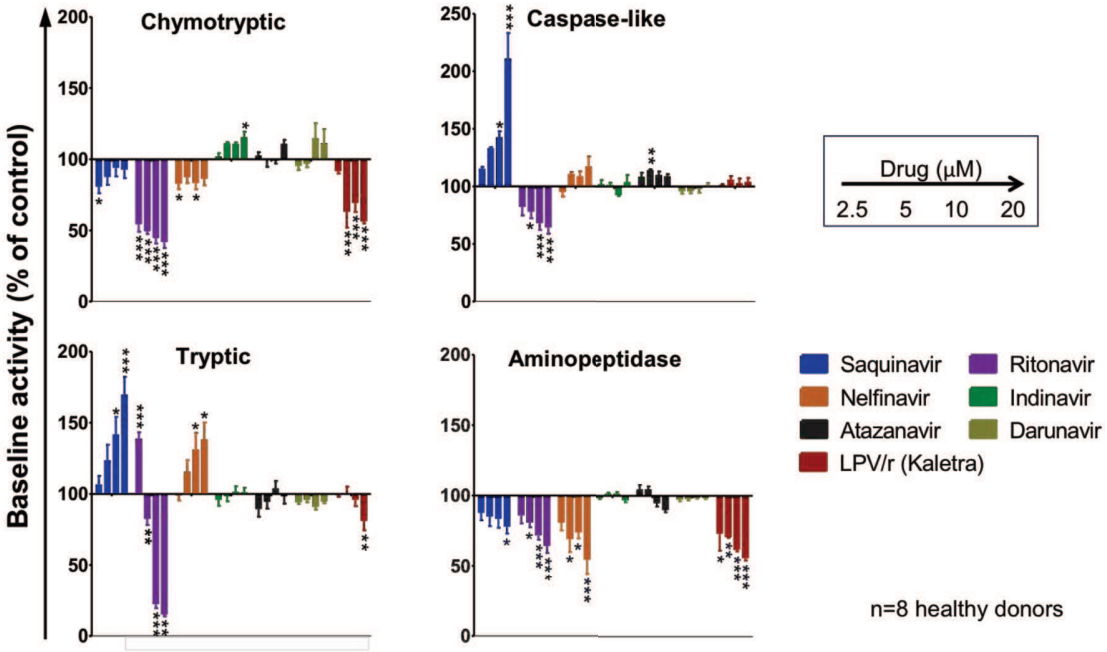

Figure 3: Effect des inhibiteurs de la protease du VIH sur les proteases cellulaire.

Pour voir si l'effet des IP sur ces activités perturbait l'apprêtement des antigènes, des peptides antigéniques issus de la protéine p24 du VIH contenant des épitopes ont été dégradés en présence d'extraits de PBMC traités ou pas avec des IP du VIH. Les produits de dégradation ont ensuite été identifiés et quantifiés par spectrométrie de masse. L'analyse des résultats montre que les IP du VIH, en perturbant les activités du protéasome et des aminopeptidases altèrent l'apprêtement antigénique et la quantité d'épitopes produits. La production de certains épitopes est augmentée alors que la production d'autres épitopes est diminuée (Figure 4).

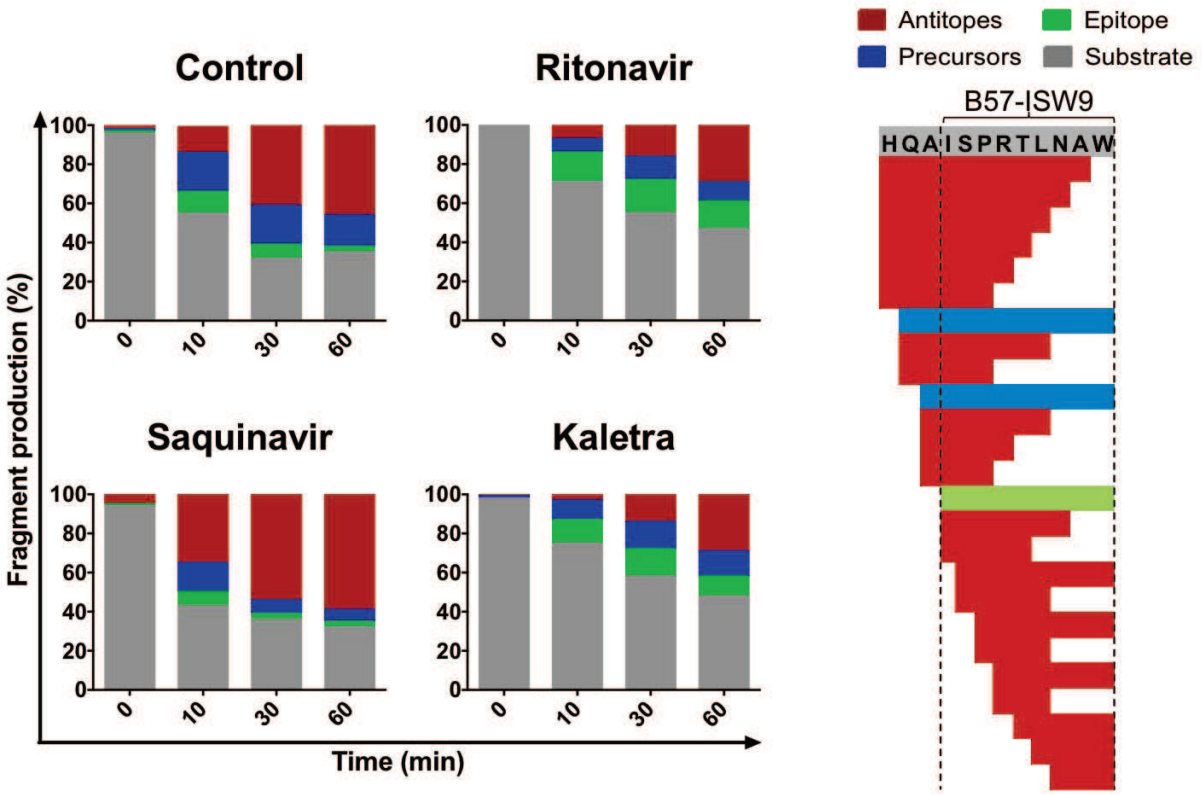

Figure 4: Effect des inhibiteurs de la protease du VIH sur l'apprêtement des antigènes.

Pour mieux comprendre cet effet variable sur la quantité d'épitopes produits, nous avons mesuré l'effet des IP sur l'hydrolyse des différents acides aminés. Les IP du VIH inhibent l'hydrolyse de certains acides aminés et augmenté l'hydrolyse des autres, suggérant que l'effet des IP du VIH sur l'apprêtement antigénique est guidé par la séquence peptidique (Figure 5).

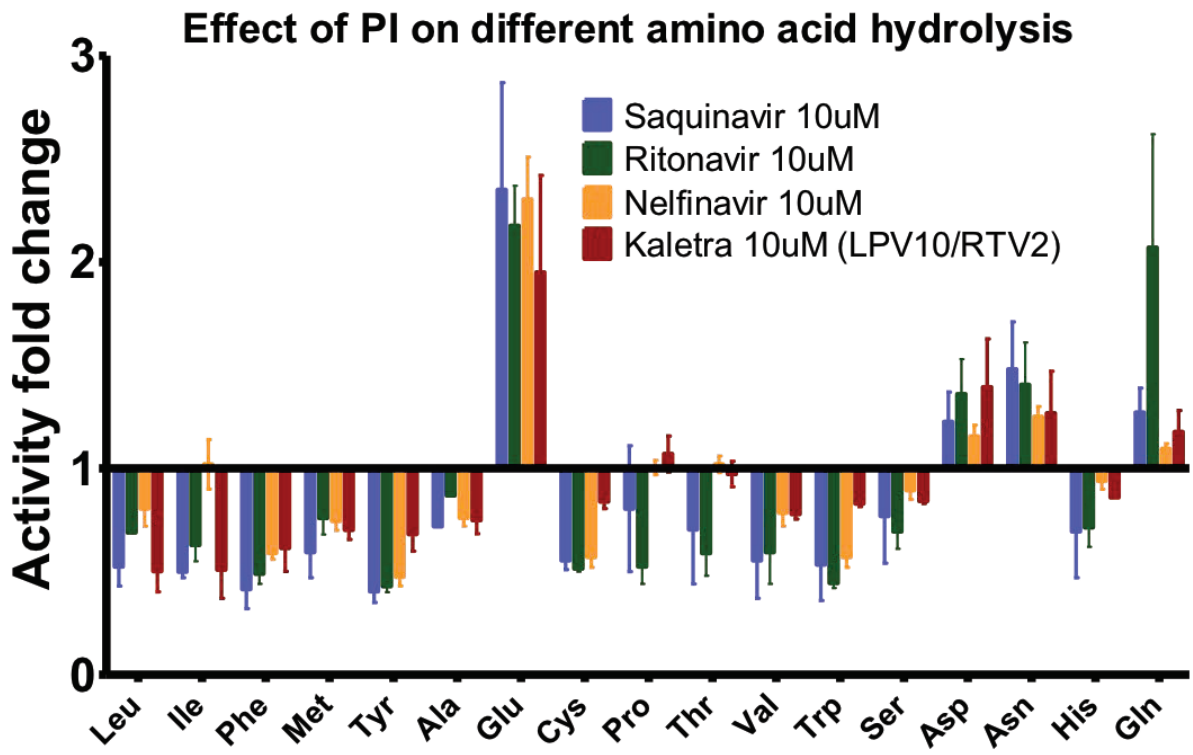

Figure 5: Effect des inhibiteurs de la protease du VIH sur l'hydrolyse des différents acides aminés.

Ensuite, pour comprendre si les changements induits par les IP sur les activités des protéases cellulaires ainsi que sur la quantité d'épitope produit dans les cellules affectaient la présentation des épitopes du VIH à la surface cellulaire, nous avons utilisé un essai fluorogénique de cytotoxité qui permet de suivre le nombre de cellules infectées par le VIH tuées par les lymphocytes T cytotoxiques spécifiques pour différents épitopes du VIH. Les résultats ont montré que les perturbations des activités des protéasomes et aminopeptidases causées par les IP du VIH altèrent l'apprêtement antigénique et la quantité d'épitope intracellulaire produit. Cette perturbation de la disponibilité intracellulaire des peptides change la quantité d'épitopes présentés à la surface cellulaire par les CMH-I (Figure 6).

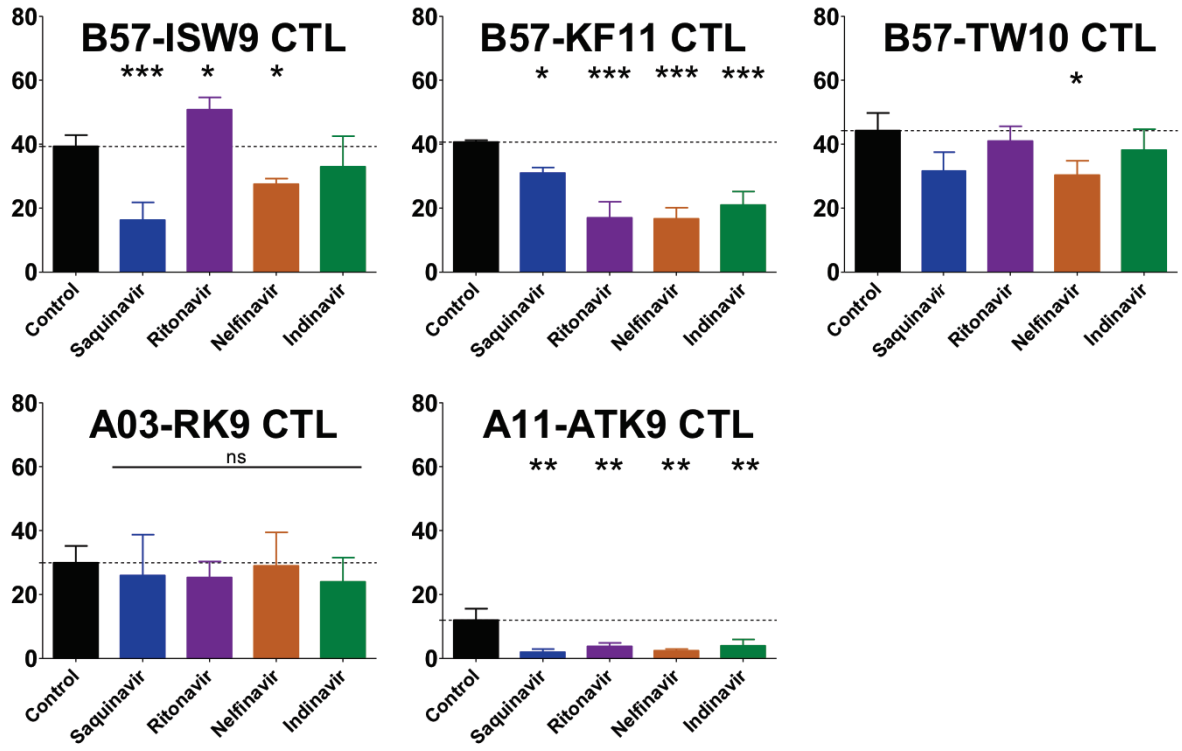

Figure 6: Les inhibiteurs de la protease du VIH changent la quantité d'épitopes présentés à la surface cellulaire par les CMH-I.

II. Effet des IP du VIH sur la présentation antigénique croisée

Les activités des cathepsines ont été mesurées dans les PBMCs ainsi que dans les lymphocytes T CD4+, cellules dendritiques et macrophages primaires traités ou pas avec cinq IP du VIH différents. L'IP ritonavir réduit les activités des cathepsines contrairement à saquinavir et nelfinavir qui eux les augmentent. Nous avons ensuite élucidé le mécanisme de l'augmentation des activités cathepsines induit par les IP. Étant donné que dans les phagosomes un des régulateurs des activités cathepsines est le pH, nous avons mesuré ce dernier en utilisant des billes liées à des fluorochromes dont l'intensité varie en fonction du pH. Une fois que ces billes sont phagocytées par les cellules traitées ou pas avec des IP, la mesure de leur fluorescence par cytométrie en flux nous a permis de quantifier le pH phagosomal. Les résultats ont montré que saquinavir et nelfinavir réduisent le pH phagosomal des cellules dendritiques et le pH endosomal des lymphocytes CD4+ d'une

unité pH, mais pas le pH phagosomal des macrophages (Figure 7).

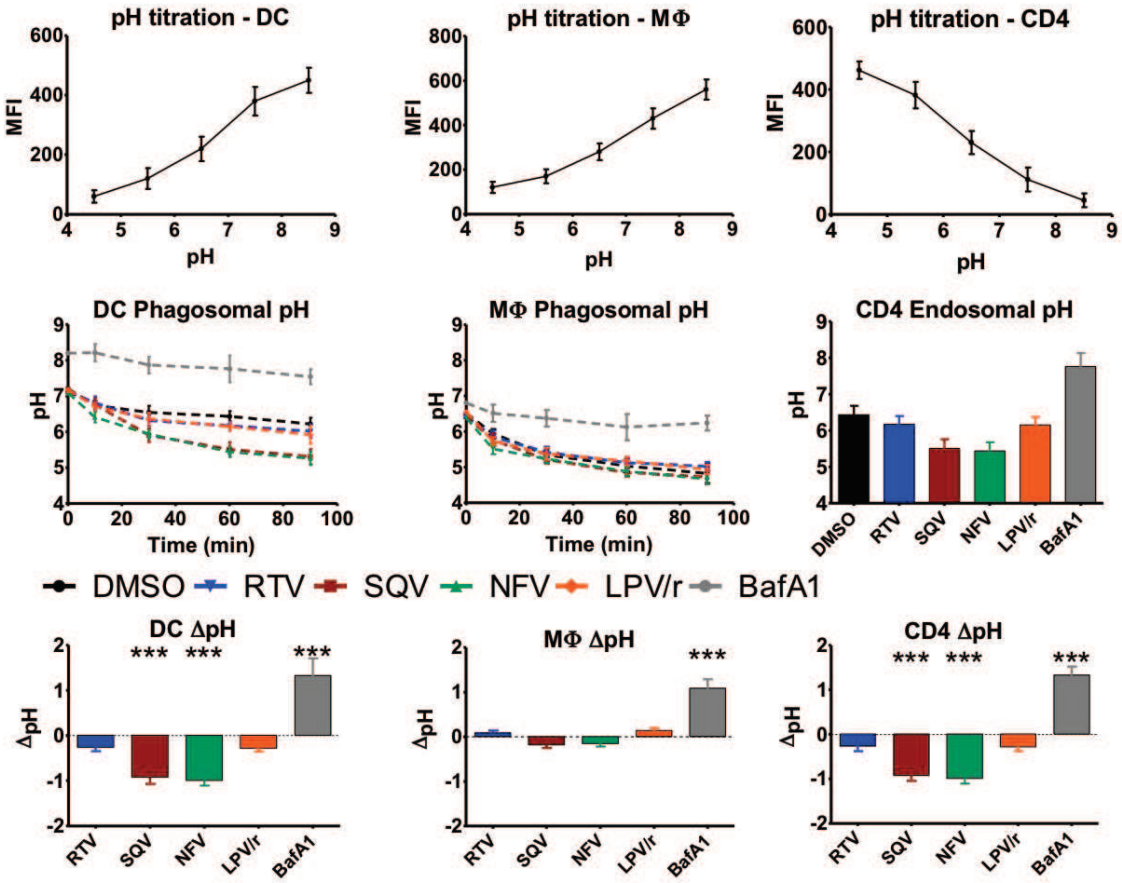

Figure 7: Les inhibiteurs de la protease du VIH changent le pH phagosomal et endosomal.

Les phagosomes des cellules dendritiques contrairement à ceux des macrophages ont la capacité de garder leur pH neutre jusqu'à 2 heures après phagocytose. Ceci est dû à l'activité enzymatique NADPH oxydase (NOX2) présent en plus grande quantité dans les phagosomes des cellules dendritiques. NOX2 produit des dérivés réactifs de l'oxygène (ROS) en utilisant les protons phagosomaux, limitant ainsi l'acidification. Pour analyser si l'effet des IP sur le pH était dû à la perturbation de l'activité NOX2, nous avons utilisé des billes liées à des fluorochromes dont l'intensité variait en fonction de la quantité de ROS produit dans les phagosomes après phagocytose. Les résultats ont montré que saquinavir et nelfinavir réduisent la production de ROS phagosomal dans les cellules dendritiques et à moindre degré dans les macrophages (Figure 8).. On a pu confirmer par Western blot que

cette réduction est due à l'inhibition de la phosphorylation de la sous-unité p47 de NOX2 par saquinavir et nelfinavir qui est une étape primordiale pour l'activation de NOX2.

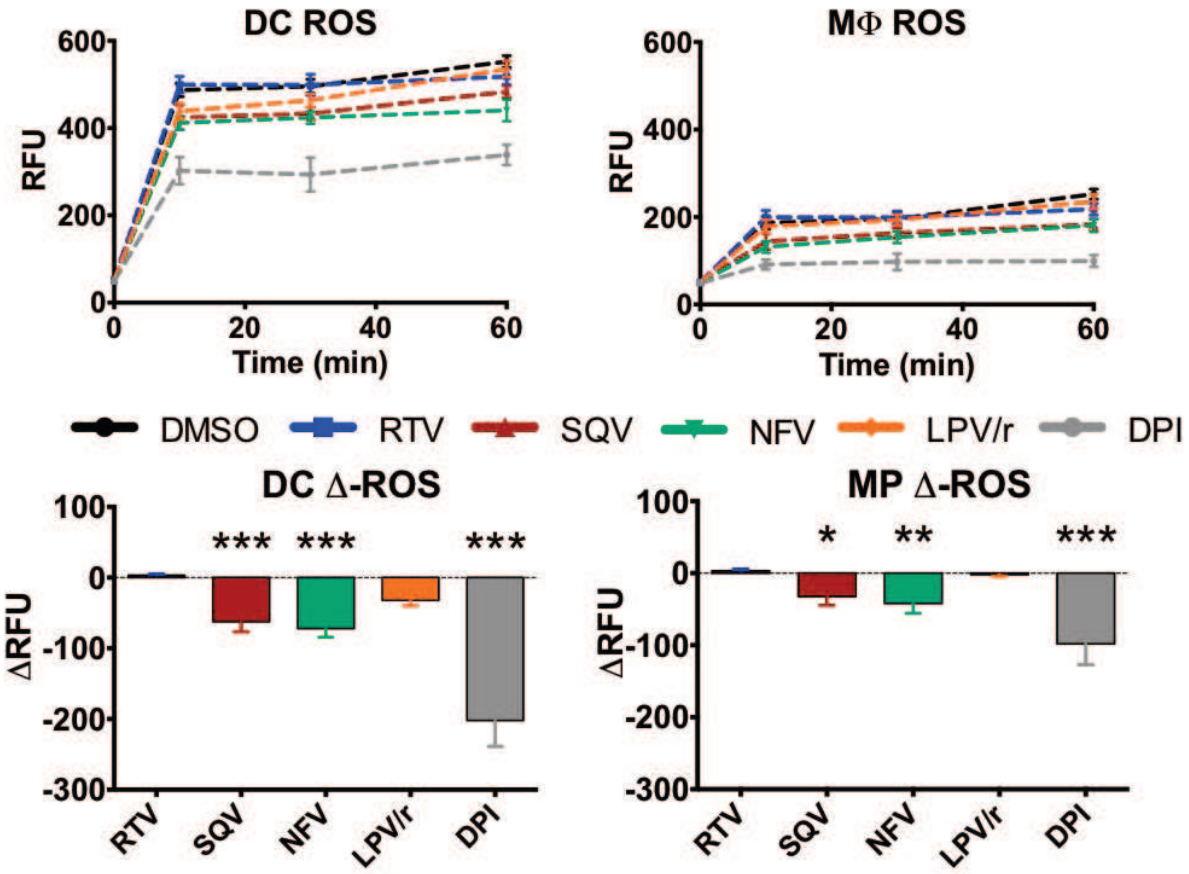

Figure 8: Les inhibiteurs de la protease du VIH changent le niveau de ROS dans les phagosomes et endosomes.

Nous avons analysé l'effet des IP sur la dégradation des protéines du VIH dans les compartiments liés à la présentation antigénique croisée. Des extraits cellulaires de PBMC, lymphocytes T CD4+, cellules dendritiques et macrophages traités ou pas avec des IP ont été utilisés comme source de cathepsines pour dégrader des peptides antigéniques issus de la protéine p24 du VIH contenant des épitopes immunogéniques. Les produits de dégradation ont ensuite été analysés par spectrométrie de masse pour identifier et quantifier les peptides issus de ces dégradations. Pour chaque type de cellule traitée par différents IP, nous avons défini un profil de coupure quantitatif des antigènes. La

comparaison des résultats avant et après traitement a montré que les IP altèrent la préférence des sites de coupure des peptides. Ceci change la quantité d'épitopes produits dans les compartiments liés à la présentation antigénique croisée (Figure 9).

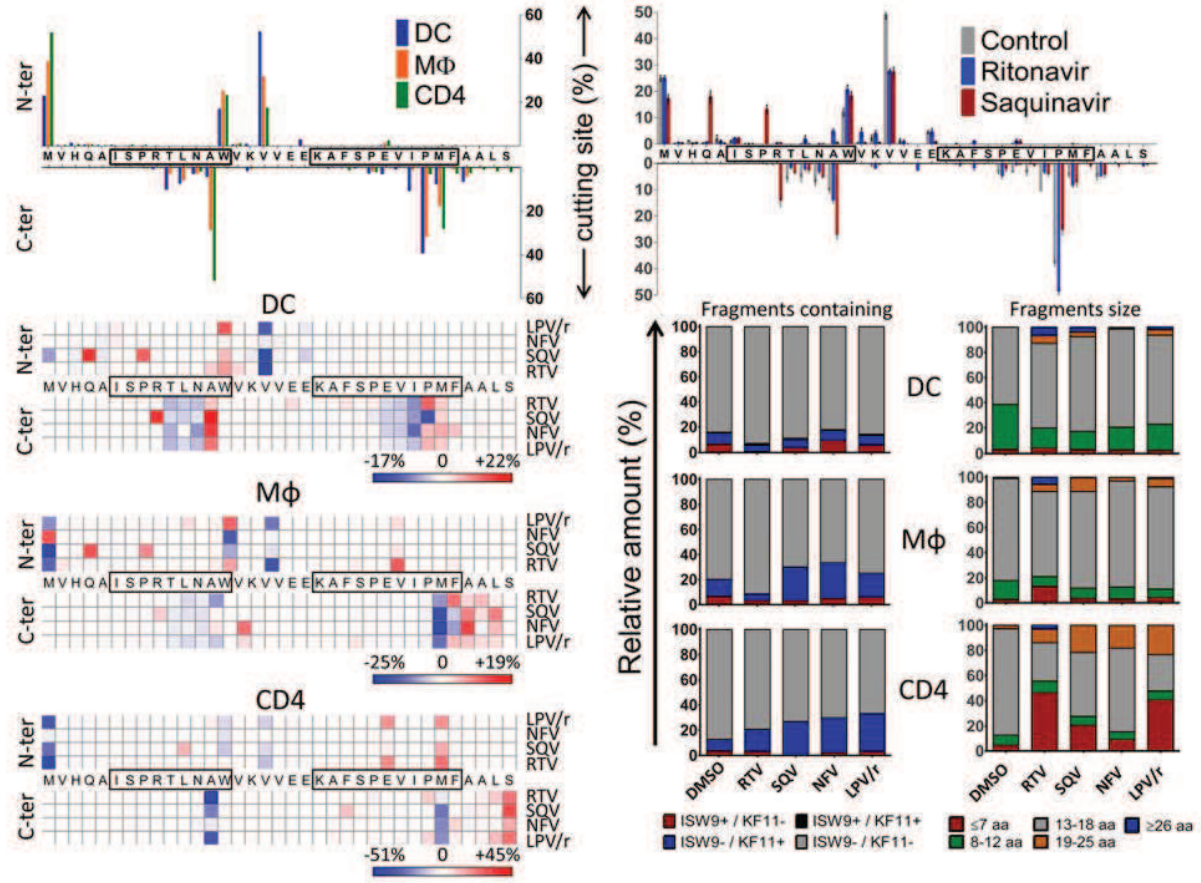

Figure 9: Effect des inhibiteurs de la protease du VIH sur l'apprêtement des antigènes dans les phagolysosomes.

Ensuite pour voir si les changements induits par les IP sur les activités des cathepsines ainsi que sur la quantité d'épitopes produits dans les phagosomes affectaient la présentation des épitopes du VIH à la surface cellulaire, nous avons utilisé un essai de cytotoxité basé sur la fluorescence qui permet de suivre la mort des cellules dendritiques présentant des épitopes du VIH grâce à la voie croisée par les lymphocytes T cytotoxiques spécifiques aux épitopes du VIH. Nous avons observé que les perturbations des activités cathepsines causées par les IP altèrent l'apprêtement antigénique croisé et la quantité d'épitopes produits dans les phagosomes. Cette perturbation de la disponibilité des

peptides change la quantité d'épitopes présentés à la surface cellulaire par la voie croisée (Figure 10).

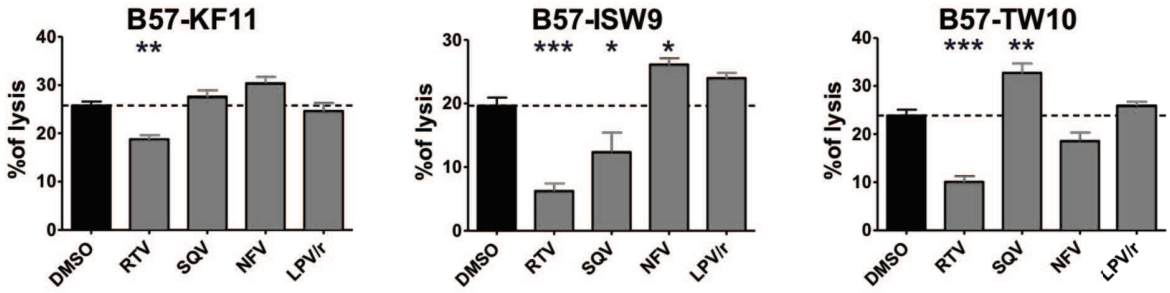

Figure 10: Effect des inhibiteurs de la protease du VIH sur la presentation-croisée.

Nous avons déterminé si les perturbations des activités du protéasome, des aminopeptidases et des cathepsines causées par les IP changent aussi la nature des peptides présentés par les cellules non-infectées. Les peptides du soi présentés à la surface des PBMCs traités ou pas avec saquinavir ont été élués par traitement acidique et identifiés par spectrométrie de masse. Le traitement avec saquinavir cause un changement significatif de 30% dans la nature des peptides du soi présentés à la surface cellulaire, suggérant que les IP non seulement changent la quantité des épitopes présentés à la surface, mais aussi partiellement la nature de ces peptides (Figure 11).

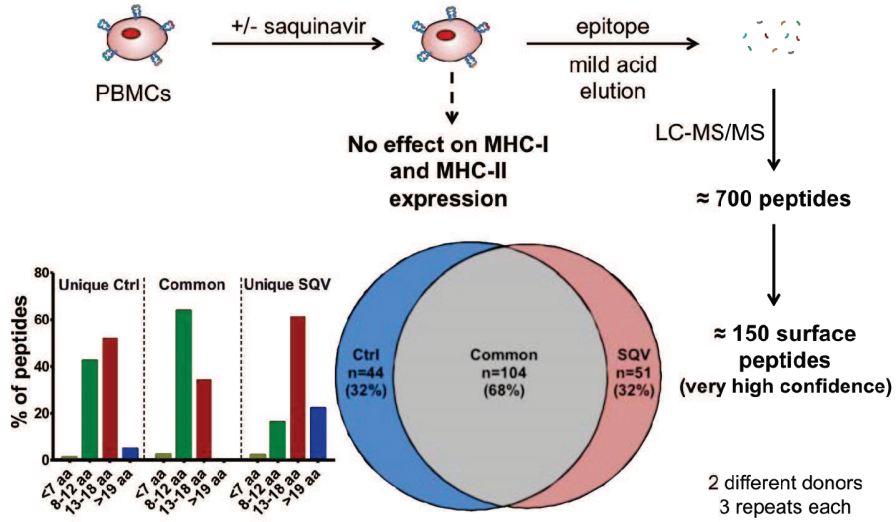

Figure 11: Effect des inhibiteurs de la protease du VIH sur la nature des peptides présentés.

En conclusion, nous avons montré que les IP du VIH perturbent les activités du protéasome, des aminopeptidases et des cathepsines en interagissant directement avec les enzymes et aussi en réduisant l'activation de NOX2 dans les phagosomes. Ces perturbations d'activité altèrent l'apprêtement antigénique dans la voie directe ainsi que croisée et changent ainsi la quantité d'épitopes présentés à la surface cellulaire par les CMH-I. En plus du changement de la quantité d'épitopes présentés, on a montré que le traitement avec des IP du VIH changent significativement le peptidome du soi présenté à la surface cellulaire. Ce travail est important dans plusieurs aspects cliniques et thérapeutiques. Par exemple, chez les patients séropositifs pour le VIH, le traitement avec certains IP pourrait causer un changement dans la quantité et/ou la nature des épitopes présentés par des cellules ayant des réplications résiduelles de VIH pouvant ainsi perturber la réponse immunitaire. Également, chez les patients séropositifs pour le VIH coinfectés avec d'autres pathogènes, le traitement IP pourrait aussi perturber la présentation d'épitopes issus des autres pathogènes et donc modifier la réponse immunitaire contre les co-infections. En outre, dans le contexte des stratégies thérapeutiques comme la réactivation des réservoirs du VIH ou la vaccination des patients séropositifs, le traitement avec des IP du VIH pourrait changer les réponses immunitaires en fonction du type d'IP utilisé et réduire l'efficacité de la thérapie. Finalement, mieux comprendre l'effet spécifique de chaque IP sur les profils de dégradation antigénique nous permettra de prédire et potentiellement d'augmenter la présentation des épitopes immunogéniques d'intérêt.

Introduction

1. AIDS/HIV Background

Since the identification of the human immunodeficiency virus (HIV) thirty-five years ago, HIV infection still remains a threatening infectious disease with considerable public health consequences. Cumulatively, acquired immunodeficiency syndrome (AIDS)-related deaths have been estimated to 39 million since the beginning of the epidemic (UNAIDS 2014). In 2013, 2.1 million new infections and 35 million people living with HIV were reported, mainly in developing countries (UNAIDS 2014). Although antiretroviral therapy (ART) has greatly increased the survival rate and quality of life among infected individuals, only 12.9 million people globally are treated, leaving 63% of the HIV positive population untreated (UNAIDS 2014). Thanks to global health initiatives more and more HIV infected individuals are getting access to ART but continuation of long-term therapy are hampered amongst other by access to care, costs, adherence and ART-related toxicities. Moreover, effective therapeutic or preventive vaccines are still elusive goals, despite considerable research efforts that have been attempted over the past three decades.

1.1 HIV origin and structure

AIDS was first recognized in 1980, but the causative pathogen, HIV, was not identified until 1983, when scientists at the Pasteur Institute in Paris isolated a retrovirus from a lymph node of a patient with AIDS [1]. Since this discovery, HIV virology has been vigorously studied with the hope of developing effective vaccines, powerful treatments, and a potential cure.

HIV belongs to the genus Lentivirus of the family Retroviridae based on shared morphology and similar mode of replication. HIV is further classified into HIV-1 and HIV-2 based on genetic variability. HIV-1, which originated in eastern and central Africa, and HIV-2 from western Africa, were both important in the early epidemic, but the current pandemic is due to HIV-1, and in particular HIV-1 Group M [2]. While HIV-1 Group M subtype C is the most prevalent in the world given its dominance in Africa, subtype B, which is most prevalent in North America and Western Europe, has traditionally been the most frequently studied.

HIV-1 is an enveloped virus with a matrix protein that surrounds a nucleoid structure in the center of the viral particle. The nucleoid structure of mature HIV-1 contains the viral dimeric RNA genome surrounded by a nucleocapsid core, which in turn is housed in the viral capsid. This nucleoid structure also contains viral enzymes integrase, reverse transcriptase (RT), and protease (PR). Surrounding the virion is a host-derived envelope, which is embedded with numerous spike-like glycoproteins that are responsible for host cell attachment and fusion [3]. Each glycoprotein is composed of three transmembrane gp41 subunits (trimer) plus a gp120 trimer that binds to the host cell's CD4 receptor and CCR5 or CXCR4 co-receptor [4](Figure 1).

The HIV genome is approximately 9 kb in length and encodes ten genes: regulatory genes tat and rev; accessory genes vpu, vpr, vif, and nef; and structural genes gag, pro, pol, env. In addition, the HIV DNA genome includes noncoding regulatory sequences, including two flanking long terminal repeats (LTR). Among the coding regions, regulatory gene rev encodes a protein that shuttles incompletely spliced RNA transcripts from cellular nucleus to cytoplasm for translation and packaging, while tat encodes a transcription factor that upregulates HIV DNA expression [5]. Accessory genes vpu, vpr, vif, and nef, encode proteins that likely inhibit cellular retroviral defenses. Gag and env encode proteins that make up the nucleoid structure and envelope respectively. Finally, pol encodes enzymes necessary for reverse transcription of viral RNA into DNA (RT and ribonuclease H), maturation (HIV PR) and integration (integrase, IN) of viral DNA into the host genome (Figure 2).

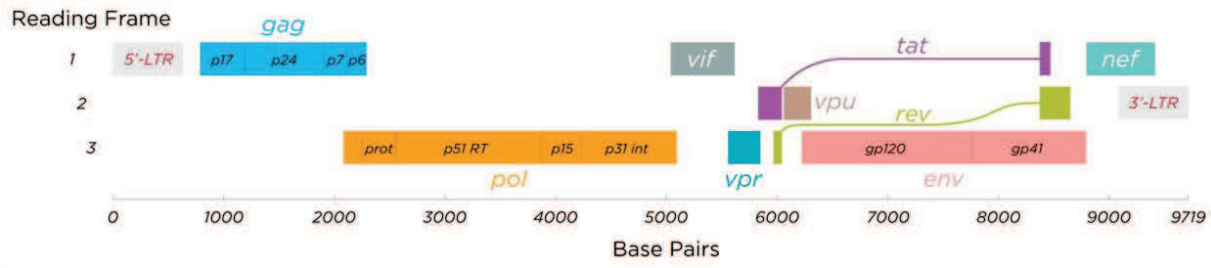

Figure 1: HIV-1 genome and transcriptional splicing organization (adapted from NIV.gov)

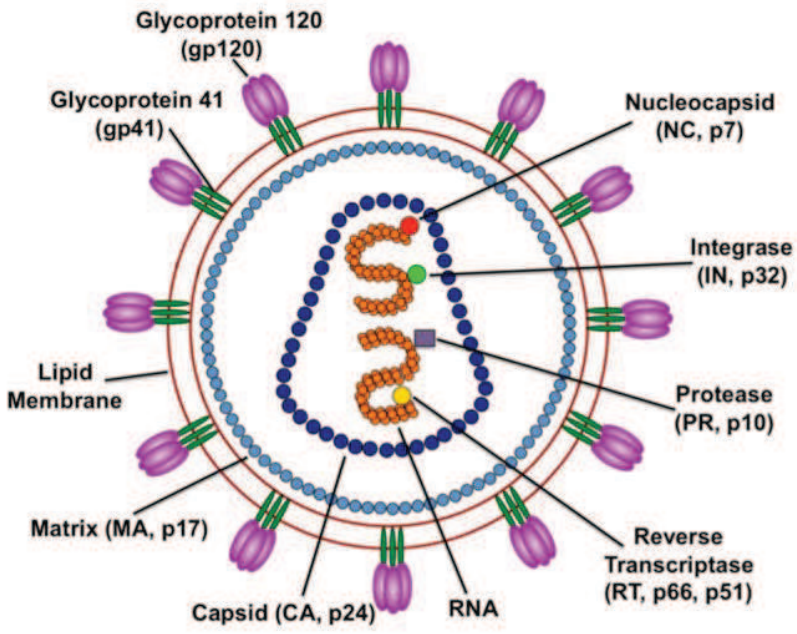

Figure 2: Schematic representation of the HIV structure (NIH.gov)

1.2 The replication cycle of HIV

Understanding the major steps of HIV replication cycle has been key to investigate molecules that could block its replication and permitted the manufacturing of antivirals directed against important steps of this cycle.

The infection cycle of HIV starts by gp120 attaching to its cellular receptor CD4 [6]. The CD4 receptor is expressed on the surface of T helper cells (Th), monocytes, macrophages (Mϕ) and dendritic cells (DC). Upon attachment, a conformational change occurs on the gp120, leading to interactions between the gp120 and co-receptors CCR5 or CXCR4. The attachment with the co-receptor brings the virus closer to the cell, and exposes the fusion domain of gp41 [7]. The fusion between viral and the host cellular membranes allows the entry of viral capsid into the cell. HIV can also enter the cell via alternative routes like phagocytosis, antibody-mediated entry or cell-to-cell transmission however these entries do not always result in productive infections.

After HIV has entered the cell, the RT copies the viral RNA into a complementary DNA (cDNA) molecule. The RT by its DNA polymerase activity generates a complementary second strand of the viral cDNA. The double-stranded viral DNA is then transported to the cell nucleus, where it is integrated into host cell DNA by the viral IN [8,9] . The integrated viral DNA is known as proviral DNA, and it can be dormant for a long time. Upon activation, the proviral DNA is transcribed to generate mRNA by the host cell RNA polymerase II. The primary mRNA transcripts contain multiple introns and can be processed to yield more than 30 alternative mRNAs by various levels of splicing [10]. Doubly spliced mRNA can translate to the major regulatory proteins, particularly Nef, Tat and Rev [11]; partially spliced mRNA has the potential to express the Env precursor (gp160), Vif, Vpu and Vpr; the unspliced mRNA can be expressed as Gag and Gag-Pol precursor proteins or serve as the genomic RNA. The gp120 and gp41 is in fact generated by an endoprotease cleavage of gp160 precursor before transportation to the plasma membrane of the cell [12]. The two nascent viral RNA are also transported to the plasma membrane with Gag and Gag-Pol precursor proteins. Assembly and package of the virion takes place by budding through plasma membrane of the cell [13,14]. During this process, the Gag and Gag-Pol precursor proteins are cleaved by the HIV PR to form the proper HIV proteins, which result in a mature virion (figure 3).

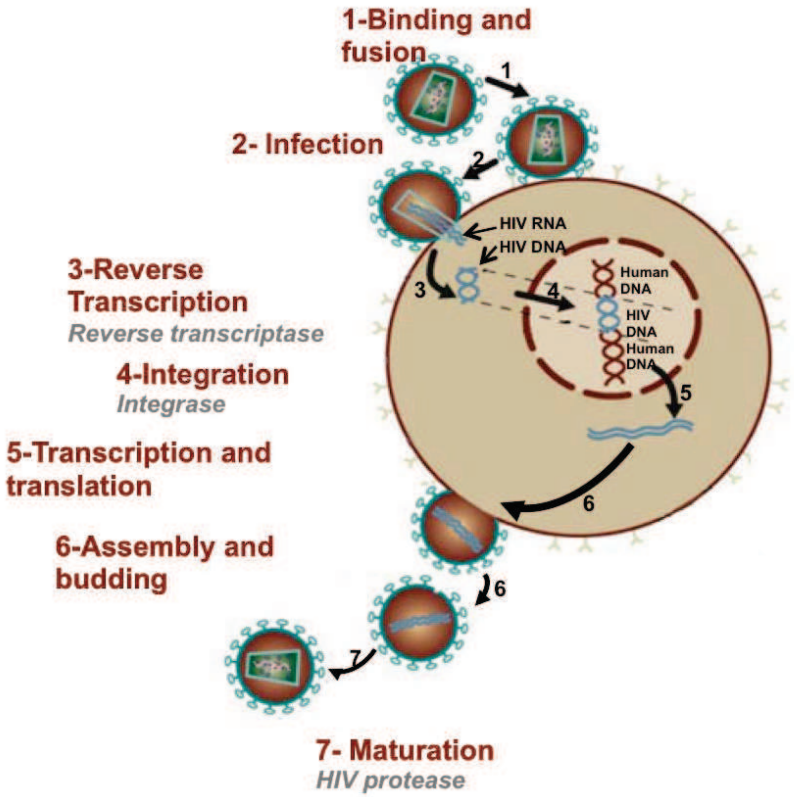

Figure 3: HIV replication cycle. (Figure adapted from www.aidsinfonet.org)

1.3 The natural course of HIV-1 infection

Sexual transmission via mucosal surfaces is the most common route of HIV-1 infection. Technical advances in molecular cloning of virus isolated within days of infection are providing clues as to the nature of the transmitted/founder virus [15]. It is now appreciated that in approximately 80% of mucosal transmission events, a single HIV-1 virion crosses the mucosal barrier and establishes productive infection [16].

Within two weeks of exposure to HIV-1, the transmitted virus has crossed the mucosal epithelial barrier, infected a small population of CD4 T cells, and expanded locally by infecting additional resting and activated CD4 T cells [17]. Having infected a seed population of target cells, the virus is transported to the local draining lymph nodes which contain a large number of target cells, gains access to the bloodstream, and fully disseminates throughout secondary lymphoid organs. By 21-28 days after infection, viral load (VL) reaches a peak, with millions of

viral copies detectable in patient plasma [18]. By this point, the hallmark of HIV-1 infection has been irreversibly established—large numbers of CD4 T cell populations in the host have been depleted (figure 4 – Acute phase).

The earliest detection of HIV-1-specific CD8 T cells coincides with the time at which VL begins to decrease. The infected host establishes a VL set point, which is predictive of the rate of disease progression; individuals with a low set point tend to have a better disease prognosis [19]. The clinical latency stage of the disease can last for several years and now for several decades thanks to the successful use of ART. This stage is accompanied by a steady VL and slow gradual decrease of CD4 T lymphocytes (figure 4 – Clinical latency). Although this period is clinical asymptomatic, it is characterized by a persistent state of immune activation, a critical contributor to disease pathogenesis. Ongoing HIV-1 replication is considered one underlying cause of this chronic activation. Host immune cells are subject to continuous stimulation, resulting in increased cell turnover, increased frequency of cells with an activated phenotype, and cell exhaustion [20,21]. More recently, translocation of microbial products was shown to be a contributing factor to this systemic activation [22]. Damage to gut epithelium facilitates translocation of microbes and/or microbial products that are normally sequestered in the gastrointestinal tract. The detection of these products was higher during chronic HIV-1 infection and correlated with proinflammatory markers. Treatment strategies to reduce the hyperactive immune state observed during chronic HIV-1 disease could help to mitigate immunological dysfunction.

The gradual loss of CD4 T lymphocytes leads to the late-stage of disease characterized by CD4 T lymphocyte count below 200 cells/mm3. This diminished level of CD4 T lymphocytes causes the infected person to be susceptible to opportunistic infections. Unfortunately, the CD4+ T lymphocytes count further decreases during this late-stage and HIV-1 VL sharply increases at least to the level of viral RNA seen during acute stage of disease. In addition to opportunistic infections and problems directly related to HIV-1, AIDS-related malignancies, such as Kaposi sarcoma and Non-Hodgkin's lymphoma, can contribute to the eventual death of HIV-1 infected patients (figure 4).

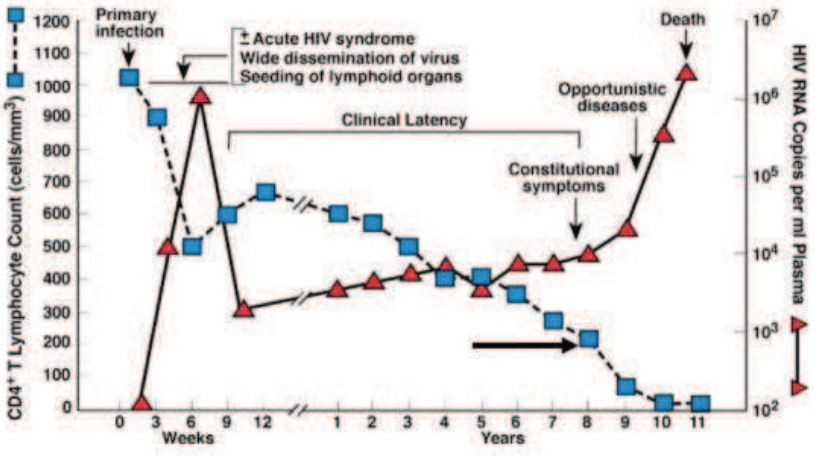

Figure 4: Typical course of HIV infection that shows the relationship between the levels of HIV (viral load) and CD4+ T cell counts over the average course of untreated HIV infection.
(Adapted from: Fauci, A.S., et al, *Ann. Intern. Med.*, 124:654, 1996)

1.4 Viral and host factors influencing susceptibility to HIV infection

In the absence of ART, the immune system of the majority of HIV-1 infected individuals eventually fails, opportunistic infections develop, and the patient succumbs to AIDS. Despite decades of research no prophylactic or therapeutic HIV vaccine strategies with satisfactory efficacy are available to date. Only one human vaccine trial (RV144) showed modest efficacy (approximately 30%) but protection seemed to wane over time [23-25]. A number of studies have identified both viral and host factors including HLA, chemokine receptors and host restriction factors (APOBEC, TRIM5α, Tetherin, SAMHD1) that are associated with a more rapid or delayed progression to AIDS [26-35]. Understanding those factors will help design treatment strategies to prevent or cure HIV infection.

One noted genetic factor associated with delayed disease progression is the Δ32CCR5 mutation, a 32-base pair deletion in the gene encoding the HIV-1 co-receptor CCR5. Individuals homozygous for this deletion fail to express CCR5 at the cell surface and are thus more resistant to infection [36,37]. Infection with viruses that lack a functional Nef protein was also associated with a less pathogenic course of disease [38].

A subset of HIV-1 infected individuals exhibit spontaneous control of HIV-1 replication in the absence of therapy [39]. Originally described as individuals who maintained CD4 cell counts above 500/ mm3 without the use of ART, long- term nonprogressors (LTNP) were a distinct subset of HIV-1 infected patients who remained healthy for long periods of time. It was later observed that many LTNPs do eventually progress, developing clinical signs of disease after 10-15 years of infection [40]. Over the years, an even smaller subset of patients arose out of the LTNPs, now commonly referred to as elite controllers (EC) [28,41]. Making up less than 1% of HIV-1 infected individuals; ECs demonstrate remarkable control of virus replication, able to maintain VL below the level of detection (<50 copies/mL) for as many as 25 years. The most common characteristic of HIV-1 controllers is the expression of certain HLA class I alleles. HLA-B*13, B*27, B*51, B*57, and B*5801 alleles are heavily represented in cohorts of patients with non-progressive HIV-1 disease [26,28,42,43]. These individuals provide "proof-of-principle" that natural immunity to HIV-1 exists and protects from disease progression. LTNPs and ECs remain the focus of a number of studies to better assess the immune response that affords long-lasting protection [44]. Understanding the mechanisms of immunologic control of HIV replication in LTNPs and EC may identify candidate markers of immune control useful for assessing HIV vaccine strategies.

1.5 Immune responses induced during HIV-1 infection

Cell-mediated immune responses are a critical component of host defense against HIV-1 replication. Hence, understanding the impact of natural killer (NK) cell, B cell and T cell effector functions on the course of HIV-1 disease is critical for defining correlates of long-lasting protection and the development of novel treatment strategies.

1.5.1 Natural killer cells

Previous studies have reported the importance of targeting HIV-1 early, as low VL set point correlates with delayed disease progression [45]. Furthermore, early control of HIV-1 replication achieved by ART during primary infection was associated with preserved HIV-specific immune responses [46]. As first responders to invasion by microbial pathogens, innate effector cells react to contain and clear infection; hence NK cells are likely an important component of immune

protection during the acute stage of disease. Rapid progression to AIDS has been associated with reduced NK cell frequency and function [47]. It is also known that HIV-1 infection alters NK cell phenotype, as the subset most responsible for antibody-dependent cell-mediated cytotoxicity (ADCC) is selectively lost during disease [48,49].

NK cell effector function is regulated by activator and inhibitory receptors expressed at the cell surface [50]. One family of NK cell activating receptors consists of three members—NKp30, NKp44, and NKp46—and it was observed that compared to uninfected controls, these receptors were expressed at lower levels in HIV-infected subjects [51]. Epidemiologic studies provide further evidence implicating NK cells as mediators of protection during HIV-1 disease. Over 1500 HIV-infected individuals were analyzed for HIV-1 disease outcome, human leukocyte antigen (HLA) genotype, and expression of killer immunoglobulin-like receptors (KIR) [52]. KIRs comprise a class of NK cell receptors specific for HLA class I molecules. This analysis demonstrated that the co-expression of activating NK cell receptor KIR3DS1 and HLA-B alleles having the Bw4 motif was associated with delayed progression to AIDS. There was no added benefit if the molecules were expressed individually. The impact of NK cell effector function on HIV-1 disease warrants further investigation as innate immunity may impact long-term prognosis of HIV-1 disease during primary infection.

1.5.2 B cells and HIV-1 Infection

Humoral responses are an essential component of adaptive immunity. For years, vaccine development focused on the induction of antigen-specific antibodies, as sterilizing immunity to a number of pathogens (measles, hepatitis B) was established if a minimum antibody titer was induced [53]. These long-lasting antibody responses are induced by immunization with killed and live attenuated viruses, or recombinant antigens. Safety issues prevent the use of attenuated HIV-1 as a vaccine agent, thus alternate vaccine strategies will be needed to induce appropriate virus-specific humoral responses.

While virus-specific antibodies can be detected within three weeks of infection, HIV-1 neutralizing antibodies (NAbs) are often not detected for months or even years after transmission [18], and these NAbs are the first antibodies from which the virus will escape. Adding

another level of complexity, NAbs to conserved regions of the HIV envelope proteins, those likely to provide the most protection, are extremely rare and often not detected for 2-3 years after infection [18].

Pre-existing circulating antibody has been shown to affect disease outcome in rhesus macaques [54-56]. Animals were passively immunized with NAbs and subsequently challenged with chimeric simian immunodeficiency virus (SIV)/HIV-1 virus. Compared to controls, macaques receiving antibody infusion showed reduced pathogenicity or a complete block of infection; this protection was observed in animals regardless of inoculation site. Recently in a phase 1 human clinical trial a passive immunization with NAbs showed up 250 times decrease of the VL in the blood of HIV infected individual [57]. These data suggest that NAbs may be important mediators of protection from HIV-1 acquisition and control. Understanding development of the more rare, HIV-1-specific NAbs isolated from infected individuals may provide insight on how to generate such responses with an effective vaccine.

1.5.3 CD8 T cell and HIV-1 Infection

CD8+ T cells are part of the adaptive branch of the immune system and are key players in mediating immunity to intracellular pathogens and tumors. CD8 T cells that carry the appropriate T-cell receptor (TCR) recognize peptide in the context of MHC class I [58,59]. Initial encounter of naive CD8 T cells with antigen induces CD8 T-cell priming and initiates a program of proliferation and differentiation into effector cytotoxic T lymphocytes (CTLs); this is known as the primary response. After the primary response peaks and antigen is cleared, most effector CD8 T cells die, leaving behind a surviving fraction that persists as long-lived memory cells. Upon second antigen encounter, those memory cells mount a faster and stronger immune response than the primary response.

CD8+ T cell priming need various stimuli to become fully activated and induce differentiation and proliferation (figure 5). These stimuli can be roughly divided into two categories: TCR signals and environmental cues, including but not limited to dendritic cell (DC) activation and costimulation (CD80/CD86), CD4 ‘help’, and soluble inflammatory and growth factors. Conditions of T cell priming impact the development of downstream CD8 T cell effector

function. The extent to which these signals influence CD8 T-cell fate and effector function is still unclear and need to be addressed.

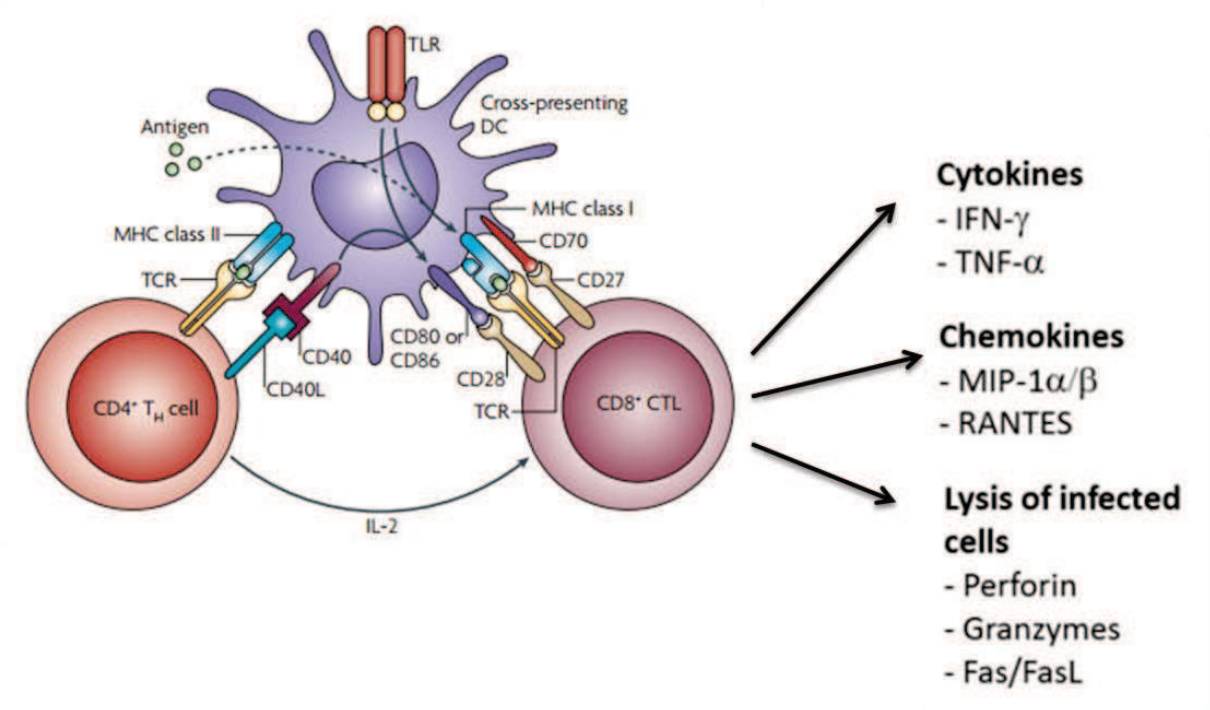

Figure 5: T cell activation by DC (MHC-TCR recognition and help of costimulatory molecules)(Front Immunol. 2011 Aug 1;2:31. doi: 10.3389)

Parameters of CD8 T cell effector function upon antigen stimulation include proliferation, production of cytokines (interferon(IFN)-γ, interleukin(IL)-2, tumor necrosis factor(TNF)-α), production of chemokines (macrophage inflammatory protein(MIP)-1 alpha, RANTES), and the release of effector molecules involved in target cell lysis (CD107a, perforin, granzymes) (figure 5). Production of IL-2 and maintenance of proliferative capacity by CD8 T cells have been associated with viral control [60,61]. More recently, simultaneous production of these soluble factors by a single CD8 T cell, defined as a polyfunctional response, has been associated with improved disease outcome [62]. However, the mechanism and precise component(s) of the CD8 T cell response critical for long-lasting protection are not clear, highlighting the need for improved methods to analyze CD8 T cell effector functions.

Many studies established the importance of CD8 T cell responses in control of HIV replication.

The emergence of HIV-1-specific CD8 T cells during primary infection coincides with the initial reduction of VL from its peak by two to four logs [63,64]. This temporal association was an early demonstration of the importance of CD8 T cell responses in controlling HIV-1 replication [65-67]. When SIV-infected macaques were treated with an anti-CD8 antibody, control of virus replication was lost and VL increased 20- to 2500-fold within six days of antibody treatment [68,69]. It was only when CD8 T cells were repopulated that control of virus replication was recovered. One caveat to these studies was the fact that NK cells may have also been depleted upon antibody treatment, another caveat is overexposure to IL15 and over activation of CD4 T cells; nonetheless, cytotoxic effector cells were playing a role in limiting virus replication.

CD8 T cells are also responsible at least in part for the control of viral replication in many ECs. For example, EC are enriched for certain HLA alleles, such as HLA-B13, B15, B51, B27, B57, and B58 [28,70-74]. EC contain a greater fraction of HIV-specific CD8+ T cells that can degranulate, produce multiple functional cytokines and chemokines and display markedly better proliferative potential upon HIV peptide stimulation than individuals with progressive disease [60,62,75-77]. Additionally, recent evidence has demonstrated that HIV-specific CD8 T-cells from EC have enhanced cytotoxic capabilities compared to progressors [78-81]. However due to the lack of understanding of the exact CD8 T cell priming mechanism it is still unclear how to induce such polyfunctional CD8 T cell response by vaccination.

Early HIV-specific CD8 T cell responses are usually narrowly focused on a few immunodominant epitopes, which facilitates viral escape [82]. Gag and Nef are highly immunodominant and command most of the HIV-1-specific CD8 T cell response, however immunodominant do not necessarily correlate with control . Gag-specific responses in contrast to Nef are associated with improved control of virus replication [83,84]. Virus mutating to evade immune pressure induced by HIV-specific CD8 T cells also confirms the importance of CD8 T cells in HIV control. Mutations within immunodominant epitopes or in its flanking motifs lead to altered antigen processing or loss of HLA class I binding, thus enabling the virus to evade host immunity. Escape from the immunodominant B*27-KK10 (Gag p24, KRWIILGLNK) CD8 T cell response is an example of significant loss of viral control as a result of mutation within a CD8 T cell epitope [43]. Substitution

of the arginine (R) residue at position 2 was associated with rapid disease progression. Interestingly, while the conversion at position 2 of this epitope enables evasion of the host immune response, it comes at a fitness cost to the virus. Additional studies have demonstrated that the virus induces compensatory mutations in an attempt to restore fitness [85,86]. During the chronic phase of the infection the immune response becomes broader but no more effective at controlling viral replication [87]. Since immunodominance established during HIV infection or reproduced by some HIV vaccines does not clear or prevent infection, breaking immunodominance hierarchies to induce the presentation of broader subdominant but protective epitopes provides an interesting alternative for vaccine design.

Although these findings highlight the critical importance of CD8 T cells in controlling HIV-1 replication, we still need to better understand the factors that influence CD8 T cell priming, proliferation and memory including MHC-I epitope and co-stimulatory molecules presented by DCs, CD4 T cell help and inflammatory and growth factor production to ultimately design a vaccine that will induce broad polyfunctional CD8 T cell responses to control HIV-1 infection.

1.5.3 CD4 T cells and HIV-1

CD4 T cells play key role in orchestrating and mediating the immune responses against viral pathogens. Naïve CD4 T cells that carry the appropriate TCR recognize antigenic peptides in the context of MHC-II presented on the surface of antigen presenting cells (APCs). Depending on the stimulatory signals and cytokines in the milieu naïve CD4 T cells can differentiate into memory CD4 T cells or a number of different effector cell subsets. The main subsets are Th1, 2 and 17. Once differentiated into an effector phenotype, T cells will migrate to sites of infection to mount immune responses. Th1 cells are marked by the secretion of IFN-γ, IL-2 and lymphotoxin-α (LTa), whereas Th2 cells are defined by the secretion of IL4, 5, 6, 10 and 13 [88]. Th1 cells provide help to the cellular arm of the immune system. They stimulate other cells such as Mϕ and in instances where pathogen infection does not trigger a strong inflammatory response, Th1 cells are vital in the stimulation of the CD8 T cell response by providing signals such as IL-2 [89]. Mice studies indicated that CD8+ T cell memory development was impaired with the depletion of CD4 T cells [90,91]. However the exact mechanism and the extent to which CD4 T

cell are needed to induce an optimal CD8 T cell response is still not clear. Th2 cells provide help to the humoral arm of the immune system. They stimulate B cells to upregulate antibody production and undergo class switching [92]. Th17 cells are marked by the secretion of IL17, 21 and 22. They are vital for pathogen clearance and inducing tissue inflammation [93]. Another important subset of CD4 T cells are the regulatory T cells (Tregs). These cells act to suppress the immune system and are important in establishing peripheral tolerance to self-antigens (figure 6).

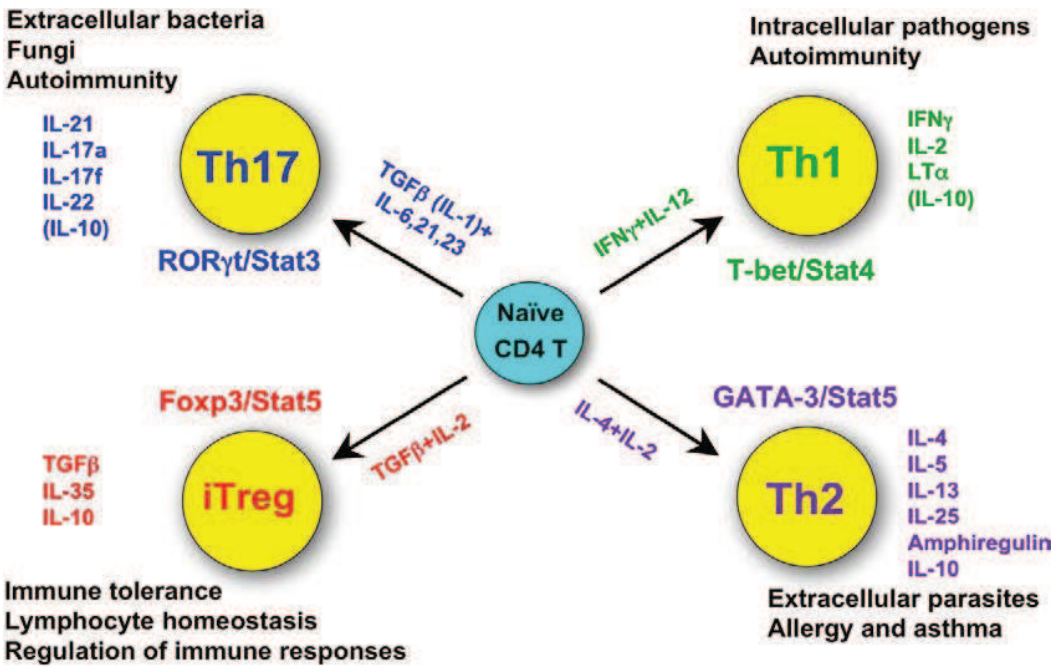

Figure 6: Summary of the 4 CD4 T helper cell fates: their functions, their unique products, their characteristic transcription factors, and cytokines critical for their fate determination. (Blood. 2008 Sep 1;112(5):1557-69. doi: 10.1182)

HIV-1 primarily infects and destroys CD4 T cells. A high rate of replication causes rapid disseminated infection of CD4 T cells in the first few weeks and a sizeable reduction in CD4 T cell numbers. Over the long term, CD4 T cell death outnumbers the thymic output of new cells, resulting in a progressive depletion. CD4 T cell response diminishes and its contribution to the immune system is severely compromised leading to poor control of HIV-1 infection and increased susceptibility to opportunistic infections. In addition, a subset of resting memory CD4

T cells harbor latent HIV-1 DNA that cannot be cleared and are largely unaffected by ART causing a major barrier to the eradication of HIV-1 within infected individuals.

Other aspects of CD4 T cell function have also provided possible insights into correlates of disease control. Increasingly reports of CD4 T cells with direct effector function are appearing in the literature [94-96]. In addition to APCs, different cell types have now been shown to upregulate the expression of MHC-II molecules under certain conditions, one such example being virus infection [97]. The expression of MHC-II molecules on virus infected cells suggests a direct role for CD4 T cells in anti-viral immunity. Indeed CD4 T cells have now been shown to control infection of many viruses including gamma herpes viruses, murine influenza and west Nile virus amongst others [98-100]. A number of reports have shown isolation of virus-specific CD4 T cells, including cytotoxic CD4+ T cells specific to viral antigens such as those of Epstein-Barr virus (EBV) and HIV [94,95,101,102]. Moreover, early expansion of CD4 T cells expressing perforin and Granzyme A is associated with spontaneous control of HIV infection, suggesting direct cytolytic activity of CD4 T cells [102]. Interestingly, prior exposure to other pathogens may also prime cross-protective CD4 T cell responses against HIV that are associated with early clearance of the virus [103] and suggests that vaccines targeted to induce CD4 T cell responses may be useful. However additional studies are needed to understand the exact mechanism leading to the generation of functional virus-specific cytotoxic CD4 T cells.

1.5.5 Benefit of treatment

Nowadays, we are in the era where most of HIV-infected patients who have access to ART have achieved controlled plasma VLs. The control of HIV viremia has a substantial role in the management of HIV infection and its consequences. The control of viremia has been translated in a series of immunological and clinical benefits. The restoration of CD4 cell count occurs following the initiation of ART and a rise of 50 to 100 cells/mm3 is usually observed in the first year of therapy, however CD4 reconstitution is not even for all patients and factors that control it are not well understood. In a long-term observational study that prospectively followed patients initiating ART, the majority of increase in CD4 cell counts was in the first two years with little increase afterwards [104]. Moreover, the increase in CD4 T cells count by ART reconstitutes

CD4 T cell help to maintain functional CTLs crucial for HIV control [105]. In addition, ART treatment also decreases viral antigen exposure, which reduces the persistent immune activation and inflammation and leads to immune reconstitution [105-107]. Controlled VL and restored immunity upon ARV therapy resulted in significant differences in the incidence of AIDS-defining illnesses (esophageal candidiasis, Kaposi's sarcoma, pulmonary and extrapulmonary tuberculosis, non-Hodgkins lymphoma, bacterial pneumonia and recurrent herpes simplex) before and after ART as well as over the different periods of ART [108,109]. Furthermore, dramatic decrease in mortality was observed upon successful ART treatment [110-112] as well as increased survival probabilities reaching life expectancy values comparable to HIV uninfected individuals [113] .

In addition to the immunological and clinical benefits, the control of viremia (<50copies/mL) has been shown to prevent the selection of resistance mutations. In patients with persistent low-level viremia under ART, new resistance mutations were detected and the magnitude of viremia was the primary driver of the evolution rate of the emergent drug resistance mutation [114,115].

Beside the individual benefits, ART has led to a decrease of transmission of HIV to non-infected partners through the control of viral replication. Data from prospective cohort analysis of serodiscordant couples showed a 92% reduction of HIV transmission between patients on treatment and those not receiving it. Transmission occurred more among couples where the non-treated HIV-infected partner had low CD4 cell counts and higher plasma HIV-1 concentrations [116]. In the HPTN 052 Study, 1763 serodiscordant couples in which HIV-1–infected participants had a CD4 count of 350 to 550 cells/mm3 were randomly assigned to receive ART either immediately or after a decline in the CD4 count or the onset of HIV-1-related symptoms. Of the 28 linked transmissions, only 1 occurred in the early-therapy group suggesting a relative reduction of 96% in the number of linked HIV-1 transmissions resulting from the early initiation of ART, as compared with delayed therapy [117].

2. Antiretroviral therapy

2.1 Different classes of antiretroviral therapy

The significant advancement in the understanding of HIV replication and its pathogenesis has helped in the identification of various pharmacological targets. The first anti-HIV agent licensed for clinical use was Zidovudine (AZT), in 1987. Since then, several anti-HIV compounds have been approved by the FDA (US Food and Drug Administration) and EMEA (European Medicine Agency) for treating HIV infections. These compounds fall within different categories depending on the target within the HIV replicative cycle they interact with (figure 7).

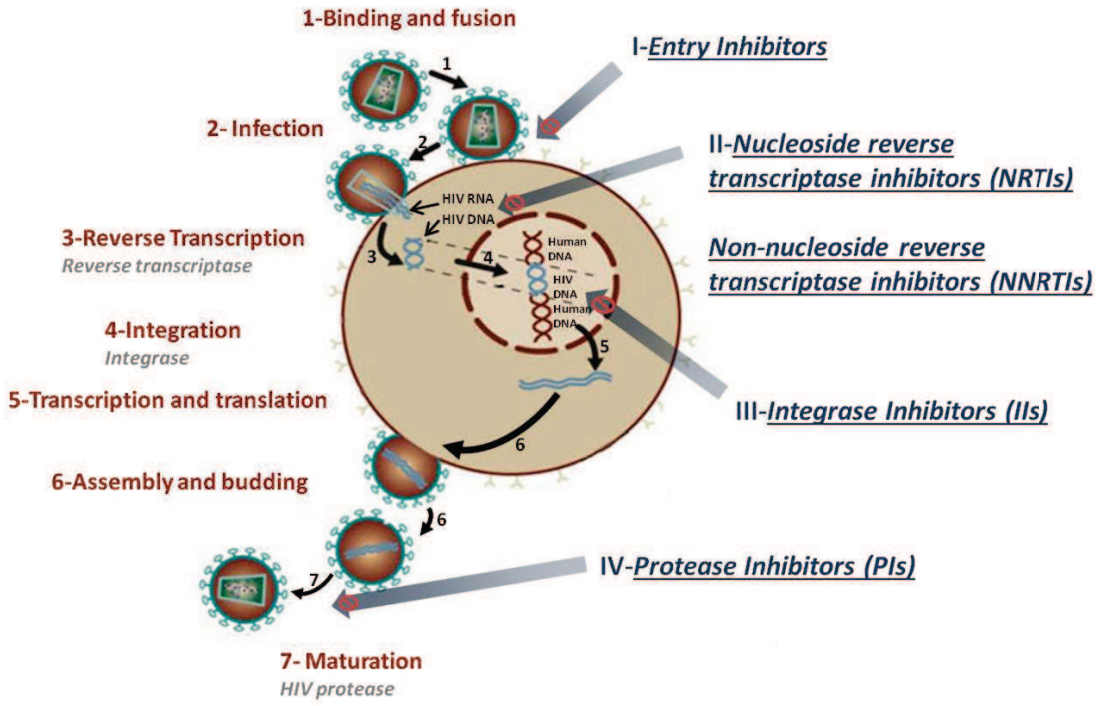

Figure 7: Antiretroviral classes and their targets in HIV replication cycle. (Figure adapted from www.aidsinfonet.org)

2.1.1 The reverse transcriptase inhibitors

The RT inhibitors interfere with the generation of a DNA copy from the viral RNA. There are two classes of RT inhibitors, distinguished by their mode of action.

First of them is the group of nucleoside reverse transcriptase inhibitors (NRTIs). These are nucleoside analogues that are incorporated by the viral RT into the newly synthesized DNA strand. They are inactive in their initial forms and require successive phosphorylation steps by host cell kinases and phosphotransferases to form deoxynucleoside triphosphate (dNTP) analogs capable of viral inhibition. In their respective triphosphate (TP) forms, NRTIs compete with their corresponding endogenous dNTPs for incorporation by HIV RT. Once incorporated, they serve as chain-terminators of viral RT, thus, acting early in the viral replication cycle by inhibiting a critical step of proviral DNA synthesis prior to integration into the host cell genome [118] (figure 8). The currently approved HIV NRTIs are listed in the table below (table 1).

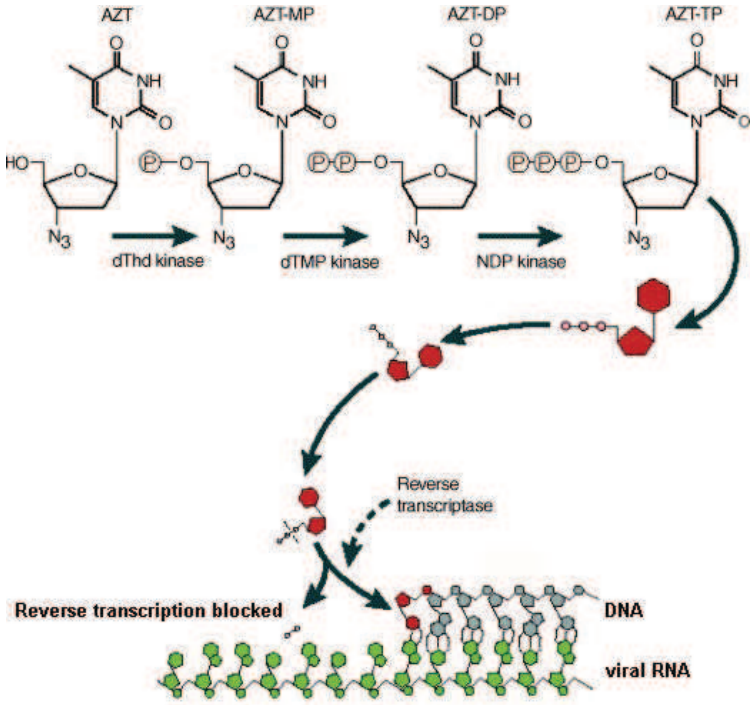

Figure 8: Nucleoside reverse transcriptase inhibitors mode of action (AZT as an example)(adapted from http://biochemistryformedics.com/)

Table 1: HIV nucleoside/nucleotide reverse transcriptase inhibitors.

Generic name	Abbreviation	Brand Name	Date of FDA approval
zidovudine	AZT (ZDV)	Retrovir	1987
stavudine	d4T	Zerit	1994
lamivudine	3TC	Epivir	1995
abacavir	ABC	Ziagen	1998
didanosine	ddI	Videx EC	2000
tenofovir	TDF	Viread	2001
emtricitabine	FTC	Emtriva	2003

The second group of RT inhibitors is the non-nucleoside reverse transcriptase inhibitors (NNRTIs). They are small molecules that carry out the inhibition of RT by binding to a hydrophobic pocket in the proximity of the active site of the enzyme. After the inhibitor is bound, it impairs the flexibility of the RT resulting in its inability to synthesize DNA (figure 9). Mutations can cause resistance to NNRTIs which results in reduced affinity of the inhibitor to the protein. Usually, a single mutation selected by one NNRTI is sufficient to confer complete resistance to all compounds of the drug class [119] [120]. The currently approved HIV NNRTIs are listed in the table below (table 2).

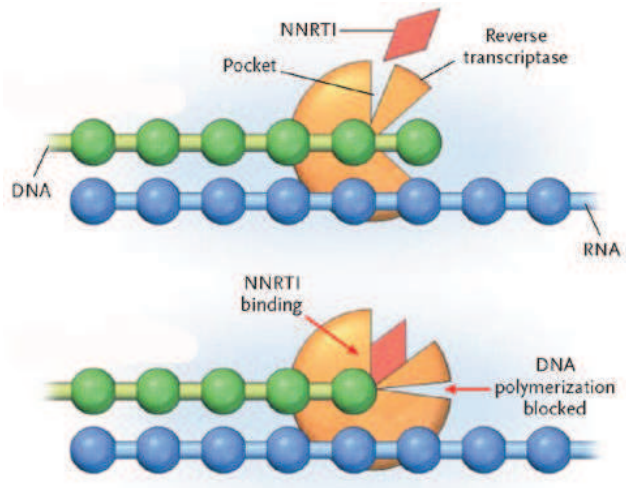

Figure 9: Non-nucleoside reverse transcriptase inhibitors mode of action (adapted from massmed.org).

Table 2: HIV non-nucleoside reverse transcriptase inhibitors.

Generic name	Abbreviation	Brand Name	Date of FDA approval
nevirapine	NVP	Viramune	1996
delavirdine	DLV	Rescriptor	1997
efavirenz	EFV	Sustiva (US) - Stocrin (Europe)	1998
etravirine	ETR	Intelence	2008
rilpivirine		Edurant	2011

2.1.2 The protease inhibitors

Protease Inhibitors (PIs) interfere with the process of forming new infectious viral particles. The viral protease is engaged in virion maturation. Protease targets the amino acid sequences in the gag and gag–pol polyproteins, which must be cleaved before the nascent viral particles (virions) can mature. Cleavage of the gag polyprotein produces three large proteins (p24, p17, and p7) that contribute to the structure of the virion and to RNA packaging. The design of the first-generation HIV PIs is based on the transition-state mimetic of the Phe-Pro bond, the major substrate of HIV-I protease. PIs by binding to the active site of the protease compete with its natural substrates. PIs prevent cleavage of gag and gag–pol protein precursors in acutely and chronically infected cells, arresting maturation and hence blocking the infectivity of nascent virions [121] (figure 10).

The resistance of HIV against PIs can be achieved by two mechanisms. The first one involves mutations in the protease catalytic site such that the affinity of the inhibitor is decreased while the natural substrates (gag and gag–pol polyproteins) can still be bound efficiently [119]. Those mutations can sometime reduce the efficiency of the protease by reducing the affinity to its natural substrate. Thus, the second mechanism introduces compensatory mutations aiming at re-establishing the efficiency of the enzyme while maintaining resistance against the inhibitor. These compensatory mutations can occur either in the protease or at the cleavage site of its natural substrate [122,123].

The currently approved HIV PIs are listed in the table below (table 3).

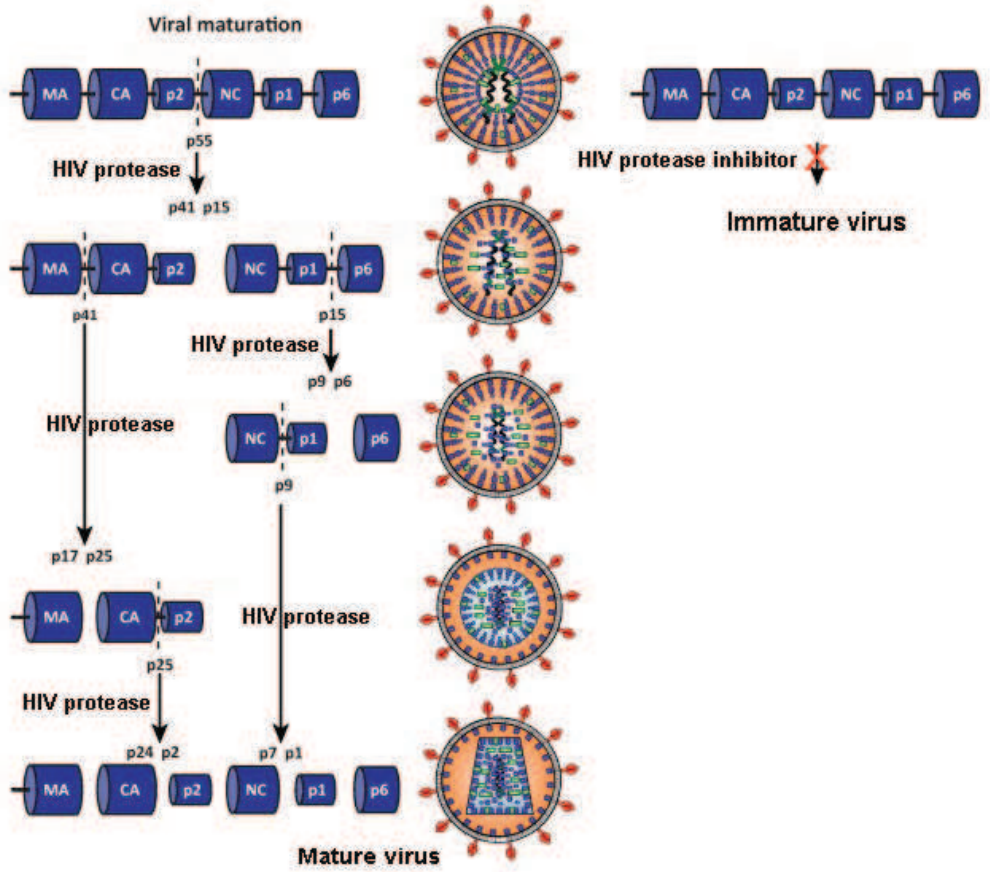

Figure 10: HIV protease inhibitor role in blocking HIV maturation.

Table 3: HIV protease inhibitors.

Generic name	Abbreviation	Brand Name	Date of FDA approval
saquinavir	SQV	Invirase	1995
ritonavir	RTV	Norvir	1996
indinavir	IDV	Crixivan	1996
nelfinavir	NFV	Viracept	1997
amprenavir	APV	Agenerase	1999
lopinavir + ritonavir	LPV/RTV	Kaletra - Aluvia (developing world)	2000
fosamprenavir	FOS-APV	Lexiva (US) - Telzir (Europe)	2003
atazanavir	ATV	Reyataz	2003
tipranavir	TPV	Aptivus	2005
darunavir	DRV	Prezista	2006

2.1.3 The integrase inhibitors

Integrase inhibitors (II) are designed to block the activity of integrase, a viral enzyme that inserts the viral genome in the DNA of the host cell [124] (figure 11). Raltegravir (RAL) was the first integrase inhibitor approved by the FDA. Clinical trials indicate that RAL is safe and highly effective in the treatment of both antiretroviral-naïve and –experienced patients [125]. Following RAL two other integrase inhibitors had been approved (table 4).

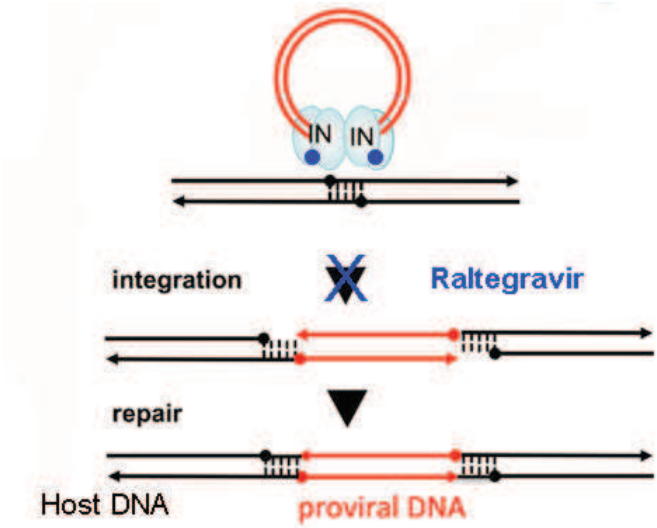

Figure 11: HIV integrase inhibitor blocks the integration of proviral DNA to the host genome (adapted from NIH.gov).

Table **4**: HIV integrase inhibitor.

Generic name	Abbreviation	Brand Name	Date of FDA approval
raltegravir	RAL	Isentress	2007
elvitegravir	EVG	Vitekta	2012
dolutegravir	DTG	Tivicay	2013

2.1.4 The entry and fusion inhibitors

These inhibitors block viral fusion and entry to the host cell. This group of inhibitors can be subdivided into classes of agents that act at different stages of entry: CD4 binding, co-receptor binding, and fusion. Currently, only antagonists that block CCR5 binding (Maraviroc) and fusion

(Enfuvirtide) have been approved by the FDA for treatment of HIV infected patients, although strategies to inhibit other aspects of HIV entry are under development [126]. Maraviroc binds to the co-receptor CCR5 and blocks the entry of the virus to the cell (figure 10). Prior to the use of co-receptor blockers, it is necessary to determine the co-receptor which is being used by the virus for entering [127]. In addition to maraviroc, more CCR5 and also CXCR4 inhibitors are under investigation [128]. Enfuvirtide prevents HIV from entering a target cell by inhibiting fusion of virus and host cell membranes. Enfuvirtide binds to a subunit of gp41 and therefore prevents the required conformational change that facilitates the fusion of host and viral membrane (figure 12). Drug resistance mutations are usually located in the Enfuvirtide binding site on gp41 (direct resistance) or confer resistance indirectly via mutations in other regions of gp41 and even in gp120 [129] (table 5).

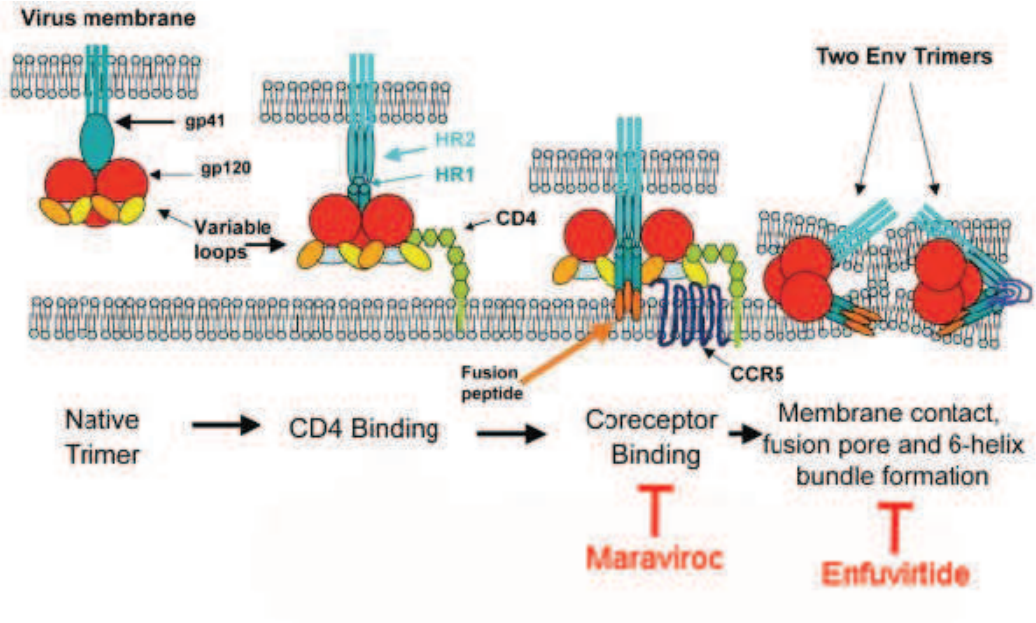

Figure 12: HIV entry and fusion inhibitor targets (PNAS 2003 Sep 16;100(19):10598-602).

Table 5: HIV entry and fusion inhibitors.

Generic name	Abbreviation	Brand Name	Date of FDA approval
enfuvirtide	T-20	Fuzeon	2003
maraviroc	MVC	Celsentri (Europe) - Selzentry (US)	2007

2.2 Treatment initiation and HAART

According to the WHO 2013 guidelines, a patient is recommended to start treatment when their CD4+ count reaches <500 cells/mm3, which is an increase from the 2010 guidelines that recommended treatment start when the count reached <350 cells/mm3. When a patient progresses from being HIV-positive to the point of needing drug treatment, sophisticated genotyping is used (in the US) to determine an optimal set of ARVs that will provide the best chance at suppressing the replication of the virus with a genetic barrier to resistance. CD4 cell count is used as a marker of the ability of the patient's immune system to function; VL is used as an indication of viral progression. When ART is working well, an infected person's VL is below the Limit of Detection (LOD) 50 copies/mL. When ARVs are not working, VL is increased, resulting in a concomitant drop in CD4 count (figure 13). When a person has reached a CD4 count <200 cells/mm3 they are diagnosed as having AIDS. A healthy person's CD4 count is usually between 500 to1000 cell/mm3.

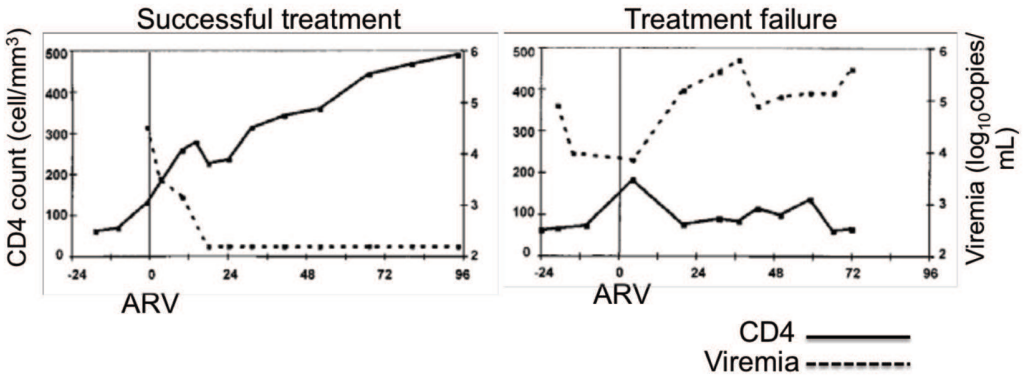

Figure 13: CD4 count and viremia during a successful and unsuccessful HAART treatment (Figure from 192)

As discussed above, the HIV develops resistance against individual drugs and inhibitors. This problem required a new pharmaceutical strategy. An approach of combination therapy was developed which involved combining several ARV compounds. This approach benefited the most from the development of drugs in NNRTIs and PI classes. Combination therapy can block the resistance effect more effectively for two reasons; first, multiple mechanisms are required for resistance to occur to all drugs in the regimen and second; multiple drugs suppress viral replication more effectively than single agents. This marked the beginning of the era of highly active antiretroviral therapy (HAART) in 1995. HAART combines a minimum of three drugs from at least two different drug classes. The first line of HAART includes two NRTIs and one NNRTI. If the first line treatment fails which could happen for many reasons including drug resistance, poor adherence, poor drug absorption or a weak drug combination, a second line treatment composed of two NRTIs and one PI is initiated. If the second line of treatment shows signs of failure then IIs or entry/fusion inhibitors are added to the treatment. Combinations of antiretrovirals with different targets create multiple barriers to the HIV replication process. This helps to keep the number of new virus production low and reduce the possibility of a superior mutation.

In 2005-06, FDA approved fixed-dose combinations of antiretrovirals (for example, Atripla). These are multiple antiretroviral drugs combined into a single pill, which helps to significantly simplify a drug treatment regimen by reducing the pill burden, helping to increase adherence and thus reducing potential development of viral resistance to the drugs. They may combine different classes of antiretrovirals or contain only a single class. Another milestone in HAART was the discovery that the protease inhibitor ritonavir interferes with the liver enzyme cytochrome P450 [130]. This enzyme is involved in the metabolic processing of most protease inhibitors. Thus, the use of a small dose of ritonavir inhibits the liver enzyme, and helps to maintain optimal levels of other protease inhibitors in the patient's blood for a longer period of time. The boosting of protease inhibitors with ritonavir is standard as of 2001 – following the introduction of Kaletra (LPV+RTV) – and is usually denoted by PI/r. Table 6 shows different antiretroviral combinations recommended by different guidelines.

Table 6: Different guidelines on the first line antiretroviral therapy.

Guideline	NRTI	NNRTI	PI	II
WHO 2013	TDF/3TC (or FTC) ABC/3TC AZT/3TC	EFV NVP	No PI	No II
US DHSS 2014	TDF/FTC ABC/3TC	EFV	ATV/r DRV/r	RAL DTG
FRANCE 2013	TDF/FTC ABC/3TC	EFV RPV	ATV/r DRV/r	No II
EACS 2013	TDF/FTC ABC/3TC	EFV RPV	ATV/r DRV/r	RAL

2.3 Side effects of HAART

The use of HAART has been associated with increasing life expectancy in HIV-infected patients. While the median age of HIV-infected patients is increasing, concerns arise concerning the long term toxicities and morbidities associated with the use of HAART. Many patients under ART displayed lipodystrophy, metabolic alterations, increased risk of cardiovascular diseases and reduced bone mineral density. Now that ART is recommended for lifelong, the challenge is to maximize antiviral efficacy and to minimize toxicity[131].

Lipodystrophy is defined as abnormal fatty tissue distribution. It could present as lipoatrophy (loss of fat tissue in the face and the extremities), lipohypertrophy (accumulation of fat tissue in the abdomen and posterior neck) or a mixture of lipoatrophy and lipohypertrophy. Several overlapping risk factors attribute for the development of lipodystrophy [132]. There is an evidence that HIV-1 infection on its own contributes to the development of the lipodystrophic phenotype by interfering with some key genes of adipocyte differentiation and mitochondrial function in patients which have not received ART [133]. Beside the role of HIV, the use of thymidine analogues NRTIs (zidovudine and stavudine) are mainly responsible for peripheral lipoatrophy. NRTIs induce mitochondrial dysfunction and modify adipocyte phenotype and adipose tissue pattern of secretion of cytokines and adipokines through the production of reactive oxygen species [134]. This deleterious effect was one of the causes behind the replacement of thymidine analogues with other nontoxic NRTIs such as abacavir or tenofovir which led to improvement in lipoatrophy. The use of PIs is associated with the development of fat hypertrophy [135]. PIs

increase cytokine and decrease adiponectin secretion and expression [136]. In a recent study, Guaraldi G et al have shown that CD8 T-cell activation was associated with lipodystrophy and the relative amount of visceral abdominal adipose tissue in ART controlled, virologically suppressed, HIV-infected patients suggesting that CD8 activation may be involved in the accumulation of central fat [137].

Beside the morphological changes (lipodystrophy) associated with PIs use, the APROCO study, which has investigated the prevalence of lipid and glucose alteration found that 23% of HIV-infected patients have glucose metabolism alterations, 28% have hypertriglyceridemia and 57% have hypercholesterolemia. Age was significantly associated with different phenotypes of lipodystrophy and metabolic alterations while among antiretrovirals, only ritonavir was associated with hypertriglyceridemia [138]. These abnormalities were associated with increased plasma levels of apolipoproteins [139]. Compared to HIV-uninfected population, the incidence of type-2 diabetes in HIV-infected men with HAART exposure was greater than 4 times in the multicenter AIDS cohort study [140]. Several cohorts reported an increased incidence of diabetes among patients on HAART and ranged from 4.4 person-years follow-up (PYFU) in the Swiss HIV cohort study to 14.1 PYFU in the APROCO-COPILOTE Cohort Study [141-143]. In addition to traditional risk factors, the use of NRTIs (stavudine, zidovudine, lamivudine and didanosine) and the protease inhibitor (indinavir) containing regimens was associated with the risk of developing diabetes.

The risk of myocardial infarction (MI) among HIV-infected patients is higher than general population [144]. Endothelial dysfunction is possibly the most plausible link between HIV infection and atherosclerosis [145]. The mechanisms underlying the regulation of endothelial function in HIV-infected persons appear to be multifactorial, including direct effects of HIV on the endothelium, indirect effects of HIV on lipids and inflammatory cytokines and ART-related effects [146]. After the reported association between the use of ART and the risk of MI in the DAD study [147], several studies have reported an association between abacavir use and risk of MI. However, in a case-control study (matched for age, sex, and clinical center) nested within the French Hospital Database on HIV found that the risk of MI was increased by cumulative

exposure to all the studied PIs except saquinavir, whereas the association with abacavir cannot be considered causal [144].

Reduced bone mineral density (osteoporosis and osteopenia) is another complication of both HIV and current antiretroviral drugs. In a meta-analysis of 20 studies, the prevalence of osteoporosis was more than three times greater compared to HIV-uninfected controls. In addition, ART-exposed and PI-exposed patients had a higher prevalence of osteoporosis [148]. The change in bone mineral density (BMD) was compared in a randomized trial that assigned the patients into three treatment arms: an NNRTI and a PI/r, a PI/r and NRTIs or an NNRTI and NRTIs using DEXA scan. After 1 year, the decrease in lumbar spine BMD was more in patients receiving PI/r-containing regimen compared with NNRTI and NRTIs suggesting that BMD should be monitored during lifelong ART [149]. Another study evaluated osteopenia in HIV-1-infected men receiving HAART for a median of 7.5 years, showed that tenofovir exposure was independently associated with a larger decline in BMD at lumbar and hip spine [150].

Beside the evaluation of BMD, some studies evaluated the risk of fractures. In Danish population-based cohort study evaluating the development of low and high energy fractures in HIV-infected patients, an increased risk of fracture compared with population controls was found. Among HIV-monoinfected patients, the increased risk was observed for low-energy but not for high-energy fractures, and the increased risk of low-energy fracture was only observed in HAART-exposed patients [151]. Further study found that the cumulative exposure to TDF and lopinavir/ritonavir was independently predictive of increased risk of osteoporotic fracture in the HAART era [152].

Despite the evidence showing a clear association between HAART and side effects there is still no clear understanding of the cellular mechanisms leading to these alterations. Minimizing toxicity and undesirable effects are of outmost importance now that HAART is recommended for lifelong use by HIV infected individuals. Therefore additional studies are needed to unveil the cellular targets and the mechanisms leading to these alterations.

2.4 Limitations of HAART

The expanded use of HAART has changed the course of HIV infection. Nowadays, about 90% of patients on ART have plasma HIV-RNA levels below the levels of detection for long periods of time. Despite this success, failure of HIV eradication due to established reservoirs, residual viremia and persistent immune activation and inflammation remain a challenge in HIV research [153-155].

In the mid-nineties, the persistence of small detectable pool of latently infected, CD4 T-cells carrying replication-competent virus was documented in several independent studies among patients who received clinically effective HAART [156-158]. In addition, several studies demonstrated rapid viral rebound after discontinuation of therapy in patients in whom sustained suppression of plasma viremia had been achieved for prolonged periods [159-161]. These latently infected, CD4 T-cells serve as HIV reservoir and present an impediment to viral eradication.

The establishment of HIV reservoir is initiated early in the course of infection at time of virus penetration. This conclusion is based on the observation that the initiation of HAART in infected patients as early as 10 days after the onset of symptoms of primary HIV-1 infection did not prevent generation of latently infected, resting CD4 T cells carrying integrated HIV-1 DNA as well as infectious HIV-1 despite the successful control of plasma viremia shortly after institution of HAART [162]. In addition, ART initiation as early as 3 days post-infection, did not prevent viral rebound in monkeys after discontinuation of ART following 24 weeks of fully suppressive therapy [163]. Considerable progress has been achieved regarding our knowledge in the pathogenesis of HIV reservoirs and the mechanisms of viral latency even though a lot remains to be understood. Two hypotheses are suggested to explain the persistence of HIV reservoir despite the effective HAART use for long time. First, the memory phenotype with the long half-life of the latently infected resting CD4 T cells which allows these cells to harbor the virus without expressing viral antigens on their surface thus enables them to escape host immune responses. Second, ongoing low-level of HIV replication with de novo viral infection, due to partial suppression and/or to inadequate drug penetration [154,164].

The most widely discussed approach to eradicate HIV reservoirs is reactivating HIV genomes in resting CD4 T cells. To date, histone deacetylase (HDAC) inhibitors have been tested as potential latency-reversing agents. Of these, valproic acid has been tested in different studies with no measurable effect [165-167]. Other HDAC inhibitors (vorinostat, romidepsin, panobinostat, givinostat and belinostat) have been tested and showed promising results in the reactivation of virus in latently infected cells [168]. Disulfiram, which has been used in the treatment of alcoholism, is being evaluated [169-171]. The use of cytokines has been envisioned as an additional therapeutic strategy. Interleukin-2 use was not successful [172]. Interleukin-7 is being tested with more success than IL-2 in reactivating latently HIV-1 infected cells [173,174]. These reactivation strategies are being tested on patients treated with HAART. Different ARTs have been associated with off-target effects resulting in the adverse effects described above. Therefore it is of interest to study the direct effect of ARTs on reservoir reactivation and elimination of infected cells.

The use of sensitive single-copy assays for HIV-1 RNA allowed the detection of residual amounts of free virus in the plasma of patients on HAART [175]. However the source of this residual viremia is still unclear. Several lines of evidence support the hypothesis that the source of such viremia is the release of HIV-1 from cells infected before the initiation of HAART rather than ongoing replication. First, clinical experience has shown that adherent patients who maintain plasma VLs less than 50 copies/ml do not develop resistance to therapy. Secondly, intensification studies that added potent antiretroviral drug to suppressive HAART did not find any further decrease in the amount of residual viremia. Third, phylogenetic studies of residual plasma viremia show no sequence evolution in patients on effective HAART [176-178], although it is still not clear if viral sequence evolution can be detected in tissues.

In contrast, some experts believe that the decrease in CD8+ T-cell activation and the transient increase of episomal HIV-1 DNA observed after the intensification of HAART with raltegravir, provide evidence that active HIV-1 replication continues despite HAART [179,180]. Therefore one therapeutic vaccination strategy is to activate HIV specific CD8+ T cells to eliminate cells with

active HIV-1 replication. However it is still unclear if those HIV infected cell with low replication efficiently present HIV-derived MHC-I bond peptides required for CTL recognition killing.

Despite the benefits of HAART on CD4 count and immune reconstitution, individuals on HAART continue to have elevated activated CD4 and CD8 T-cells compared to healthy HIV-negative individuals. Moreover, CD8 T cell from individuals on HAART have a lower proliferative and cytotoxic capacity compared to LTNPs [81,181]. In addition individuals on HAART are shown to have an imbalanced cytokine and chemokine environment [182-184]. The specific mechanisms underlying the persistence of chronic immune activation are still unclear. HIV reservoirs and residual viremia have been shown to correlate with persistent immune activation [180,185,186]. Several studies have also indicated that microbial translocation is a driver of chronic immune activation among HIV-infected patients [187]. HIV also induces immune activation through indirect pathway. During HIV-1 infection, the depletion of CD4 T cells may result in suboptimal immune control of other persistent viruses such as cytomegalovirus (CMV) and EBV[188,189].

Observations of residual immune activation and inflammation have led to interest in early initiation of HAART. A study of long-term HAART initiated during early HIV-1 infection suggested that there is potential for better immune system preservation and a functional cure [190]. A functional cure is defined as the ability to control infection without the need for medication. For example, while not successful in the long-term, very early HAART initiation in an infant showed the potential for a functional cure (absence of virus for extended period of time after treatment interruption), however this effect turned out to be only transient and ultimately viral rebound was observed [191]. Therefore, the timing of HAART initiation could aid in preserving the immune system, and may also help avoid damage that may persist in individuals who initiate HAART later.

The following figure (figure 14) summarizes the potential reasons leading to persistent immune activation and inflammation in patients on HAART. It has been shown that ARV treatment is associated with many off-target effects including direct effects on the immune system independent from HIV infection. However it is still unclear if ARV treatment per se contributes

to the persistent immune activation and inflammation. The next chapter will discuss the known off-target effects of ARVs and their consequences.

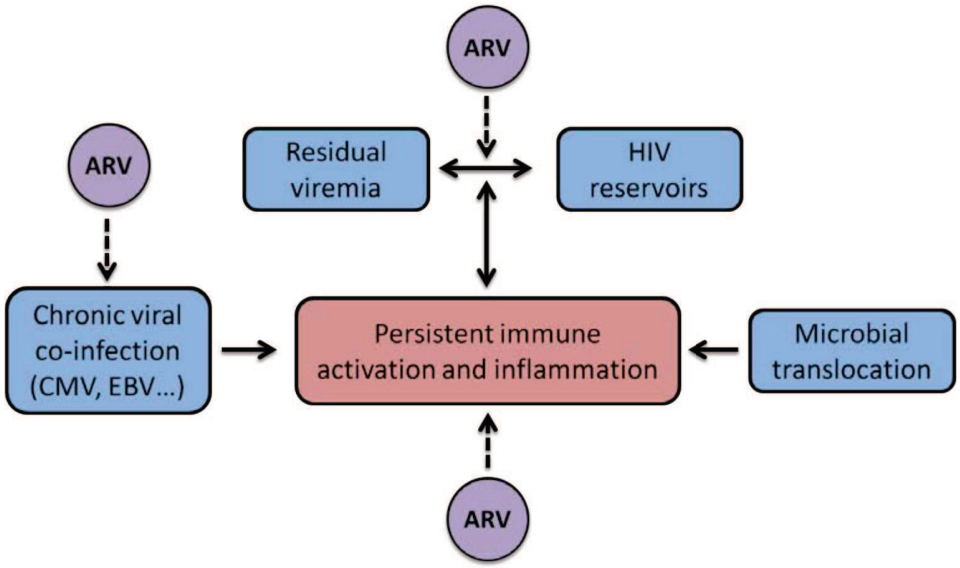

Figure 14: Potential reasons contributing to the persistent immune activation and inflammation in patients on HAART.

2.5 Off-target effects of HAART

Unfortunately in some cases suppression of viral replication fail due to viral resistance to ART. Despite the development of resistant viral mutants, a substantial proportion of treated patients show a steady increase in CD4 cell counts and do not develop HIV associated disorders [192,193] (figure 15). These observations suggested that HAART might be affecting the immune system independently of viral suppression.

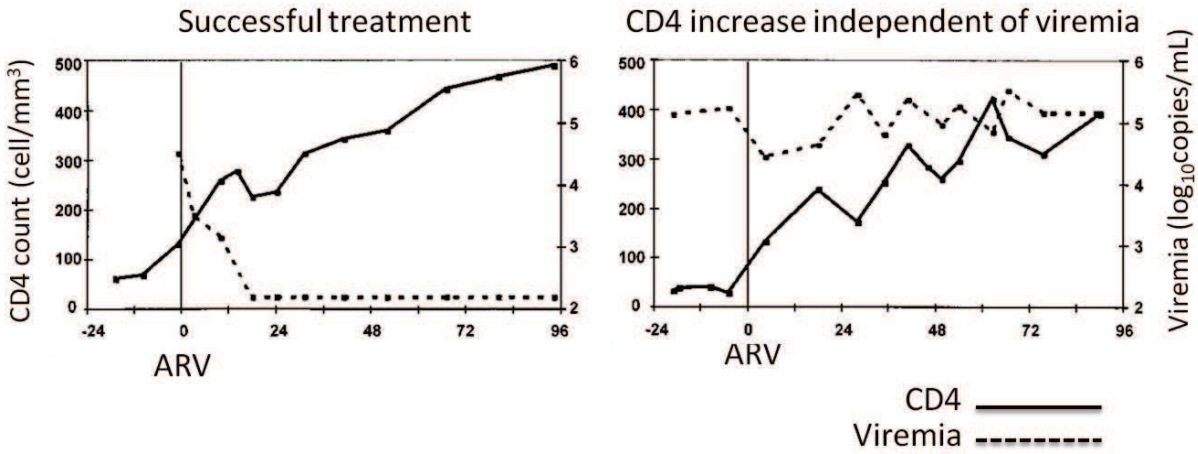

Figure 15: HAART increasing CD4 count independently of viral suppression (figure from [192]).

Several studies in HIV-positive and HIV-negative patients showed increased thymic T cell output caused directly by HAART treatment that include HIV protease inhibitors [194-197]. Importantly, thymic production of naive T cells with new antigen specificities might replenish the HIV-depleted T cell repertoire and explain the beneficial effect of HAART in patients with unaffected VL. Additionally, evidence highlighted the direct immunomodulatory effects of antiretroviral drugs [198,199]. For example significant reduction of cytokine production by peripheral blood mononuclear cells (PBMCs) from HIV-uninfected subjects was observed after HAART prophylaxis following exposure to contaminated blood [197,200]. This decrease in cytokine production might be reducing the continuous stimulation and cell exhaustion caused during the chronic phase of the infection explaining the non-HIV related clinical benefits of HAART. Moreover, HIV PIs improved the survival of CD4 and CD8 T cells and restored impaired T-cell proliferative response in vivo and in vitro [199]. Although these studies provide evidences for the beneficial immunosuppressive activity of certain PIs, the molecular events underlying these phenomena, as well as the cellular targets of PIs still remain not completely defined.

In addition to the effect of HAART on T cells, recent studies showed that some HIV-PI alter DC function [201-203]. DCs play key role in orchestrating the innate and adaptive immune responses. Among other things they are involved in activating naive T-cells and NK cells regulating the links between innate and adaptive immune responses. The presence of PIs altered monocyte

differentiation toward DC lineage and led to the generation of immature DCs (iDCs) showing an altered phenotype, including low levels of surface proteins (CD1a, CD86, CD36 and CD209) essential for DC function. iDCs generated in presence of PIs failed to mature and produce the appropriate cytokines in respond to bacterial endotoxin. These PI-induced alterations weakened the ability of DCs to prime autologous NK cells and made them highly susceptible to NK cell killing. NK cell capacity to kill iDCs and mature DCs (mDC) that fail to undergo a proper maturation (also known as NK mediated DC editing) has been proposed to play a major role shaping the quality and strength of the adaptive immune response [204]. Therefore, the ability of certain PIs to sustain the generation of mDC displaying higher susceptibility to autologous NK cytotoxicity might be beneficial during HIV chronic infection by limiting excessive inflammation. Additionally, it has been shown that CD209 on DCs also known as DC-SIGN is able to bind HIV-1 and carry the virus to lymphoid tissues contributing to the rapid transmission of HIV-1 to lymphoid T-cells. HIV PIs by reducing CD209 expression and by editing of DCs by autologous NK cells would also limit the spreading of virus from migrating DC to naive T-cells trafficking in lymphoid tissues. In addition, DCs are also involved in T-cell priming and activation. However, it is still unclear if the PI-induced alteration of DC phenotype and function affect their capacity to efficiently prime T-cells. It is important to mention that PI concentration used to test the effect on DC maturation and function was very high (comparable to human peak plasma drug level) [201], it is therefore important to confirm these results using concentrations closer to the physiological levels.

Early in the HAART era, investigators reported regression of HIV-related Kaposi's sarcoma in individuals on HAART [205,206]. Kaposi's sarcoma is an angioproliferative disease characterized by angiogenesis, endothelial spindle-cell growth (Kaposi's sarcoma cells), inflammatory-cell infiltration, and oedema, which becomes progressively infected by human herpesvirus 8 [207]. At first thought to be a consequence of effective anti-HIV treatment and immune reconstitution, the effects of HAART including HIV PIs on Kaposi's sarcoma control did not always correlate with HIV load or CD4 cell counts. Progression of Kaposi's sarcoma while on HAART was not necessarily associated with virological failure in a fifth of the patients in one study [206]. These were the earliest clinical indications that HIV PIs had a non-immune-mediated antitumor

activity. Later, additional studies showed that some HIV PIs have pleiotropic antitumor effects, including inhibition of inflammatory cytokine production, proteasome activity, cell proliferation and survival, and induction of apoptosis [208-213]. Subsequently, HIV PIs use alone or in combination to chemotherapy or radiotherapy showed beneficial results in human clinical trials against different cancer types [214-216]. Different cellular targets of HIV PIs have been proposed but the exact anti-tumor mechanism is still unclear. One of the cellular targets of some HIV PIs is the proteasome. Evidence showing that the proteasome can cleave the gag-pol natural substrate of HIV protease raised questions about a possible interaction between HIV PI and proteasome [217]. Indeed, it has been confirmed that ritonavir, saquinavir and nelfinavir inhibit proteasome activities in cells [218-220]. Proteasomes are involved in many cellular mechanisms and their inhibition is proved to be beneficial in some cancer types. For instance Bortezomib is a FDA approved proteasome inhibitor for treating multiple myeloma. Therefore, the inhibitory effect of HIV PIs on the proteasome might explain in part their anti-cancer effect. Proteasome also play a crucial role in the antigen processing machinery. It is responsible for the generation of most antigenic peptides, as its inhibition blocks most antigen presentation on MHC-I molecules [221]. However it is still unclear how the PI-induced proteasome activity inhibition affects the antigen processing machinery and alters the immunopeptidome presented by MHC-I for CD8 T cell recognition which will be the focus of the first part of the results (study 1).

3. Antigen processing and epitope presentation

As previously discussed, the ability of a T cell to function relies on its intrinsic capacity to recognize target cells that are infected by a pathogen or have internalized pathogen-derived proteins. To facilitate this recognition, cells express MHC molecules that bind peptide fragments derived from those proteins. These peptide-MHC complexes are then displayed on the cell surface. In order for this to occur antigen processing is required to degrade proteins within cells and generate these peptide fragments.

In the classical model of antigen processing, MHC class I molecules bind peptides derived from endogenously expressed proteins whereas MHC class II molecules bind peptides derived from

extracellular proteins that have been phagocytosed by the cell. However this model has proved to be an oversimplification of reality. It has been shown that MHC-I bound peptides on APCs could derive from phagocytosed extracellular proteins processed in the pathway called “cross-presentation”. In the following sections only the MHC-I peptide processing and presentation pathways will be discussed.

3.1 Direct antigen processing machinery

3.1.1 Antigen processing in the cytosol

Intracellular proteins and peptides are constantly degraded as part of the normal process of turnover and recycling of proteins and organelles within cell. Degradation is a tightly regulated process and different proteins have different half-lives that can range from minutes to weeks. Within the cytosol, degradation is mostly carried out by the 26S proteasome [222]. The proteasome is responsible for the generation of most antigenic peptides, as its inhibition blocks most antigen presentation on MHC-I molecules [221]. The 26S proteasome is a multicatalytic enzyme responsible for the degradation of polyubiquitinated as well as other proteins. It consists of a 20S core, representing the catalytic core, and two 19S regulator complexes that confer the binding and unfolding of ubiquitylated substrates [223]. The two inner rings are composed of seven β subunits, three of which (β1, β2 and β5) contain active sites and are responsible for this enzyme’s hydrolyzing activity [224]. Although they share a common mechanism, these subunits have distinct substrate specificities; β1, β2 and β5 cleave after acidic, basic and hydrophobic residues, respectively (termed the caspase-like, tryptic and chymotryptic activities) [225 226 227] (figure 16).

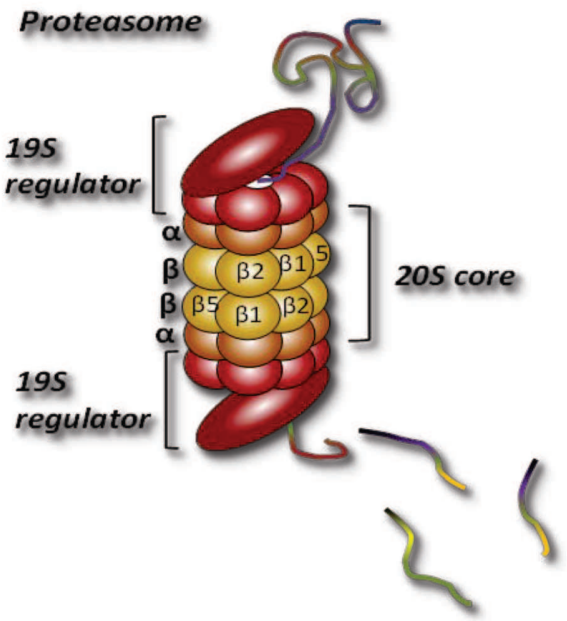

Figure 16: Schematic representation of the proteasome. The proteasome is composed of a 20S core attached to two 19S caps to form the 26S proteasome. The 20S core is composed of four stacked heptameric ring structures. The two inner β rings contain the three subunits responsible for the specific hydrolyzing activities of this enzyme. The two outer rings are composed of α subunits that bind 19S regulatory caps.

Besides constitutive proteasomes expressed in all cell types, immunoproteasomes are present in lymphoid tissues and can be induced in other cell types upon infection or cytokine exposure [228]. IFN-γ induces the expression of catalytic immunosubunits and PA28 lids leading to the assembly of 20S and 26S immunoproteasomes [229]. Immunoproteasomes tend to produce longer peptides ending with C-terminal hydrophobic residues, the most frequent C-terminal anchor for most MHC-I isotypes, and may favor the production of epitopes [230]. The presence of both proteasomes and immunoproteasomes in the same cell is associated with a greater variety of peptides available for presentation [231]. Moreover, another type of proteasome called thymoproteasome is expressed by thymic cortical epithelial cells and are involved in the generation and the presentation of thymoproteasome-specific peptide-MHC-I complexes essential for the positive selection of major and diverse repertoire of MHC-I-restricted T cells.

In addition to the proteasomes, other proteases in the cytoplasm have been shown to play a role in the generation or destruction of antigenic peptides as well, although the sequence of

degradation events leading to optimal epitope production is poorly defined. Leucine aminopeptidase (LAP) activity in the cytoplasm can be enhanced by IFN-y and has been shown to have the ability to trim the N-terminus of antigenic peptides [232]. Two other proteases, bleomycin hydrolase (BH) and puromycin-sensitive aminopeptidase (PSA), were shown to trim the N-terminus of antigenic peptides, although they both have the ability to destroy epitopes as well [233]. Thimet oligopeptidase (TOP) was once thought to play a role in generating antigenic peptides [234,235]. Later work revealed that TOP primarily plays a destructive role and limits the supply of peptides for MHC-I presentation [236]. The multicatalytic protease tripeptidyl peptidase II (TPPII) also has conflicting evidence of being involved in the generation and/or destruction of antigenic peptides [237,238].

While antigenic peptides and N-terminally-extended precursors are generated in the cytoplasm, a majority of peptides are actually destroyed before ever entering the ER for final processing and MHC-I loading. Studies from the Neefjes and other groups have demonstrated that only 0.1% of antigenic proteins may ever yield an antigenic peptide [239,240]. It is this massive destruction of peptides in the cytoplasm that makes the antigen processing pathway inherently inefficient, and makes the eventual binding of a final antigenic peptides to MHC-I a rare event.

Among all of this destruction in the cytoplasm, protective components also exist. It has been shown that specific motifs within and outside epitopes determine the sensitivity of peptide to degradation by cytosolic peptidases, the kinetics of epitope production, and contribute to the amount of peptides available for presentation to CTL [241-243]. The combination of specific sequences within proteins and intracellular peptidase hydrolytic activities shapes the kinetics of production and amount of peptides available for loading onto MHC-I. In addition, cytoplasmic chaperones play a key role in protecting antigenic fragments from destruction before they enter the endoplasmic reticulum (ER). The multisubunit chaperonin TriC was found to play a key role in the protection of antigenic fragments from AAF-CMK-sensitive proteases, which include several cytoplasmic proteases and TPP II [244]. The chaperone hsp90 and cochaperone CHIP were found to protect large antigenic fragments from destruction, possibly before they are delivered to the proteasome [245].

3.1.2 Antigen processing in the ER

Cytosolic peptides of mostly 8–16 aa long with adequate anchor residues for the transporter associated to antigen processing (TAP) [246] are translocated into the ER where they can be loaded onto the MHC-I and exported to the cell surface. Prior to MHC-I presentation peptides may still need final trimming. It has been shown that aminopeptidase activity in the ER is crucial for the generation of antigenic peptides [247], and that MHC-I molecules are somehow involved in the trimming process [248]. The major ER aminopeptidase responsible for generating these final N-terminal cuts was later identified as ERAP1 and ERAP2 (ER aminopeptidase associated with antigen processing) [247,249-252]. ERAP was shown to trim antigenic peptides to the appropriate length for MHC-I binding and presentation, and to synergize with MHC-I molecules in this process [253]. In fact, ERAP knockout in mice altered the degradation of proteins, changed the repertoire of peptides presented on MHC-I molecules and modified CTL responses [254]. After peptides are trimmed by ERAP and loaded onto MHC-I molecules with the peptide loading complex composed of tapasin, calnexin, calreticulin and ERp57, they are exported to the cell surface and presented to CD8+ T cells (figure 17).

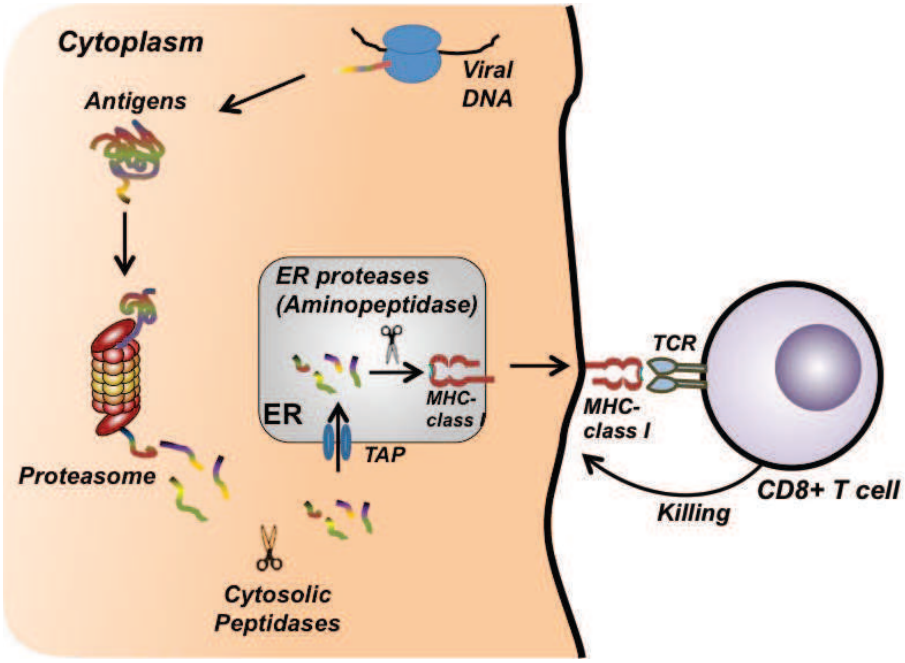

Figure 17: Endogenous antigen processing and epitope presentation pathway.

3.1.3 Endogenous sources of antigens

There are a variety of endogenous sources of antigen to be found in any given cell, and these sources may vary depending on the cell type. Properly translated and folded proteins that are degraded as part of natural protein turnover by the proteasome represent one source of antigenic material. However the use of stable proteins as an antigenic source has a major caveat: it cannot be an accurate representation of the protein milieu inside the cell at any given time. If a cell is virally infected, for example, it would be highly inefficient to wait until viral proteins had lived out their full lives before being processed and presented as antigens. Studies have shown that inhibition of protein translation rapidly effects antigen presentation (Reits et al., 2000; Schubert et al., 2000; Yewdell et al., 2001), indicating that the pool of proteins utilized as a source of endogenous antigens are newly synthesized proteins.

Since this observation several years ago, efforts have been made to further understand the mechanism by which the cell preferentially uses newly synthesized proteins as a source of antigen. Described as “DRiPs" (defective ribosomal products) by Yewdell (Yewdell et al., 1996), this pool of proteins is thought to be degraded immediately after translation due to defects in translation or misfolding that occur naturally in the cell. These mistakes occur as a normal part of cellular metabolism, and are thought to be the source of newly synthesized proteins used for antigenic material. When a cell is virally infected, mechanisms may be employed to increase the use of DRiPs for antigen presentation. In fact one study using an LCMV model showed that although an epitope-containing viral protein was long-lived, only neosynthesized viral protein was actually used as a source of antigenic peptides (Khan et al., 2001).

With the goal of providing a real-time representation of the proteins inside of a cell, other less-than-perfect sources of protein may also be preferentially used as antigenic sources. The products of cryptic translation are one of these sources. Cryptic translation products are proteins translated outside of the normal open reading frame, and/or initiated with non-AUG start codons. As shown by members of the Shastri lab, cryptic translation products are an important source of antigenic material (Malarkannan et al., 1999; Schwab et al., 2003; Schwab et al., 2000). Susan Schwab also went on to show that cryptic translation products initiated

using a CUG start codon were actually encoded as a leucine on their first residue, rather than solely as a methionine residue through a wobble mechanism as previously thought (Schwab et al., 2004). It has also been shown that cryptic HIV-1 epitopes derived from alternate reading frames of the HIV-1 genome are recognized and targeted by the host immune system [255,256]. These cryptically-translated protein products may contribute significantly to a DRiP-like pool of proteins, and therefore serve as early warning flags in the form of peptides presented to CD8+ T cells. Because part of the antiviral response involves shutting down regular host translation, cryptically translated viral proteins may be some of the first detectable antigenic sources.

3.1.4 Factors affecting antigen processing efficiency

Many factors including intracellular epitope stability, kinetics of epitope production and motifs within epitopes or in the sequences flanking the epitopes have been shown to affect the efficiency of antigen processing and epitope presentation [243 241 257 258].

Surface MHC-I epitope presentation is dependent on the amount of epitope available in the cell at a given time for loading onto the MHC-I. The amount of epitope availability depends on the production kinetics and the intracellular stability of the epitope. It has been shown that motifs surrounding optimal epitopes favorable for degradation leads to the production of peptides that include epitopes [243]. For instances, endogenous processing and presentation of human immunodominant HIV-1 epitope is more efficient than that of a subdominant epitope. This is explained by the increased cleavage of the flanking regions of the immunodominant epitopes that constitute portable motifs, which are absent in the regions surrounding subdominant epitopes. The presence of these cleavable motifs increases the production of fragments containing immunodominant epitopes. Moreover, naturally occurring mutations in those flanking motifs have been shown to impair the processing and presentation of HIV epitopes and to lead to CTL escape [243]. In addition to kinetics of epitope production, the intracellular stability of the epitopes affects the amount available for MHC-I loading. Epitope stability is defined as the intracellular half-life of the epitope, which is dependent on the sensitivity of the epitope to cytosolic degradation. Higher sensitivity to cytosolic degradation reduces the amount of peptides displayed at the cell surface and hinders recognition by CTLs. Intracellular stability is

associated with specific motifs located throughout the peptide sequences. Multiple HLA-associated mutations occurring within HIV epitopes including B57-TW10 (TSTLQEQIGW, aa 108-117 in Gag p24) G9D mutation introduces cleavage sites and increases the sensitivity of the epitope for degradation [241,259]. This dramatically decreases the intracellular stability of peptides and reduces surface MHC-I epitope presentation thus constituting a mechanism of immune escape [241]. Furthermore, kinetics of epitope production and stability are dependent on the proteases and peptidases involved in the generation and further degradation of those epitopes. Any alterations in the activities of the peptidases might increase or decrease the amount of epitope available for MHC-I loading. Therefore understanding of the factors that affect peptidase activities might allow us to uncover new ways used by the virus to alter epitope presentation and escape or enable us to increase the presentation of some epitopes by modifying the activities of the peptidases.

3.2 Cross-presentation

As previously discussed, CD8+ T cells recognize pathogen infected cells through peptide complexed to MHC-I molecules. However, CTLs cannot gain cytotoxic function without first being primed by DCs. This priming occurs through peptide-MHC-I recognition in addition to the co-stimulatory molecules presented by DCs. The peptides presented by MHC-I on DCs or Mϕs can be generated by two distinct pathways. The first is the classical endogenous antigen-processing pathway described above where presented MHC-I bound peptides are derived from proteins expressed in the cell. The second pathway called cross-presentation occurs when the presented MHC-I bound peptides derive from phagocytosed or endocytosed exogenous antigens.

3.2.1 Intracellular trafficking

Cross-presentation requires antigen transit through endosomes or phagosomes and eventually partial proteolysis by cathepsins [260]. Peptides generated after the initial proteolysis can further undergo mainly two different pathways (“cytosolic” and “vacuolar”). Cross-presentation through the cytosolic pathway is sensitive to proteasome inhibitors, which suggests that generated peptides access the cytosol, where they are degraded by the proteasome [261].

Proteasome-generated peptides can then feed into the classical endogenous MHC-I antigen presentation pathway, which involves the transport of peptides into the ER by TAP for loading on newly formed MHC-I molecules [261]. Alternatively, it has been shown that ER-resident proteins including TAP and the MHC-I loading machinery can be recruited to phagosomes and perhaps even to endosomes [262]; thus, peptides generated by the proteasome might be translocated back into the lumen of endocytic compartments for loading on MHC-I molecules, which could then recycle back to the plasma membrane.

By contrast, cross-presentation through the vacuolar pathway is resistant to proteasome inhibitors and generally independent of TAP [263], but is sensitive to inhibitors of lysosomal proteolysis (in particular, cathepsin S inhibitors [264]). The MHC-I molecules in this pathway likely access endocytic compartments by recycling from the plasma membrane, and would bind peptides independently of proteasomal degradation, TAP transporters or the MHC-I loading complex [265,266] (figure 18).

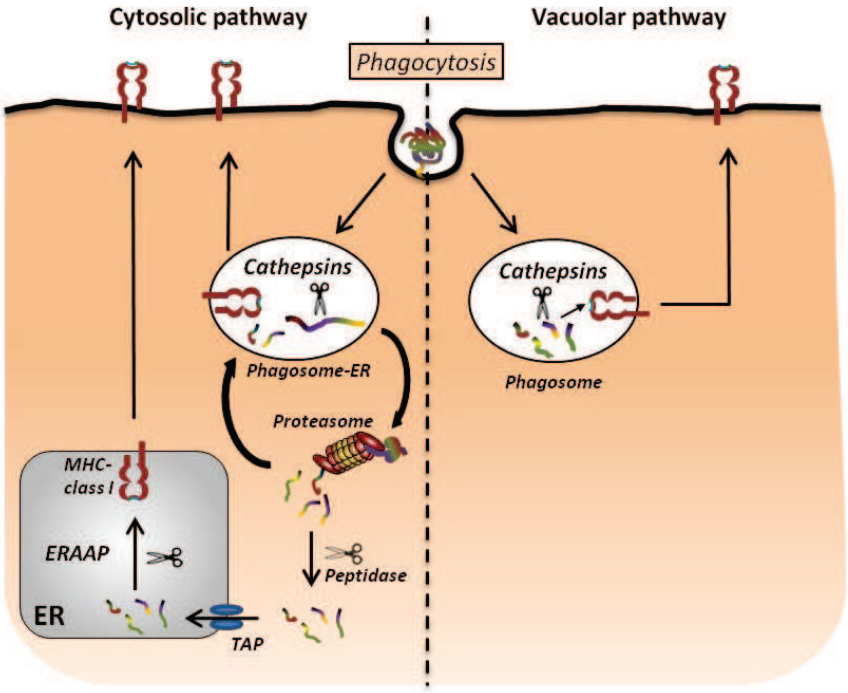

Figure 18: Cytosolic and vacuolar pathways of cross-presentation.

The experimental evidence supporting the cross-presentation of a particular antigen through the vacuolar or cytosolic pathways comes from interfering with either endocytic (lysosomal proteases), cytosolic (proteasomal proteolysis) or ER-related (TAP or loading complex) functions. All three intracellular compartments being involved in the cross-presentation pathway makes it extremely challenging to uncover the exact contribution on each compartment. Proteasome inhibition or TAP knockout reduced the export of new synthesized MHC-I to the plasma membrane thus inhibiting the amount of MHC-I recycled to the endosomal compartments. On the other hand inhibiting endocytic function to prevent the generation of MHC-I binding peptides in endosomes and phagosomes also interferes with the initial partial degradation steps that are required for the export of some antigens to the cytosol. Therefore, most of the arguments in favor or against the use of the vacuolar or cytosolic pathways for presentation of particular antigens are to be taken with caution.

3.2.2 Role of cathepsins, pH and NOX2

In addition to their role in generating MHC-II epitopes, cathepsins play a key role in shaping the repertoire of antigenic MHC-I peptides generated in the cross-presentation pathway. Phagocytosed antigens are initially degraded by cathepsins present in the phagolysosomal compartments. There are two groups of cathepsins: Cysteine cathepsins such as cathepsin S, B, H and L; and aspartate cathepsins such as cathepsins D and E. They differ mainly by their substrate specificity and their activity levels at different pH [267,268].

It has been shown that degradation patterns in the different cross-presentation compartments contribute to HIV immunodominance [269]. More immunodominant epitopes compared to subdominant were produced when HIV proteins were degraded by cathepsins in cross-presentation compartments, which led to higher CTL responses specific for immunodominant epitopes after cross-presentation. Immunodominant epitopes also had higher intracellular stability in cross-presentation compartments. In addition, common HLA-associated mutations in a dominant epitope appearing during acute HIV infection modified the degradation patterns of long HIV peptides, reduced intracellular stability and epitope production in cross-presentation-

competent cell compartments, showing that impaired epitope production in the cross-presentation pathway contributes to immune escape [269].

One of the hallmarks of the endocytic pathway of DCs is its decreased cathepsin activity compared with that of other phagocytes, such as Mϕs and neutrophils [268]. Using models of antigen endocytosis, several groups have shown that limited antigen degradation correlates with efficient cross-presentation [268,270]. Moreover, antigens that are artificially delivered to highly degradative, late endocytic compartments by dedicated liposomes are presented on MHC-II molecules more efficiently than on MHC- I molecules [271]. By contrast, antigens are cross-presented more efficiently when the liposomes are targeted to less degradative, early endocytic compartments.

The decreased proteolysis that occurs in the endocytic compartments of DCs compared with other phagocytes is mainly due to the low levels of lysosomal proteases in DC endosomes and phagosomes, and to decreased activity of the proteases that are present. The decreased activity of these proteases is caused by a high pH maintained in the phagosomes (approximately pH 6.5-7), which is itself a result of both low levels of V-ATPase activity (due to its incomplete assembly) and high levels of NADPH oxidase 2 (NOX2) activity in phagosomal and endosomal compartments [268,272]. NOX2 uses protons from the phagosome to generate reactive oxygen species (ROS) thus limiting the acidification and maintaining low cathepsin activity in DC phagosomes [272,273]. It has been shown that NOX2 knock-down DCs and DCs from patients with chronic granulomatous disease (which is caused by a genetic defect in NOX2) have increased phagosomal acidification and impaired antigen cross-presentation [272,273]. This NOX2-mediated regulation of cathepsin activities allows the low levels of protein degradation in phagosomes to preserve potential MHC-I-binding epitopes. However, some degree of degradation favors cross-presentation, probably because smaller peptides are exported to the cytosol with a higher efficiency than large ones [274] (figure 19). Therefore understanding the factors that control the phagocytic environment favorable for cross-presentation will be crucial for the design of vaccines that will be optimally processed and presented by APCs to induce a strong and broad CTL response.

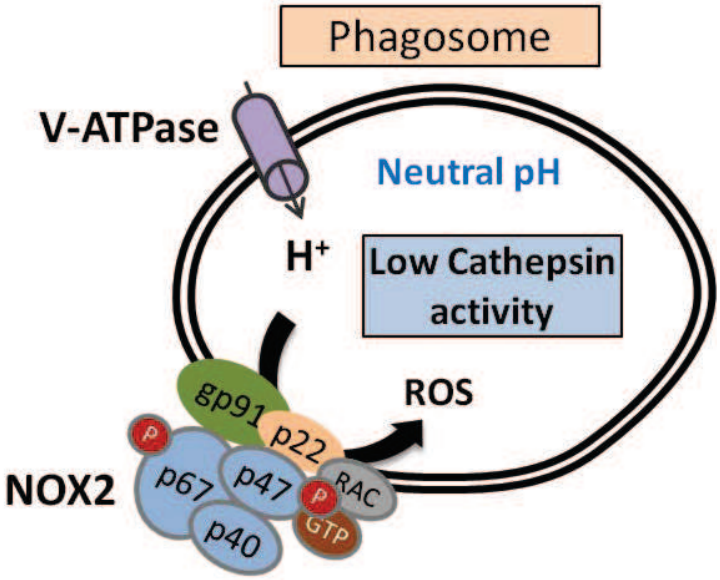

Figure 19: NOX2-mediated control of DC phagosomal pH. NOX2 uses H+ to produce ROS thus limiting phagosome acidification. Neutral pH keeps cathepsin activity low which is favorable for antigen cross-presentation.

Hypothesis and aims

The ability of CTL to clear virus-infected cells depends on the processing of viral antigens by cellular proteases and peptidases and peptide display by MHC-I. In addition to the presentation of epitopes derived from endogenous proteins, APCs have the ability to process exogenous antigens by phagosomal cathepsins and cross-present the epitopes by MHC-I.

It has been shown that perturbations of cellular proteases involved in antigen processing modify protein degradation patterns, epitope amount and intracellular stability, and consequently epitope presentation by MHC-I. For instance, the inhibition of the proteasome by N-acetyl-leucyl-leucyl-norleucinal or ERAAP1 knockout in mice altered the degradation of proteins, changed the repertoire of peptides presented on MHC-I molecules and modified CTL responses [221,254,275]. Inhibitors of cathepsins affected antigen processing in the endolysosomal compartment and altered epitope cross-presentation [264,267,268]. In addition, alterations in DC phagosome's controlled environment including NOX2 inhibition or increased acidification led to impairment in DC ability to cross-present antigenic peptides [272].

Despite the evidence showing that HIV PIs inhibit the proteasome activity, no study has assessed in human primary cells the effect of PIs on aminopeptidase and cathepsins equally important in antigen processing, the link between PI-induced alterations of cellular peptidases, HIV protein degradation patterns, and HIV epitope presentation to CTLs. Therefore, we hypothesized that HIV PIs by altering the activities of cellular proteases and peptidases involved in antigen processing, modify antigen degradation pattern thus enhancing or impairing the presentation of various MHC-I epitopes.

The first aim was to study in human primary cells the effect of HIV PIs on the proteasome and aminopeptidase activities, understand the impact of these PI-induced activity changes on HIV protein degradation pattern and epitope production kinetics, and analyze the consequence of these alterations on HIV epitope presentation to CTLs.

The second aim was to assess the effect of HIV PIs on cathepsin activities, phagosomal pH and NOX2 activity as well as on the overall impact on epitope cross-presentation by DCs and Mϕs.

The context of the PhD:

After a successful master thesis in Sylvie Le Gall's lab working on the antigen degradation pathway, I started my PhD in the form of "co-tutelle" under the co-supervision of Pr. Etienne Weiss and Pr. Sylvie Le Gall. One of the objectives was to develop intrabodies (Single-chain Fv fragment) [276-280] with Pr. Weiss' expertise in this field to target and block specific peptidases in particular cellular compartments with the goal of shaping antigen degradation patterns and ultimately changing epitope presentation. The entire PhD project was done in Pr. Sylvie Le Gall's lab at the Ragon Institute of MGH, MIT and Harvard in the United States of America.

Results

Study n°1

Sequence-Specific Alterations of Epitope Production by HIV Protease Inhibitors

HIV protease inhibitors (PIs) are one of the antiretroviral classes used by HIV infected people to control HIV replication. In addition to their inhibitory effect on HIV protease, PIs have been associated with other off target effects including proteasome inhibition. Proteasomes are involved in antigen degradation and presentation of epitopes on MHC-I. This process is critical for the recognition of pathogen-infected cells by CD8+ T lymphocytes. In this study we investigated the effect of PIs on aminopeptidase activities equally important for antigen processing and the impact of PI-induced peptidase activity alteration on antigen degradation pattern, epitope production and presentation, and recognition by cytotoxic T lymphocytes.

Paper published

Sequence-Specific Alterations of Epitope Production by HIV Protease Inhibitors

Georgio Kourjian, Yang Xu, Ijah Mondesire-Crump, Mariko Shimada, Pauline Gourdain and Sylvie Le Gall

J Immunol published online 10 March 2014
http://www.jimmunol.org/content/early/2014/03/07/jimmunol.1302805

The Journal of Immunology is published twice each month by The American Association of Immunologists, Inc., 9650 Rockville Pike, Bethesda, MD 20814-3994.

Print ISSN: 0022-1767 Online ISSN: 1550-6606.

Published March 10, 2014, doi:10.4049/jimmunol.1302805

Sequence-Specific Alterations of Epitope Production by HIV Protease Inhibitors

Georgio Kourjian, Yang Xu, Ijah Mondesire-Crump, Mariko Shimada, Pauline Gourdain, and Sylvie Le Gall

Ag processing by intracellular proteases and peptidases and epitope presentation are critical for recognition of pathogen-infected cells by CD8$^+$ T lymphocytes. First-generation HIV protease inhibitors (PIs) alter proteasome activity, but the effect of first- or second-generation PIs on other cellular peptidases, the underlying mechanism, and impact on Ag processing and epitope presentation to CTL are still unknown. In this article, we demonstrate that several HIV PIs altered not only proteasome but also aminopeptidase activities in PBMCs. Using an in vitro degradation assay involving PBMC cytosolic extracts, we showed that PIs altered the degradation patterns of oligopeptides and peptide production in a sequence-specific manner, enhancing the cleavage of certain residues and reducing others. PIs affected the sensitivity of peptides to intracellular degradation, and altered the kinetics and amount of HIV epitopes produced intracellularly. Accordingly, the endogenous degradation of incoming virions in the presence of PIs led to variations in CTL-mediated killing of HIV-infected cells. By altering host protease activities and the degradation patterns of proteins in a sequence-specific manner, HIV PIs may diversify peptides available for MHC class I presentation to CTL, alter the patterns of CTL responses, and provide a complementary approach to current therapies for the CTL-mediated clearance of abnormal cells in infection, cancer, or other immune disease. ***The Journal of Immunology*****, 2014, 192: 000–000.**

Highly active antiretroviral therapy (HAART), which is a combination of nucleoside reverse transcriptase inhibitors (NRTIs), non-NRTIs (nNRT1s), protease inhibitors (PIs), and integrase inhibitors given to HIV-infected patients, efficiently suppresses HIV replication, leading to partial immune restoration and turning AIDS into a chronic disease (1).

HIV PIs block the HIV aspartyl protease, preventing the cleavage of HIV Gag and Pol polyproteins that include essential structural and enzymatic components of the virus. This blockage prevents the conversion of HIV particles into their mature infectious form (2). Currently, nine different HIV PIs are available on the market and used in HAART (3). Long-term treatment of responder patients with PI-containing HAART has been linked with several unpredicted adverse effects, such as hyperbilirubinemia, hyperlipidemia, or hypolipidemia (4), body fat redistribution (5), insulin resistance (6), osteopenia, and osteoporosis (7, 8); these adverse effects occur more so with first-generation PIs such as saquinavir or ritonavir than with newer PIs such as darunavir (9). The design of the first-generation HIV PIs is based on the transition-state mimetic of the Phe-Pro bond, the major substrate of HIV-I protease (10). Evidence showing the ability of the 20S proteasome to cleave similar bonds (11) raised questions about possible interactions between HIV PIs and the proteasome catalytic sites.

Proteasomes play a key role in the degradation of full-length proteins and defective ribosomal products into peptides (12) that can be further shortened or degraded by cytosolic aminopeptidases and endopeptidases such as thimet oligopeptidase (13, 14) or tripeptidyl peptidase II (15). Some of these peptides are translocated by the TAP complex into the endoplasmic reticulum (ER), where they can be further trimmed by ER-resident aminopeptidases (ERAP1 or ERAP2) (16, 17) and, provided they contain appropriate anchor residues, loaded onto MHC class I (MHC-I) and displayed at the cell surface.

Epitopes can be solely produced by the proteasome or a combination of proteasomes and aminopeptidases and/or endopeptidases, although the sequence of degradation events leading to epitope production is poorly defined. Peptides produced during protein degradation can be subjected to hydrolysis by various peptidases, thus limiting the amount of peptides available for MHC-I presentation (18–20). The specificity of each peptidase is determined by length and motifs in the substrate. Proteasomes have the broadest cleavage capacity and often define the C terminus of extended epitopes because of frequent cleavages after hydrophobic residues (21).

Aminopeptidases cleave N-terminal extensions of peptides shorter than 16 aa and have well-defined hierarchy of cleavable residues and noncleavable residues (22–24) that influence the kinetics of production of adjacent epitopes (24). We showed that specific motifs within and outside epitopes determine the sensitivity of peptide to degradation by cytosolic peptidases, the kinetics of epitope production, and contribute to the amount of peptides available for presentation to CTL (18, 24, 25). In addition, differences in peptidase activities among cell types also influence the kinetics and amount of epitope produced (26). The combination of specific sequences

Ragon Institute of MGH, MIT and Harvard, Massachusetts General Hospital, Harvard Medical School, Cambridge, MA 02139

Received for publication October 18, 2013. Accepted for publication February 8, 2014.

This work was supported by National Institute of Allergy and Infectious Diseases/National Institutes of Health Grants AI084753 and AI084106 (to S.L.G.).

Address correspondence and reprint requests to Dr. Sylvie Le Gall, Ragon Institute of MGH, MIT and Harvard, Massachusetts General Hospital, Harvard Medical School, 400 Technology Square, Cambridge, MA 02139. E-mail address: sylvie_legall@hms.harvard.edu

The online version of this article contains supplemental material.

Abbreviations used in this article: ART, antiretroviral therapy; ER, endoplasmic reticulum; ERAP, ER-resident aminopeptidase; HAART, highly active ART; Kaletra, lopinavir/ritonavir; LC-MS/MS, liquid chromatography tandem mass spectrometry; LCMV, lymphocytic choriomeningitis virus; MHC-I, MHC class I; nNRTI, non-nucleoside reverse transcriptase inhibitor; NRTI, nucleoside reverse transcriptase inhibitor; PI, protease inhibitor; RP-HPLC, reverse-phase HPLC; VSVg, vesicular stomatitis virus G glycoprotein; WT, wild type.

within proteins and intracellular peptidase hydrolytic activities shapes the kinetics of production and amount of peptides available for loading onto MHC-I. Therefore, natural or artificial variations in cellular peptidase activities may change the balance between production and further cleavage of peptides, enhancing or impairing the presentation of various MHC-I epitopes. For instance, the inhibition of the proteasome by *N*-acetyl-leucyl-leucyl-norleucinal or ERAP-1 knockout in mice altered the degradation of proteins and changed the repertoire of peptides presented on MHC-I molecules and CTL responses (27–29). The three HIV PIs ritonavir, saquinavir, and nelfinavir inhibit the activity of purified mouse or human 20S proteasomes and the proteasome activity in immortalized cells (30–32), causing intracellular accumulation of polyubiquitinated proteins (33, 34). In mice infected with lymphocytic choriomeningitis virus (LCMV) and treated with ritonavir, the cytotoxic immune response against two T cell epitopes of LCMV was reduced and prevented the expansion of LCMV reactive CTL (30). One possible explanation for these changes in CTL responses might be PI-induced alteration of proteasome activity leading to modification of epitope production. No study has assessed in human primary cells the effect of PIs on postproteasomal peptidases equally important in Ag processing, the link between PI-induced alterations of cellular peptidases, HIV protein degradation patterns, and HIV epitope presentation to CTL (when HIV replication is not fully inhibited by HAART) (35, 36), or the effect of PIs on the processing of other pathogens that HAART-treated patients may encounter during coinfection.

In this article, we investigate the effect of seven HIV PIs (saquinavir, ritonavir, nelfinavir, indinavir, atazanavir, darunavir, and lopinavir/ritonavir [Kaletra]) on proteasome and aminopeptidase activities of PBMCs. Our results showed that HIV PIs variably altered not only proteasomal but also aminopeptidase activities. Furthermore, using an in vitro epitope processing assay (25), we showed that HIV PIs changed HIV peptide degradation patterns, the cytosolic stability, and amount of epitopes produced. In addition, by measuring the lysis of PI-treated and HIV-infected cells by epitope-specific CTL, we found that HIV PIs variably altered the presentation of HIV epitopes and the recognition by CTL. Finally, we identified motifs whose cleavage is enhanced or reduced by HIV PIs, leading to increased or decreased production of neighboring epitopes.

Altogether, these results show that by variably altering cellular protease activities, HIV PIs modify HIV protein degradation patterns, epitope production, and presentation, leading to variations in CTL responses.

Materials and Methods

Preparation of antiretroviral drug stocks

The antiretroviral tablets used in this study were obtained from two sources: 1) National Institutes of Health AIDS Research and Reference Reagent Program (National Institute of Allergy and Infectious Diseases), or 2) the Massachusetts General Hospital Inpatient pharmacy. The following reagents were donated by the National Institutes of Health AIDS Reagent Program: indinavir, lamivudine, and nelfinavir. From the Massachusetts General Hospital inpatient pharmacy we obtained ritonavir, saquinavir, atazanavir sulfate, delavirdine, darunavir, and Kaletra. The purified form of the antiretroviral drugs was obtained from Selleckchem (ritonavir, lopinavir, and darunavir), Sigma (saquinavir), and Santa Cruz (nelfinavir). All drugs were dissolved in 100% DMSO. Kaletra was prepared by combining lopinavir and ritonavir with 5:1 ratio, respectively; subsequently, Kaletra concentrations mentioned in this article correspond to lopinavir amount. Stock solutions of 50 mM were kept at −20°C, and fresh aliquots were used for each experiment.

PBMC isolation from donors

The use of buffy coats from anonymous blood donors was approved under Protocol No. 2005P001218 by the Partners Human Research Committee (Boston, MA). PBMCs were isolated from buffy coats (Massachusetts General Hospital, Boston, MA) by Ficoll-Hypaque (Sigma-Aldrich, St. Louis, MO) density gradient centrifugation. The needed amount of PBMCs for live cell proteolytic activity measurement was taken for immediate use, and the remaining PBMCs were used for cytosol extraction (25).

Measuring proteolytic activities in live cells or purified enzymes

Chymotryptic, tryptic, and caspase-like activities of proteasomes present in live PBMCs or purified PBMC proteasome obtained using the protocol described by Kisselev and Goldberg (37) were measured with specific fluorogenic substrates (50 μmol/L Suc-LLVY-Amc, 50 μmol/L BocLRR-Amc, and 75 μmol/L ZLLE-Amc, respectively; Bachem) (26, 29). Different amino acid cleavage activities required 5 μmol/L X-Amc substrate, where X represents any amino acid (26). Pan-caspase activity was measured using 50 μmol/L Ac-DEVD-AMC fluorogenic substrate. PBMCs, purified PBMC proteasomes, or purified aminopeptidase ERAP1 (obtained from R&D Systems) were pretreated with increasing drug concentrations for 30 min at 37°C before adding the fluorogenic substrates. The specificity of the reaction was assessed by preincubating cells with inhibitors of proteasomes (MG-132; 10 μmol/L), aminopeptidases (Bestatin; 120 μmol/L), or pan-caspase (Z-VAD-FMK; 20 μmol/L). Digitonin was added to the cells at final amount of 0.0025% to facilitate the entry of the drugs and the substrates into the cells. The fluorescence was measured at 37°C every 5 min for 5 h using a VICTOR X Multilabel Plate Reader (Perkin Elmer, Boston, MA).

Drug toxicity measurement assay

PBMCs at 500,000 cells/ml were incubated overnight with different PIs in 48-well plates. Cells were stained with annexin and 7-aminoactinomycin D (Annexin V APC Apoptosis Detection Kit I; BD Pharmingen), and the percentage of apoptotic and necrotic cells were determined by flow cytometry.

HIV epitope processing assay

A total of 2 nmol purified peptide (>95% pure; Massachusetts General Hospital peptide core facility) was degraded in 20 μg PBMC cytosol pretreated with different PIs for 30 min. The degradation reaction was stopped at various time points with 1% formic acid, and degradation products were analyzed by liquid chromatography tandem mass spectrometry (LC-MS/MS). Peptides present in the digestion mix were purified by TCA precipitation at each time point. Equal amounts of peptide degradation samples at different time points were injected into a Nano-HPLC (NanoLC Ultra; Eksigent) and online nanosprayed into an Orbitrap mass spectrometry (LTQ Orbitrap Discovery; Thermo) at a flow rate of 400 nl/min. A Nano cHiPLC trap column (200 μm × 0.5 mm ChromXP c18-CL 5 μm 120 Å; Eksigent) was used to remove salts and contaminants in the sample buffers. Peptides were separated in a Nano cHiPLC column (75 μm × 15 cm ChromXP c18-CL 5 μm 300 Å; Eksigent) over a gradient of 2–40% buffer B (buffer A: water w/0.1% formic acid; buffer B: acetonitrile w/0.1% formic acid) in 20 min. Mass spectra were recorded in the range of 370–2000 Daltons. In the tandem mass spectrometry mode, the eight most intense peaks were selected with a window of 1 Dalton and fragmented. The collision gas is helium and collision voltage is 35 V. Peaks in the mass spectra were searched against the source peptides databases with Proteome Discoverer (version 1.3; Thermo) and quantitatively analyzed. The integrated area of a peak generated by a given peptide is proportional to the relative abundance of the peptide present. Each degradation time point was run on the mass spectrometer at least twice.

Cytosolic peptide stability assay

A total of 2 nmol purified peptide (Massachusetts General Hospital peptide core facility; >95% pure) was degraded at 37°C in 20 μg PBMC cytosol pretreated with different PIs for 30 min. The reaction was stopped with 1% formic acid at various time points. The degradation of the peptide was analyzed by reverse-phase HPLC (RP-HPLC; Waters) as described previously (18). The peptide corresponds to one peak whose amount is proportional to the surface under peak. One hundred percent corresponds to the surface under peak for each peptide at time 0. Peptides incubated at 37°C in buffer without extracts are similarly analyzed.

CTL induced killing assay

HLA-matched B cells were incubated with PI for 30 min before being infected with vesicular stomatitis virus G glycoprotein (VSVg)–pseudotyped Gag-Pol-GFP–expressing or NL4.3 HIV-GFP–expressing in-house–made virus. Thirty-six hours postinfection, half of the cells was stained with HLA-A/B/C allophycocyanin (BD Biosciences) and analyzed by flow

cytometry for the infection percentage and the HLA-A/B/C surface expression level. The other half of the cells was incubated with epitope-specific CTL clones at E:T ratio of 4:1. All conditions were done in triplicates. Noninfected cells were pulsed 30 min with decreasing concentration of CTL-matched or nonmatched epitopes and subjected to CTL killing to test the CTL specificity. To measure cell death, we used Vybrant fluorescence-based cytotoxic assay kit (Invitrogen). Percentage specific lysis was determined by using the following formula: ([experimental release − spontaneous release]/[maximum release − spontaneous release]) × 100%. Maximum release was determined by lysis of all target cells with detergent (5% Triton X-100), and spontaneous release was determined by incubating nontarget cells (not infected) with CTL (38).

Statistical analysis

Data were analyzed using GraphPad Prism 5 software.

Results

HIV PIs alter cellular proteasome and aminopeptidase activities

We first aimed to assess the effect of seven HIV PIs (saquinavir, ritonavir, nelfinavir, indinavir, atazanavir, darunavir, and Kaletra), one NRTI (lamivudine), and one nNRTI (delavirdine) on the main proteolytic activities—chymotryptic, tryptic, and caspase-like activities of proteasomes (i.e., cleaving after hydrophobic, basic, and acidic amino acids, respectively)—and aminopeptidase in freshly isolated PBMCs from at least six different HIV$^-$ donors.

The concentrations of the PIs used in this study correspond to the level of PIs found in the plasma of ART-treated persons (39–43). Using annexin and 7-aminoactinomycin D staining as markers for apoptosis and necrosis, we detected no toxicity on PBMCs treated at therapeutic concentrations of PIs ranging from 5 to 20 μM (Supplemental Fig. 1A). Furthermore, pan-caspase activity measurement showed no caspase induction after PI treatment (Supplemental Fig. 1B). Each protease activity was measured with a fluorogenic substrate composed of a peptide specific for each proteolytic activity and a fluorogenic coumarin-derivative moiety (24, 37) (Fig. 1A). For each protease activity, fluorescence was measured over time, and the hydrolysis kinetics was calculated as the maximum slope of fluorescence emission after subtraction of fluorescence in the absence of cells. For each substrate, 100% represents the maximum slope of fluorescence emission by cells incubated with substrate and DMSO control.

The specificity of substrate cleavage was checked by preincubation of cells with cognate inhibitors of proteasome (MG132) or aminopeptidase (Bestatin). In the presence of the specific inhibitor (Bestatin), aminopeptidase activity was reduced by 20-fold compared with the control (maximum slope of 145.35 for control and 7.25 for Bestatin). Increasing concentrations of ritonavir (2.5–20 μM) reduced aminopeptidase activities by 1.11- to 1.73-fold, respectively (Fig. 1B).

The effects of each PI at increasing concentrations on all three proteasome and aminopeptidase activities were assessed (Fig. 1C). Chymotryptic activity of proteasome (Fig. 1C, *upper left panel*) was decreased upon saquinavir, ritonavir, nelfinavir, or Kaletra treatment by 1.23- to 2-fold. In contrast, indinavir increased the chymotryptic activity by 1.15-fold, and atazanavir or darunavir did not change it. Saquinavir and atazanavir increased the proteasomal caspase-like activity (Fig. 1C, *upper right panel*) by 1.15- to 1.9-fold, whereas ritonavir decreased it by 1.54-fold; unlike the latter, the activity was not affected by nelfinavir, indinavir, darunavir, or Kaletra. Saquinavir and nelfinavir increased the proteasomal tryptic activity (Fig. 1C, *lower left panel*) by 1.38- to 1.7-fold. Ritonavir increased the activity at low concentration (2.5 μM) by 1.39-fold and decreased tryptic activity at higher concentrations by 5.5-fold. Kaletra also decreased the proteasomal tryptic activity by 1.24-fold. Proteasome tryptic activity was not affected by indinavir, atazanavir, or darunavir.

Saquinavir, ritonavir, nelfinavir, and Kaletra decreased aminopeptidase activities (Fig. 1C, *lower right panel*) by 1.21- to 1.83-fold, but no change was seen upon indinavir, atazanavir, or darunavir treatment. Delavirdine (nNRTI) and lamivudine (NRTI) did not have any significant effect on the proteasomal and aminopeptidase activities (G. Kourjian, unpublished observations).

The effect of the PIs on chymotryptic, caspase-like, tryptic, and aminopeptidase activities was similar when using live PBMCs, purified PBMC proteasome, and aminopeptidase ERAP1 (Fig. 1D) or PBMC cytosolic extracts (G. Kourjian, unpublished observations). This shows that the alterations induced by PIs are specific and validate the use of PI-treated cellular extracts as one approach to assess the impact of PIs on the processing of epitopes.

These results show that saquinavir, ritonavir, nelfinavir, and Kaletra altered proteasomal activities in human primary cells in agreement with previous studies testing first-generation PIs on purified proteasomes or immortalized cell lines (31, 33). In addition, we showed that these four PIs inhibited aminopeptidase activities known to play an important role in defining the composition of MHC-I peptide repertoire (17). Indinavir, atazanavir, and darunavir, the newer PIs, as well as reverse transcriptase inhibitors lamivudine and delavirdine, did not significantly affect peptidase activities tested in PBMCs.

Peptide degradation patterns are altered by HIV PIs

To assess the effect of HIV PI on peptide degradation patterns and epitope production, we used PBMC cytosolic extracts to degrade 3ISW9 (HQAISPRTLNAW) fragment, which is a precursor of an HLA-B57–restricted ISW9 epitope (ISPRTLNAW, aa 15–23 in Gag p24) that elicits frequent CTL responses in HLA-B57 HIV-infected individuals (18). Fig. 2A shows degradation products of substrate 3ISW9 identified by LC-MS/MS after a 60-min degradation in PBMC extracts in the absence of PIs. They included peptides encompassing epitope ISW9, termed precursors, optimal epitope ISW9, and peptides containing only part of the optimal peptide that will not bind to HLA-B57, termed antitopes.

To assess and compare the production of all peptides over time in each condition, we calculated the contribution of each peptide to the degradation products detected at a given time point. We first checked that the amount of peptide injected on the mass spectrometer directly correlated with the surface of the peptide's corresponding peak (Supplemental Fig. 2A, 2B). Three peptides were mixed at various ratios while keeping the total femtomole constant. The total intensity of all peaks was constant (<10% variation among mixes), and for each peptide the peak surface was proportional to the amount of the peptides (Supplemental Fig. 2C), thus validating the measurement of the relative contribution of each peptide to the total intensity of degradation peptides in the presence of various drugs. In PBMC extracts treated with 10 μM ritonavir or Kaletra, 3ISW9 degradation started slower compared with DMSO control or saquinavir-treated extracts (71–75 versus 43–55% 3ISW9 remaining at 10 min). However, the production of ISW9 was increased by 4.6- or 3.36-fold at 60 min upon ritonavir or Kaletra treatment, respectively (14 and 10% of total peptides upon ritonavir and Kaletra, respectively, compared with 3% in control; Fig. 2B–D), suggesting that peptide trimming was shifted toward epitope production. Saquinavir treatment of 10 μM produced 3.3-fold less ISW9 and 1.8-fold more antitopes compared with the control, suggesting that in the presence of saquinavir, precursors are being cut into peptides destroying epitopes (Fig. 2C). These changes in the ratios of categories of peptides were confirmed by comparing individual fragment intensities in the presence of various PIs. For instance, upon saquinavir treatment, the antitope QAISPRTL was produced up to 4-7-fold more than in control or Kaletra treatment, whereas

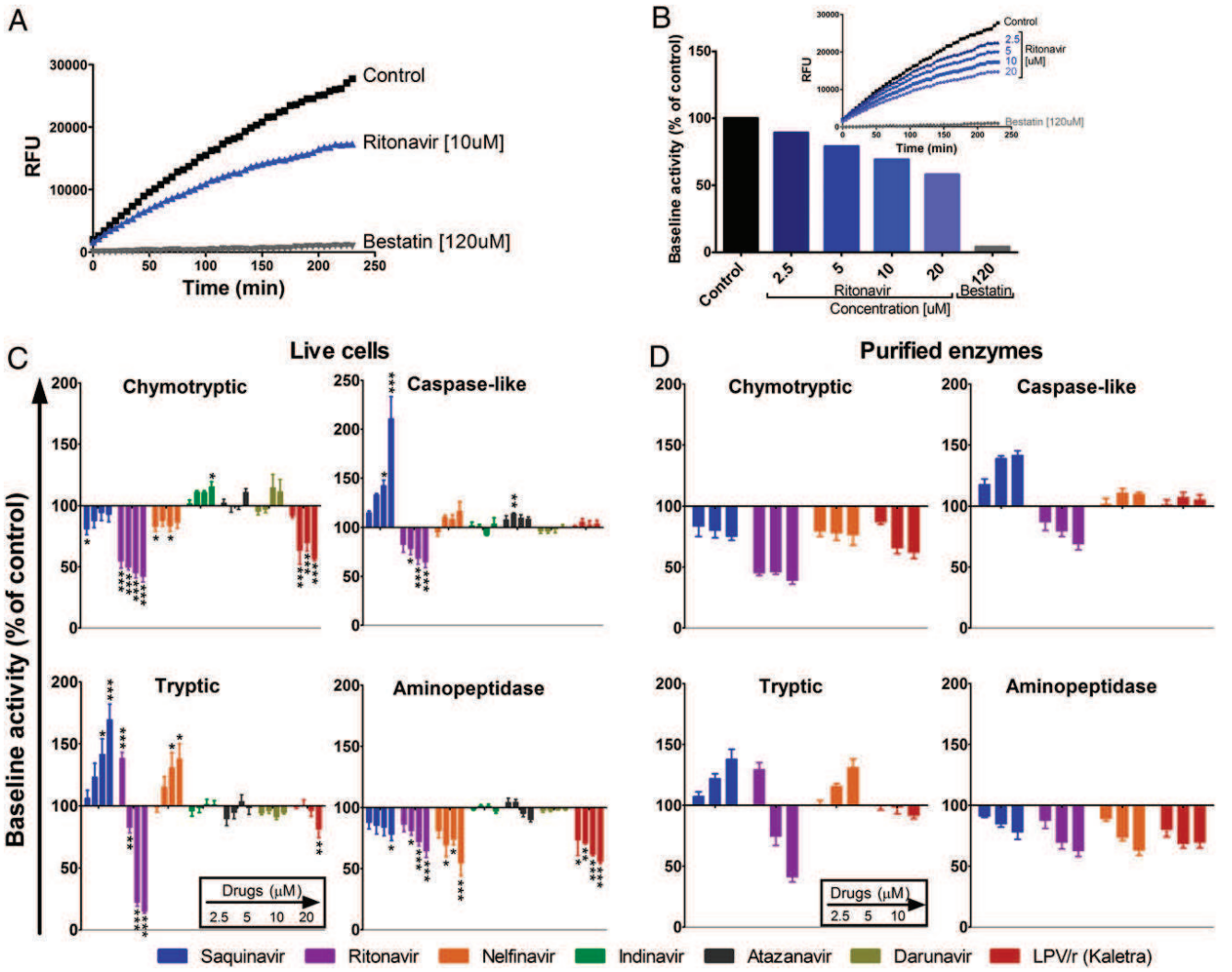

FIGURE 1. HIV PIs variably alter proteasome and aminopeptidase activities in human PBMCs. (**A**) Aminopeptidase substrate Leu-amc was added to PBMCs pretreated with DMSO (control, squares), 10 μM ritonavir (triangles), or 120 μM Bestatin (inverse triangles) and incubated for 4 h at 37°C, during which fluorescence emission was monitored every 5 min. (**B**) PBMCs were preincubated with increasing concentrations of ritonavir or 120 μM Bestatin before addition of Leu-amc. The maximum slope of fluorescence emission over 1 h was calculated for each condition. One hundred percent represents the maximum slope of fluorescence emission of the control (153.9). Maximum slope of fluorescence upon each treatment was compared with control. (**C**) PBMCs or (**D**) purified proteasomes or ERAP1 were pretreated with DMSO (control) or increasing concentrations of each PI (saquinavir, ritonavir, nelfinavir, indinavir, atazanavir, darunavir, and Kaletra [left to right bars on each graph]) before adding specific substrate for each activity (chymotryptic and caspase-like [*top panels*], tryptic and aminopeptidase [*lower panels*]). In each panel, 100% represents the maximum slope of DMSO-treated PBMCs (1161.8 for chymotryptic, 194 for caspase-like, 475 for tryptic, and 1063.6 for aminopeptidase) or purified proteasomes or ERAP1 (186.8 for chymotryptic, 27.1 for caspase-like, 91.8 for tryptic, and 507 for aminopeptidase). The maximum slope of treated PBMCs was compared with that of control. Average of six to eight healthy donors. $*p < 0.05$, $**p < 0.01$, $***p < 0.001$, one-way ANOVA with Dunnett's posttest.

2-ISW9 (QAISPRTLNAW) precursor was produced at least twice less (Fig. 2E, 2F), suggesting that in the presence of saquinavir, precursors are being cut to antitopes from the C-terminal side (or overtrimmed from the N-terminal side), whereas in the presence of ritonavir or Kaletra, they are preferentially trimmed to epitopes. Two other epitopes are present in substrate 3ISW9: HLA-A25–restricted QW11 (QAISPRTLNAW) and HLA-B15–restricted HL9 (HQAISPRTL). In contrast with their positive effect on B57-ISW9 production, ritonavir and Kaletra reduced the production of A25-QW11 and B15-HL9 epitopes, suggesting that the effect of HIV PIs on epitope production is variable and peptide dependent (Supplemental Fig. 3). We had previously shown that variations in epitope production (caused by mutations or variations in peptidase activities) measured by mass spectrometry correlated with changes in CTL-mediated killing of infected cells endogenously processing and presenting HIV epitopes (18, 24, 25). Altogether, these results indicate that HIV PIs differently altered peptide degradation patterns, resulting in increased or decreased epitope production and changing the ratio of cytosolic peptides available for loading onto MHC-I.

The intracellular stability of optimal HIV epitopes is altered upon HIV PI treatment

Peptides produced during protein degradation can be subjected to hydrolysis by multiple cytosolic proteases, thus altering the amount of peptides available for MHC-I presentation. The cytosolic stability of peptides is highly variable, defined by specific motifs, and contributes to defining the amount of peptides displayed to CTL (18, 19, 44). We hypothesized that PIs -by variably altering intracellular peptidase activities- might modify the cytosolic stability of peptides and consequently peptide availability for MHC-I loading.

To test the effect of HIV PI on the intracellular HIV epitope stability, we incubated highly purified peptides with cytosol from healthy human PBMCs pretreated with DMSO (control) or HIV PIs. The amount of peptide remaining over time was measured by

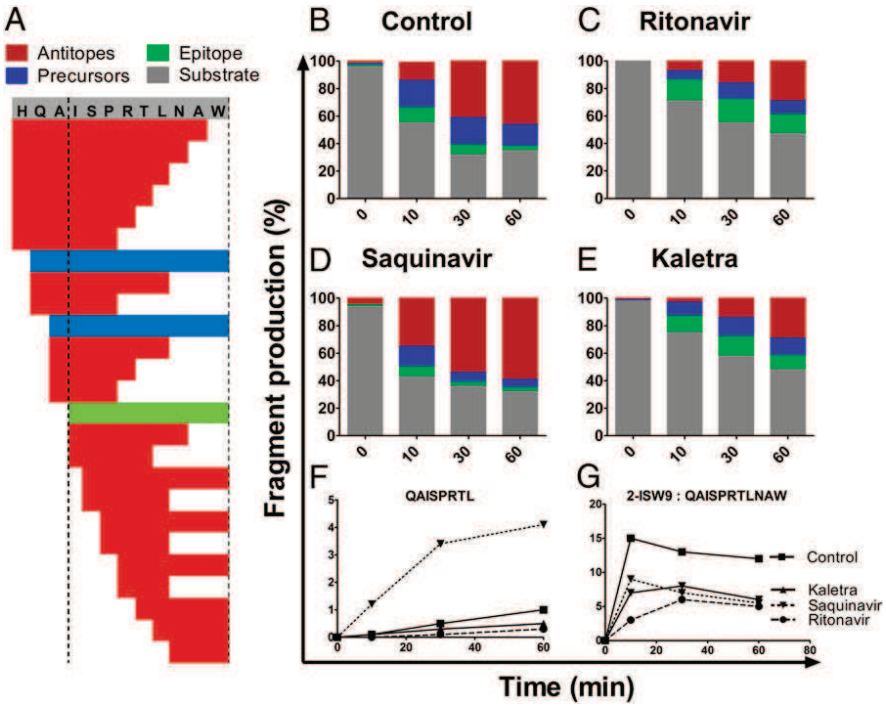

FIGURE 2. HIV PIs alter peptide degradation patterns. 3ISW9 (HQAISPRTLNAW) peptide containing HLA-B57–restricted ISW9 epitope (ISPRTLNAW) was degraded in PBMC cytosolic extracts preincubated with DMSO (**A** and **B**) or 10 μM ritonavir (**C**), saquinavir (**D**), or Kaletra (**E**). Resulting degradation products at 0, 10, 30, and 60 min were analyzed by LC-MS/MS. Degradation peptides were categorized as substrate 3-ISW9 (gray), epitope ISW9 (green), precursors—peptides that include the epitope (blue) or antitopes (peptides including only part of the epitope (red) (A–E). Each peptide identified by a specific mass and charge corresponds to a peak of a specific intensity, and the proportion of each category of peptides to the total peak intensity (ranging from 7.1E+8 to 8.4E+8 at a given time point) was calculated at each time point in the presence of DMSO (B), ritonavir (C), saquinavir (D), or Kaletra (E). Percentage of antitope QAISPRTL (**F**) and precursor 2-ISW9 (QAISPRTLNAW) (**G**) production over time upon PI treatment. Figure is representative of one of three independent experiments using PBMC extracts from three different donors and run in duplicates on the mass spectrometer.

RP-HPLC profile analysis, where each peak defined by its elution time represents one peptide, and the surface area under the peak is proportional to the amount of peptide (25). The degradation of the peptide results in reduction of its peak and the appearance of additional peaks corresponding to truncated peptides. A value of 100% was assigned to the amount of input peptide present at time 0, and the amount of peptides remaining was calculated at each time point. The time at which 50% of the peptide was degraded defines its half-life. Fig. 3A illustrate the degradation rates of HLA-A02–restricted SL9 (SLYNTVATL, aa 77–85 in Gag p17) in extracts preincubated with control DMSO, saquinavir, or nelfinavir. Pretreating PBMC cytosol with saquinavir decreased SL9 degradation rate, thus increasing its half-life to 52 min (compared with 37 min in control), whereas nelfinavir treatment increased SL9 degradation and reduced its half-life to 24 min (Fig. 3A). We measured the half-life of five optimally defined HIV epitopes that elicit frequent CTL responses in HIV-infected persons in the presence or absence of 2 or 5 μM HIV PIs: HLA-A02–restricted SL9, HLA-A11–restricted ATK9 (AIFQSSMTK, aa 158–166 in reverse transcriptase of HIV-1 polymerase), HLA-B57–restricted KF11 (KAFSPEVIPMF, aa 30–40 in Gag p24), HLA-B57–restricted ISW9, and HLA-B57–restricted TW10 (TSTLQEQIGW, aa 108–117 in Gag p24) (45). The half-lives of these epitopes in untreated cytosol, which were highly variable (119.4, 37.2, 33.9, 25.7, and 14.8 min for TW10, ATK9, SL9, KF11, and ISW9, respectively) as we previously showed (18), was compared with their half-lives upon different PI treatments. A02-SL9 epitope half-life was increased by 1.4- ($p < 0.001$) and 1.2-fold ($p < 0.05$) by saquinavir and ritonavir, respectively, whereas nelfinavir and atazanavir reduced it by 1.25- ($p < 0.05$) and 1.33-fold ($p < 0.01$), respectively (Fig. 3B). Darunavir did not change the half-life of SL9 and four other peptides. B57-KF11 half-life was increased by 1.44- ($p < 0.05$) and 1.52-fold ($p < 0.05$) by saquinavir and ritonavir, respectively (Fig. 3C). No other tested drug showed any effect on B57-KF11 half-life. B57-ISW9 half-life was increased by 1.48-fold ($p < 0.05$) by saquinavir (Fig. 3D). Other PIs tested did not significantly change B57-ISW9 half-life. A11-ATK9 and B57-TW10 half-life was not changed by any of the PIs tested (Fig. 3E, 3F). These results demonstrate that HIV PIs, by changing activities of cellular proteases, modified the cytosolic stability of several HIV epitopes, thus increasing or decreasing their availability for transfer into the ER, loading onto MHC-I, and display to CTL.

HIV PIs alter HIV epitope processing and presentation by HIV-infected cells to CTL

Having demonstrated that HIV PIs modified the degradation patterns of long peptides into epitopes and the intracellular stability of epitopes (two parameters that we previously identified to be critical to define the amount of MHC-bound peptides available for CTL recognition) (18, 24, 25), we next assessed whether HIV PIs could affect the endogenous processing and presentation of HIV epitopes and the subsequent CTL-mediated killing of HIV-infected cells. Because HIV PIs affect the late stages of replication, we performed single-round infections with nonreplicative virus to monitor epitope presentation. Upon PI treatment, single-round infection with either VSVg-pseudotyped lentivirus expressing HIV-1 Gag, Pol, and GPF or VSVg expressing HIV-1 NL4.3 without Env led to similar infection rates (67.3–68.5%) and did not affect the surface expression of HLA-A/B/C (mean fluorescence intensity ≈60; Supplemental Fig. 4). The PIs blocked the replication and release of HIV-1 NL4.3 in Jurkat cells, confirming the stability and the activity of the PIs (data not shown).

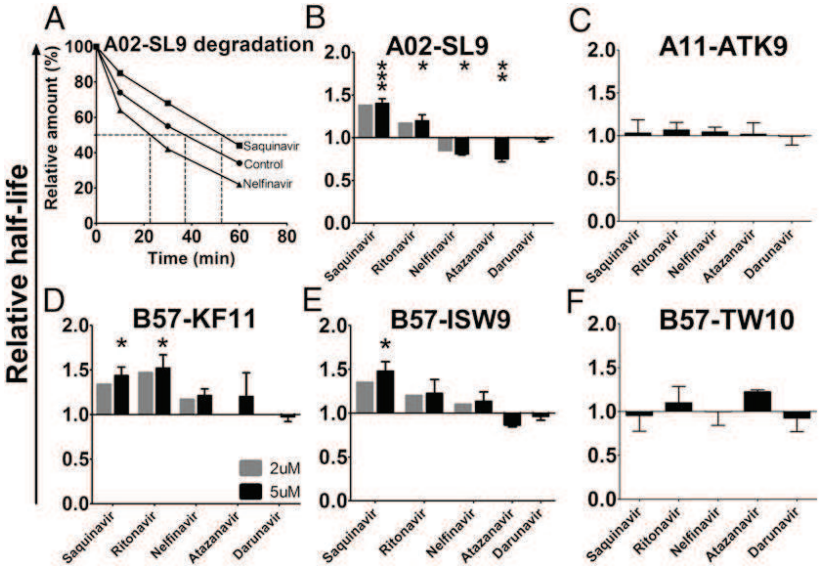

FIGURE 3. HIV PIs variably alter intracellular HIV epitope stability. (**A**) HLA-A02–restricted SL9 epitope (SLYNTVATL, aa 77–85 in HIV-1 Gag p17) was degraded in PBMC extracts pretreated with DMSO (control, circles), 5 μM nelfinavir (triangles), or 5 μM saquinavir (squares). Remaining peptide was quantified by RP-HPLC analysis after 0, 10, 30, and 60 min. One hundred percent represents the amount of peptide at time 0 calculated as the surface under the peptide peak detected by RP-HPLC (815.986, 821.569, and 813.118 for DMSO, saquinavir, and nelfinavir, respectively). Times at which 50% of the SL9 peptide remained correspond to peptide half-lives (37, 52, and 24 min for control, saquinavir, and nelfinavir, respectively). (**B**–**F**) HLA-A02–SL9 (B), HLA-B57-KF11 (C), HLA-B57-ISW9 (D), HLA-B57-TW10 (E), and HLA-A11-ATK9 (F) epitopes were degraded in PBMC extracts pretreated with DMSO, 2 μM PI, or 5 μM PI (saquinavir, ritonavir, nelfinavir, atazanavir, or darunavir). The cytosolic half-lives in control condition were 33.87, 25.66, 14.83, 119.4, and 37.21 min for SL9, KF11, ISW9, TW10, and ATK9, respectively. Fold differences of each epitope half-life upon treatment compared with control are presented in each panel. All data represent the average of four different experiments using four different PBMC extracts. *$p < 0.05$, **$p < 0.01$, ***$p < 0.001$, one-way ANOVA with Dunnett's posttest.

HLA-matched B cell lines were pretreated with DMSO or 5 μM PI before being infected with either VSVg-pseudotyped lentivirus expressing HIV-1 Gag, Pol, and GPF or VSVg expressing HIV-1 NL4.3 without Env and used as targets in a fluorescence-based killing assay with various epitope-specific CTL clones (38). Killing is monitored with an extracellular fluorogenic substrate that fluoresces after cleavage by an intracellular enzyme released by dying cells (46). Fluorescence is monitored every 5 min after addition of CTL to target cells, allowing for real-time measurement of CTL-mediated killing in conditions where the percentage lysis at 4 h is similar to those obtained in Cr-based killing assay (38). HIV PIs did not affect CTL-mediated lysis of uninfected cells pulsed with various amounts of cognate peptides, in accordance with the lack of effect of PIs on MHC-I expression (Supplemental Fig. 4) and absence of toxicity on CTL (G. Kourjian, unpublished observations). Fluorescence emission after synchronized addition of B57-KF11 or B57-ISW9 CTL to HIV-infected B57 expressing B cells was similar, indicative of similar kinetics of killing of infected targets by the two clones recognizing these two p24 epitopes (Fig. 4A). However, preincubation of target cells with ritonavir before infection had opposite effects on the kinetics of killing by the two CTL clones. The kinetics of killing by B57-KF11 CTL was slower and the maximum lysis reduced upon ritonavir treatment, whereas they were enhanced for B57-ISW9 CTL (Fig. 4A). We compared the specific lysis of HLA-B57 HIV-infected B cells 4 h after parallel addition of three B57-restricted, Gag-specific CTL clones in the presence of various PIs (Fig. 4B–D), and similarly the killing of A03/11 HIV-infected B cells by A03 Gag-specific or A11-restricted RT-specific CTL (Fig. 4E–F). Saquinavir, ritonavir, nelfinavir, and indinavir reduced the killing of HIV-infected cells by the B57-KF11 CTL by 1.31-fold ($p < 0.05$), 2.4-fold ($p < 0.001$), 2.44-fold ($p < 0.001$), and 1.9-fold ($p < 0.001$), respectively (Fig. 4B). The killing of HIV-infected cells by B57-ISW9 CTL was inhibited 2.44-fold ($p < 0.001$) and 1.2-fold ($p < 0.05$) by saquinavir and nelfinavir, respectively (Fig. 4C). In contrast, ritonavir increased it by 1.2-fold ($p < 0.05$) and nelfinavir had no effect. The lysis of HIV-infected cells by B57-TW10 CTL was decreased only by nelfinavir (1.46-fold, $p< 0.05$; Fig. 4D). None of the drugs tested altered the recognition and killing of HIV-infected cells by A03-RK9 CTL, an epitope that is efficiently produced and highly stable in the cytosol (18, 25) (Fig. 4E). The killing of HIV-infected cells by A11-ATK9 CTL, which was lower due to the lesser amount of RT present in incoming virions compared with Gag, was reduced by saquinavir, ritonavir, nelfinavir, and indinavir by 8-fold ($p < 0.01$), 4-fold ($p < 0.01$), 4.8-fold ($p < 0.01$), and 3-fold ($p < 0.01$), respectively (Fig. 4F). These results show that HIV PIs altered the endogenous processing and the presentation of HIV epitopes to CTL in various ways and underscore the link between drug-induced alterations of epitope production and subsequent changes in epitope-specific CTL responses. Ritonavir enhanced both in vitro production and intracellular stability of ISW9 (Figs. 2C, 3D), and led to enhanced killing of infected cells that endogenously processed ISW9, whereas the reduced in vitro production of ISW9 in the presence of saquinavir correlated with the reduced killing of HIV-infected cells by B57-ISW9 CTL. Therefore, PI-induced modulations of cellular peptidase activities leading to changes in peptide degradation patterns, epitope production, or intracellular peptide stability affected epitope presentation and recognition of HIV-infected cells by CTL.

HIV PIs variably modify the cleavage of amino acids, resulting in sequence-specific alterations of epitope production

Because HIV PIs variably affected the activities of cellular peptidases and the processing and presentation of epitopes in different ways, we hypothesized that alterations induced by PIs may be sequence specific. To individually test the impact of each PI on amino acid cleavage, we measured the hydrolysis of fluorogenic substrate X-amc (where X can be any amino acid) in PBMCs pretreated with 10 μM of various PIs. We compared the hydrolysis of 17 aa in

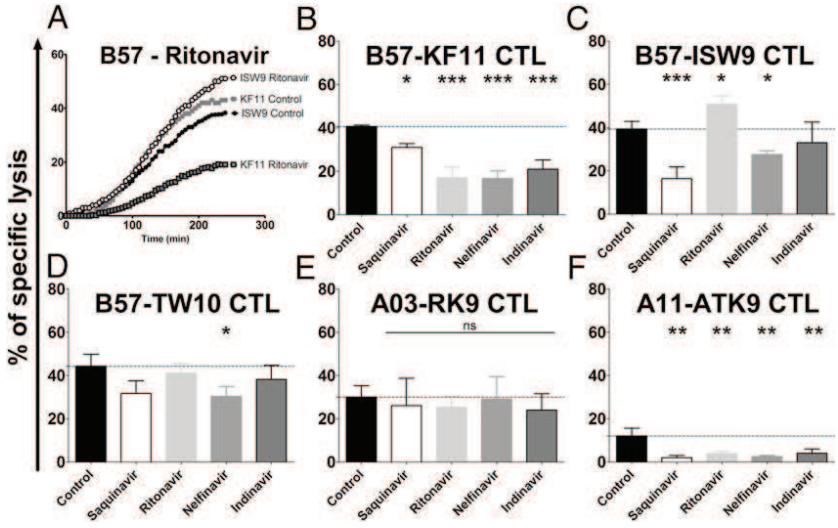

FIGURE 4. HIV PIs variably alter the endogenous processing and presentation of HIV epitopes by infected cells to CTLs. (**A**) HLA-B57 B cells were treated with DMSO or 5 μM ritonavir before being infected with VSVg-NL4.three-dimensionalEnv and used as targets in a fluorescence-based killing assay with KF11- and ISW9-specific CTLs. Fluorescence emission was recorded every 5 min from the moment ISW9-specific (circles) or KF11-specific (squares) CTLs were added to HIV-infected cells pretreated with DMSO (no line) or with ritonavir (black lines). Specific lysis was calculated as [(CTL-induced release − spontaneous release)/(maximum release − spontaneous release)] × 100%. Maximum release was determined by lysis of all target cells with detergent (5% Triton), and spontaneous release was determined by incubating noninfected cells with CTLs. (**B**–**F**) HLA-matched B cells were treated with DMSO (control; black bars) or 5 μM PI (saquinavir, ritonavir, nelfinavir, atazanavir, or darunavir) before being infected with VSVg-NL4.three-dimensionalEnv and used as targets in fluorescence-based killing assay with (B) KF11-, (C) ISW9-, (D) TW10-, (E) RK9-, or (F) ATK9-specific CTLs. The lysis percentage of target cells at 4 h after addition of an epitope-specific CTL was compared among cells pretreated with indicated PIs or DMSO control. All data represent the average of four experiments. $*p < 0.05$, $**p < 0.01$, $***p < 0.001$, one-way ANOVA with Dunnett's posttest.

PBMCs pretreated with saquinavir, ritonavir, nelfinavir, Kaletra, or control DMSO (Fig. 5A). The hydrolysis of 13 aa was inhibited by 1.2- to 2.5-fold. Twelve of 13 aa corresponded to substrates cleavable by aminopeptidases (24). The inhibition of their hydrolysis by HIV PIs is similar to that observed in Fig. 1C using the standard leucine-amc substrate. The cleavage of Proamc performed by prolylpeptidases, but not by aminopeptidases (47), was also reduced, suggesting that these PIs can also inhibit prolylpeptidase activities. In contrast, the hydrolysis of glutamic acid, aspartic acid, glutamine, and asparagine, substrates not cleavable by aminopeptidases, was increased, on average, by 2.2-, 1.3-, 1.35-, and 1.4-fold, respectively (Fig. 5A), becoming as cleavable as valine and other residues slowly cleavable in the cytosol. Thus, by modifying the cleavage of various amino acids in opposite ways, certain PIs may change the patterns of peptide degradation in the cytosol. To test the relevance of these residue-specific changes on epitope processing, we measured the production of an HIV epitope flanked by residues whose cleavage was either reduced (isoleucine, I) or enhanced (glutamic acid, E) by PIs. The processing of this epitope is proteasome and aminopeptidase dependent, and we previously showed that the trimming efficiency of extended KF11 (VXX-KF11) into KF11 correlated with that of fluorogenic X-amc (24). We compared the degradation of peptide 3KF11 (VEEKAFSPEVIPMF), which is a precursor of HLA-B57–restricted KF11, with that of an artificial mutant 2I-3KF11 (VIIKAFSPEVIPMF), in the presence or absence of 10 μM ritonavir. In the absence of PI, the degradation rates of 3KF11 and 2I-3KF11 proceeded with similar kinetics over 60 min, although, on average, 3.4-fold more epitope (KF11) and less 1KF11 precursors were produced from 2I-3KF11 because of faster N-terminal trimming of isoleucine compared with glutamic acid as we previously reported (24) (Fig. 5B). However, upon ritonavir treatment, 3KF11 degradation produced less precursors (on average, 1.8-fold less for EEKAFSPEVIPMF and 1.4-fold less for EKAFSPEVIPMF) and 1.5-fold more epitopes compared with the control (Fig. 5C, *upper panels*), suggesting that ritonavir, by increasing the hydrolysis of glutamic acid, increased the trimming of precursors toward epitope KF11. In contrast, during 2I-3KF11 degradation, because of the decreased hydrolysis of isoleucine upon ritonavir treatment, the trimming of 2I-3KF11 toward epitopes was inhibited, resulting in increased amounts of precursors (on average, 1.6-fold more for IIKAFSPEVIPMF and 1.8-fold more for IKAFSPEVIPMF) and 1.46-fold less epitopes (Fig. 5C, *lower panels*). These opposite variations in in vitro production of KF11 (from 1.8-fold more to 1.5-fold less) fell within the range that affected endogenous processing and presentation of KF11 to CTL in our previous study (24). Together, these results indicate that the effect of PI on peptide degradation is sequence specific, thus increasing the production of some epitopes and decreasing the production of others, and modifying the ratios of peptides available for loading onto MHC-I and presentation to CTL.

Discussion

The ability of CTL to clear virus-infected cells is dependent on the processing of viral Ags by cellular proteases and peptidases and peptide display by MHC-I. Any perturbation of cellular peptidase activity could modify protein degradation patterns and consequently epitope presentation. In this study, we showed that several HIV PIs, by changing not only cellular proteasome but also aminopeptidase activities, altered HIV Ag degradation patterns and cytosolic stability of peptides in a sequence-specific manner, leading to variations in lysis of HIV-infected cells by $CD8^+$ T cells.

Four of seven PIs affected at least one cellular peptidase activity. Saquinavir could either enhance or reduce proteasome and aminopeptidase hydrolytic activities, whereas other PIs such as Kaletra mostly reduced proteasome and/or aminopeptidase activities, suggesting different interactions between each drug and each cellular enzyme. It was previously shown using molecular docking that ritonavir can bind to the active center of the yeast proteasome PRE2 subunit that is homologous to human proteasome β5 subunit (48), elucidating the inhibition of the chymotryptic activity by ritonavir (30, 48, 49).

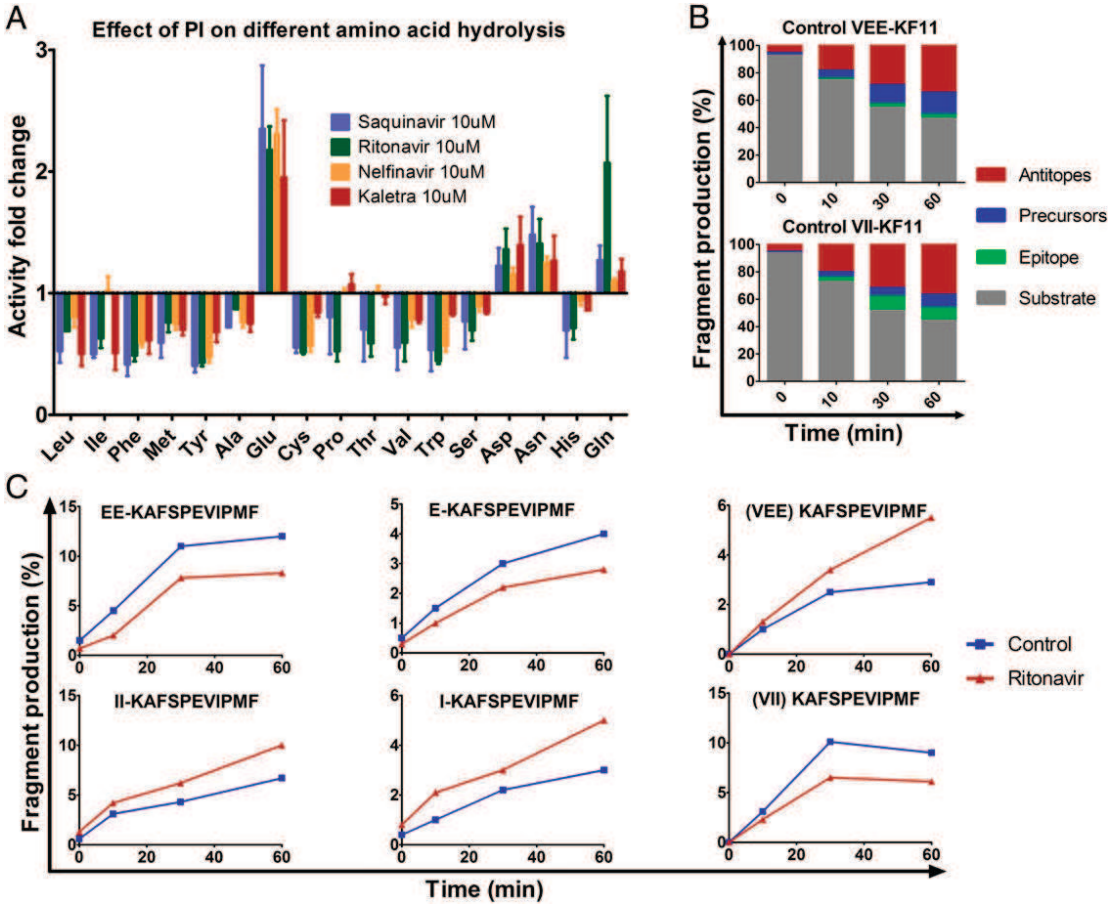

FIGURE 5. HIV PIs modify HIV peptide degradation in a sequence-specific manner. (**A**) The hydrolysis of various amino acids was measured with fluorogenic substrate in PBMCs pretreated with 10 μM saquinavir (blue), ritonavir (green), nelfinavir (yellow), or Kaletra (red). Fluorescence emission was measured over 1 h, and the maximum slope of fluorescence was measured in each condition. The fold difference of the maximum slope of PI-treated PBMCs over DMSO control was calculated for each condition. Data represent average results of four different experiments using four different PBMC donors. (**B**) The 3KF11 (VEEKAFSPEVIPMF, *upper panel*) and 2I-3KF11 (VIIKAFSPEVIPMF, *lower panel*) peptides were degraded using PBMC extracts. The resulting degradation products were analyzed by LC-MS/MS at 0, 10, 30, and 60 min. The distribution of substrate (3KF11 or 2I-3KF11, in gray), epitope (KF11, in green), precursors (blue), or antitopes (red) is shown at each time point. (**C**) The relative amount of epitope precursors (EEKAFSPEVIPMF and EKAFSPEVIPMF) and epitope KF11 (*upper panels*), and 2I-3KF11 epitope precursors (IIKAFSPEVIPMF and IKAFSPEVIPMF), and epitope (*lower panels*) were calculated at each time point of degradation with extracts pretreated with DMSO (control, blue) or with ritonavir (red). (B and C) One experiment representative of two independent experiments using PBMC extracts from two different donors and run in duplicate on the mass spectrometer.

Likewise, HIV PIs might interact with noncatalytic effector sites in the proteasome and aminopeptidases that were shown in enzymatic studies to regulate the different catalytic activities (50–52). This would provide a potential mechanism of either inhibition or enhancement of cellular peptidases by HIV PIs, although molecular modeling and structural studies are required to test this hypothesis.

First-generation PIs like ritonavir, saquinavir, and nelfinavir showed stronger effect on proteasome and aminopeptidase activities than newer PIs like atazanavir and darunavir. First-generation PIs induced more rapid and profound adverse effects on lipid and glucose metabolism than did newer PIs (4, 7, 8, 53–55). Rats treated with ritonavir developed hyperlipidemia and displayed higher RNA expression of proteasome subunits (56, 57). Although there is no clear mechanistic link between the two observations, ritonavir-induced proteasome inhibition may trigger a feedback loop leading to increased proteasome expression as observed with proteasome inhibitors (58). PI-induced proteasome inhibition may modify the half-life of proteins involved in glucose or lipid metabolism, such as the documented accumulation of sterol regulatory binding proteins 1/2 inducing constitutive lipid biosynthesis in mice (59). Whether the modification of intracellular aminopeptidase activities would affect glucose or lipid metabolism remains unknown. Surface aminopeptidases such as membrane-bound ectoenzyme aminopeptidase N/CD13 or intracellular aminopeptidases trafficking to the surface such as insulin-responsive aminopeptidase are involved in peptide cleavage, cholesterol uptake for aminopeptidase N (60, 61), or glucose transport uptake for insulin-responsive aminopeptidase (62). Considering the conservation between aminopeptidase catalytic sites, it will be important to examine whether first- and second-generation PIs modify surface aminopeptidase activities, as well as other peptidases, in each subcellular compartment and affect the biological functions of these enzymes. Finally, because various cell subsets present different levels of peptidase activities (26), it will be necessary to assess the effect of PIs not only on PBMCs, but also on specific cell subsets.

We showed that alteration of proteasome and aminopeptidase activities by HIV PIs modified both the degradation patterns of long HIV peptides and the sensitivity of epitopes to intracellular degradation before loading onto MHC-I, and therefore the amount of peptides available for display to CTL. The effect was both drug and sequence dependent. Variations in degradation patterns were

explained by the intriguing observation that the cleavage of specific residues was enhanced, whereas others were reduced. Twelve residues whose cleavage was reduced by four drugs corresponded to residues cleavable by aminopeptidases, thus suggesting that HIV PIs may reduce the efficiency of aminopeptidase-dependent trimming of many N-extended peptides into epitopes. Surprisingly, these four drugs enhanced the cleavage of acidic residues, mostly E and, to some extent, D, H, Q, which are poorly cleavable by aminopeptidases. Sequential incubation of cells with ritonavir or Kaletra followed by aminopeptidase inhibitor reduced PI-enhanced cleavage of E by 53–59%, suggesting that PI modified aminopeptidase activities to facilitate the cleavage of acidic residues but also enhanced another unidentified peptidase activity. Ritonavir or Kaletra did not enhance caspase-like activity of the proteasome or the activity of caspases (which can cleave motifs containing acidic residues), at least when measured with a pan-caspase substrate (63) (Supplemental Fig. 1), thus ruling out a major involvement of proteasomes and caspases in the changes in residue-specific cleavage patterns. Whether HIV PIs enhance additional cytosolic peptidases cleaving acidic residues or whether it may modify aminopeptidase hydrolytic capacity to enhance cleavage of acidic residues and reduce cleavage of other residues remains to be determined.

These findings have implications for the degradation of HIV proteins and beyond. First, in the context of HIV protein degradation, specifically relevant for HIV-infected, ART-treated persons with ongoing replication of drug-resistant mutated strains, we have shown that HLA-restricted mutations flanking residues tend to evolve from aminopeptidase-cleavable to poorly cleavable residues (24). In the presence of HIV PIs such as Kaletra used as booster in ART treatments, we may expect that the production of the wild type (WT) peptide would be decreased, whereas flanking mutations leading to an acidic residue would enhance epitope production as shown in this study with an isoleucine-to-glutamic acid mutation. Alternatively, a mutation toward an acidic residue within an epitope could enhance the intracellular degradation of the mutated epitope and the production of the WT version. Overall, these changes could affect the ratio of HIV peptides presented by infected cells. Mutated epitopes can elicit CTL responses (64–66); thus, the change of ratio of WT and mutated peptides could contribute to shifts in immunodominance, as seen after immune escape in acute HIV infection (67–70). Although the lack of appropriate longitudinal clinical samples precludes us to test this hypothesis, PI-induced modification of epitope landscape may contribute to broadening of immune responses against HIV in ART-treated patients with ongoing viral replication. In addition, studying the impact of PI on HIV epitope presentation is relevant to approaches to purge HIV reservoirs by combining provirus reactivation in the presence of ART to prevent replication, and therapeutic vaccination to boost immune responses against HIV (71, 72). If ART needed to prevent replication after provirus reactivation calls for inclusion of HIV PIs, it will be important to assess the repertoire of HIV epitopes presented in the context of these therapeutic strategies to define the complementary vaccination strategy better suited to clear reservoirs.

Second, because certain PIs modify Ag processing in a sequence-specific manner, the effect will likely be observed for the degradation of host proteins or proteins derived from other pathogens. The cytosolic stability of optimal epitopes derived from CMV, HCV, influenza, or EBV was variably affected by PI treatment, with ritonavir/Kaletra increasing the cytosolic stability of several peptides (G. Kourjian, unpublished observations). Because intracellular peptide stability contributes to the amount of peptides displayed to CTL (18), HIV PIs may alter the presentation of epitopes derived from other pathogens infecting ART-treated persons. More than half of HIV^+ individuals worldwide become coinfected with other pathogens such as tuberculosis or HCV, and effective drug combinations to curb both infections are needed (73–75). Assessing whether and how ART, beyond reducing HIV viral load and cellular activation, may possibly contribute to diversifying immune responses against coinfecting pathogens by modifying the degradation patterns of these pathogens provides a new outlook of the use of HIV PIs. Similarly, saquinavir, ritonavir, and nelfinavir, because of their inhibitory effect on the proteasome and other cellular targets, have been shown in previous studies and clinical trials to have beneficial effects on several cancers (31, 34, 76–81). In the repositioning of PIs as cancer therapy, another potential benefit could be a PI-induced altered processing of cancer Ags (the intracellular stability of an MAGE3 epitope was modified by ritonavir/Kaletra; G. Kourjian, unpublished observations), potentially leading to presentation of a different cancer Ag-derived peptide and new immune responses.

Our results indicate that HIV PIs, by altering several cellular peptidase activities, modify Ag processing and epitope presentation. Additional structural studies are needed to understand how HIV PIs modify peptide hydrolytic activity and specificity. However, if HIV PIs allow diversification of epitope presentation, they may provide complementary approaches to treat various immune diseases, considering that temporary PI treatment would not induce toxicity and adverse effects observed in long-term HAART.

Acknowledgments

We thank Drs. M. Hirsch, S. Fortune, D. Kavanagh, F. Pereyra, and B. Zanoni for stimulating discussions and input on the manuscript.

Disclosures

The authors have no financial conflicts of interest.

References

1. Autran, B., G. Carcelain, T. S. Li, C. Blanc, D. Mathez, R. Tubiana, C. Katlama, P. Debré, and J. Leibowitch. 1997. Positive effects of combined antiretroviral therapy on CD4+ T cell homeostasis and function in advanced HIV disease. *Science* 277: 112–116.
2. Flexner, C. 1998. HIV-protease inhibitors. *N. Engl. J. Med.* 338: 1281–1292.
3. Fernández-Montero, J. V., P. Barreiro, and V. Soriano. 2009. HIV protease inhibitors: recent clinical trials and recommendations on use. *Expert Opin. Pharmacother.* 10: 1615–1629.
4. Carr, A., K. Samaras, S. Burton, M. Law, J. Freund, D. J. Chisholm, and D. A. Cooper. 1998. A syndrome of peripheral lipodystrophy, hyperlipidaemia and insulin resistance in patients receiving HIV protease inhibitors. *AIDS* 12: F51–F58.
5. Ena, J., C. Benito, P. Llácer, F. Pasquau, and C. Amador. 2004. [Abnormal body fat distribution and type of antiretroviral therapy as predictors of cardiovascular disease risk in HIV-infected patients]. *Med. Clin. (Barc.)* 122: 721–726.
6. Yarasheski, K. E., P. Tebas, C. Sigmund, S. Dagogo-Jack, A. Bohrer, J. Turk, P. A. Halban, P. E. Cryer, and W. G. Powderly. 1999. Insulin resistance in HIV protease inhibitor-associated diabetes. *J. Acquir. Immune Defic. Syndr.* 21: 209–216.
7. Brown, T. T., and R. B. Qaqish. 2006. Antiretroviral therapy and the prevalence of osteopenia and osteoporosis: a meta-analytic review. *AIDS* 20: 2165–2174.
8. Boesecke, C., and D. A. Cooper. 2008. Toxicity of HIV protease inhibitors: clinical considerations. *Curr. Opin. HIV AIDS* 3: 653–659.
9. Orkin, C., E. DeJesus, H. Khanlou, A. Stoehr, K. Supparatpinyo, E. Lathouwers, E. Lefebvre, M. Opsomer, T. Van de Casteele, and F. Tomaka. 2013. Final 192-week efficacy and safety of once-daily darunavir/ritonavir compared with lopinavir/ritonavir in HIV-1-infected treatment-naïve patients in the ARTEMIS trial. *HIV Med.* 14: 49–59.
10. Erickson, J., D. J. Neidhart, J. VanDrie, D. J. Kempf, X. C. Wang, D. W. Norbeck, J. J. Plattner, J. W. Rittenhouse, M. Turon, N. Wideburg, et al. 1990. Design, activity, and 2.8 A crystal structure of a C2 symmetric inhibitor complexed to HIV-1 protease. *Science* 249: 527–533.
11. Diez-Rivero, C. M., E. M. Lafuente, and P. A. Reche. 2010. Computational analysis and modeling of cleavage by the immunoproteasome and the constitutive proteasome. *BMC Bioinformatics* 11: 479.
12. Goldberg, A. L. 2003. Protein degradation and protection against misfolded or damaged proteins. *Nature* 426: 895–899.
13. York, I. A., A. X. Mo, K. Lemerise, W. Zeng, Y. Shen, C. R. Abraham, T. Saric, A. L. Goldberg, and K. L. Rock. 2003. The cytosolic endopeptidase, thimet

oligopeptidase, destroys antigenic peptides and limits the extent of MHC class I antigen presentation. *Immunity* 18: 429–440.
14. Saric, T., C. I. Graef, and A. L. Goldberg. 2004. Pathway for degradation of peptides generated by proteasomes: a key role for thimet oligopeptidase and other metallopeptidases. *J. Biol. Chem.* 279: 46723–46732.
15. Kawahara, M., I. A. York, A. Hearn, D. Farfan, and K. L. Rock. 2009. Analysis of the role of tripeptidyl peptidase II in MHC class I antigen presentation in vivo. *J. Immunol.* 183: 6069–6077.
16. Serwold, T., F. Gonzalez, J. Kim, R. Jacob, and N. Shastri. 2002. ERAAP customizes peptides for MHC class I molecules in the endoplasmic reticulum. *Nature* 419: 480–483.
17. York, I. A., S. C. Chang, T. Saric, J. A. Keys, J. M. Favreau, A. L. Goldberg, and K. L. Rock. 2002. The ER aminopeptidase ERAP1 enhances or limits antigen presentation by trimming epitopes to 8-9 residues. *Nat. Immunol.* 3: 1177–1184.
18. Lazaro, E., C. Kadie, P. Stamegna, S. C. Zhang, P. Gourdain, N. Y. Lai, M. Zhang, S. A. Martinez, D. Heckerman, and S. Le Gall. 2011. Variable HIV peptide stability in human cytosol is critical to epitope presentation and immune escape. *J. Clin. Invest.* 121: 2480–2492.
19. Herberts, C. A., J. J. Neijssen, J. de Haan, L. Janssen, J. W. Drijfhout, E. A. Reits, and J. J. Neefjes. 2006. Cutting edge: HLA-B27 acquires many N-terminal dibasic peptides: coupling cytosolic peptide stability to antigen presentation. *J. Immunol.* 176: 2697–2701.
20. Reits, E., A. Griekspoor, J. Neijssen, T. Groothuis, K. Jalink, P. van Veelen, H. Janssen, J. Calafat, J. W. Drijfhout, and J. Neefjes. 2003. Peptide diffusion, protection, and degradation in nuclear and cytoplasmic compartments before antigen presentation by MHC class I. *Immunity* 18: 97–108.
21. Kisselev, A. F., T. N. Akopian, K. M. Woo, and A. L. Goldberg. 1999. The sizes of peptides generated from protein by mammalian 26 and 20 S proteasomes. Implications for understanding the degradative mechanism and antigen presentation. *J. Biol. Chem.* 274: 3363–3371.
22. Hearn, A., I. A. York, and K. L. Rock. 2009. The specificity of trimming of MHC class I-presented peptides in the endoplasmic reticulum. *J. Immunol.* 183: 5526–5536.
23. Schatz, M. M., B. Peters, N. Akkad, N. Ullrich, A. N. Martinez, O. Carroll, S. Bulik, H. G. Rammensee, P. van Endert, H. G. Holzhütter, et al. 2008. Characterizing the N-terminal processing motif of MHC class I ligands. *J. Immunol.* 180: 3210–3217.
24. Zhang, S. C., E. Martin, M. Shimada, S. B. Godfrey, J. Fricke, S. Locastro, N. Y. Lai, P. Liebesny, J. M. Carlson, C. J. Brumme, et al. 2012. Aminopeptidase substrate preference affects HIV epitope presentation and predicts immune escape patterns in HIV-infected individuals. *J. Immunol.* 188: 5924–5934.
25. Le Gall, S., P. Stamegna, and B. D. Walker. 2007. Portable flanking sequences modulate CTL epitope processing. *J. Clin. Invest.* 117: 3563–3575.
26. Lazaro, E., S. B. Godfrey, P. Stamegna, T. Ogbechie, C. Kerrigan, M. Zhang, B. D. Walker, and S. Le Gall. 2009. Differential HIV epitope processing in monocytes and CD4 T cells affects cytotoxic T lymphocyte recognition. *J. Infect. Dis.* 200: 236–243.
27. Rock, K. L., C. Gramm, L. Rothstein, K. Clark, R. Stein, L. Dick, D. Hwang, and A. L. Goldberg. 1994. Inhibitors of the proteasome block the degradation of most cell proteins and the generation of peptides presented on MHC class I molecules. *Cell* 78: 761–771.
28. York, I. A., M. A. Brehm, S. Zendzian, C. F. Towne, and K. L. Rock. 2006. Endoplasmic reticulum aminopeptidase 1 (ERAP1) trims MHC class I-presented peptides in vivo and plays an important role in immunodominance. *Proc. Natl. Acad. Sci. USA* 103: 9202–9207.
29. Blanchard, N., T. Kanaseki, H. Escobar, F. Delebecque, N. A. Nagarajan, E. Reyes-Vargas, D. K. Crockett, D. H. Raulet, J. C. Delgado, and N. Shastri. 2010. Endoplasmic reticulum aminopeptidase associated with antigen processing defines the composition and structure of MHC class I peptide repertoire in normal and virus-infected cells. *J. Immunol.* 184: 3033–3042.
30. André, P., M. Groettrup, P. Klenerman, R. de Giuli, B. L. Booth, Jr., V. Cerundolo, M. Bonneville, F. Jotereau, R. M. Zinkernagel, and V. Lotteau. 1998. An inhibitor of HIV-1 protease modulates proteasome activity, antigen presentation, and T cell responses. *Proc. Natl. Acad. Sci. USA* 95: 13120–13124.
31. Gaedicke, S., E. Firat-Geier, O. Constantiniu, M. Lucchiari-Hartz, M. Freudenberg, C. Galanos, and G. Niedermann. 2002. Antitumor effect of the human immunodeficiency virus protease inhibitor ritonavir: induction of tumor-cell apoptosis associated with perturbation of proteasomal proteolysis. *Cancer Res.* 62: 6901–6908.
32. Kelleher, A. D., B. L. Booth, Jr., A. K. Sewell, A. Oxenius, V. Cerundolo, A. J. McMichael, R. E. Phillips, and D. A. Price. 2001. Effects of retroviral protease inhibitors on proteasome function and processing of HIV-derived MHC class I-restricted cytotoxic T lymphocyte epitopes. *AIDS Res. Hum. Retroviruses* 17: 1063–1066.
33. Piccinini, M., M. T. Rinaudo, A. Anselmino, B. Buccinnà, C. Ramondetti, A. Dematteis, E. Ricotti, L. Palmisano, M. Mostert, and P. A. Tovo. 2005. The HIV protease inhibitors nelfinavir and saquinavir, but not a variety of HIV reverse transcriptase inhibitors, adversely affect human proteasome function. *Antivir. Ther. (Lond.)* 10: 215–223.
34. Pajonk, F., J. Himmelsbach, K. Riess, A. Sommer, and W. H. McBride. 2002. The human immunodeficiency virus (HIV)-1 protease inhibitor saquinavir inhibits proteasome function and causes apoptosis and radiosensitization in non-HIV-associated human cancer cells. *Cancer Res.* 62: 5230–5235.
35. Hill, A., A. McBride, A. W. Sawyer, N. Clumeck, and R. K. Gupta. 2013. Resistance at virological failure using boosted protease inhibitors versus non-nucleoside reverse transcriptase inhibitors as first-line antiretroviral therapy—implications for sustained efficacy of ART in resource-limited settings. *J. Infect. Dis.* 207(Suppl. 2): S78–S84.
36. Hosseinipour, M. C., R. K. Gupta, G. Van Zyl, J. J. Eron, and J. B. Nachega. 2013. Emergence of HIV drug resistance during first- and second-line antiretroviral therapy in resource-limited settings. *J. Infect. Dis.* 207(Suppl. 2): S49–S56.
37. Kisselev, A. F., and A. L. Goldberg. 2005. Monitoring activity and inhibition of 26S proteasomes with fluorogenic peptide substrates. *Methods Enzymol.* 398: 364–378.
38. Gourdain, P., J. Boucau, G. Kourjian, N. Y. Lai, E. Duong, and S. Le Gall. 2013. A real-time killing assay to follow viral epitope presentation to CD8 T cells. *J. Immunol. Methods* 398–399: 60–67.
39. Acosta, E. P., T. N. Kakuda, R. C. Brundage, P. L. Anderson, and C. V. Fletcher. 2000. Pharmacodynamics of human immunodeficiency virus type 1 protease inhibitors. *Clin. Infect. Dis.* 30(Suppl. 2): S151–S159.
40. Cardiello, P. G., T. Monhaphol, A. Mahanontharit, R. P. van Heeswijk, D. Burger, A. Hill, K. Ruxrungtham, J. M. Lange, D. A. Cooper, and P. Phanuphak. 2003. Pharmacokinetics of once-daily saquinavir hard-gelatin capsules and saquinavir soft-gelatin capsules boosted with ritonavir in HIV-1-infected subjects. *J. Acquir. Immune Defic. Syndr.* 32: 375–379.
41. Hennessy, M., S. Clarke, J. P. Spiers, D. Kelleher, F. Mulcahy, P. Hoggard, D. Back, and M. Barry. 2004. Intracellular accumulation of nelfinavir and its relationship to P-glycoprotein expression and function in HIV-infected patients. *Antivir. Ther. (Lond.)* 9: 115–122.
42. Jackson, A., V. Watson, D. Back, S. Khoo, N. Liptrott, D. Egan, K. Gedela, C. Higgs, R. Abbas, B. Gazzard, and M. Boffito. 2011. Plasma and intracellular pharmacokinetics of darunavir/ritonavir once daily and raltegravir once and twice daily in HIV-infected individuals. *J. Acquir. Immune Defic. Syndr.* 58: 450–457.
43. van Heeswijk, R. P., A. I. Veldkamp, J. W. Mulder, P. L. Meenhorst, J. M. Lange, J. H. Beijnen, and R. M. Hoetelmans. 2000. Once-daily dosing of saquinavir and low-dose ritonavir in HIV-1-infected individuals: a pharmacokinetic pilot study. *AIDS* 14: F103–F110.
44. Reits, E., J. Neijssen, C. Herberts, W. Benckhuijsen, L. Janssen, J. W. Drijfhout, and J. Neefjes. 2004. A major role for TPPII in trimming proteasomal degradation products for MHC class I antigen presentation. *Immunity* 20: 495–506.
45. Frahm, N., B. Baker, and C. Brander. 2008. Identification and optimal definition of HIV-derived cytotoxic T lymphocyte (CTL) epitopes for the study of CTL escape, functional avidity and viral evolution. In *HIV Molecular Immunology 2008*. B. T. Korber, C. Brander, and B. F. Haynes, et al., eds. Los Alamos National Laboratory, Los Alamos, NM, p. 1–24.
46. Batchelor, R. H., and M. Zhou. 2004. Use of cellular glucose-6-phosphate dehydrogenase for cell quantitation: applications in cytotoxicity and apoptosis assays. *Anal. Biochem.* 329: 35–42.
47. Rosenblum, J. S., and J. W. Kozarich. 2003. Prolyl peptidases: a serine protease subfamily with high potential for drug discovery. *Curr. Opin. Chem. Biol.* 7: 496–504.
48. Schmidtke, G., H. G. Holzhütter, M. Bogyo, N. Kairies, M. Groll, R. de Giuli, S. Emch, and M. Groettrup. 1999. How an inhibitor of the HIV-I protease modulates proteasome activity. *J. Biol. Chem.* 274: 35734–35740.
49. Sato, A., T. Asano, K. Ito, and T. Asano. 2012. Ritonavir interacts with bortezomib to enhance protein ubiquitination and histone acetylation synergistically in renal cancer cells. *Urology* 79:966.e13-21.
50. Ruschak, A. M., and L. E. Kay. 2012. Proteasome allostery as a population shift between interchanging conformers. *Proc. Natl. Acad. Sci. USA* 109: E3454–E3462.
51. Jankowska, E., M. Gaczynska, P. Osmulski, E. Sikorska, R. Rostankowski, S. Madabhushi, M. Tokmina-Lukaszewska, and F. Kasprzykowski. 2010. Potential allosteric modulators of the proteasome activity. *Biopolymers* 93: 481–495.
52. Kisselev, A. F., T. N. Akopian, V. Castillo, and A. L. Goldberg. 1999. Proteasome active sites allosterically regulate each other, suggesting a cyclical bite-chew mechanism for protein breakdown. *Mol. Cell* 4: 395–402.
53. Spector, A. A. 2006. HIV protease inhibitors and hyperlipidemia: a fatty acid connection. *Arterioscler. Thromb. Vasc. Biol.* 26: 7–9.
54. Anuurad, E., A. Bremer, and L. Berglund. 2010. HIV protease inhibitors and obesity. *Curr. Opin. Endocrinol. Diabetes Obes.* 17: 478–485.
55. Noor, M. A., O. P. Flint, J. F. Maa, and R. A. Parker. 2006. Effects of atazanavir/ritonavir and lopinavir/ritonavir on glucose uptake and insulin sensitivity: demonstrable differences in vitro and clinically. *AIDS* 20: 1813–1821.
56. Waring, J. F., R. Ciurlionis, K. Marsh, L. L. Klein, D. A. Degoey, J. T. Randolph, B. Spear, and D. J. Kempf. 2010. Identification of proteasome gene regulation in a rat model for HIV protease inhibitor-induced hyperlipidemia. *Arch. Toxicol.* 84: 263–270.
57. Lum, P. Y., Y. D. He, J. G. Slatter, J. F. Waring, N. Zelinsky, G. Cavet, X. Dai, O. Fong, R. Gum, L. Jin, et al. 2007. Gene expression profiling of rat liver reveals a mechanistic basis for ritonavir-induced hyperlipidemia. *Genomics* 90: 464–473.
58. Meiners, S., D. Heyken, A. Weller, A. Ludwig, K. Stangl, P. M. Kloetzel, and E. Krüger. 2003. Inhibition of proteasome activity induces concerted expression of proteasome genes and de novo formation of Mammalian proteasomes. *J. Biol. Chem.* 278: 21517–21525.
59. Riddle, T. M., D. G. Kuhel, L. A. Woollett, C. J. Fichtenbaum, and D. Y. Hui. 2001. HIV protease inhibitor induces fatty acid and sterol biosynthesis in liver and adipose tissues due to the accumulation of activated sterol regulatory element-binding proteins in the nucleus. *J. Biol. Chem.* 276: 37514–37519.
60. Kramer, W., F. Girbig, D. Corsiero, A. Pfenninger, W. Frick, G. Jähne, M. Rhein, W. Wendler, F. Lottspeich, E. O. Hochleitner, et al. 2005. Aminopeptidase N (CD13) is a molecular target of the cholesterol absorption inhibitor ezetimibe in the enterocyte brush border membrane. *J. Biol. Chem.* 280: 1306–1320.
61. Levy, E., S. Spahis, D. Sinnett, N. Peretti, F. Maupas-Schwalm, E. Delvin, M. Lambert, and M. A. Lavoie. 2007. Intestinal cholesterol transport proteins: an update and beyond. *Curr. Opin. Lipidol.* 18: 310–318.

62. Yeh, T. Y., J. I. Sbodio, Z. Y. Tsun, B. Luo, and N. W. Chi. 2007. Insulin-stimulated exocytosis of GLUT4 is enhanced by IRAP and its partner tankyrase. *Biochem. J.* 402: 279–290.
63. Thornberry, N. A., T. A. Rano, E. P. Peterson, D. M. Rasper, T. Timkey, M. Garcia-Calvo, V. M. Houtzager, P. A. Nordstrom, S. Roy, J. P. Vaillancourt, et al. 1997. A combinatorial approach defines specificities of members of the caspase family and granzyme B. Functional relationships established for key mediators of apoptosis. *J. Biol. Chem.* 272: 17907–17911.
64. Feeney, M. E., Y. Tang, K. Pfafferott, K. A. Roosevelt, R. Draenert, A. Trocha, X. G. Yu, C. Verrill, T. Allen, C. Moore, et al. 2005. HIV-1 viral escape in infancy followed by emergence of a variant-specific CTL response. *J. Immunol.* 174: 7524–7530.
65. Allen, T. M., X. G. Yu, E. T. Kalife, L. L. Reyor, M. Lichterfeld, M. John, M. Cheng, R. L. Allgaier, S. Mui, N. Frahm, et al. 2005. De novo generation of escape variant-specific CD8+ T-cell responses following cytotoxic T-lymphocyte escape in chronic human immunodeficiency virus type 1 infection. *J. Virol.* 79: 12952–12960.
66. O'Connell, K. A., R. W. Hegarty, R. F. Siliciano, and J. N. Blankson. 2011. Viral suppression of multiple escape mutants by de novo CD8(+) T cell responses in a human immunodeficiency virus-1 infected elite suppressor. *Retrovirology* 8: 63.
67. Turnbull, E. L., M. Wong, S. Wang, X. Wei, N. A. Jones, K. E. Conrod, D. Aldam, J. Turner, P. Pellegrino, B. F. Keele, et al. 2009. Kinetics of expansion of epitope-specific T cell responses during primary HIV-1 infection. *J. Immunol.* 182: 7131–7145.
68. Liu, M. K., N. Hawkins, A. J. Ritchie, V. V. Ganusov, V. Whale, S. Brackenridge, H. Li, J. W. Pavlicek, F. Cai, M. Rose-Abrahams, et al; CHAVI Core B. 2013. Vertical T cell immunodominance and epitope entropy determine HIV-1 escape. *J. Clin. Invest.* 123: 380–393.
69. Borrow, P., H. Lewicki, X. Wei, M. S. Horwitz, N. Peffer, H. Meyers, J. A. Nelson, J. E. Gairin, B. H. Hahn, M. B. Oldstone, and G. M. Shaw. 1997. Antiviral pressure exerted by HIV-1-specific cytotoxic T lymphocytes (CTLs) during primary infection demonstrated by rapid selection of CTL escape virus. *Nat. Med.* 3: 205–211.
70. Nowak, M. A., R. M. May, R. E. Phillips, S. Rowland-Jones, D. G. Lalloo, S. McAdam, P. Klenerman, B. Köppe, K. Sigmund, C. R. Bangham, et al. 1995. Antigenic oscillations and shifting immunodominance in HIV-1 infections. *Nature* 375: 606–611.
71. Archin, N. M., A. L. Liberty, A. D. Kashuba, S. K. Choudhary, J. D. Kuruc, A. M. Crooks, D. C. Parker, E. M. Anderson, M. F. Kearney, M. C. Strain, et al. 2012. Administration of vorinostat disrupts HIV-1 latency in patients on antiretroviral therapy. *Nature* 487: 482–485.
72. Siliciano, J. D., and R. F. Siliciano. 2013. HIV-1 eradication strategies: design and assessment. *Curr. Opin. HIV AIDS* 8: 318–325.
73. Jalali, Z., and J. K. Rockstroh. 2012. Antiviral drugs and the treatment of hepatitis C. *Curr. HIV/AIDS Rep.* 9: 132–138.
74. Naidoo, K., C. Baxter, and S. S. Abdool Karim. 2013. When to start antiretroviral therapy during tuberculosis treatment? *Curr. Opin. Infect. Dis.* 26: 35–42.
75. Walker, N. F., G. Meintjes, and R. J. Wilkinson. 2013. HIV-1 and the immune response to TB. *Future Virol.* 8: 57–80.
76. Bono, C., L. Karlin, S. Harel, E. Mouly, S. Labaume, L. Galicier, S. Apcher, H. Sauvageon, J. P. Fermand, J. C. Bories, and B. Arnulf. 2012. The human immunodeficiency virus-1 protease inhibitor nelfinavir impairs proteasome activity and inhibits the proliferation of multiple myeloma cells in vitro and in vivo. *Haematologica* 97: 1101–1109.
77. Kawabata, S., J. J. Gills, J. R. Mercado-Matos, J. Lopiccolo, W. Wilson, III, M. C. Hollander, and P. A. Dennis. 2012. Synergistic effects of nelfinavir and bortezomib on proteotoxic death of NSCLC and multiple myeloma cells. *Cell Death Dis.* 3: e353.
78. Kraus, M., E. Malenke, J. Gogel, H. Müller, T. Rückrich, H. Overkleeft, H. Ovaa, E. Koscielniak, J. T. Hartmann, and C. Driessen. 2008. Ritonavir induces endoplasmic reticulum stress and sensitizes sarcoma cells toward bortezomib-induced apoptosis. *Mol. Cancer Ther.* 7: 1940–1948.
79. Sgadari, C., P. Monini, G. Barillari, and B. Ensoli. 2003. Use of HIV protease inhibitors to block Kaposi's sarcoma and tumour growth. *Lancet Oncol.* 4: 537–547.
80. Zeng, J., A. P. See, K. Aziz, S. Thiyagarajan, T. Salih, R. P. Gajula, M. Armour, J. Phallen, S. Terezakis, L. Kleinberg, et al. 2011. Nelfinavir induces radiation sensitization in pituitary adenoma cells. *Cancer Biol. Ther.* 12: 657–663.
81. Kimple, R. J., A. V. Vaseva, A. D. Cox, K. M. Baerman, B. F. Calvo, J. E. Tepper, J. M. Shields, and C. I. Sartor. 2010. Radiosensitization of epidermal growth factor receptor/HER2-positive pancreatic cancer is mediated by inhibition of Akt independent of ras mutational status. *Clin. Cancer Res.* 16: 912–923.

Supplemental figure 1

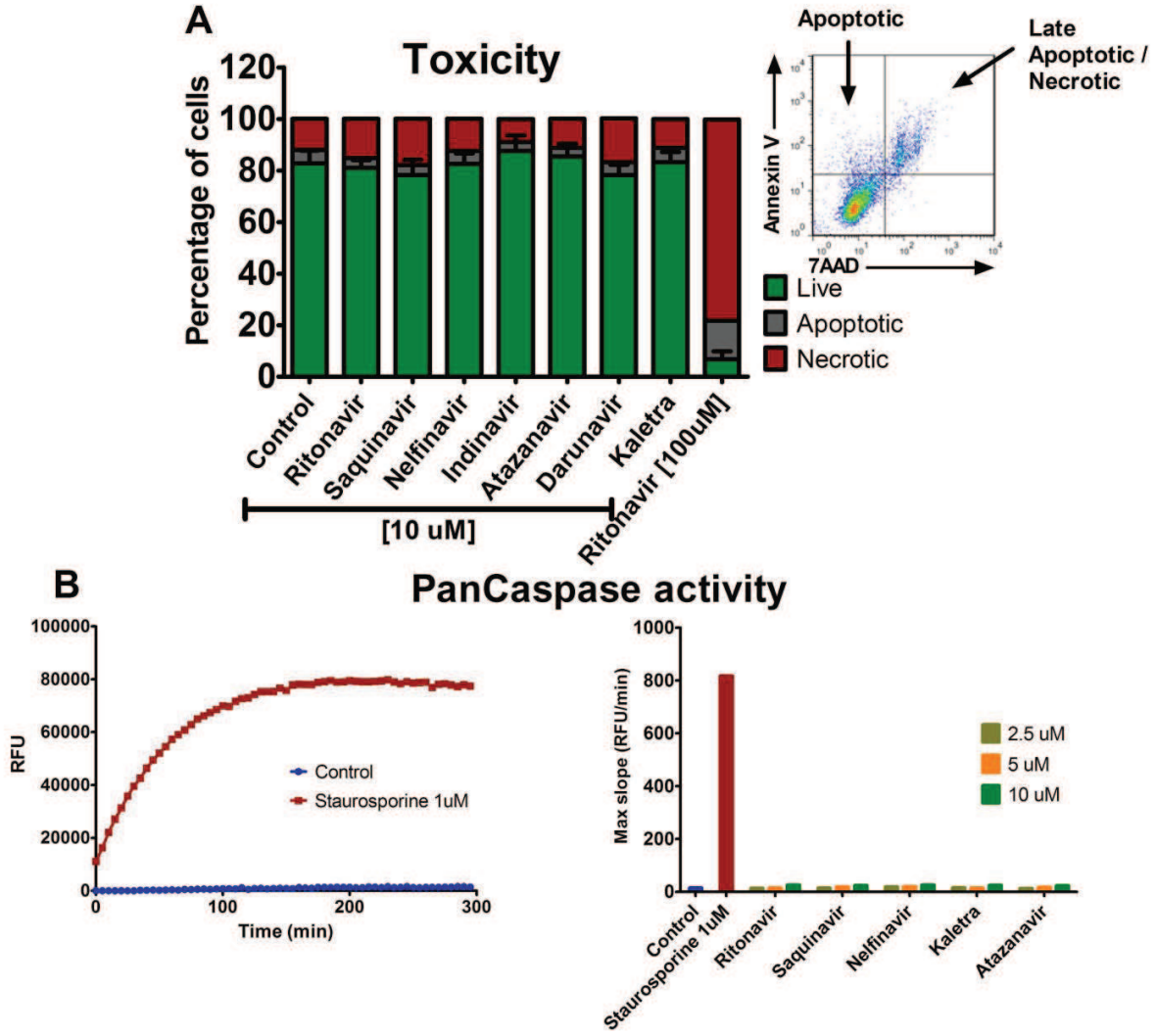

Supplemental figure 1. Plasma concentrations of HIV PIs are not toxic to PBMCs used in this study. **(A)** PBMCs were incubated with DMSO (control), 10μM of PI (Ritonavir, Saquinavir, Nelfinavir, Indinavir, Atazanavir, Darunavir or Kaletra) or 100μM of Ritonavir overnight. Cells were stained with Annexin 5/7AAD and analyzed by Flow cytometry (inset). The percentage of live (green), apoptotic (grey) and necrotic (red) cells upon each drug treatment were compared to control DMSO. 100μM of Ritonavir was used as a positive control to induce cell apoptosis and necrosis. All data represent the average of 3 experiments performed in PBMC from 3 different donors. **(B)** PanCaspase substrate Ac-DEVD-AMC was added to PBMCs pretreated with DMSO (blue), 1μM Staurosporine (red) or increasing concentration of HIV PIs and incubated for 5 h at 37˚C, during which fluorescence emission was monitored every 5 min. Left panel presents the fluorescence over time and right panel the maximum slope of fluorescence emission over 1 hour for each condition.

Supplemental figure 2

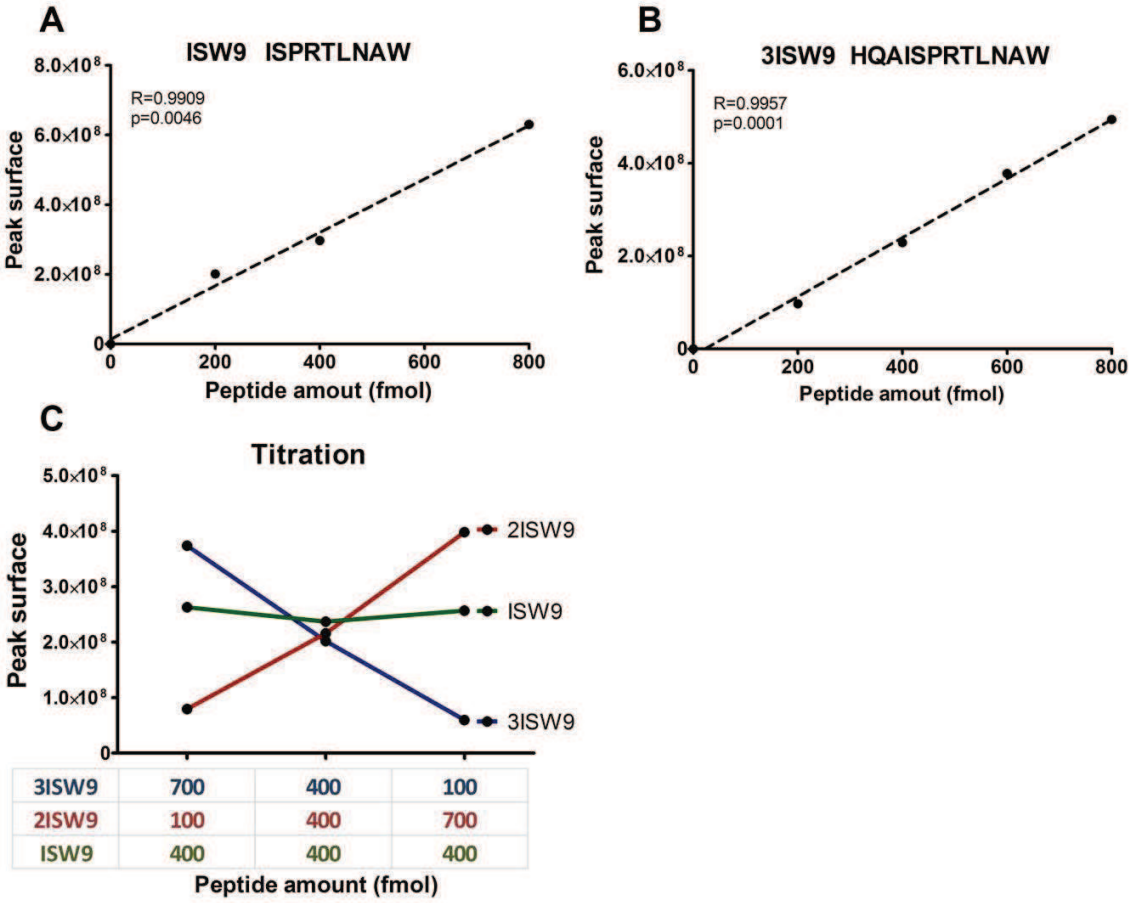

Supplemental figure 2. Validation of the mass spectrometry detection, quantification and analysis of peptide degradation. Increasing amounts of peptides ISW9 **(A)**, 3ISW9 **(B)** or various amounts of 3ISW9, 2ISW9 and ISW9 mixed together **(C)** were diluted in 80% water, 15% acetonitril, 5% trifluoroethanol and analyzed by mass spectrometry. The peptide sequence and area under peak were calculated with Proteome Discover. Correlation between peptide amount and area under peak were calculated by linear regression.

Supplemental figure 3

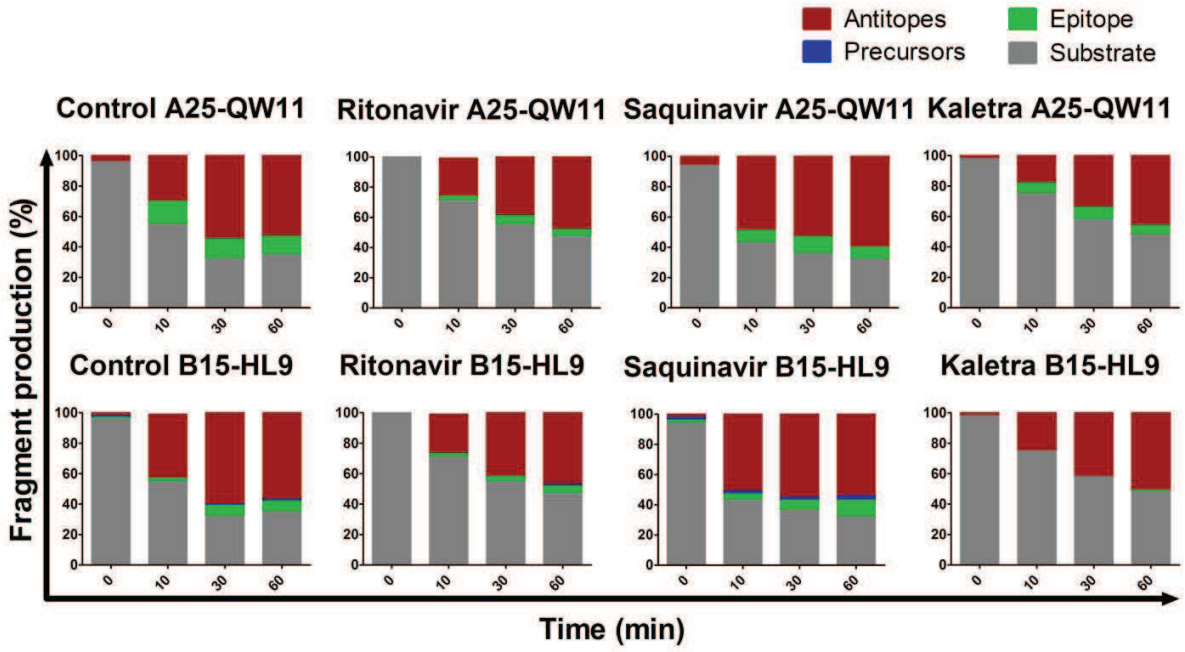

Supplemental figure 3. HIV PIs variably alter the degradation patterns of different peptides. The 3ISW9 (HQAISPRTLNAW) peptide was degraded using PBMC extracts and the reaction was stopped at 0, 10, 30 and 60min. Resulting degradation products were analyzed by LC-MS-MS. The production of A25-QW11 (QAISPRTLNAW; upper panels) and B15-HL9 (HQAISPRTL; lower panels) were assessed in the presence of DMSO control or 10uM of Ritonavir, Saquivanir, Kaletra (left to right).

Supplemental figure 4

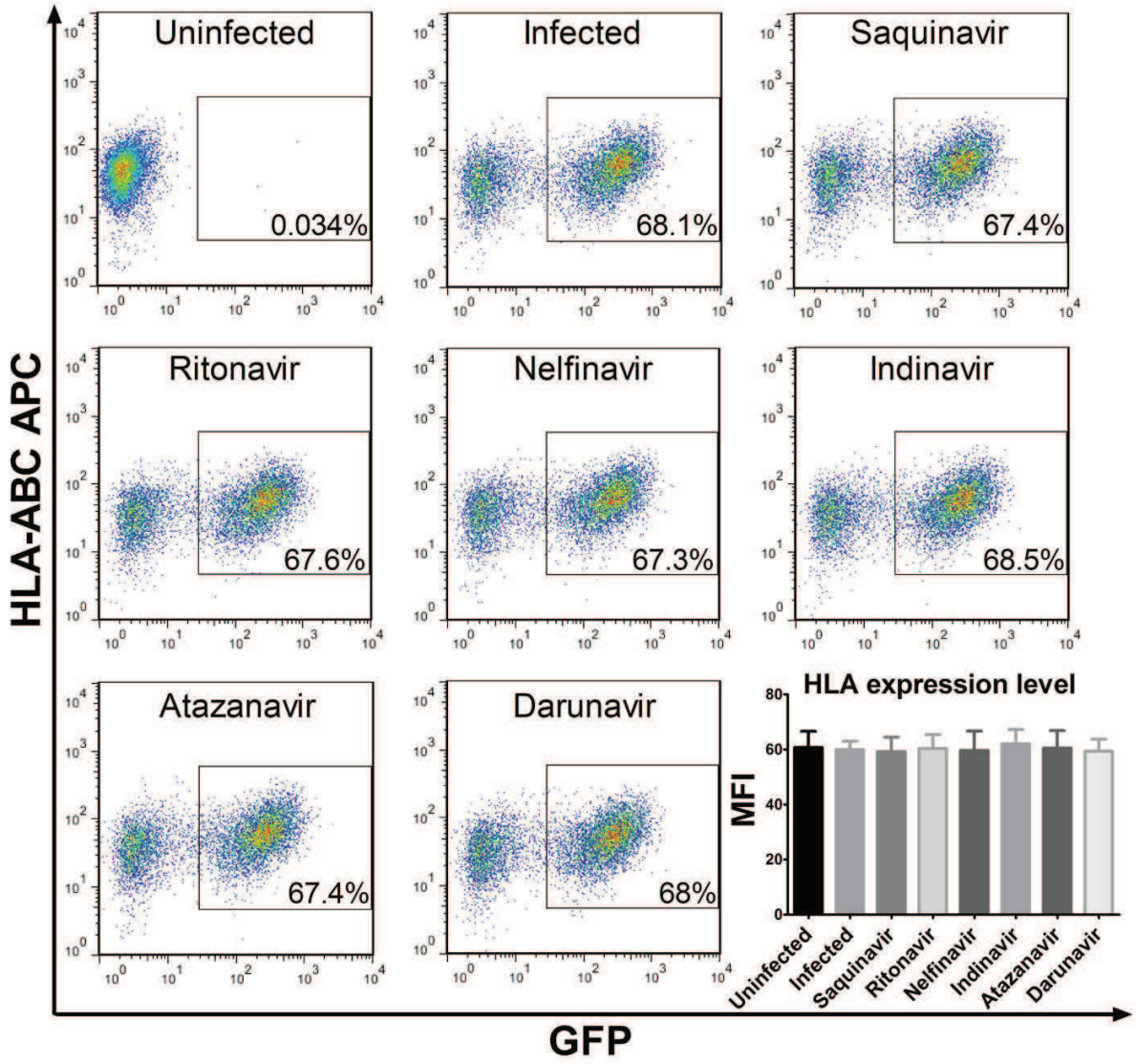

Supplemental figure 4. HIV PIs do not affect HLA-A/B/C surface expression levels or VSV-pseudotyped HIV infection rates. B cells pretreated with DMSO (control) or 5uM PI (Saquinavir, Ritonavir, Nelfinavir, Indinavir, Atazanavir and Darunavir) were infected with VSVg-NL4.3DEnv or VSVg-LV expressing GFP. Two days after infection the surface expression of HLA-A/B/C and the percentage of GFP positive cells were measured by flow cytometry. Mean fluorescence intensity of HLA-ABC surface expression after HIV-infection is shown as an average and standard deviation of 3 experiments (lower right panel).

Study n°2

HIV protease inhibitors modulate NOX2 and cathepsin activities leading to altered antigen processing and epitope cross-presentation

Antigen presenting cells have the ability to process exogenous antigens by phagosomal cathepsins and cross-present the epitopes on MHC-I to CD8+ T lymphocytes. To avoid the excessive cleavage and the destruction of potential antigenic peptides, cathepsin activities are limited by the maintenance of a neutral phagosomal pH. This controlled phagosomal pH is mediated by the NADPH oxidase NOX2 which uses protons from the phagosome to produce reactive oxygen species thus limiting the acidification. In this study we investigated the effect of HIV PIs on cathepsin activities as well as the tightly controlled phagosomal environment. We assessed the impact of PI-induced alteration on exogenous antigen degradation, epitope production and presentation, and recognition by cytotoxic T lymphocytes.

Final preparation before submission in May 2015

HIV protease inhibitors modulate NOX2 and cathepsin activities leading to altered antigen processing and epitope cross-presentation

Georgio Kourjian[1], Marijana Rucevic[1], Matthew Berberich[1], Jens Dinter[1] Daniel Wambua[1], Julie Boucau[1] and Sylvie Le Gall[1]

[1] Ragon Institute of Massachusetts General Hospital, Massachusetts Institute of Technology and Harvard, Cambridge, MA 02139, United States of America

Contact Information: sylvie_legall@hms.harvard.edu

Additional Title Page Footnotes:

Summary

To initiate adaptive cytotoxic immune responses, phagocytosed antigens are degraded by cathepsins and the proteolytic peptides are presented by antigen presenting cells to CD8+ T lymphocytes through a process called antigen cross-presentation. The controlled degradation of antigens mediated by the limited cathepsin activity is enabled by the NADPH oxidase NOX2 induced alkalinization of the early phagosomes. HIV protease inhibitors (PIs) used by HIV infected people are shown to alter cellular protease activities. We now describe that HIV PIs by inhibiting Akt and protein kinase C activity, reduce NOX2 activation thus phagosomal alkalinization leading to excessive cathepsin activation in the phagosomes and alterations in antigen processing patterns. Accordingly, here we show that HIV PIs alter HIV protein degradation in DC phagosomes, HIV epitope cross-presentation by MHC-I and CTL-mediated killing. Moreover, sequencing by mass spectrometry (MS) of surface MHC-bound self-peptidome of primary human cells revealed significant modifications of peptide-MHC presentation caused by PI treatment. Therefore, by altering NOX2 and cathepsin activities and the degradation patterns of proteins, HIV PIs may diversify peptides available for cross-presentation, alter the patterns of CTL responses, and provide a complementary approach to current therapies for the CTL-mediated clearance of abnormal cells in infection, cancer, or other immune disease.

INTRODUCTION

HIV infection has been considered as a chronic illness since the availability of highly active antiretroviral treatments (HAART), which is a combination of nucleoside reverse transcriptase inhibitors (NRTIs), non-NRTIs (nNRTIs), protease inhibitors (PIs), and integrase inhibitors given to HIV-infected patients to suppress HIV replication (Autran et al., 1997). HIV PIs are designed to block the HIV aspartyl protease preventing the cleavage of HIV Gag and Pol polyproteins that include essential structural and enzymatic components of the virus. This blockage prevents the conversion of HIV particles into their mature infectious form (Flexner, 1998). The design of the first-generation HIV PIs is based on the transition-state mimetic of the Phe-Pro bond, the major substrate of HIV-I protease (Erickson et al., 1990). Evidence showing the ability of the 20S proteasome to cleave similar bonds (Diez-Rivero et al., 2010) raised questions about possible interactions between HIV PIs and the proteasome catalytic sites. Proteasomes are the central proteolytic system of the eukaryotic cell (Rock et al., 1994) and play an important role in the generation of MHC-class I (MHC-I) peptides. Degradation products that result from proteasomal cleavage of full-length proteins and defective ribosomal products (Goldberg, 2003), are transported into the endoplasmic reticulum (ER) where they are further trimmed by ER-resident aminopeptidases (ERAP1 or ERAP2) (Saveanu et al., 2005; York et al., 2002) and loaded onto MHC-I molecules and exported to the cell surface. It has been shown that natural or artificial variations in proteasome and aminopeptidase activities change the balance between production and further cleavage of peptides, enhancing or impairing the presentation of various MHC-I epitopes. For instance, the inhibition of the proteasome by N-acetyl-leucyl-leucyl-norleucinal or ERAP-1 knockout in mice altered the degradation of proteins and changed the repertoire of peptides presented on MHC-I molecules and CTL responses (Blanchard et al., 2010; Rock et al., 1994). The three HIV PIs ritonavir (RTV), saquinavir (SQV), and nelfinavir (NFV) inhibit the activity of purified mouse or human 20S proteasomes and the proteasome activity in immortalized cells (Andre et al., 1998; Gaedicke et al., 2002), causing intracellular accumulation of polyubiquitinated proteins (Pajonk et al., 2002). In mice infected with lymphocytic choriomeningitis virus (LCMV) and treated with RTV, the cytotoxic immune response against two T cell epitopes of LCMV was reduced and prevented the expansion of

LCMV reactive CTL (Andre et al., 1998). We previously showed that HIV PIs by variably altering cellular proteasome and aminopeptidase activities in primary cells modify HIV protein degradation pattern, epitope production, and presentation, leading to variations in CTL responses (Kourjian et al., 2014).

In addition to the direct antigen presentation pathway, professional antigen presenting cells (APCs) have the ability to acquire exogenous antigens and present them on MHC-I molecules, by a mechanism known as cross-presentation (Guermonprez et al., 2002; Heath et al., 2004). Cross-presentation requires antigen transit through endosomes or phagosomes and eventually partial proteolysis by cathepsins (Amigorena and Savina, 2010). Peptides generated after the proteolysis can either escape into the cytosol and be further degraded in the direct antigen processing pathway (Kovacsovics-Bankowski and Rock, 1995) or they can be transported into a specialized mix ER-phagosome compartments (Bertholet et al., 2006) where they can be directly loaded onto the MHC-I and presented to the cell surface. Phagolysosomal cathepsin activities are tightly controlled, allowing the limited degradation of antigens without the destructing of potential antigenic peptides (Delamarre et al., 2005). Upon phagocytosis, phagosomes fuse first with early and late endosomes and then with lysosomes, thus acquiring progressively both the acidification machinery which is mainly the V-ATPase complex and the lysosomal proteases from the endocytic pathway (Claus et al., 1998). Acidification results in strong activation of cathepsins because their optimal proteolytic activities lie between pH 4.5 and pH 6, and vary among cathepsins (Claus et al., 1998; Dinter et al., 2015). In dendritic cell (DC) phagosomes, the acidification is delayed because protons are being used by NADPH oxidase NOX2 to generate reactive oxygen species (ROS), thus limiting cathepsin activities (Savina et al., 2006). The NOX2-mediated regulation of cathepsin activities allows the controlled degradation of antigens without the destruction of potential antigenic peptides. An alteration of this controlled environment by variations in NOX2 or cathepsin activities change the balance between production and further destruction of antigenic peptides, enhancing or impairing the cross-presentation of various MHC-I epitopes. For instance, DCs lacking NOX2 show enhanced phagosomal acidification and increased antigen degradation, resulting in impaired cross-presentation (Savina et al., 2006). Inhibitors of cathepsins affected antigen processing in the

endolysosomal compartment and altered epitope cross-presentation (Delamarre et al., 2005; Shen et al., 2004). Despite the role of cathepsins in the degradation of exogenous antigens in the endolysosomal compartment, no study has yet assessed in human primary cells the effect of PIs on cathepsin activities, the link between PI-induced alterations of cathepsins, antigen degradation in phagolysosomal compartments, and HIV epitope cross-presentation to CTLs.

The aim of this study was to investigate the effect of five HIV PIs (RTV, SQV, NFV, LPV/RTV [Kaletra] and darunavir (DRV)) on cathepsin activities in monocyte derived DCs, macrophages (MØ) and primary CD4 T cells. Our results showed that RTV reduce cathepsin activities but surprisingly SQV and NFV enhance the activities. Furthermore, by measuring phagosomal pH and oxidation, we found that the increase of cathepsin activity is caused by faster phagosome acidification and lower levels of ROS generation upon SQV and NFV treatment. This was due to lower phox-p47 phosphorylation and NOX2 assembly caused by SQV and NFV induced Akt and protein kinase C inhibition. Moreover, we showed that PI-induced alterations of cathepsin activity modify antigen degradation patterns and the amount of epitope precursor produced in compartments involved in cross-presentation. The alterations in the quantity of epitopes produced caused by HIV PIs, resulted in variable cross-presentation of HIV epitopes and recognition by CTLs. On top of the changes in the quantity of cross-presented epitopes, PI-induced alteration of cathepsin activities as well as activities of proteases involved in the direct antigen processing machinery (Kourjian et al., 2014) caused 32% change in the identity of the surface MHC-bound self peptidome upon treating PBMCs with SQV.

Altogether, these results show that by changing phagosomal physiology, HIV PIs modify cathepsin activities leading to altered antigen degradation, change the amount of epitope cross-presented to CTLs and modify cell surface immunopeptidome.

RESULTS

HIV PIs alter endolysosomal cathepsin activities

Exogenous antigens internalized by DCs and MØs are first degraded by proteases called cathepsins located in the endolysosomal compartments. We aimed to assess the effect of five HIV PIs (RTV, SQV, NFV, Kaletra and DRV) on cathepsin S and omnicathepsin activities which measures the combined activities of cathepsin S, cathepsin L, and cathepsin B, using fluorogenic peptide substrates as described previously (Dinter et al., 2014; Kourjian et al., 2014; Lazaro et al., 2009). We previously showed that the concentrations of the PIs used in this study corresponding to the level of PIs found in the plasma of ART-treated persons are not toxic for the cells (Acosta et al., 2000; Kourjian et al., 2014). For each protease activity, fluorescence was measured over time, and the hydrolysis kinetics was calculated as the maximum slope of fluorescence emission after subtraction of fluorescence in the absence of cells (Figure 1A). For each substrate, 100% represents the maximum slope of fluorescence emission by cells incubated with substrate and DMSO control. The specificity of substrate cleavage was checked by preincubation of cells with cognate inhibitors of omnicathepsin (E64) or cathepsin S (Z-FL-COCHO). In the presence of the specific inhibitor (E64), omnicathepsin activity was reduced by 14-fold compared to the control (maximum slope of 67 for control and 5 for E64). SQV increased the omnicathepsin activity by 6.7-fold and RTV reduced it by 1.9-fold (maximum slope of 430 for SQV and 36 for RTV) (Figure 1B). The effects of 5uM of RTV, SQV, NFV, Kaletra and DRV on omnicathepsin and cathepsin S activities were assessed in freshly isolated PBMCs, CD4 T cells, monocyte derived DCs and MØs from at least six different HIV- donors (Figure 1 C, D, E and F respectively). In PBMCs, RTV reduced both the omnicathepsin and cathepsin S activities by 3.3-fold. In contract, SQV and NFV increased the omnicathepsin activity by 3.6-fold and 3.2-fold respectively. Cathepsin S activity was increased 2-fold by SQV but not NFV. Kaletra and DRV did not significantly change these activities in PBMCs (Figure 1C). Similar alterations were seen in CD4 T cells, DCs and MØs but the activity fold change was different across the different cell types. SQV, NFV and Kaletra increased omnicathepsin and cathepsin S activities more than 10-fold in CD4 T cells compared to an average of 1.6-fold increase in DCs and MØs.

RTV reduced omnicathepsin and cathepsin S activities on average by 2.5-fold and 2.7-fold respectively (Figure 1 D, E, F). To further understand if HIV PIs are affecting the enzymes directly, PBMC whole cell extracts were used as source of enzymes. The pH of cell extracts was reduced to pH 4 in order to activate the cathepsins (Vaithilingam et al., 2013) and their activity was measured in presence of different PIs. Similar activity alterations were observed in PBMC extracts compared to live cells, however the fold change due to PIs was smaller in extracts (data not shown). The effect of PIs was also tested on recombinant cathepsin S and cathepsin D. RTV, NFV and Kaletra reduced cathepsin S activities by 1.85-fold, 1.35-fold and 2.6-fold respectively, in contrast SQV increased the activity by 1.24-fold (Figure 1G). Cathepsin D activity was reduced only by RTV 1.5-fold, in contrast SQV and NFV increased the activity by 1.7-fold and 1.9-fold respectively (Figure 1 H). We further wanted to test whether HIV PIs maturation of cathepsins. Most cathepsins are synthesized in their inactive procathepsin form. The activation process is triggered by a pH drop in the endolysosomal compartments, which induces the proteolytic removal of amino terminal pro-domain blocking the catalytic site of the cathepsin. To assess the impact of PIs on cathepsin activation procathepsin K was treated with 5uM of different PIs at different pH and then cathepsin K activity was measured. At pH 7 only SQV and NFV from the PIs tested activated the procathepsin K resulting in 7.5-fold activity increase compared to control (Figure 1I). Similarly at pH 5.5 SQV and NFV were able to activate more procathepsin K leading to an average of 1.75-fold activity increase. The alterations by HIV PIs seen on recombinant enzymes confirm that the drugs have a direct effect on cathepsins but the differences in the effect seen in live cells compared to extracts or recombinant enzymes suggest that other cellular mechanism might be causing additional alterations in live cells.

HIV PIs increase phagolysosomal acidification

Phagolysosomal cathepsin activities are tightly controlled allowing the limited degradation of antigens without destroying potential antigenic peptides. One of the most direct ways of controlling the activity of endolysosomal cathepsins is the pH (Claus et al., 1998; Dinter et al., 2015). To assess if the effect of HIV PIs on cathepsin activities are in part due to changes

in phagolysosomal pH we measured phagosomal pH in DCs, MØ and CD4 T cells in presence of different HIV PIs. In order to measure phagosomal pH in DCs and MØ accurately, we set up phagosomal pH measurement by flow cytometry (Savina et al., 2010). Latex beads were coated with pH-sensitive (fluorescein isothiocyanate, or FITC) and pH-insensitive (FluoProbe647) fluorescent dyes. After different times of phagocytosis of the beads, the fluorescence intensity was quantified using flow cytometry. The pH-insensitive dye allowed us to gate on cells that phagocytosed only one bead and the fluorescence intensity of the pH-sensitive dye reflected the pH in the phagosomal environment (Figure 2A). Similarly, E.coli-pHrodo® was used as another method to measure phagosomal pH in MØ and Dextran-pHrodo as a method to measure endosomal pH in CD4 T cells. Standard curves were obtained by permeabilizing cells and incubating them in predetermined pH media. FITC intensity decreased and pHrodo® intensity increased upon acidification (Figure 2B). HIV PI treatment did not affect bead uptake rate (Figure S1A) and confocal microscopy visually confirmed particle uptake (Figure S1B). The pH values in phagosomes were determined by reporting the mean fluorescence intensity in the cell population to the pH standard curves.

As previously shown (Savina et al., 2006), the pH in DC phagosomes stayed around 7-6.5 after 20min pulse and 90 min incubation at 37C (chase) (Figure 2C left). In contrast the pH in MØ phagosomes was below 6 after a 20 min pulse and a 10 min chase and acidified further over a 90 min chase, reaching values around pH 5 (Figure 2C middle). Similarly, using E.coli-pHrodo® the pH in MØ phagosomes after 60 min chase was around 5 (Figure S2B). SQV and NFV but not RTV and Kaletra reduced DC phagosomal pH after 60min chase by approximately 1 pH point and as expected, bafilomycin increased the pH by 1.3 pH points (Figure 2C and D left panel). HIV PIs did not significantly affect the phagosomal pH in MØs using the fluorochrome-coated bead assay (Figure 2C and D middle panel). However in the case of the E.coli-pHrodo® assay SQV but not the other PIs reduced the MØ phagosomal pH by 0.5 pH point after 60min chase (Figure S2C). In CD4 T cells, dextran-pHrodo® was used to measure endosomal pH (Figure 2A). The pH values were determined by reporting the mean fluorescence intensity to the standard curve (Figure 2B right panel) obtained similarly as before. CD4 T cell endolysosomal pH was reduced by SQV and NFV treatment by approximately 1 pH points after 60min chase.

RTV and Kaletra did not significantly change the pH (Figure 2C and D right panel). Bafilomycin treatment increased the pH on average by 1.3 pH point in all the cells tested. These results suggest that SQV and NFV but not RTV and Kaletra reduce phagosomal pH, which might explain the PI-induced increase of cathepsin activities.

HIV PIs reduce ROS generation in phagolysosomes

It was previously shown that phagosomal pH is in part regulated by the consumption of protons through the generation of ROS by NOX2 (Savina et al., 2006; Segal, 2005). To check that in our experimental model we incubated DCs with diphenylene iodonium (DPI), a specific inhibitor of flavin-containing enzymes such as NOX2. As expected phagosomal pH was reduced by approximately 1 pH point confirming that ROS in part regulate phagosomal pH (Figure 3A). Similarly, DPI treatment increased omnicathepsin and cathepsin S activities in DCs by 2.2-fold and 1.95-fold respectively confirming that phagosomal ROS by regulating the pH affect cathepsin activities (Figure 3B). We therefore hypothesized that HIV PIs might be modulating ROS generation by NOX2, subsequently affecting phagosomal pH, which in turn is altering cathepsin activities in the phagosomes (Figure 3C). To address the possible affect of HIV PIs on generation of ROS specifically in phagosomes, latex beads were coated with dihydrorhodamine 123 (DHR), a dye that only emits fluorescence under oxidative conditions (Savina et al., 2010), and an oxidation-insensitive (FluoProbe647) fluorescent dyes. After different times of phagocytosis, gating on cells that phagocytosed only one bead and quantifying the fluorescent intensity of DHR allowed us to measure ROS generation in the phagosomes (Figure 3D). As expected, in DC phagosomes at least two times more ROS was produced compared to MØs (Savina et al., 2006) (Figure 3E-F). ROS generation was strongly inhibited by DPI treatment. RTV and Kaletra did not significantly alter ROS production in DCs and MØs. In contrast, SQV and NFV significantly reduced ROS generation in DCs (-63 and -72 RFUs respectively) and to a lesser extent in MØs (-33 and -42 RFUs respectively) (Figure 3E-F-G-H). We concluded that SQV and NFV inhibit ROS generation, leading to phagosome acidification and increase in cathepsin activity.

The NOX2 is composed of multiple subunits and its activation is triggered by the phosphorylation of the phox-p47 subunit at multiple locations and by different kinase including Akt and PKC (El-Benna et al., 2009). Therefore, to examine whether SQV and NFV induced NOX2 activity reduction is due to lower phox-p47 phosphorylation level, we analyzed the phosphorylation of phox-p47 at serine 345 and serine 359 after PI treatment by western blot (Figure 4A). SQV and NFV reduced p47-ser359 phosphorylation by average of 1.7-fold but did not effect p47-ser345 phosphorylation (Figure 4B). To assess if this reduction in phosphorylation is caused by direct inhibition of kinase activities, we measured the Akt, protein kinase A, protein kinase C and Phosphoinositide-dependent kinase-1 activities in presence or absence of different PIs. SQV and NFV moderately reduced all 4 kinase activities tested by an average of 1.5-fold suggesting that kinase inhibition is causing less phox-p47 phosphorylation, which is leading to lower NOX2 activity and less ROS production in phagosomes.

HIV PIs alter degradation pattern and cutting site frequencies of antigenic peptides

Exogenous antigens internalized by DCs and MØs are first processed by cathepsins located in the endo-lysosomal compartments (Colbert et al., 2009). In order to analyze how the cathepsin activity alteration by HIV PIs is affecting antigen processing in compartments involved in cross-presentation we used in vitro antigen degradation assay previously developed in the lab (Kourjian et al., 2014; Vaithilingam et al., 2013). Whole cell extracts from DCs, MØs and CD4 T cells in acidic conditions were used as a source of proteases to degrade a synthetic 35-mer peptide representing HIV-1 Gag p24 (MVHQAISPRTLNAWVKVVEEKAFSPEVIPMFAALS, aa 10-44 in Gag p24) containing the epitopes ISW9 and KF11. Figure S3 shows degradation products of the 35-mer p24 peptide identified by LC-MS/MS after a 60-min degradation in DC, MØ and CD4 T cell extracts in the absence of PIs. The intensity of peptides cut at the same amino acid location from the N-terminus side of the peptide were added and divided by the total degradation product intensity giving us the percentage of cut at that specific amino acid location. This cutting site analysis was done at each amino acid location from the N-terminus side of the peptide as well as the C-terminus side. The analysis shows how much the peptide is cut at each amino acid location relatively to other positions. We observed differences in the

frequency of the cutting sites when we compared degradations using DC, MØ and CD4 T cell extracts confirming the differential antigen-processing activities by different cell types which was previously reported by our lab (Dinter et al., 2014; Lazaro et al., 2009) (Figure 5A left panel). Similar analysis was performed for degradations done in presence of different HIV PIs. In DCs, RTV and SQV changes the cleavage pattern of the peptide. SQV introduced new cutting sites within the ISW9 epitope (N-ter of proline position 8 and C-ter of arginine position 9). RTV and SQV also changed the frequency of certain cutting sites (for example N-ter of valine position 17 and C-ter of proline position 29) (Figure 5A right panel). In order to display the changes in the degradation patterns induced by the PIs, heat maps were generated showing the difference in the frequency of the cuts at each amino acid location. Figure 5B shows that HIV PIs change the degradation pattern of epitopes increasing the cuts at some locations and decreasing it in others. For instance SQV increased the cleavage within the ISW9 epitope in DCs (Figure 5B top panel), potentially leading to the destruction of the epitope and the reduction of the amount available for surface presentation. To further understand the effect of the PIs on epitope production, we analyzed the changes in the amount of epitope-containing fragments generated. In DCs, SQV reduced the production of B57-ISW9-containing fragments by 1.7-fold which was expected because of the increased cleavage within the epitope seen in Figure 5 B top panel. RTV reduced the production of B57-KF11 containing fragments by 1.8-fold and B57-ISW9 containing fragments by 6-fold. In MØs, RTV and SQV reduced both by 2-fold the amount of B57-ISW9 containing fragment. The amount of B57-KF11-containing fragments was reduced 2.6-fold by RTV and increased 2-fold by SQV, 2-fold by NFV and 1.4-fold by Kaletra. In CD4 T cells, B57-ISW9 containing fragment amount was reduced 6-fold by SQV. B57-KF11 containing fragment amount was increased 2-fold by RTV and 3-fold by SQV, NFV and Kaletra (Figure 5C). Beside the PI-induced changes in the amount of ISW9 and KF11-containing fragments, HIV PI treatments changed the size distribution of the degradation products. The amount of 8-12 aa long peptides was reduced by all PIs by an average of 2-fold in DCs and MØs. In CD4 T cells the amount of 13-18 aa long peptides was reduced 2.7-fold by RTV, 1.7-fold by SQV, 1.4-fold by NFV and 3-fold by Kaletra (Figure 5D). Together these results suggest that PIs by altering cathepsin activities are changing the frequency of different cutting sites. These changes are

affecting the amount of different epitope production wich in turn may affect the amount of epitopes presented to the cell surface by MHC-I.

HIV PIs alter the cross-presentation of HLA-B57-restricted Gag p24 KF11, ISW9 and TW10.

In order to understand if cathepsin activity alteration and epitope degradation pattern modification by HIV PIs affect epitope presentation to the cell surface by MHC-I we analyzed the cross-presentation of the three optimally defined HLA-B57 restricted HIV-epitopes originating from HIV-1 p24 protein by DCs: HLA-B57-restricted ISW9 (ISPRTLNAW, aa 15-23 in Gag p24), HLA-B57-restricted KF11 (KAFSPEVIPMF, aa 30-40 in Gag p24), and HLA-B57-restricted TW10 (TSTLQEQIGW, aa 108-117 in Gag p24) (Goulder et al., 1996; Yusim, 2013). DCs were derived from HLA-B57+ patients' monocytes, loaded with HIV-1 p24 protein in presence of different HIV PIs and challenged with epitope specific cytotoxic T cells (CTLs). The killing was monitored using a florescent-based assay developed in the lab (Gourdain et al., 2013). We first assessed the effect of HIV PIs on the level of MHC-I surface expression in DCs. No significant difference was observed upon HIV PIs treatment as previously seen in B cell lines (Kourjian et al., 2014) (Figure 6A). DCs pulsed with increasing concentration of peptides showed increased killing when challenged with the appropriate CTLs validating the sensitivity of our system (Figure 6B). RTV unlike the other PIs tested reduced by 1.4-fold the B57-KF11 cross-presentation by DCs compared to control (Figure 6C). B57-ISW9 cross-presentation was reduced by RTV and SQV (3.2-fold and 1.6-fold respectively). In contract, NFV increased the killing by 1.35-fold (Figure 6D). RTV reduced B57-TW10 cross-presentation by 2.4-fold while SQV increased it by 1.4-fold (Figure 6E). The amount of epitope cross-presented to the cell surface depends to the amount of this epitope produced in compartments involved in cross-presentation. HIV PI-induced alterations in the amount of epitope containing fragments produced led to changes in the amount of epitope cross-presentation. For instance, SQV enhanced the cutting site frequency within the B57-ISW9 epitope (Figure 5B) leading to reduced production of B57-ISW9 containing fragments (Figure 5C), which resulted in lower cross-presentation of B57-ISW9 by DCs (Figure 6D) confirming the link between drug-induced

alteration of epitope production and subsequent changes in epitope-specific CTL responses to cross-presented epitopes.

HIV PI alter PBMC self surface MHC peptidome

To further investigate if HIV PIs alter surface MHC peptide presentation, we directly sequenced by MS the surface self-peptidome of human PBMCs treated or not with SQV. Peptides eluted directly from the live cells surface) were identified and comparatively mapped by high resolution MS.

In total we identified, with the high mass accuracy, 686 and 680 host derived MHC peptides presented by control and SQV treated PBMCs, respectively. However, among them, only 148 Control-PBMC and 155 SQV-PBMC derived peptides that were identified with the highest confidence, highly scored and highly reproducible between multiple runs were considered for further analysis (Table S1). SQV treatment altered the surface self-peptidome of PBMCs. The comparative mapping revealed that 68% of peptides were commonly presented between control and SQV treated PBMCs whereas, 32% of MHC peptides were uniquely presented by either, control or treated cells (Figure 7A). Analysis of the length of the peptides showed that the peptides uniquely presented upon SQV treatment were longer in size compared to peptides presented by control-PBMCs. More than 80% of the peptides presented uniquely on SQV-PBMCs were longer than 13 amino acid compared to only 60% of the peptides presented uniquely on Control-PBMCs and 40% of peptides commonly present on Control-PBMCs and SQV-PBMCs (Figure 7B). Assuming that surface peptides longer than 13 amino acid correspond to MHC-II bound peptides and knowing that SQV does not increase MHC-II surface expression level (data not know), these data suggest that SQV might be increasing the diversity of the peptidome bound to MHC-II.

MHC peptidome of treated and untreated PBMCs were sampled from similar number of the host proteins. Many of the commonly identified MHC peptides were derived from the same protein and were sampled as nested peptides with an average of 3 peptides per protein (Figure

7C). However, uniquely identified peptidome from both, treated and untreated PBMCs were sampled rather from diverse proteins and more often with one peptide derived from one protein (Figure 7C).

Further analysis of the proteins of origin revealed that 64% of all proteins identified were represented by both treated and untreated PBMCs, whereas 18% were uniquely represented on control-PBMCs and another 18% only on SQV-PBMCs suggesting that SQV is changing the origin of proteins represented on the surface (Figure 7D). This might be explained by a possible SQV-induced alteration of protein expressions. The group of proteins represented by both treated and untreated PBMCs was further divided into subgroups depending on the diversity of the locations the peptides derived from. Peptides presented commonly or uniquely were derived from the same location in 64% of the case of proteins represented by both treated and untreated PBMCs (Figure 7D - similar). In 22% of the proteins from this group SQV treatment narrowed the location from which the peptides are derived (Figure 7D – narrowing), whereas in the remaining 14% of the proteins SQV broadened the location of the peptides (Figure 7D – broadening).

These data suggest that SQV treatment is changing MHC surface peptidome including broadening the presentation of peptides coming from some proteins and narrowing the presentation of peptides coming from others.

DISCUSSION

In addition to the presentation of epitopes derived from endogenous proteins, APCs have the ability to process exogenous antigen by phagosomal cathepsins and cross-present the epitopes on MHC-I to CTLs. Any perturbation of protease or peptidase activities could modify protein degradation patterns and consequently epitope cross-presentation. In this study, we showed that several HIV PIs, by changing phagosomal acidification and affecting cathepsin activities, alter HIV Ag degradation patterns leading to variations in HIV epitope cross-presentation and recognition by CD8 T cells.

We discovered that four of the five PIs tested affect cellular cathepsin activities. NFV for instance reduced cathepsin S activity and enhanced cathepsin D activity, whereas RTV mostly reduced all cathepsin activities tested, suggesting different interactions between each drug and cathepsins. HIV PIs might bind directly to the catalytic site or might interact with noncatalytic effector sites on cathepsins that were shown in enzymatic studies to regulate the hydrolytic activities (Novinec et al., 2014). This would provide a potential mechanism of either inhibition or enhancement of cathepsin activities by HIV PIs, although molecular modeling and structural studies are required to test this hypothesis. We discovered that SQV and NFV facilitate the maturation of procathepsin K even at neutral pH. Most cathepsins are synthesized in their inactive procathepsin form. The activation process is triggered by a pH drop in the endolysosomal compartments, which induces the proteolytic removal of amino terminal pro-domain blocking the catalytic site of the cathepsin. This pH dependent activation restricts cathepsin hydrolytic activity only to lysosomal compartments. It was discovered that glycoaminoglycans (GAG) can at neutral pH loosen the binding of the propeptide on the catalytic site and accelerate the autocatalytic removal of the propeptide subsequently activating cathepsins (Caglic et al., 2007; Vasiljeva et al., 2005). Similarly, SQV and NFV might be using the same mechanism as GAG to facilitate the maturation of cathepsins at neutral pH, although structural studies are needed to test this hypothesis. Excessive cathepsin activation and extracellular presence of active cathepsins are linked to inflammation of the mucosa and damage to the musocal barrier (Menzel et al., 2006). Therefore HIV PI-induced cathepsin activation and increased maturation might be involved in damaging the mucosa, allowing

microbial translocation and causing chronic immune activation in patients on ART. In addition, cathepsin dysregulation is also associated with various other pathological conditions, such as cancer, rheumatoid arthritis, atherogenesis and muscular dystrophy (Turk et al., 2012). Additional research is needed to investigate if PI-induced cathepsin alteration contributes to the development of such disease in patients using long term ART.

First-generation PIs like RTV, SQV, and NFV showed stronger effect on cathepsin activities than newer PIs like DRV. First-generation PIs also induced more rapid and profound adverse effects on lipid metabolism and reduced bone mineral density than did newer PIs (Brown and Qaqish, 2006; Carr et al., 1998; Duvivier et al., 2009). It has been proposed that lipid metabolism disorder associated with NFV is caused in part by enhanced lysosome-mediated perilipin proteolysis which is a protein involved in regulating adipocyte lipolysis. NFV induced 6-fold reduction of perilipin half-life was reversed by NH4Cl but not by proteasome inhibition suggesting the involvement of lysosomal proteases in NFV-induced perilipin proteolysis. However the exact mechanism of this enhanced degradation is not clear (Kovsan et al., 2007). NFV-induced lysosomal cathepsin activity increase showed in this study might directly explain the enhancement of perilipin proteolysis in the lysosomes that is contributing to the lipid metabolism disorders in patients on ART.

Osteoporosis and osteopenia are side effect associated with first generation PI use (Brown and Qaqish, 2006; Duvivier et al., 2009). Cathepsins play a crucial role in bone remodeling by degrading type I collagens in the bone resorption pits (Saftig et al., 1998). SQV- and NFV-induced cathepsin activity increase that we showed in this study might explain the excessive bone collagen degradation and the bone density reduction seen in patients on PIs, however further studies are needed to confirm this hypothesis.

SQV and NFV have been shown to have pleiotropic anti-cancer activity and are now repurposed for cancer treatment. Experimental studies connect the anticancer effects of some PIs to the suppression of the Akt signaling pathway, but the actual molecular targets remain unknown (Plastaras et al., 2008). Our results show that SQV and NFV are able to directly inhibit multiple members of the protein kinase-like superfamily, which are involved in the regulation of cellular processes vital for carcinogenesis and metastasis. This finding provides a molecular

basis to explain the broad-spectrum anti-cancer effect of SQV and NFV. Since, kinases regulate many complex processes in cells and the extent to which the PI-induced kinase activity alterations affect other cellular processes is unknown and needs to be addressed.

In this study we showed that SQV and NFV -by inhibiting Akt kinase and protein kinase C (PKC)- reduce the phosphorylation of phox-p47 which is required for the assembly of active NOX2 (El-Benna et al., 2009). The multicomponent NOX2 enzyme produces ROS in the phagosomes of neutrophils, eosinophils, monocytes and MØs contributing to the destruction of the engulfed pathogens (Segal, 2005). The phagosomal NOX2 and ROS production play key role in host defense against microbial pathogens as illustrated by a human genetic disorder called chronic granulomatous disease (CGC), which is associated with life-threatening bacterial and fungal infections and is characterized by an absence of ROS production due to a deficiency in one of the components of NOX2 (Meischl and Roos, 1998). The NOX2 complex is composed of multiple subunits and its activation is triggered by the phosphorylation of the phox-p47 subunit at multiple locations and by different kinase including Akt and PKC (El-Benna et al., 2009). SQV and NFV by inhibiting Akt and PKC activity partially reduce the phosphorylation of phox-p47 thus inhibiting NOX2 activity and reducing ROS production in DC and MØ phagosomes. The impact of the PI-induced NOX2 activity inhibition on MØ capacity to kill phagocytosed pathogens remains unknown and needs to be further investigated. In addition to their role in microbial killing, NOX2 by consuming protons to produce ROS is involved in maintaining neutral DC phagosomal pH. This controlled pH confers DCs the ability to cross-present by limiting degradation of the phagocytosed antigens without the destruction of potential antigenic peptides. This was confirmed by NOX2 deficient DC's inability to cross-present (Savina et al., 2006). In this study we showed that SQV and NFV by inhibiting NOX2 activity increase the DC phagosome acidification and lead to enhancement in cathepsin activities. The HIV PI-induced direct and indirect (via increased phagosome acidification) alteration of cathepsin activity modified long HIV peptide and full protein degradation patterns in lysosomal compartments. These changes in antigen processing resulted in alterations in the amount of peptides available for direct MHC-I loading in the vacuolar pathway or further processing in the cytosolic pathway and subsequently led to altered HIV epitope cross-presentation to CTL. Cutting site analysis

showed that HIV PI effect on phagosomal antigen processing was drug and sequence dependent as well as variable depending on the cell subset tested which is in line with our previous data showing that various cell subsets present different levels of peptidase activities (Dinter et al., 2014; Lazaro et al., 2009). Given that each cathepsin has different sequence specificities (Turk et al., 2012), a given PI -by variably changing the activities of the different cathepsins available- may increase the cleavage of certain motifs and decrease the degradation of others. Further in depth analysis of PI induced enhancement or reduction of the cutting intensity at each amino acid location of full HIV proteins (Figure S4) will allow us to predict the effect of each PIs treatment on the amount of different epitope production.

These findings have implications for the degradation of HIV proteins and beyond. First, in the context of HIV protein degradation, specifically in ART-treated persons with ongoing replication of drug-resistant mutated strains, PIs by altering cathepsin activities might be changing the cross-presentation of HIV derived epitopes by APCs. Although the lack of appropriate clinical samples precludes us to test this hypothesis, PI-induced modification of the self-immunopeptidome landscape on PBMC surface observed in this study suggest that HIV PIs may contribute to broadening some CTL responses against HIV and narrowing others in ART-treated patients with ongoing viral replication. In addition, studying the impact of PIs on HIV epitope cross-presentation is relevant to approaches to purge HIV reservoirs by combining provirus reactivation in the presence of ART to prevent replication, and therapeutic vaccination to boost immune responses against HIV (Archin et al., 2012; Siliciano and Siliciano, 2013). If ART needed to prevent replication after provirus reactivation calls for inclusion of HIV PIs, it will be important to assess the impact of HIV PIs on the cross-presentation efficiency of the therapeutic vaccines and the induction of broad CTL responses needed to eliminate the reactivated HIV-epitope presenting cells (Deng et al., 2015).

Second, HIV PIs by modifying cathepsin activities might also alter the degradation and the cross-presentation of proteins derived from other pathogens infecting ART-treated persons. More than half of HIV+ individuals worldwide become coinfected with other pathogens such as tuberculosis or HCV, and effective drug combinations to curb both infections are needed (Jalali and Rockstroh, 2012; Naidoo et al., 2013). Assessing whether and how ART, beyond reducing

HIV viral load and cellular activation, may possibly contribute to diversifying immune responses against coinfecting pathogens by modifying the degradation patterns of these pathogens provides a new outlook of the use of HIV PIs. Similarly, in the repositioning of PIs as cancer therapy, another potential benefit could be a PI-induced altered processing of cancer Ags, potentially leading to the cross-presentation of different cancer Ag-derived peptide leading to the activation of new immune responses.

Third, because endolysosomal pH and cathepsin activity regulate MHC-II epitope processing, it is very likely that HIV PI-induced modifications of phagosomal acidification and cathepsin activities alter antigen processing and MHC-II epitope presentation. The increase upon SQV treatment in the number of 13-18 amino acid long self-peptidome presented on the surface of PBMCs suggest that SQV might be broadening the MHC-II surface peptidome, however, more immunological and quantitative studies are needed to confirm this hypothesis.
Our results indicate that HIV PIs, by altering Akt and PKC, NOX2 and cathepsin activities, modify antigen processing in lysosomal compartments and epitope cross-presentation. Additional structural studies are needed to understand the mechanism behind the PI-induced alterations of various classes of enzymes. However, if HIV PIs allow diversification of epitope presentation, they may provide complementary approaches to broaden the immune responses against various immune diseases, considering that temporary PI treatment would not induce toxicity and adverse effects observed in long-term HAART.

Experimental Procedures

Antiretroviral drugs

HIV PIs were obtained from Selleckchem (RTV, LPV, and DRV), Sigma (SQV), and Santa Cruz (NFV). All drugs were dissolved in 100% DMSO. Kaletra was prepared by combining LPV and RTV with 5:1 ratio, respectively; subsequently, Kaletra concentrations mentioned in this article correspond to LPV amount. Stock solutions of 10 mM were kept at -20C, and fresh aliquots were used for each experiment.

Cell culture

Cells were isolated from HLA-typed blood donors or anonymous buffy coats after written informed consent and approval by the institutional review board. Human peripheral blood mononuclear cells (PBMCs) were isolated by Ficoll-Hypaque (Sigma-Aldrich, USA) density centrifugation. Monocytes and CD4 T cells were isolated using CD14+ and CD4+ magnetic isolation kits respectively (StemCell, Canada). Monocytes were differentiated into DCs and Møs (Dinter et al., 2014).

Measurement of phagosomal pH and ROS production

Phagosomal pH and ROS production was measured as described in (Savina et al., 2010). Briefly, beads were covalently coupled with FITC and FluoProbes 647 DHR 123 (Life Technologies). Cells treated for 30min with different HIV PIs (5uM) or inhibitors (10 uM of DPI or 1 uM Bafilomycin) were pulsed with the beads for 20 min and then extensively washed in cold PBS. The cells were then incubated at 37C (‘‘chased’’) for the indicated times and immediately analyzed by flow cytometry. Ecoli-pHrodo (Life Technologies) and 10,000MW Dextran-pHrodo (Life Technologies) were used in the same way as described above.

In vitro peptide degradation assay and MS analysis

Peptide degradation and MS analysis was performed as we previously described in (Dinter et al., 2015; Kourjian et al., 2014). Briefly, 2nmol of pure peptides were digested with 15µg of whole cell extracts at 37°C in pH4 degradation buffer (Vaithilingam et al., 2013). The degradation was stopped with 2.5µL of 100% formic acid and peptide fragments were purified by 5% trichloroacetic acid precipitation. Peptides in the digestion mix were identified by in house MS as previously described (Dinter et al., 2015; Kourjian et al., 2014).

Fluorescent measurement of proteolytic activities in live cells and cell extracts

Proteolytic activity measurement was performed as we previously described in (Dinter et al., 2015; Kourjian et al., 2014; Lazaro et al., 2009). Briefly, 5x104 DCs, Møs or CD4T cells were pretreated with the indicated PIs and the omnicathepsin or cathepsin S activities were measured using specific fluorogenic substrates. Specific inhibitors were used to confirm the specificity of the reactions. The rate of fluorescence emission, which is proportional to the proteolytic activity, was measured every 5 minutes at 37°C in a Victor-3 Plate Reader (Perkin Elmer).

Phox-p47 expression and phosphorylation level by Western blot, and kinase activity measurement

Protein extracts (30 ug/lane) from treated or untreated DCs were subjected to SDS-PAGE on 4%–12% gradient gel. After transferring, the membranes were blocked and incubated with primary antibodies and secondary antibodies IRDye® Li-Cor). Protein bands were visualized by dual infrared fluorophore Odyssey Infrared Imaging System, and densitometric quantification was performed (Li-cor Biosciences). To measure kinase activities, the "Kinase Selectivity Profiling System: AGC-1" (Promega) was used in addition to "Kinase-Glo® Luminescent kit" (Promega). The assays were done in accordance with the protocols from Promega.

Cross-presentation assay

Immature DCs were exposed to recombinant HIV-1 p24-protein (Abcam, USA) for 1hr at 37C. Cells pulsed with the indicated concentrations of the optimal epitopes were used as controls for antigen presentation and CTL clone specificity. DCs were thoroughly washed and cultured for 4 hours before adding the epitope-specific CTL clones at a 4:1 effector-to-target ratio in 96-well plates (Millipore). The target lysis was measured using a fluorescent-based cell lysis measurement method previously developed in the lab (Gourdain et al., 2013).

Acid elution of MHC peptides and identification by MS

Peptides bound to MHC molecules and presented at the surface of control and drug treated PBMCs were isolated directly from the live cells and identified by high resolution tandem. In brief, 5x107 cells were shortly exposed to mild acid treatment (10% acetic acid, 5 min) and peptide pool obtained was immediately subjected to ultrafiltration (3 kDa cut-off) for MHC peptides enrichment. The pools of eluted peptides were further subjected to LC-ESI-MS/MS analysis using an Eksigent HPLC system (Eksigent) directly interfaced with an Orbitrap LTQ XL MS (Thermo Fisher). Ten most abundant multiply charged ions were selected for high resolution MS/MS sequencing. Data were analyzed with Proteome Discoverer 1.4 (Thermo Fisher) software and searched against SwissProt human database using MASCOT search engine. To ensure high accuracy of identified sequences, the mass tolerance on precursor was set to 5 ppm and 0.02 Da for fragment ions with all assignments made at 1% FDR. The candidate MHC peptides identified were selected based on their presence in replicate samples. All identified MHC peptides were blasted against nonredundant SwissProt database restricted to human entries to identify their corresponding source proteins.

Dextran-pHrodo and Ecoli-pHrodo uptake visualization using confocal microscopy

CD4 T cell or MØs were plated in poly-L-lysine-coated glass chambers (Nunc™ Lab-Tek™ Chambered Coverglass - Themoscientific) and incubated for 1h at 37C and 5% CO2. Dextran-pHrodo 10,000MW (Lifesciences) was added to CD4 T cells and Ecoli-pHrodo (Lifesciences) was added to MØs and incubated for 1 hour. After extensive wash the glass chamber was incubated in the environmental chamber for live cell imaging and the fluorescence was visualized by Zeiss confocal microscope (LSM 510) using 63 3 1.4 NA oil immersion objective. Images were analyzed using Imaris 7.6 software.

AUTHOR CONTRIBUTIONS

Conceived and designed the experiments: GK SLG. Performed the experiments: GK MR MB DW. Analyzed the data: GK MR MB SLG. Contributed reagents/materials: JD BJ MR. Wrote the paper: GK MR SLG.

ACKNOWLEDGMENTS

We thank Drs. D. Kavanagh, F. Pereyra, and S. Pillai for stimulating discussions and input on the manuscript.

REFERENCES

Acosta, E.P., Kakuda, T.N., Brundage, R.C., Anderson, P.L., and Fletcher, C.V. (2000). Pharmacodynamics of human immunodeficiency virus type 1 protease inhibitors. Clinical infectious diseases : an official publication of the Infectious Diseases Society of America *30 Suppl 2*, S151-159.

Amigorena, S., and Savina, A. (2010). Intracellular mechanisms of antigen cross presentation in dendritic cells. Current opinion in immunology *22*, 109-117.

Andre, P., Groettrup, M., Klenerman, P., de Giuli, R., Booth, B.L., Jr., Cerundolo, V., Bonneville, M., Jotereau, F., Zinkernagel, R.M., and Lotteau, V. (1998). An inhibitor of HIV-1 protease modulates proteasome activity, antigen presentation, and T cell responses. Proceedings of the National Academy of Sciences of the United States of America *95*, 13120-13124.

Archin, N.M., Liberty, A.L., Kashuba, A.D., Choudhary, S.K., Kuruc, J.D., Crooks, A.M., Parker, D.C., Anderson, E.M., Kearney, M.F., Strain, M.C*., et al.* (2012). Administration of vorinostat disrupts HIV-1 latency in patients on antiretroviral therapy. Nature *487*, 482-485.

Autran, B., Carcelain, G., Li, T.S., Blanc, C., Mathez, D., Tubiana, R., Katlama, C., Debre, P., and Leibowitch, J. (1997). Positive effects of combined antiretroviral therapy on CD4+ T cell homeostasis and function in advanced HIV disease. Science *277*, 112-116.

Bertholet, S., Goldszmid, R., Morrot, A., Debrabant, A., Afrin, F., Collazo-Custodio, C., Houde, M., Desjardins, M., Sher, A., and Sacks, D. (2006). Leishmania antigens are presented to CD8+ T cells by a transporter associated with antigen processing-independent pathway in vitro and in vivo. Journal of immunology *177*, 3525-3533.

Blanchard, N., Kanaseki, T., Escobar, H., Delebecque, F., Nagarajan, N.A., Reyes-Vargas, E., Crockett, D.K., Raulet, D.H., Delgado, J.C., and Shastri, N. (2010). Endoplasmic reticulum aminopeptidase associated with antigen processing defines the composition and structure of MHC class I peptide repertoire in normal and virus-infected cells. Journal of immunology *184*, 3033-3042.

Brown, T.T., and Qaqish, R.B. (2006). Antiretroviral therapy and the prevalence of osteopenia and osteoporosis: a meta-analytic review. Aids *20*, 2165-2174.

Caglic, D., Pungercar, J.R., Pejler, G., Turk, V., and Turk, B. (2007). Glycosaminoglycans facilitate procathepsin B activation through disruption of propeptide-mature enzyme interactions. The Journal of biological chemistry *282*, 33076-33085.

Carr, A., Samaras, K., Burton, S., Law, M., Freund, J., Chisholm, D.J., and Cooper, D.A. (1998). A syndrome of peripheral lipodystrophy, hyperlipidaemia and insulin resistance in patients receiving HIV protease inhibitors. Aids *12*, F51-58.
Claus, V., Jahraus, A., Tjelle, T., Berg, T., Kirschke, H., Faulstich, H., and Griffiths, G. (1998). Lysosomal enzyme trafficking between phagosomes, endosomes, and lysosomes in J774 macrophages. Enrichment of cathepsin H in early endosomes. The Journal of biological chemistry *273*, 9842-9851.
Colbert, J.D., Matthews, S.P., Miller, G., and Watts, C. (2009). Diverse regulatory roles for lysosomal proteases in the immune response. European journal of immunology *39*, 2955-2965.
Delamarre, L., Pack, M., Chang, H., Mellman, I., and Trombetta, E.S. (2005). Differential lysosomal proteolysis in antigen-presenting cells determines antigen fate. Science *307*, 1630-1634.
Deng, K., Pertea, M., Rongvaux, A., Wang, L., Durand, C.M., Ghiaur, G., Lai, J., McHugh, H.L., Hao, H., Zhang, H.*, et al.* (2015). Broad CTL response is required to clear latent HIV-1 due to dominance of escape mutations. Nature *517*, 381-385.
Diez-Rivero, C.M., Lafuente, E.M., and Reche, P.A. (2010). Computational analysis and modeling of cleavage by the immunoproteasome and the constitutive proteasome. BMC bioinformatics *11*, 479.
Dinter, J., Duong, E., Lai, N.Y., Berberich, M.J., Kourjian, G., Bracho-Sanchez, E., Chu, D., Su, H., Zhang, S.C., and Le Gall, S. (2015). Variable processing and cross-presentation of HIV by dendritic cells and macrophages shapes CTL immunodominance and immune escape. PLoS pathogens *11*, e1004725.
Dinter, J., Gourdain, P., Lai, N.Y., Duong, E., Bracho-Sanchez, E., Rucevic, M., Liebesny, P.H., Xu, Y., Shimada, M., Ghebremichael, M.*, et al.* (2014). Different antigen-processing activities in dendritic cells, macrophages, and monocytes lead to uneven production of HIV epitopes and affect CTL recognition. Journal of immunology *193*, 4322-4334.
Duvivier, C., Kolta, S., Assoumou, L., Ghosn, J., Rozenberg, S., Murphy, R.L., Katlama, C., Costagliola, D., and group, A.H.s. (2009). Greater decrease in bone mineral density with protease inhibitor regimens compared with nonnucleoside reverse transcriptase inhibitor regimens in HIV-1 infected naive patients. Aids *23*, 817-824.
El-Benna, J., Dang, P.M., Gougerot-Pocidalo, M.A., Marie, J.C., and Braut-Boucher, F. (2009). p47phox, the phagocyte NADPH oxidase/NOX2 organizer: structure, phosphorylation and implication in diseases. Experimental & molecular medicine *41*, 217-225.
Erickson, J., Neidhart, D.J., VanDrie, J., Kempf, D.J., Wang, X.C., Norbeck, D.W., Plattner, J.J., Rittenhouse, J.W., Turon, M., Wideburg, N.*, et al.* (1990). Design, activity, and 2.8 A crystal structure of a C2 symmetric inhibitor complexed to HIV-1 protease. Science *249*, 527-533.
Flexner, C. (1998). HIV-protease inhibitors. The New England journal of medicine *338*, 1281-1292.
Gaedicke, S., Firat-Geier, E., Constantiniu, O., Lucchiari-Hartz, M., Freudenberg, M., Galanos, C., and Niedermann, G. (2002). Antitumor effect of the human immunodeficiency virus protease inhibitor ritonavir: induction of tumor-cell apoptosis associated with perturbation of proteasomal proteolysis. Cancer research *62*, 6901-6908.
Goldberg, A.L. (2003). Protein degradation and protection against misfolded or damaged proteins. Nature *426*, 895-899.
Goulder, P.J., Bunce, M., Krausa, P., McIntyre, K., Crowley, S., Morgan, B., Edwards, A., Giangrande, P., Phillips, R.E., and McMichael, A.J. (1996). Novel, cross-restricted, conserved, and immunodominant cytotoxic T lymphocyte epitopes in slow progressors in HIV type 1 infection. AIDS research and human retroviruses *12*, 1691-1698.
Gourdain, P., Boucau, J., Kourjian, G., Lai, N.Y., Duong, E., and Le Gall, S. (2013). A real-time killing assay to follow viral epitope presentation to CD8 T cells. Journal of immunological methods *398-399*, 60-67.
Guermonprez, P., Valladeau, J., Zitvogel, L., Thery, C., and Amigorena, S. (2002). Antigen presentation and T cell stimulation by dendritic cells. Annual review of immunology *20*, 621-667.

Heath, W.R., Belz, G.T., Behrens, G.M., Smith, C.M., Forehan, S.P., Parish, I.A., Davey, G.M., Wilson, N.S., Carbone, F.R., and Villadangos, J.A. (2004). Cross-presentation, dendritic cell subsets, and the generation of immunity to cellular antigens. Immunological reviews *199*, 9-26.
Jalali, Z., and Rockstroh, J.K. (2012). Antiviral drugs and the treatment of hepatitis C. Current HIV/AIDS reports *9*, 132-138.
Kourjian, G., Xu, Y., Mondesire-Crump, I., Shimada, M., Gourdain, P., and Le Gall, S. (2014). Sequence-specific alterations of epitope production by HIV protease inhibitors. Journal of immunology *192*, 3496-3506.
Kovacsovics-Bankowski, M., and Rock, K.L. (1995). A phagosome-to-cytosol pathway for exogenous antigens presented on MHC class I molecules. Science *267*, 243-246.
Kovsan, J., Ben-Romano, R., Souza, S.C., Greenberg, A.S., and Rudich, A. (2007). Regulation of adipocyte lipolysis by degradation of the perilipin protein: nelfinavir enhances lysosome-mediated perilipin proteolysis. The Journal of biological chemistry *282*, 21704-21711.
Lazaro, E., Godfrey, S.B., Stamegna, P., Ogbechie, T., Kerrigan, C., Zhang, M., Walker, B.D., and Le Gall, S. (2009). Differential HIV epitope processing in monocytes and CD4 T cells affects cytotoxic T lymphocyte recognition. The Journal of infectious diseases *200*, 236-243.
Meischl, C., and Roos, D. (1998). The molecular basis of chronic granulomatous disease. Springer seminars in immunopathology *19*, 417-434.
Menzel, K., Hausmann, M., Obermeier, F., Schreiter, K., Dunger, N., Bataille, F., Falk, W., Scholmerich, J., Herfarth, H., and Rogler, G. (2006). Cathepsins B, L and D in inflammatory bowel disease macrophages and potential therapeutic effects of cathepsin inhibition in vivo. Clinical and experimental immunology *146*, 169-180.
Naidoo, K., Baxter, C., and Abdool Karim, S.S. (2013). When to start antiretroviral therapy during tuberculosis treatment? Current opinion in infectious diseases *26*, 35-42.
Novinec, M., Korenc, M., Caflisch, A., Ranganathan, R., Lenarcic, B., and Baici, A. (2014). A novel allosteric mechanism in the cysteine peptidase cathepsin K discovered by computational methods. Nature communications *5*, 3287.
Pajonk, F., Himmelsbach, J., Riess, K., Sommer, A., and McBride, W.H. (2002). The human immunodeficiency virus (HIV)-1 protease inhibitor saquinavir inhibits proteasome function and causes apoptosis and radiosensitization in non-HIV-associated human cancer cells. Cancer research *62*, 5230-5235.
Plastaras, J.P., Vapiwala, N., Ahmed, M.S., Gudonis, D., Cerniglia, G.J., Feldman, M.D., Frank, I., and Gupta, A.K. (2008). Validation and toxicity of PI3K/Akt pathway inhibition by HIV protease inhibitors in humans. Cancer biology & therapy *7*, 628-635.
Rock, K.L., Gramm, C., Rothstein, L., Clark, K., Stein, R., Dick, L., Hwang, D., and Goldberg, A.L. (1994). Inhibitors of the proteasome block the degradation of most cell proteins and the generation of peptides presented on MHC class I molecules. Cell *78*, 761-771.
Saftig, P., Hunziker, E., Wehmeyer, O., Jones, S., Boyde, A., Rommerskirch, W., Moritz, J.D., Schu, P., and von Figura, K. (1998). Impaired osteoclastic bone resorption leads to osteopetrosis in cathepsin-K-deficient mice. Proceedings of the National Academy of Sciences of the United States of America *95*, 13453-13458.
Saveanu, L., Carroll, O., Lindo, V., Del Val, M., Lopez, D., Lepelletier, Y., Greer, F., Schomburg, L., Fruci, D., Niedermann, G*., et al.* (2005). Concerted peptide trimming by human ERAP1 and ERAP2 aminopeptidase complexes in the endoplasmic reticulum. Nature immunology *6*, 689-697.
Savina, A., Jancic, C., Hugues, S., Guermonprez, P., Vargas, P., Moura, I.C., Lennon-Dumenil, A.M., Seabra, M.C., Raposo, G., and Amigorena, S. (2006). NOX2 controls phagosomal pH to regulate antigen processing during crosspresentation by dendritic cells. Cell *126*, 205-218.

Savina, A., Vargas, P., Guermonprez, P., Lennon, A.M., and Amigorena, S. (2010). Measuring pH, ROS production, maturation, and degradation in dendritic cell phagosomes using cytofluorometry-based assays. Methods in molecular biology *595*, 383-402.
Segal, A.W. (2005). How neutrophils kill microbes. Annual review of immunology *23*, 197-223.
Shen, L., Sigal, L.J., Boes, M., and Rock, K.L. (2004). Important role of cathepsin S in generating peptides for TAP-independent MHC class I crosspresentation in vivo. Immunity *21*, 155-165.
Siliciano, J.D., and Siliciano, R.F. (2013). HIV-1 eradication strategies: design and assessment. Current opinion in HIV and AIDS *8*, 318-325.
Turk, V., Stoka, V., Vasiljeva, O., Renko, M., Sun, T., Turk, B., and Turk, D. (2012). Cysteine cathepsins: from structure, function and regulation to new frontiers. Biochimica et biophysica acta *1824*, 68-88.
Vaithilingam, A., Lai, N.Y., Duong, E., Boucau, J., Xu, Y., Shimada, M., Gandhi, M., and Le Gall, S. (2013). A simple methodology to assess endolysosomal protease activity involved in antigen processing in human primary cells. BMC cell biology *14*, 35.
Vasiljeva, O., Dolinar, M., Pungercar, J.R., Turk, V., and Turk, B. (2005). Recombinant human procathepsin S is capable of autocatalytic processing at neutral pH in the presence of glycosaminoglycans. FEBS letters *579*, 1285-1290.
York, I.A., Chang, S.C., Saric, T., Keys, J.A., Favreau, J.M., Goldberg, A.L., and Rock, K.L. (2002). The ER aminopeptidase ERAP1 enhances or limits antigen presentation by trimming epitopes to 8-9 residues. Nature immunology *3*, 1177-1184.
Yusim, K.e.a. (2013). HIV Molecular Immunology 2013. Los Alamos National Laboratory, Theoretical Biology and Biophysics, Los Alamos, New Mexico.

Figure 1

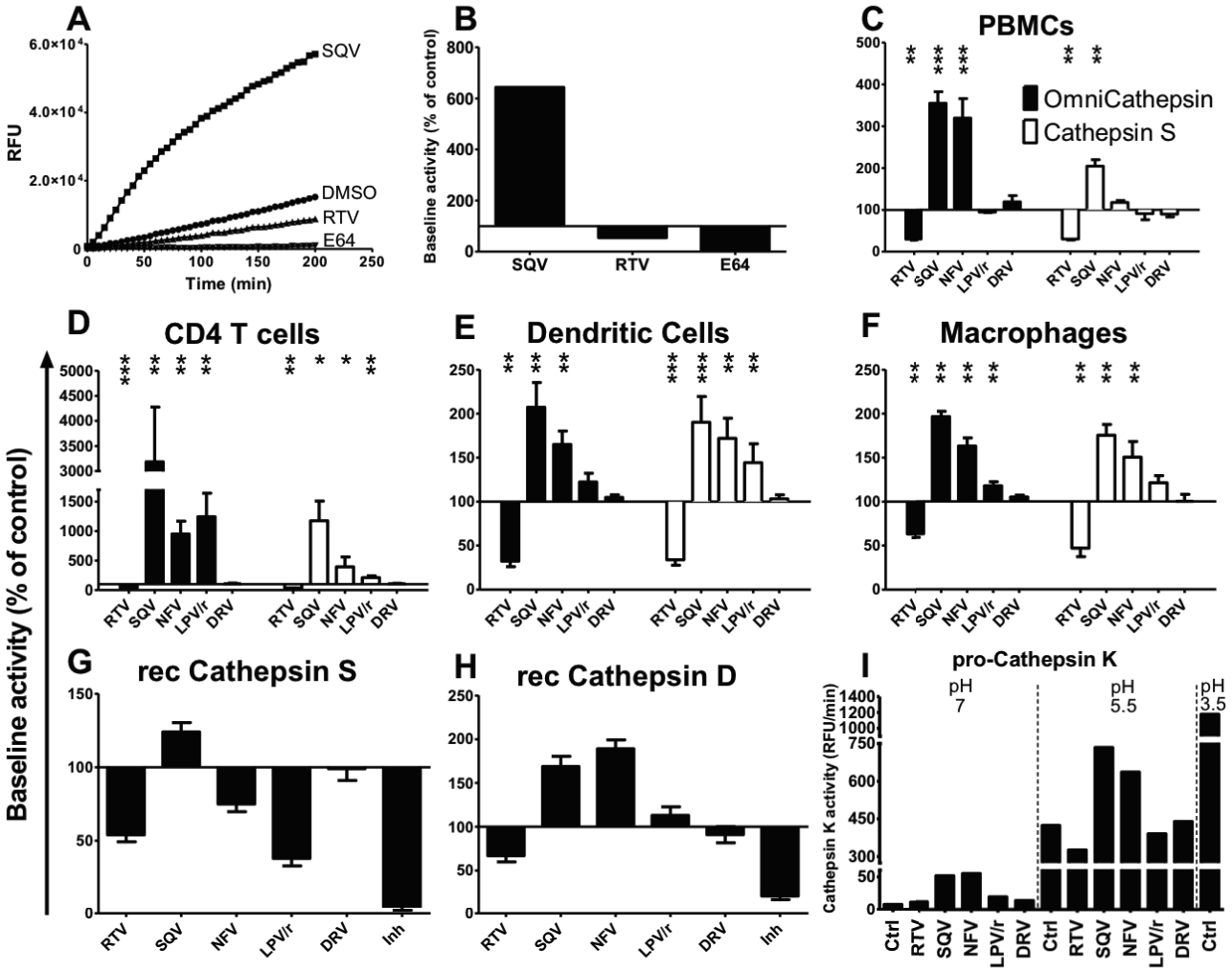

FIGURE 1. HIV PIs variably alter cathepsin activities in human CD4 T cell, DC cells and MØs. (A) Omnicathepsin substrate was added to PBMCs pretreated with DMSO, 5 µM RTV, 5 µM SQV or 10µM E64 and fluorescence emission was monitored every 5 min. (B) The maximum slope of fluorescence emission over 1 h calculated from panel A and represented as hundred percent. Maximum slope of fluorescence upon each treatment was compared with control. (C) PBMCs, (D) CD4 T cells, (E) DCs or (F) MØs were pretreated for 30min with DMSO (control) or with 5 µM of the indicated PIs before adding specific substrate for each activity (Omnicathepsin black bars, Cathepsin S white bars). In each panel, 100% represents the maximum slope of DMSO-treated PBMCs. Data represent average +/- SD of cells from 6 healthy donors. (G) Recombinant cathepsin S or (H) recombinant cathepsin D were pretreated with DMSO or 5 µM of the indicated PIs or inhibitor (10µM ZFL-COCHOO for cathepsin S and 100µM Pepstatin A for cathepsin D) before adding specific substrate for each activity. In each panel, 100% represents the maximum slope of DMSO-treated PBMCs. Data represent average +/- SD of 3 independent experiments. (I) Pro-cathepsin K was incubated with 5 µM of the indicated PIs for 30min at different pH before adding the specific substrate. The emission fluorescence was measured and the maximum slope is represented in the figure. *p , 0.05, **p , 0.01, ***p , 0.001.

Figure 2

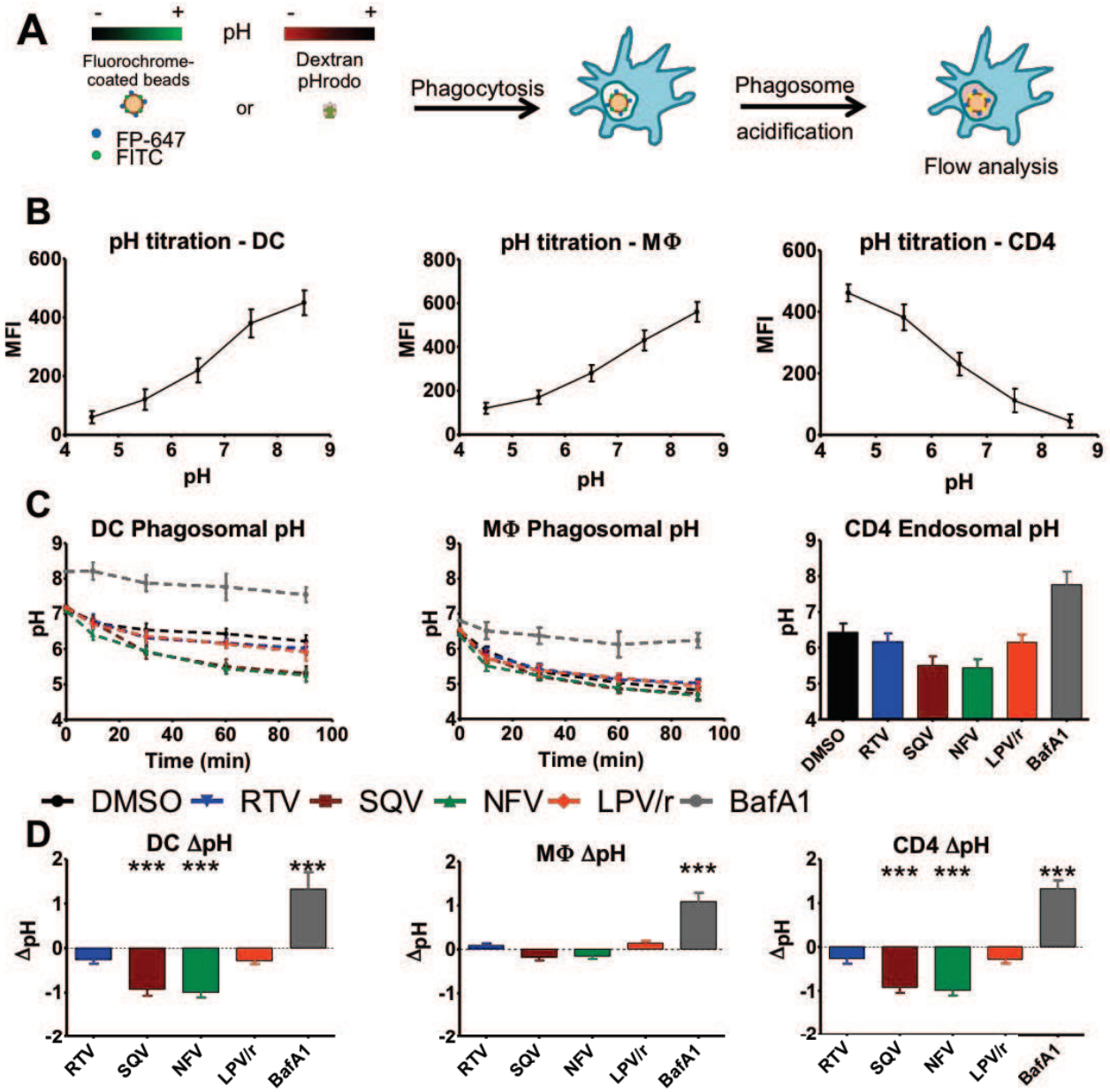

FIGURE 2. HIV PIs alter phagosomal and endosomal pH. (A) Representation of the experimental method of phagosomal and endosomal pH measurement. (B) pH titration curves obtained using fluorochrome-coated beads in DCs (left panel) and MØs (middle panel) or using dextran pHrodo in CD4 T cells (right panel). (C) Phagosomal pH measurement over time after 30min pretreatment of cells with 5 µM of different PIs or 1 µM Bafilomycin A1. Fluorescence measured by flow cytometry was reported to the titration curves in B for pH values. (D) Difference in pH of phagosomes in cells treated with 5 µM of different PIs or 1 µM Bafilomycin A1 compared to DMSO 60min after phagocytosis. Data represent average +/- SD of cells from 5 healthy donors. ***p , 0.001. See also Figure S1 and Figure S2.

Figure 3

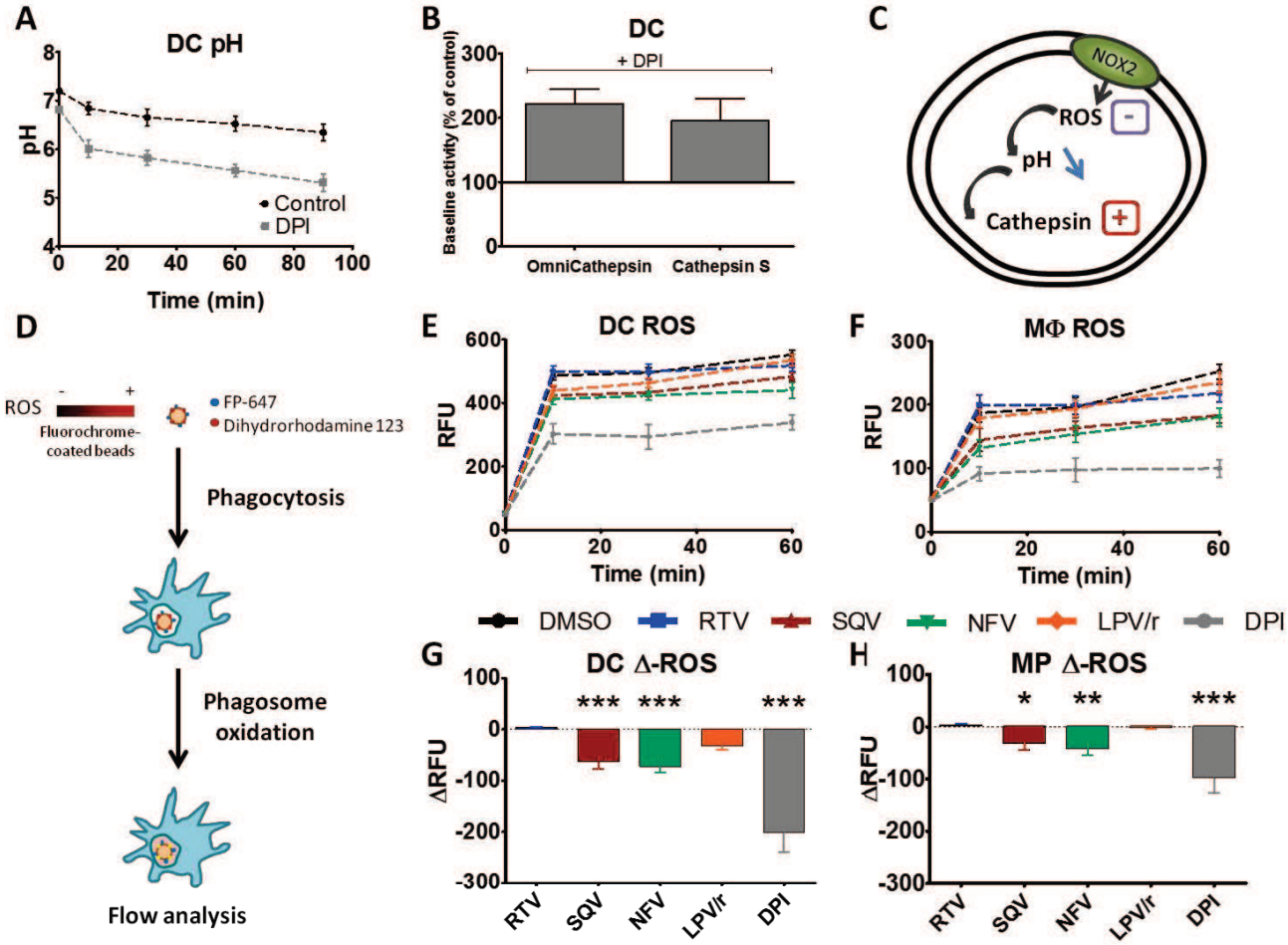

FIGURE 3. HIV PIs alter ROS production in DC phagosomes. (A) DC phagosome pH measurement over time after 30min treatment with DMSO (black) or 10 µM DPI (gray). Average +/- SD of 3 independent experiments. (B) Omnicathepsin and cathepsin S activity measurement in DCs after 30min treatment with 10 µM DPI. 100% represents the maximum slope of DMSO-treated DCs. Average +/- SD of 3 independent experiments. (C) Representation of the hypothesis: PIs inhibit ROS production, leading to phagosome acidification and cathepsin activation. (D) Representation of the experimental method of phagosomal ROS measurement. ROS measurement in DCs (E) and MØ (F) over time after 30min pretreatment of cells with 5 µM of different PIs or 10 µM DPI. Difference in ROS production in DC (G) and MØ (H) phagosomes in cells treated with 5 µM of different PIs or 10 µM DPI compared to DMSO (control) 60min after phagocytosis. Data represent average of cells from 5 healthy donors. *p , 0.05, **p , 0.01, ***p , 0.001.

Figure 4

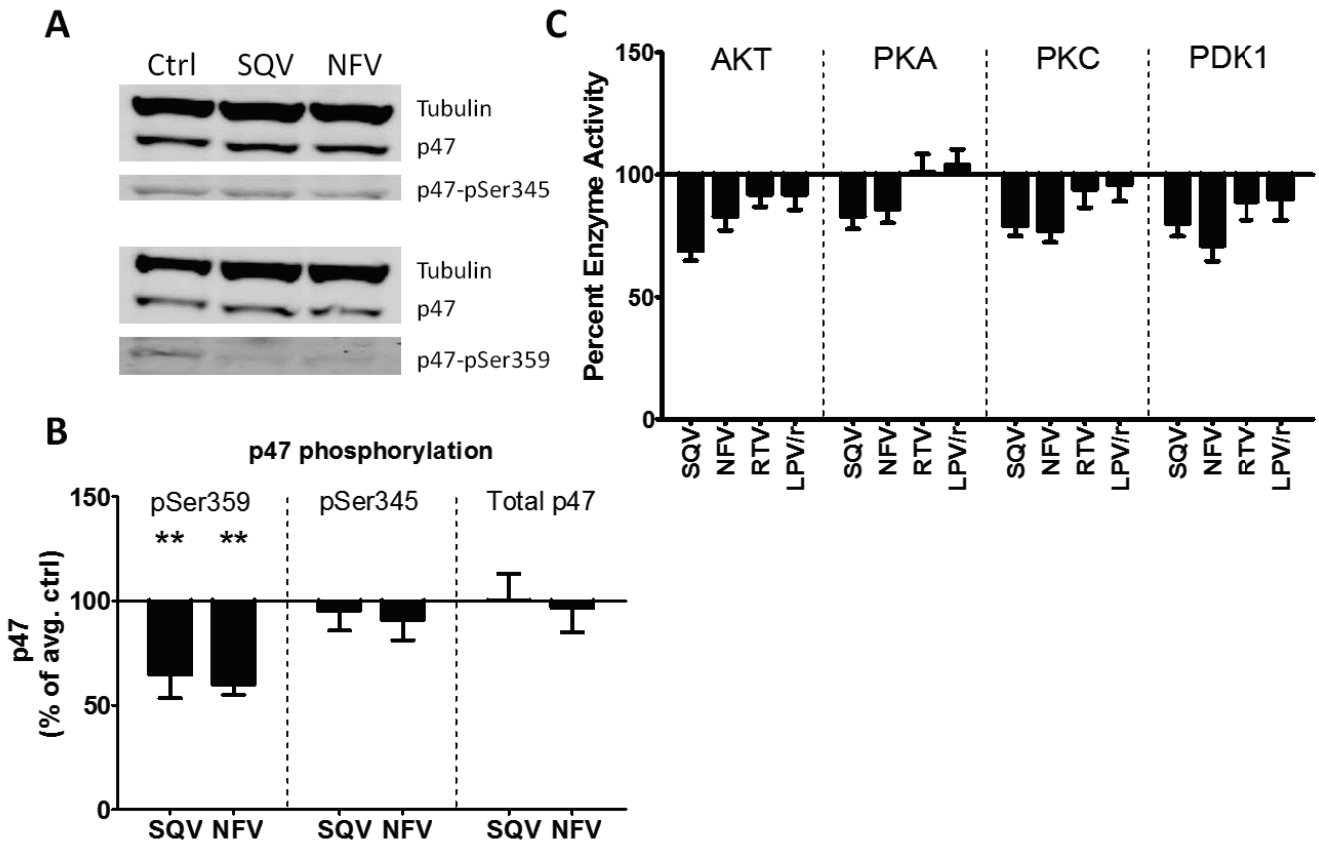

FIGURE 4. HIV PIs inhibit kinase activity and reduce p47 phosphorylation. (A) Western-Blot using extracts of DCs pretreated with DMSO, SQV or NFV and antibodies against tubulin, p47, p47-pSer345 and p47-pSer359. (B) Quantification of tubulin normalized bands. 100% represents the normalized band value of the control. Data represent average +/- SD of 4 independent experiments using cells from 4 healthy donors. (C) Different kinase activity measurement after 30min pretreatment with 5 µM of different PIs. 100% represents the baseline activity of the control. Data represent average +/- SD of 3 independent experiments.

Figure 5

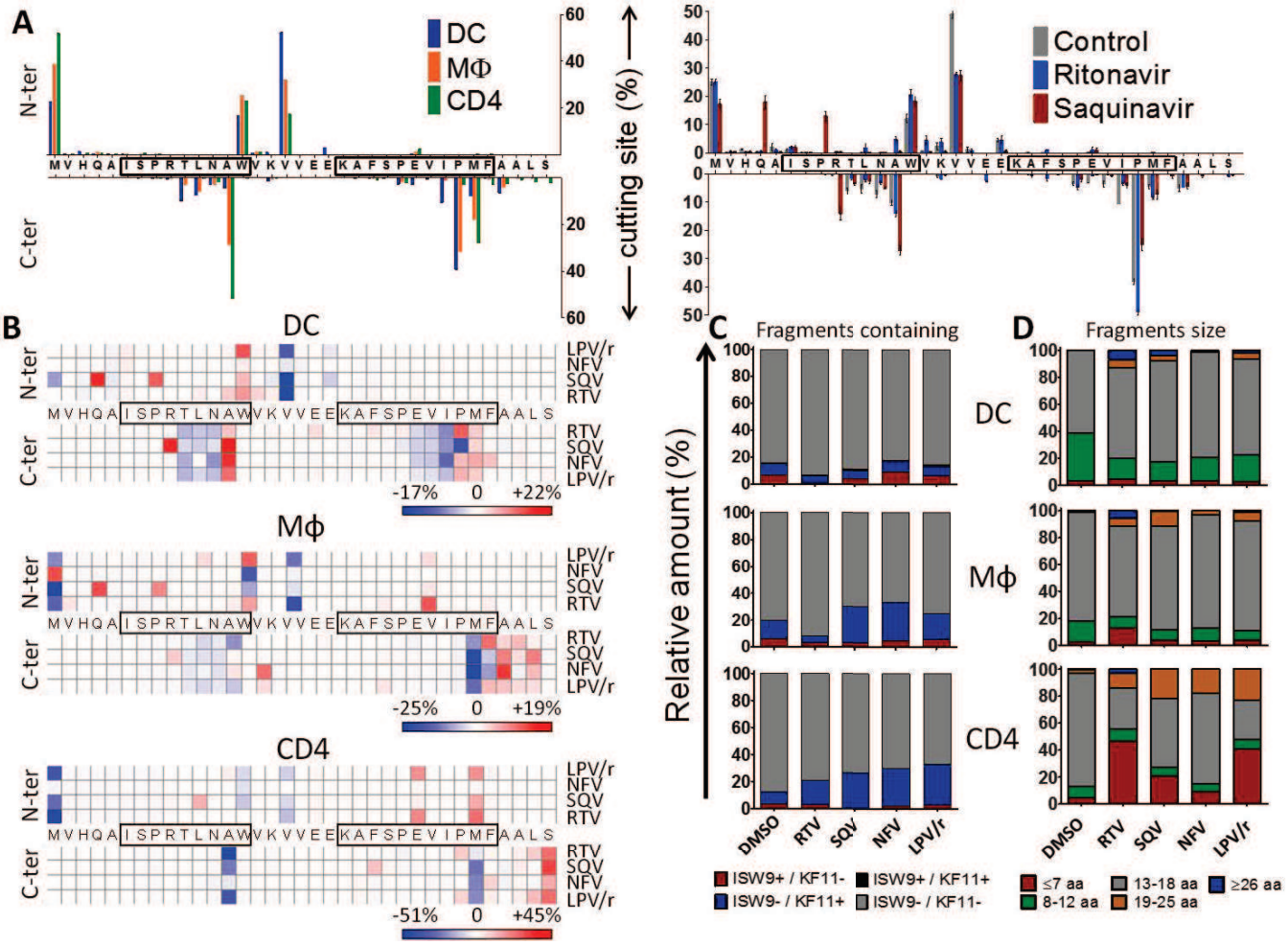

FIGURE 5. HIV PIs change the degradation pattern, epitope production and size distribution of long HIV peptide in lysosomal compartments. (A) Right panel- Cleavage patterns of p24–35mer incubated with DC (blue), MØ (orange) or CD4 (green) cell extracts for 60 minutes at pH4.0, Left panel DC cell extracts preincubated with DMSO (gray), RTV (blue) or SQV (red) for 60 minutes at pH4.0 are shown as the contribution of each cleavage site, presented as cleavage N-terminal or C-terminal to a specific amino acid, to the total intensity of all degradation products. (B) Cleavage patterns of p24–35mer incubated with DC (upper panel), MØ (middle panel) or CD4 (lower panel) cell extracts preincubated with 5 µM of different PIs for 60 minutes at pH4.0 are shown as heat maps of the contribution of each cleavage site compared to control, presented as cleavage N-terminal or C-terminal to a specific amino acid, red represents increase cleavage and blue reduced cleavage compared to control. (C) Degradation products from B identified by MS were grouped into fragments containing B57-ISW9 and B57-KF11 epitopes (black), containing only B57-KF11 epitope (blue), containing only B57-ISW9 epitope (red), or neither epitope (gray), respectively. The contribution of each category of peptides to the total intensity of all degradation products is shown at each condition. (D) All peptides from B were grouped according to their lengths of fragments: equal or longer than 26 aa (blue), 19–

25 aa (orange), 13–18 aa (gray), 8–12 aa (green), and fragments equal or shorter than 7 aa (red). The contribution of each category of peptides to the total intensity of all degradation products is shown at each condition. For (A-D) data are representative of three independent experiments with three different donors. See also Figure S3 and Figure S4.

Figure 6

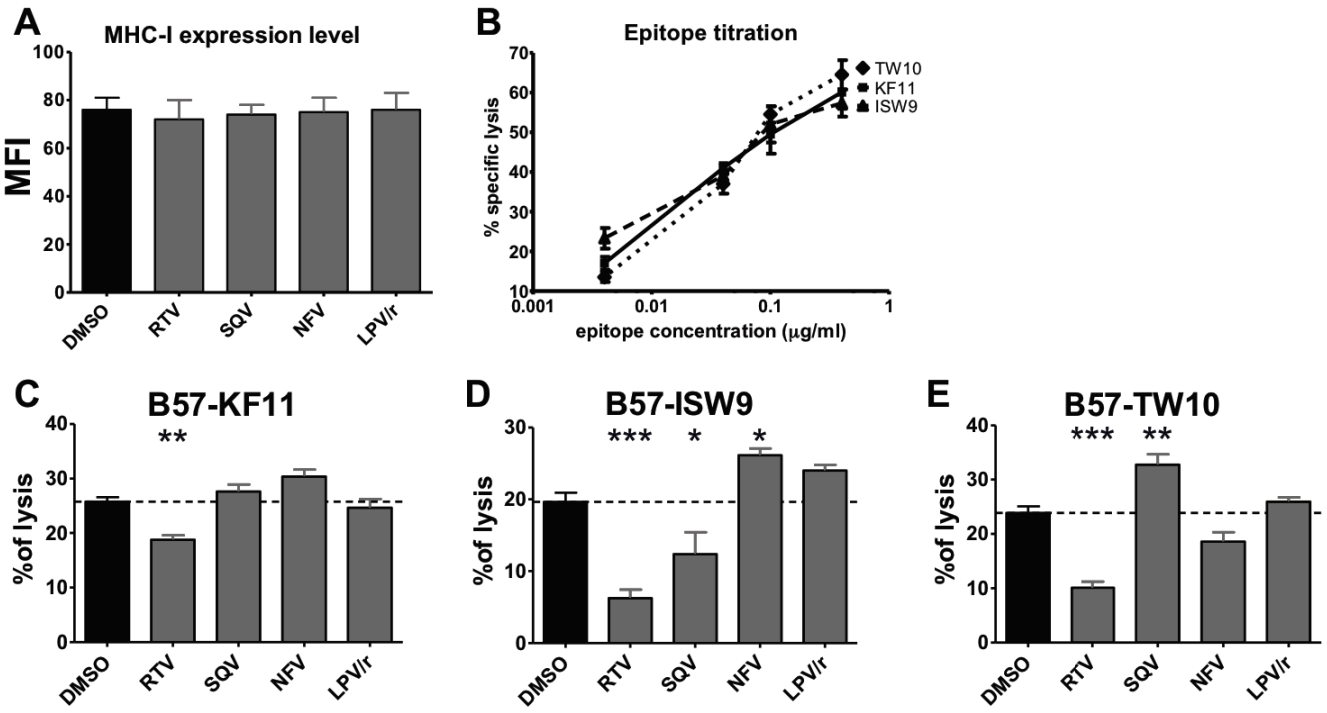

FIGURE 6. HIV PIs variably alter the processing and the cross-presentation of exogenous HIV p24. (A) MFI representing the MHC-I expression level measured by flow cytometry of DCs pretreated with 5 µM of the indicated PIs. (B) Percent of lysis by CTLs of DCs pulsed with different concentrations of optimal epitope B57-TW10, B57-KF11 or B57-ISW9 measured using a fluorescence-based method. Data represents the average +/- SD of 3 experiments. (C-E)Monocyte derived DCs from HLA-B57+ donors were pretreated with 5 µM of the indicated PIs and loaded with HIV p24 for 1h. After extensive wash and 4h incubation B57-KF11 (C), B57-ISW9 (D) or B57-TW10 (E) CTLs were added and the cell lysis was measured using a fluorescence-based method. Data represents the average +/- SD of 5 independent experiments with 5 different donors.

Figure 7

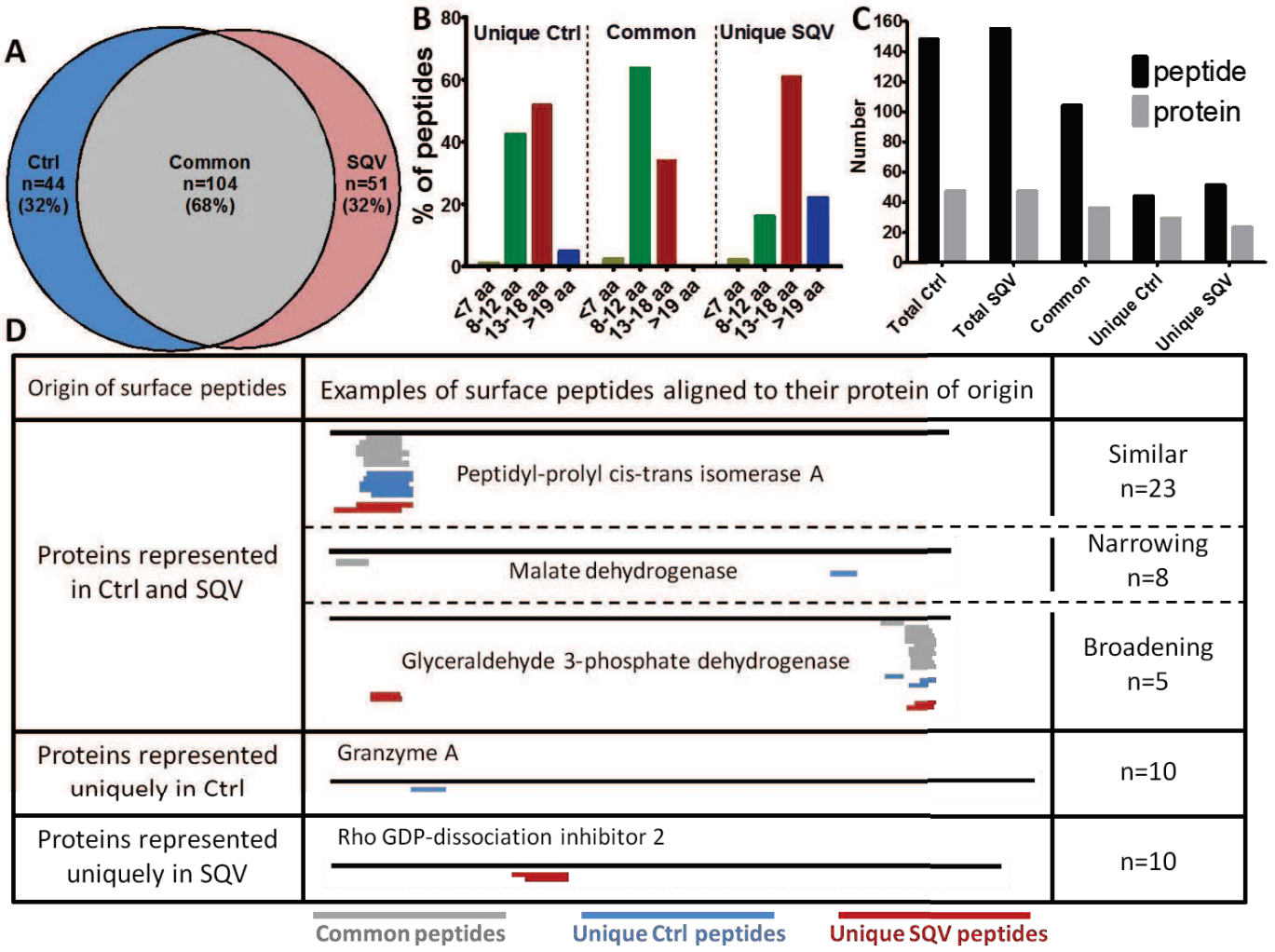

FIGURE 7. HIV PIs alter the surface MHC self-immunopeptidome. The surface MHC peptidome of PBMCs treated with DMSO or SQV for 2 days were eluted and analyzed by MS. (A) Venn diagram representation of the number and percentage of peptides commonly or uniquely present on PBMCs treated with DMSO or SQV. (B) Uniquely or commonly presented peptides were grouped according to their lengths: equal or longer than 19 aa (blue), 13–18 aa (red), 8–12 aa (green), and fragments equal or shorter than 7 aa (gray). (C) Number of total, common or uniquely presented peptides on PBMCs treated with DMSO or SQV and the number of protein they originate from. (D) The proteins of origin of the surface peptides were grouped into: proteins represented in DMSO and SQV treatment, proteins represented uniquely in DMSO treatment and proteins represented uniquely in SQV treatment. The group of proteins represented in DMSO and SQV treatment was further divided into 3 subgroups: similar (unique and common peptides coming from similar location on the protein), narrowing (SQV narrowing the location of the peptides coming from this group of proteins), broadening (SQV broadening the location of the peptides coming from this group of proteins). See also Table S1.

Figure S1

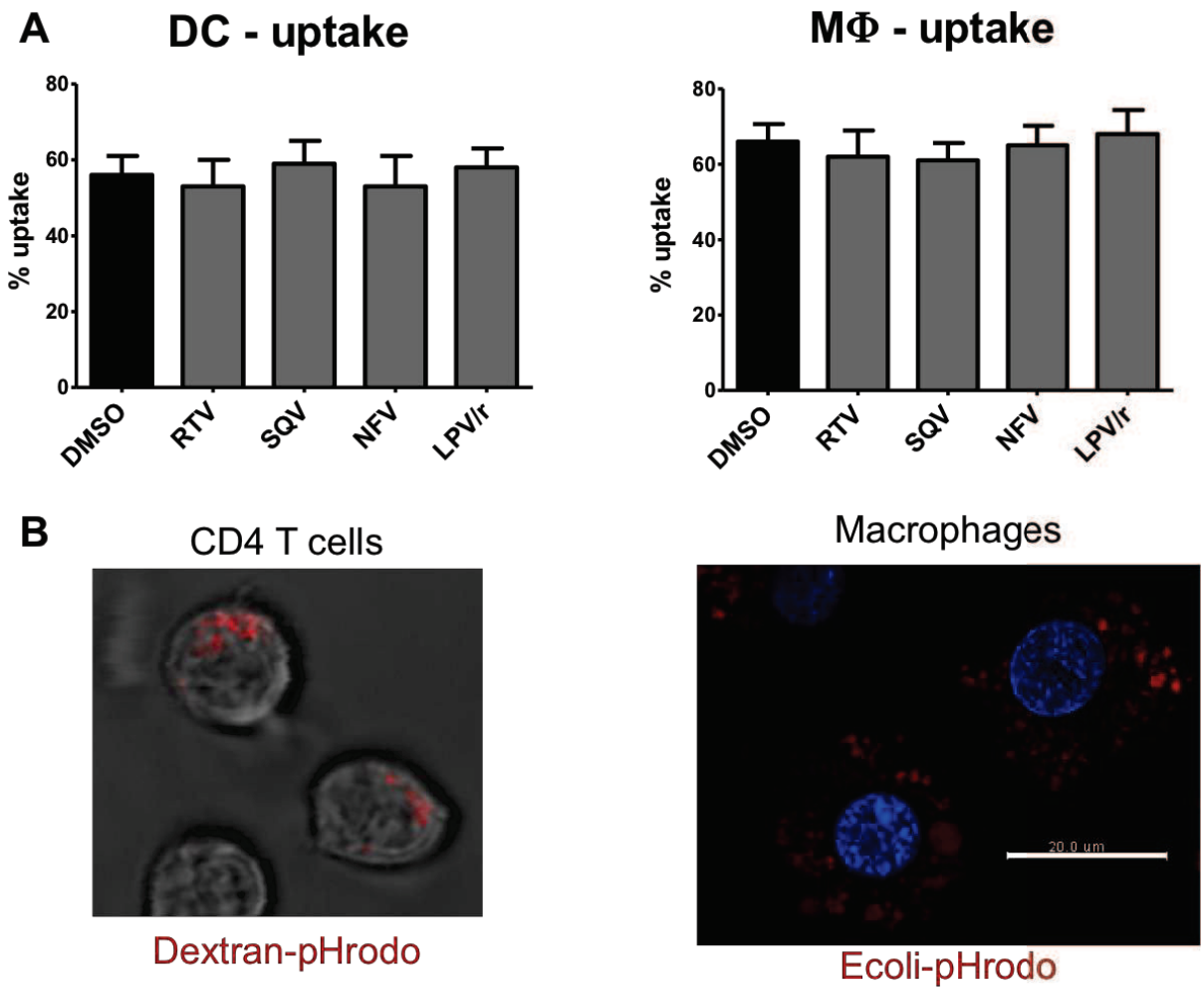

Figure S1. HIV PIs Do not Change Dendritic Cell and Macrophage Uptake Capacity. (A) Fluorochrome-coated beads were phagocytosed by dendritic cells (left panel) or macrophages (right panel) pretreated with 5 µM of the indicated PIs. Using flow cytometry the percentage of the cell population that phagocytosed one or more beads was quantified. Data represents average of 4 indipendent experiments (B) Untreated CD4 T cell endocytosis of dextran-pHrodo (left panel) and macrophage phagocytosis of Ecoli-pHrodo (right panel) was visualized using live cell confocal microscopy. pHrodo fluoresces (red in the figure) only at acidic pH confirming their presence in endolysosomal compartments.

Figure S2

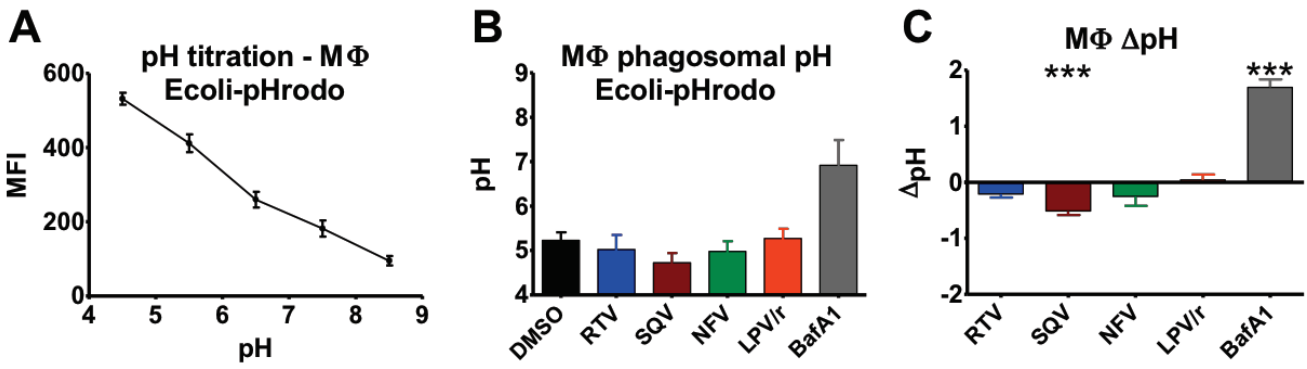

Figure S2. Saquinavir Moderately Alter Macrophage Phagosomal pH. (A) pH titration curve obtained using Ecoli-pHrodo in macrophages incubated at indicated pH. (B) Phagosomal pH measurement after 60min phagocytosis of macrophages pretreated with 5 µM of different PIs or 1 µM Bafilomycin A1 for 30min. (C) Difference in pH of phagosomes in macrophages treated with 5 µM of different PIs or 1 µM Bafilomycin A1 compared to DMSO (control) 60min after phagocytosis. Data represent average of cells from 5 healthy donors. ***p , 0.001, one-way ANOVA with Dunnett's post-test.

Figure S3

Figure S3. Variable Degradation Pattern in Dendritic Cells, Macrophages and CD4 T Cells. HIV p24–35mer (MVHQAISPRTLNAWVKVVEEKAFSPEVIPMFAALS, aa 10–44 in Gag p24) was incubated with DC, macrophage or CD4 T cell extracts for 60 minutes at pH4.0. Degradation products were analyzed by mass spectrometry and aligned to the original p24-35 sequence.

Figure S4

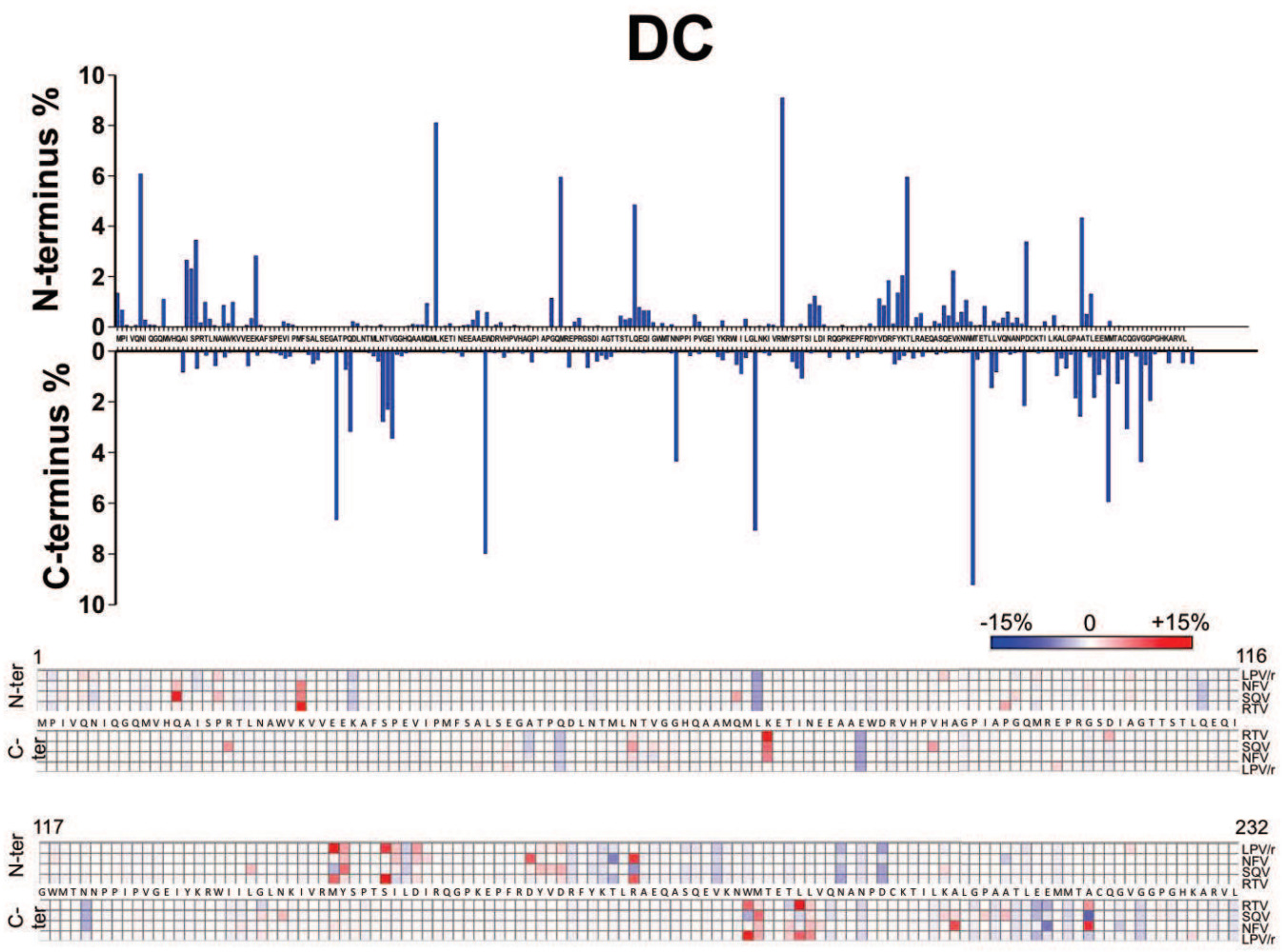

Figure S4. HIV PIs Alter Full HIV p24 Protein Degradation Pattern. Full HIV p24 protein was incubated with DC extracts for 60 minutes at pH4.0. Degradation products were analyzed by MS and the contribution of the cleavage of each amino acid position (N-ter and C-ter) to the total intensity of all degradation products was quantified. The upper panel represents the cutting site intensity at each amino acid location of full HIV p24 protein by DC without PI treatment. The lower panel shows a heat map representing the difference in cutting intensity at each amino acid location of HIV full p24 protein by DCs treated with 5 μM of different PIs compared to control.

Table S1

Common Peptides	Protein AC	Protiens
AVEQNTLQEFLK EQNTLQEFLK VEAVEQNTLQEFLK VEQNTLQEFLK	Q9H299	SH3 domain-binding glutamic acid-rich protein
KGNYAERVGAGAPVYM KGNYAERVGAGAPVY	Q96KK5;Q16777	Histone H2A
LGHLNWPPF	Q6ZRI0	Otogelin
IEILNPNKM	Q04760	Lactoylglutathione lyase
ALKAAHYHTHKE	P80511	Protein S100-A12
AAHLPAEFTPAVHASLDK AAHLPAEFTPAVHASL AAHLPAEFTPAVHAS AAHLPAEFTPAVH ASVSTVLTSKYR FLASVSTVLTSKYR KVGAHAGEYGAEALER LAAHLPAEFTPAVHASLDK LASVSTVLTSKYR LVTLAAHLPAEFTPAVHASLDK PAEFTPAVHASLDK PAVHASLDK PVNFKLLSH SVSTVLTSKYR TPAVHASLDK VDPVNFKLLSH	P69905	Hemoglobin subunit alpha
LVVYPWTQ LVVYPWTQR LVVYPWTQRF LVVYPWTQRFF LVVYPWTQRFFE VDPENFRLLGNVL VGGEALGRLL VVYPWTQRF VVYPWTQRFF VVYPWTQRFFE YPWTQRF	P68871;P02042	Hemoglobin subunit beta/delta

Common Peptides	Protein AC	Protiens
EVGGEALGRLL KVNVDEVGGEALG KVNVDEVGGEALGRL KVNVDEVGGEALGRLL LTPEEKSAVTALWG VCVLAHHFG VDEVGGEALGRL VHLTPEEKSAVTAL VHLTPEEKSAVTALWG WGKVNVDEVGGEA WGKVNVDEVGGEAL WGKVNVDEVGGEALG WGKVNVDEVGGEALGR WGKVNVDEVGGEALGRL	P68871	Hemoglobin subunit beta
KVNVDAVGGEALGRL	P02042	Hemoglobin subunit delta
WTSDTQGDEAEAGEGGEN	P63104	14-3-3 protein zeta/delta
AVDGEPLGR DIAVDGEPLGR FDAAVDGEPLGR FDAAVDGEPLGRVS IAVDGEPLGR IAVDGEPLGRVS	P62937	Peptidyl-prolyl cis-trans isomerase A
VTVPVTTFKNLQT	P62899	60S ribosomal protein L31
AIIDPGDSDIIRSMPE AIIDPGDSDIIRSMPEQ	P62888	60S ribosomal protein L30
MIREADIDGDGQVN	P62158	Calmodulin
FRDGDILGKYVD	P61604	10 kDa heat shock protein
ISKQEYDESGPSIVHRKCF SKQEYDESGPSIVHRKCF WISKQEYDESGPSIVHRKCF	P60709	Actin
LTAFEATDNQAIK	P58546	Myotrophin
AKVAVLGASGGIGQPLS	P40926	Malate dehydrogenase
IGGLAMACHDSF	P31949	Protein S100-A11
SDVLELTDDNFESR	P30101	Protein disulfide-isomerase A3
GLDLWQVKSGTIFD WQVKSGTIFD	P27797	Calreticulin

Common Peptides	Protein AC	Protiens
LVSNLNPERVTPQ	P26599	Polypyrimidine tract-binding protein 1
FVEGGPLDL	P23458	Tyrosine-protein kinase JAK1
ATPFLVVRHQLLKT PFLVVRHQLLKT	P15954	Cytochrome c oxidase subunit 7C
LNETGDEPFQYKN	P15104	Glutamine synthetase
IVNTNVPRASVPDG YDMNAANVGWNN	P14174	Macrophage migration inhibitory factor
MATGDLDQDGRIS	P13796	Plastin-2
MAADGDFKIKC	P09382	Galectin-1
NRIPESGGDNSVFD	P07996	Thrombospondin-1
GTCQDAAIVGYKDSPS	P07737	Profilin-1
MQQKLVDQNIFS	P07339	Cathepsin D
ALIYNEALKG	P06703	Protein S100-A6
GAGIALNDHFVK ISWYDNEFGYSNR ISWYDNEFGYSNRVV ISWYDNEFGYSNRVVD ISWYDNEFGYSNRVVDL NEFGYSNRVVDL WYDNEFGYSNRVVD WYDNEFGYSNRVVDL YDNEFGYSNRVV YDNEFGYSNRVVD YDNEFGYSNRVVDL	P04406	Glyceraldehyde-3-phosphate dehydrogenase
ADDRVNPCIGGVIL	P04075	Fructose-bisphosphate aldolase A
APPGSKEAEVQAKQQA LGLTAPPGSKEAEVQAKQQA PPGSKEAEVQAKQQA	O75368	SH3 domain-binding glutamic acid-rich-like protein
IELLNWVVNA ILRGSNCHKITAPG PAVAGHTLTA VMDKPLDL		Unassignd

Unique to Control	Protein AC	Protein
AVDGEPLGRVSF	P62937	Peptidyl-prolyl cis-trans isomerase A
QNTLQEFLK	Q9H299	SH3 domain-binding glutamic acid-rich-like protein 3
SYGAQPVVQTQLNS	Q96PK6	RNA-binding protein 14
MAVLPGLSSP	Q8IXN7	N-acetylaspartylglutamate synthase A
IEILNPNKMA IEILNPNKMAT IQKCDFPIMK	Q04760	Lactoylglutathione lyase
FTPAVHASLDK HLPAEFTPAVHASLDK SPADKTNVKAAWG	P69905	Hemoglobin subunit alpha
VYPWTQRF EVGGEALGRL	P68871;P02042	Hemoglobin subunit beta / delta
DIAVDGEPLGRVS DIAVDGEPLGRVSF IAVDGEPLGRVSF VDGEPLGRVSF	P62937	Peptidyl-prolyl cis-trans isomerase A
VTVPVTTFKNL YVPVTTFKNLQT	P62899	60S ribosomal protein L31
FILPDSLPLDT	P62314	Small nuclear ribonucleoprotein Sm D1
IREADIDGDGQVNY	P62158	Calmodulin
DGDILGKYVD	P61604	10 kDa heat shock protein, mitochondrial
GPGLVAGANYGHVY	P51553	Isocitrate dehydrogenase [NAD] subunit gamma
GVISDGNSYGVPDD	P40925	Malate dehydrogenase, cytoplasmic
ESRISDTGSAGLML	P30101	Protein disulfide-isomerase A3
WQVKSGTIFDN	P27797	Calreticulin
WTSDSAGEECDAAEGAEN	P27348	14-3-3 protein theta
MSNLDSNRDNEVEDF	P26447	Protein S100-A4
DVGQTVDDPYAT	P23528	Cofilin-1
PFLVVRHQLLK	P15954	Cytochrome c oxidase subunit 7C
LNETGDEPFQYK	P15104	Glutamine synthetase
YDMNAANVGWNNST	P14174	Macrophage migration inhibitory factor
VEVNPKMVMT	P13796	Plastin-2
GGNEVTPHSRPYM	P12544	Granzyme A
WSVDPLDR	P06396	Gelsolin
GIALNDHFVK GYSNRVVDL WYDNEFGYSNR	P04406	Glyceraldehyde-3-phosphate dehydrogenase
FEADPPGQVAASPDPTT	O43598	2'-deoxynucleoside 5'-phosphate N-hydrolase 1
NITLEPMEIRT	O00754	Lysosomal alpha-mannosidase
IVVYAGH WSLLATPPA DLNMLLEV MASIPLPDK GLMFEVVDL		Unasssigend

Proteins uniquely represented in Control

Unique to SQV	Protein AC	Protein
AIVEALNGKEVAAQVKAPLVLK	Q99497	Protein DJ-1
AIVEALNGKEVAAQVKAPLVLKD		
KGNYAERVGAGAPVYL	Q96KK5	Histone H2A
YYAQTSPQGMPQHPAPQ	Q96AE4	Far upstream element-binding protein 1
AHLPAEFTPAVHASLDK DKFLASVSTVLTSKYR GKVGAHAGEYGAEALER PADKTNVKAAWGKVG PADKTNVKAAWGKVGAHAGEYGAEALER SPADKTNVKAAWGKVG TLAAHLPAEFTPAVH TLAAHLPAEFTPAVHASLDK VLSPADKTNVKAAWGKVGAHAGEYG VTLAAHLPAEFTPAVHASLDK	P69905	Hemoglobin subunit alpha
PDAVMGNPKVKAHGKKVLG PWTQRFFE YPWTQRFFE KVNVDEVGGEAL KVNVDEVGGEALGR VDEVGGEALGRLL VHLTPEEKSAVTA VHLTPEEKTAVNALWG VTALWGKVNVDEVGGEA WGKVNVDEVGG	P68871;P02042	Hemoglobin subunit beta/delta
FDIAVDGEPLGRVSF VNPTVFFDIAVDGEPLGR	P62937	Peptidyl-prolyl cis-trans isomerase A
AIIDPGDSDIIRSMPEQTG	P62888	60S ribosomal protein L30
FAGDDAPRAVFPS	P60709	Actin
DGPVVTDPKAPNVVVTR VTDPKAPNVVVTR	P52566	Rho GDP-dissociation inhibitor 2
IAVFQKYAGKDG	P31949	Protein S100-A11
LTDDNFESRISDTGSAG SDVLELTDDNFESRISDTG SDVLELTDDNFESRISDTGSAG	P30101	Protein disulfide-isomerase A3
PVDLSKWSGPLSL	P30086	Phosphatidylethanolamine-binding protein 1
DVGQTVDDPYATFVK	P23528	Cofilin-1
LPGELAKHAVSEGTKAVTKYTSSK	P23527	Histone H2B type 1
ATPFLVVRHQLLKT	P15954	Cytochrome c oxidase subunit 7C
IVNTNVPRASVPD	P14174	Macrophage migration inhibitory factor
MLDNLLDI	P09874	Poly [ADP-ribose] polymerase 1
ASPEYVNLPINGNGKQ	P09211	Glutathione S-transferase P
SFLPWIR	P08311	Cathepsin G
FVNWIDSIIQR	P08246	Neutrophil elastase
MQQKLVDQNIFSF	P07339	Cathepsin D
FNSGKVDIVAINDPFI FNSGKVDIVAINDPFID NEFGYSNRVVD SWYDNEFGYSNRVVD	P04406	Glyceraldehyde-3-phosphate dehydrogenase
IAEQPVSEVETRVIA PGSKEAEVQAKQQA PPGSKEAEVQAKQ	O75380	NADH dehydrogenase [ubiquinone] iron-sulfur protein

Proteins uniquely represented in SQV

Table S1: Peptides eluted from SQV treated and untreated PBMCs and their protein of origin. Top tables represent the peptides commonly present on treated and untreated PBMCs. Bottom left table represents peptides uniquely present on untreated PBMCs. Bottom middle table represents peptides uniquely present on SQV treated PBMCs. Blue cells are the proteins represented uniquely in control and pink proteins represented uniquely in SQV treatment.

Discussion

The ability of CTL to clear virus-infected cells depends on the recognition of viral derived epitopes presented by MHC-I. Those epitopes are generated by the intracellular degradation of proteins by cytosolic or ER resident proteases in the direct antigen processing pathway or by endolysosomal cathepsins in the cross-presentation pathway. Any perturbation of cellular peptidase activity could modify protein degradation patterns and consequently epitope presentation to CTLs.

The focus of my thesis was to investigate the effect of HIV PIs on the different enzymes involved in the direct antigen processing as well as the cross-presentation pathway and to understand the impact of these activity alterations on HIV epitope production and presentation to CTLs.

1. Mechanism of protease and peptidase activity alteration

We discovered that four of seven PIs affected at least one cellular peptidase activity. Nelfinavir for instance could either enhance or reduce proteasome, aminopeptidase and cathepsin hydrolytic activities, whereas other PIs such as Ritonavir mostly reduced all activities tested, suggesting different interactions between each drug and each cellular enzyme. HIV PIs might bind directly to the catalytic site of the enzymes and inhibit their activity. It was previously shown using molecular docking that ritonavir can in fact bind to the active center of the yeast proteasome PRE2 subunit that is homologous to human proteasome b5 subunit [281], elucidating the inhibition of the chymotryptic activity by ritonavir [218,281,282]. Likewise, HIV PIs might interact with noncatalytic effector sites in the proteasome, aminopeptidases and cathepsins that were shown in enzymatic studies to regulate the different catalytic activities [283-286]. This would provide a potential mechanism of either inhibition or enhancement of cellular peptidases by HIV PIs, although molecular modeling and structural studies are required to test this hypothesis.

In addition, we discovered that Saquinavir and Nelfinavir facilitate the maturation of procathepsin K even at neutral pH. Most cathepsins are synthesized in their inactive procathepsin form. The activation process is triggered by a pH drop in the endolysosomal

compartments, which induces the proteolytic removal of amino terminal pro-domain blocking the catalytic site of the cathepsin. This pH dependent activation restricts cathepsin hydrolytic activity only to lysosomal compartments. It was discovered that glycoaminoglycans (GAG) can at neutral pH loosen the binding of the propeptide on the catalytic site and accelerate the autocatalytic removal of the propeptide subsequently activating cathepsins [287,288]. Similarly, Saquinavir and Nelfinavir might be using the same mechanism as GAG to facilitate the maturation of cathepsins at neutral pH, although structural studies are needed to test this hypothesis.

2. Link between side effects and peptidase activity alteration

First-generation PIs like ritonavir, saquinavir, and nelfinavir showed stronger effect on proteasome, aminopeptidase and cathepsin activities than newer PIs like atazanavir and darunavir. First-generation PIs induced more rapid and profound adverse effects on lipid and glucose metabolism, increased risk of cardiovascular diseases and reduced bone mineral density than did newer PIs [148,149,289-292]. Rats treated with ritonavir developed hyperlipidemia and displayed higher RNA expression of proteasome subunits [293,294]. Although there is no clear mechanistic link between the two observations, ritonavir-induced proteasome inhibition may trigger a feedback loop leading to increased proteasome expression as observed with proteasome inhibitors [295]. PI-induced proteasome inhibition may modify the half-life of proteins involved in glucose or lipid metabolism, such as the documented accumulation of sterol regulatory binding proteins 1/2 inducing constitutive lipid biosynthesis in mice [296]. Whether the modification of intracellular aminopeptidase activities would affect glucose or lipid metabolism remains unknown. Surface aminopeptidases such as membrane-bound ectoenzyme aminopeptidase N/CD13 or intracellular aminopeptidases trafficking to the surface such as insulin-responsive aminopeptidase are involved in peptide cleavage, cholesterol uptake for aminopeptidase N [297,298], or glucose transport uptake for insulin-responsive aminopeptidase [299]. Considering the conservation between aminopeptidase catalytic sites, it will be important to examine whether first- and second-generation PIs modify surface aminopeptidase activities, as

well as other peptidases, in each subcellular compartment and affect the biological functions of these enzymes.

Excessive cathepsin activation and extracellular presence of active cathepsins are linked to inflammation of the mucosa and damage to the musocal barrier [300]. Therefore HIV PI-induced cathepsin activation and increased maturation might be involved in damaging the mucosa, allowing microbial translocation and causing chronic immune activation in patients on ART. Moreover, it has been proposed that lipid metabolism disorder associated with Nelfinavir is caused in part by enhanced lysosome-mediated perilipin proteolysis which is a protein involved in regulating adipocyte lipolysis. Nelfinavir induced 6-fold reduction of perilipin half-life was reversed by NH4Cl but not by proteasome inhibition suggesting the involvement of lysosomal proteases in nelfinavir-induced perilipin proteolysis. However the exact mechanism of this enhanced degradation was not clear [301]. Nelfinavir induced lysosomal cathepsin activity increase showed in this study might directly explain the enhancement of perilipin proteolysis in the lysosomes that is contributing to the lipid metabolism disorders in patients on ART.

Osteoporosis and osteopenia are side effect associated with first generation PI use Brown, 2006 #98;Duvivier, 2009 #247}. Cathepsins play a crucial role in bone remodeling by degrading type I collagens in the bone resorption pits [302,303]. Saquinavir- and Nelfinavir-induced cathepsin activity increase that we showed in this study might explain the excessive bone collagen degradation and the bone density reduction seen in patients on PIs, however further studies are needed to confirm this hypothesis.

Cathepsins are also involved in processing pro-granzymes into proteolytically active forms in cytotoxic immune cells [304]. Therefore, additional research is needed to investigate whether HIV PI-induced modulation of cathepsin activity alter the cytotoxic capacity of CTLs and NK cells in patients on PI-including HAART. Cathepsin dysregulation is also associated with various other pathological conditions, such as cancer [305,306], rheumatoid arthritis [307], atherogenesis [308] and muscular dystrophy [309]. Additional research is needed to investigate if PI-induced cathepsin alteration contributes to the development of such disease in patients using long term ART.

3. HIV PIs and cancer

studies showed that some HIV PIs have pleiotropic antitumor effects, including inhibition of inflammatory cytokine production, proteasome activity, cell proliferation and survival, and induction of apoptosis [208-213]. Subsequently, HIV PIs use alone or in combination to chemotherapy or radiotherapy showed beneficial results in human clinical trials against different cancer types [214-216]. Different cellular targets of HIV PIs have been proposed but the exact anti-tumor mechanism is still unclear. One of the cellular targets of some HIV PIs is the proteasome as seen in our and others studies [218-220,310]. Proteasomes are involved in many cellular mechanisms and their inhibition is proved to be beneficial in some cancer types. For instance Bortezomib is a FDA approved proteasome inhibitor for treating multiple myeloma. Therefore, the inhibitory effect of HIV PIs on the proteasome might explain in part their anti-cancer effect. In addition, experimental studies connect the anticancer effects of some PIs to the suppression of the Akt signaling pathway, but the actual molecular targets remain unknown [311]. Our results show that Saquinavir and Nelfinavir are able to directly inhibit multiple members of the protein kinase-like superfamily, which are involved in the regulation of cellular processes vital for carcinogenesis and metastasis. This finding provides a molecular basis to explain the broad spectrum anti-cancer effect of Saquinavir and Nelfinavir.

4. HIV PIs and NOX2

Since, kinases regulate many complex processes in cells and the extent to which the PI-induced kinase activity alterations affect other cellular processes is unknown and needs to be addressed. In this study we showed that Saquinavir and Nelfinavir -by inhibiting Akt kinase and protein kinase C (PKC)- reduce the phosphorylation of phox-p47 which is required for the assembly of active NOX2 [312]. The multicomponent NOX2 enzyme produces ROS in the phagosomes of neutrophils, eosinophils, monocytes and macrophages contributing to the destruction of the engulfed pathogens [313-316]. The phagosomal NOX2 and ROS production play key role in host defense against microbial pathogens as illustrated by a human genetic disorder called chronic granulomatous disease (CGC), which is associated with life-threatening bacterial

and fungal infections and is characterized by an absence of ROS production due to a deficiency in one of the components of NOX2 [313,315,317,318]. The NOX2 complex is composed of multiple subunits and its activation is triggered by the phosphorylation of the phox-p47 subunit at multiple locations and by different kinase including Akt and PKC [312]. Saquinavir and Nelfinavir by inhibiting Akt and PKC activity partially reduce the phosphorylation of phox-p47 thus inhibiting NOX2 activity and reducing ROS production in DC and macrophage phagosomes. The impact of the PI-induced NOX2 activity inhibition on macrophage capacity to kill phagocytosed pathogens remains unknown and needs to be further investigated. In addition to their role in microbial killing, NOX2 by consuming protons to produce ROS is involved in maintaining neutral DC phagosomal pH. This controlled pH confers DCs the ability to cross-present by limiting degradation of the phagocytosed antigens without the destruction of potential antigenic peptides. This was confirmed by NOX2 deficient DC's inability to cross-present [272]. In this study we showed that Saquinavir and Nelfinavir by inhibiting NOX2 activity increase the DC phagosome acidification and lead to enhancement in cathepsin activities.

5. Alteration of antigen degradation patterns by HIV PIs

5.1 In the direct antigen processing pathway

We showed that alteration of proteasome and aminopeptidase activities by HIV PIs modified both the degradation patterns of long HIV peptides and the sensitivity of epitopes to intracellular degradation before loading onto MHC-I, and therefore the amount of peptides available for display to CTL. The effect was both drug and sequence dependent. Variations in degradation patterns were explained by the intriguing observation that the cleavage of specific residues was enhanced, whereas others were reduced. Twelve residues whose cleavage was reduced by four drugs corresponded to residues cleavable by aminopeptidases, thus suggesting that HIV PIs may reduce the efficiency of aminopeptidase-dependent trimming of many N-extended peptides into epitopes. Surprisingly, these four drugs enhanced the cleavage of acidic residues, mostly E and, to some extent, D, H, Q, which are poorly cleavable by aminopeptidases. Sequential incubation of cells with ritonavir or Kaletra followed by

aminopeptidase inhibitor reduced PI-enhanced cleavage of E by 53– 59%, suggesting that PI modified aminopeptidase activities to facilitate the cleavage of acidic residues but also enhanced another unidentified peptidase activity. Ritonavir or Kaletra did not enhance caspase-like activity of the proteasome or the activity of caspases (which can cleave motifs containing acidic residues), at least when measured with a pan-caspase substrate [319], thus ruling out a major involvement of proteasomes and caspases in the changes in residue-specific cleavage patterns. Whether HIV PIs enhance additional cytosolic peptidases cleaving acidic residues or whether it may modify aminopeptidase hydrolytic capacity to enhance cleavage of acidic residues and reduce cleavage of other residues remains to be determined.

5.2 In the cross-presentation pathway

The HIV PI-induced direct and indirect (via NOX2 inhibition and increased phagosome acidification) alteration of cathepsin activity modified long HIV peptide and full protein degradation patterns in lysosomal compartments. These changes in antigen processing resulted in alterations in the amount of peptides available for direct MHC-I loading in the vacuolar pathway or further processing in the cytosolic pathway and subsequently led to altered HIV epitope cross-presentation to CTL. Cutting site analysis showed that HIV PI effect on phagosomal antigen processing was drug and sequence dependent as well as variable depending on the cell subset tested which is in line with previous data showing that various cell subsets present different levels of peptidase activities [320,321]. Given that each cathepsin has different sequence specificities [322], a given PI -by variably changing the activities of the different cathepsins available- increase the cleavage of certain motifs and decrease the degradation of others. Further in depth analysis by our collaborators at Microsoft research of PI induced enhancement or reduction of the cleavage intensity at each amino acid location of full HIV proteins will enable the generation of an algorithm to predict the effect of each PIs treatment on the amount of different epitope production. The use of such algorithm might allow us in the future to increase or decrease the presentation of certain epitopes by using a predefined combination of certain HIV PIs.

6. Effect of HIV PIs on epitope presentation and CTL recognition

These findings have implications for the degradation of HIV proteins and beyond.

6.1 In the context of HIV

First, in the context of HIV protein degradation, specifically relevant for HIV-infected, ART-treated persons with ongoing replication of drug-resistant mutated strains, we have shown that HLA-restricted mutations flanking residues tend to evolve from aminopeptidase-cleavable to poorly cleavable residues[242]. In the presence of HIV PIs such as Ritonavir used as booster in ART treatments, we may expect that the production of the wild type (WT) peptide would be decreased, whereas flanking mutations leading to an acidic residue would enhance epitope production as shown in this study with an isoleucine-to-glutamic acid mutation. Alternatively, a mutation toward an acidic residue within an epitope could enhance the intracellular degradation of the mutated epitope and the production of the WT version. Overall, these changes could affect the ratio of HIV peptides presented by infected cells. Mutated epitopes can elicit CTL responses[323-325]; thus, the change of ratio of WT and mutated peptides could contribute to shifts in immunodominance, as seen after immune escape in acute HIV infection[326-329]. Although the lack of appropriate longitudinal clinical samples precludes us to test this hypothesis, PI-induced modification of the self-immunopeptidome landscape on PBMC surface observed in this study using mass spectrometry suggest that HIV PIs may contribute to broadening of immune responses against HIV in ART-treated patients with ongoing viral replication. In addition, studying the impact of PI on HIV epitope presentation is relevant to approaches to purge HIV reservoirs by combining provirus reactivation in the presence of ART to prevent replication, and therapeutic vaccination to boost immune responses against HIV[330,331]. If ART needed to prevent replication after provirus reactivation calls for inclusion of HIV PIs, it will be important to assess the repertoire of HIV epitopes presented by the reactivated latently infected cells in presence of PIs. Moreover, it will be crucial to investigate the impact of HIV PIs on the cross-presentation efficiency of therapeutic vaccines and the induction of broad CTL responses needed to eliminate the reactivated HIV-epitope presenting cells[332].

6.2 In the context of other pathogens and cancer

Because certain PIs modify antigen processing in a sequence-specific manner and because PI-treated PBMCs showed 32% alteration of their self surface peptidome it is very likely that degradation and presentation of proteins derived from other pathogens will be altered by HIV PIs. In this study cytosolic stability of optimal epitopes derived from CMV, HCV, influenza, or EBV was variably affected by PI treatment, with ritonavir/Kaletra increasing the cytosolic stability of several peptides. Because intracellular peptide stability contributes to the amount of peptides displayed to CTL [241], HIV PIs may alter the presentation of epitopes derived from other pathogens infecting ART-treated persons. More than half of HIV+ individuals worldwide become coinfected with other pathogens such as tuberculosis or HCV, and effective drug combinations to curb both infections are needed [333-335]. Assessing whether and how ART, beyond reducing HIV viral load and cellular activation, may possibly contribute to diversifying immune responses against coinfecting pathogens by modifying the degradation patterns of these pathogens provides a new outlook of the use of HIV PIs. Similarly, saquinavir, ritonavir, and nelfinavir, because of their inhibitory effect on the proteasome, kinase and other cellular targets, have been shown in previous studies and clinical trials to have beneficial effects on several cancers [209,219,336-341]. In the repositioning of PIs as cancer therapy, another potential benefit could be a PI-induced altered processing of cancer Ags (the intracellular stability of an MAGE3 epitope was modified by ritonavir/Kaletra), potentially leading to presentation of a different cancer Antigen-derived peptide and new immune responses.

6.3 MHC-II epitope presentation

Because endolysosomal pH and cathepsin activity regulate MHC-II epitope processing, it is very likely that HIV PI-induced modifications of phagosomal acidification and cathepsin activities alter antigen processing and MHC-II epitope presentation. The increase upon Saquinavir treatment in the number of 13-18 amino acid long self-peptidome presented on the surface of PBMCs suggest that Saquinavir might be broadening the MHC-II surface peptidome, however, more immunological and quantitative studies are needed to confirm this hypothesis.

Conclusion

In conclusion our results indicate that HIV PIs, by altering Akt and PKC, NOX2 and cellular peptidase activities, modify antigen processing in cytosolic, ER and lysosomal compartments leading to changes in epitope presentation to CTLs. Additional structural studies are needed to understand the mechanism behind the PI-induced alterations of various classes of enzymes. If HIV PIs allow diversification of epitope presentation, they may provide complementary approaches to broaden the immune responses against various immune diseases, considering that temporary PI treatment would not induce toxicity and adverse effects observed in long-term HAART.

In addition, even though the intended collaboration to develop intrabodies with Pr. Weiss unfortunately didn't work out, targeting specific peptidases or NOX2 and altering their activities using intrabodies or chemical compounds might be a new therapeutic approach to diversify epitope presentation and broaden immune responses against various diseases.

Bibliography

1 Barre-Sinoussi, F. *et al.* Isolation of a T-lymphotropic retrovirus from a patient at risk for acquired immune deficiency syndrome (AIDS). *Science* **220**, 868-871 (1983).

2 Buonaguro, L., Tornesello, M. L. & Buonaguro, F. M. Human immunodeficiency virus type 1 subtype distribution in the worldwide epidemic: pathogenetic and therapeutic implications. *Journal of virology* **81**, 10209-10219, doi:10.1128/JVI.00872-07 (2007).

3 Freed, E. O. HIV-1 replication. *Somatic cell and molecular genetics* **26**, 13-33 (2001).

4 Scarlatti, G. *et al.* In vivo evolution of HIV-1 co-receptor usage and sensitivity to chemokine-mediated suppression. *Nature medicine* **3**, 1259-1265 (1997).

5 Adams, M. *et al.* Cellular latency in human immunodeficiency virus-infected individuals with high CD4 levels can be detected by the presence of promoter-proximal transcripts. *Proceedings of the National Academy of Sciences of the United States of America* **91**, 3862-3866 (1994).

6 Dalgleish, A. G. *et al.* The CD4 (T4) antigen is an essential component of the receptor for the AIDS retrovirus. *Nature* **312**, 763-767 (1984).

7 Sattentau, Q. J. & Moore, J. P. Conformational changes induced in the human immunodeficiency virus envelope glycoprotein by soluble CD4 binding. *The Journal of experimental medicine* **174**, 407-415 (1991).

8 Brown, P. O., Bowerman, B., Varmus, H. E. & Bishop, J. M. Retroviral integration: structure of the initial covalent product and its precursor, and a role for the viral IN protein. *Proceedings of the National Academy of Sciences of the United States of America* **86**, 2525-2529 (1989).

9 Bushman, F. D., Fujiwara, T. & Craigie, R. Retroviral DNA integration directed by HIV integration protein in vitro. *Science* **249**, 1555-1558 (1990).

10 Schwartz, S., Felber, B. K., Benko, D. M., Fenyo, E. M. & Pavlakis, G. N. Cloning and functional analysis of multiply spliced mRNA species of human immunodeficiency virus type 1. *Journal of virology* **64**, 2519-2529 (1990).

11 Greene, W. C. & Peterlin, B. M. Charting HIV's remarkable voyage through the cell: Basic science as a passport to future therapy. *Nature medicine* **8**, 673-680, doi:10.1038/nm0702-673 (2002).

12 Hallenberger, S. *et al.* Inhibition of furin-mediated cleavage activation of HIV-1 glycoprotein gp160. *Nature* **360**, 358-361, doi:10.1038/360358a0 (1992).

13 Freed, E. O. & Martin, M. A. Domains of the human immunodeficiency virus type 1 matrix and gp41 cytoplasmic tail required for envelope incorporation into virions. *Journal of virology* **70**, 341-351 (1996).

14 Booth, A. M. *et al.* Exosomes and HIV Gag bud from endosome-like domains of the T cell plasma membrane. *The Journal of cell biology* **172**, 923-935, doi:10.1083/jcb.200508014 (2006).

15 Salazar-Gonzalez, J. F. *et al.* Genetic identity, biological phenotype, and evolutionary pathways of transmitted/founder viruses in acute and early HIV-1 infection. *The Journal of experimental medicine* **206**, 1273-1289, doi:10.1084/jem.20090378 (2009).

16 Keele, B. F. *et al.* Identification and characterization of transmitted and early founder virus envelopes in primary HIV-1 infection. *Proceedings of the National Academy of Sciences of the United States of America* **105**, 7552-7557, doi:10.1073/pnas.0802203105 (2008).

17 Haase, A. T. Targeting early infection to prevent HIV-1 mucosal transmission. *Nature* **464**, 217-223, doi:10.1038/nature08757 (2010).

18 McMichael, A. J., Borrow, P., Tomaras, G. D., Goonetilleke, N. & Haynes, B. F. The immune response during acute HIV-1 infection: clues for vaccine development. *Nature reviews. Immunology* **10**, 11-23, doi:10.1038/nri2674 (2010).

19 Mellors, J. W. *et al.* Quantitation of HIV-1 RNA in plasma predicts outcome after seroconversion. *Annals of internal medicine* **122**, 573-579 (1995).
20 Hazenberg, M. D. *et al.* T-cell division in human immunodeficiency virus (HIV)-1 infection is mainly due to immune activation: a longitudinal analysis in patients before and during highly active antiretroviral therapy (HAART). *Blood* **95**, 249-255 (2000).
21 Lane, H. C. *et al.* Abnormalities of B-cell activation and immunoregulation in patients with the acquired immunodeficiency syndrome. *The New England journal of medicine* **309**, 453-458, doi:10.1056/NEJM198308253090803 (1983).
22 Brenchley, J. M. *et al.* Microbial translocation is a cause of systemic immune activation in chronic HIV infection. *Nature medicine* **12**, 1365-1371, doi:10.1038/nm1511 (2006).
23 Rerks-Ngarm, S. *et al.* Vaccination with ALVAC and AIDSVAX to prevent HIV-1 infection in Thailand. *The New England journal of medicine* **361**, 2209-2220, doi:10.1056/NEJMoa0908492 (2009).
24 Gilbert, P. B. *et al.* Statistical interpretation of the RV144 HIV vaccine efficacy trial in Thailand: a case study for statistical issues in efficacy trials. *The Journal of infectious diseases* **203**, 969-975, doi:10.1093/infdis/jiq152 (2011).
25 Robb, M. L. *et al.* Risk behaviour and time as covariates for efficacy of the HIV vaccine regimen ALVAC-HIV (vCP1521) and AIDSVAX B/E: a post-hoc analysis of the Thai phase 3 efficacy trial RV 144. *The Lancet. Infectious diseases* **12**, 531-537, doi:10.1016/S1473-3099(12)70088-9 (2012).
26 Kaslow, R. A. *et al.* Influence of combinations of human major histocompatibility complex genes on the course of HIV-1 infection. *Nature medicine* **2**, 405-411 (1996).
27 Learmont, J. C. *et al.* Immunologic and virologic status after 14 to 18 years of infection with an attenuated strain of HIV-1. A report from the Sydney Blood Bank Cohort. *The New England journal of medicine* **340**, 1715-1722, doi:10.1056/NEJM199906033402203 (1999).
28 Pereyra, F. *et al.* The major genetic determinants of HIV-1 control affect HLA class I peptide presentation. *Science* **330**, 1551-1557, doi:10.1126/science.1195271 (2010).
29 Alkhatib, G. The biology of CCR5 and CXCR4. *Current opinion in HIV and AIDS* **4**, 96-103, doi:10.1097/COH.0b013e328324bbec (2009).
30 Pollakis, G. & Paxton, W. A. Use of (alternative) coreceptors for HIV entry. *Current opinion in HIV and AIDS* **7**, 440-449, doi:10.1097/COH.0b013e328356e9f3 (2012).
31 Vetter, M. L., Johnson, M. E., Antons, A. K., Unutmaz, D. & D'Aquila, R. T. Differences in APOBEC3G expression in CD4+ T helper lymphocyte subtypes modulate HIV-1 infectivity. *PLoS pathogens* **5**, e1000292, doi:10.1371/journal.ppat.1000292 (2009).
32 Laguette, N. *et al.* SAMHD1 is the dendritic- and myeloid-cell-specific HIV-1 restriction factor counteracted by Vpx. *Nature* **474**, 654-657, doi:10.1038/nature10117 (2011).
33 Javanbakht, H. *et al.* Effects of human TRIM5alpha polymorphisms on antiretroviral function and susceptibility to human immunodeficiency virus infection. *Virology* **354**, 15-27, doi:10.1016/j.virol.2006.06.031 (2006).
34 Speelmon, E. C. *et al.* Genetic association of the antiviral restriction factor TRIM5alpha with human immunodeficiency virus type 1 infection. *Journal of virology* **80**, 2463-2471, doi:10.1128/JVI.80.5.2463-2471.2006 (2006).
35 Sewram, S. *et al.* Human TRIM5alpha expression levels and reduced susceptibility to HIV-1 infection. *The Journal of infectious diseases* **199**, 1657-1663, doi:10.1086/598861 (2009).
36 Huang, Y. *et al.* The role of a mutant CCR5 allele in HIV-1 transmission and disease progression. *Nature medicine* **2**, 1240-1243 (1996).
37 Liu, R. *et al.* Homozygous defect in HIV-1 coreceptor accounts for resistance of some multiply-exposed individuals to HIV-1 infection. *Cell* **86**, 367-377 (1996).

38 Kirchhoff, F., Greenough, T. C., Brettler, D. B., Sullivan, J. L. & Desrosiers, R. C. Brief report: absence of intact nef sequences in a long-term survivor with nonprogressive HIV-1 infection. *The New England journal of medicine* **332**, 228-232, doi:10.1056/NEJM199501263320405 (1995).
39 Klein, M. R. & Miedema, F. Long-term survivors of HIV-1 infection. *Trends in microbiology* **3**, 386-391 (1995).
40 Lefrere, J. J. *et al.* Even individuals considered as long-term nonprogressors show biological signs of progression after 10 years of human immunodeficiency virus infection. *Blood* **90**, 1133-1140 (1997).
41 Deeks, S. G. & Walker, B. D. Human immunodeficiency virus controllers: mechanisms of durable virus control in the absence of antiretroviral therapy. *Immunity* **27**, 406-416, doi:10.1016/j.immuni.2007.08.010 (2007).
42 Carrington, M. & O'Brien, S. J. The influence of HLA genotype on AIDS. *Annual review of medicine* **54**, 535-551, doi:10.1146/annurev.med.54.101601.152346 (2003).
43 Goulder, P. J. *et al.* Late escape from an immunodominant cytotoxic T-lymphocyte response associated with progression to AIDS. *Nature medicine* **3**, 212-217 (1997).
44 Migueles, S. A. & Connors, M. Long-term nonprogressive disease among untreated HIV-infected individuals: clinical implications of understanding immune control of HIV. *Jama* **304**, 194-201, doi:10.1001/jama.2010.925 (2010).
45 Mellors, J. W. *et al.* Prognosis in HIV-1 infection predicted by the quantity of virus in plasma. *Science* **272**, 1167-1170 (1996).
46 Oxenius, A. *et al.* Early highly active antiretroviral therapy for acute HIV-1 infection preserves immune function of CD8+ and CD4+ T lymphocytes. *Proceedings of the National Academy of Sciences of the United States of America* **97**, 3382-3387 (2000).
47 Alter, G. *et al.* Sequential deregulation of NK cell subset distribution and function starting in acute HIV-1 infection. *Blood* **106**, 3366-3369, doi:10.1182/blood-2005-03-1100 (2005).
48 Mavilio, D. *et al.* Natural killer cells in HIV-1 infection: dichotomous effects of viremia on inhibitory and activating receptors and their functional correlates. *Proceedings of the National Academy of Sciences of the United States of America* **100**, 15011-15016, doi:10.1073/pnas.2336091100 (2003).
49 Mavilio, D. *et al.* Characterization of CD56-/CD16+ natural killer (NK) cells: a highly dysfunctional NK subset expanded in HIV-infected viremic individuals. *Proceedings of the National Academy of Sciences of the United States of America* **102**, 2886-2891, doi:10.1073/pnas.0409872102 (2005).
50 Lanier, L. L. NK cell recognition. *Annual review of immunology* **23**, 225-274, doi:10.1146/annurev.immunol.23.021704.115526 (2005).
51 Fauci, A. S., Mavilio, D. & Kottilil, S. NK cells in HIV infection: paradigm for protection or targets for ambush. *Nature reviews. Immunology* **5**, 835-843, doi:10.1038/nri1711 (2005).
52 Martin, M. P. *et al.* Innate partnership of HLA-B and KIR3DL1 subtypes against HIV-1. *Nature genetics* **39**, 733-740, doi:10.1038/ng2035 (2007).
53 Plotkin, S. A. Correlates of protection induced by vaccination. *Clinical and vaccine immunology : CVI* **17**, 1055-1065, doi:10.1128/CVI.00131-10 (2010).
54 Baba, T. W. *et al.* Human neutralizing monoclonal antibodies of the IgG1 subtype protect against mucosal simian-human immunodeficiency virus infection. *Nature medicine* **6**, 200-206, doi:10.1038/72309 (2000).
55 Mascola, J. R. Passive transfer studies to elucidate the role of antibody-mediated protection against HIV-1. *Vaccine* **20**, 1922-1925 (2002).
56 Barouch, D. H. *et al.* Therapeutic efficacy of potent neutralizing HIV-1-specific monoclonal antibodies in SHIV-infected rhesus monkeys. *Nature* **503**, 224-228, doi:10.1038/nature12744 (2013).

57 Caskey, M. *et al.* Viraemia suppressed in HIV-1-infected humans by broadly neutralizing antibody 3BNC117. *Nature*, doi:10.1038/nature14411 (2015).
58 Nel, A. E. & Slaughter, N. T-cell activation through the antigen receptor. Part 2: role of signaling cascades in T-cell differentiation, anergy, immune senescence, and development of immunotherapy. *The Journal of allergy and clinical immunology* **109**, 901-915 (2002).
59 Nel, A. E. T-cell activation through the antigen receptor. Part 1: signaling components, signaling pathways, and signal integration at the T-cell antigen receptor synapse. *The Journal of allergy and clinical immunology* **109**, 758-770 (2002).
60 Horton, H. *et al.* Preservation of T cell proliferation restricted by protective HLA alleles is critical for immune control of HIV-1 infection. *Journal of immunology* **177**, 7406-7415 (2006).
61 Zimmerli, S. C. *et al.* HIV-1-specific IFN-gamma/IL-2-secreting CD8 T cells support CD4-independent proliferation of HIV-1-specific CD8 T cells. *Proceedings of the National Academy of Sciences of the United States of America* **102**, 7239-7244, doi:10.1073/pnas.0502393102 (2005).
62 Betts, M. R. *et al.* HIV nonprogressors preferentially maintain highly functional HIV-specific CD8+ T cells. *Blood* **107**, 4781-4789, doi:10.1182/blood-2005-12-4818 (2006).
63 Koup, R. A. *et al.* Temporal association of cellular immune responses with the initial control of viremia in primary human immunodeficiency virus type 1 syndrome. *Journal of virology* **68**, 4650-4655 (1994).
64 Ogg, G. S. *et al.* Longitudinal phenotypic analysis of human immunodeficiency virus type 1-specific cytotoxic T lymphocytes: correlation with disease progression. *Journal of virology* **73**, 9153-9160 (1999).
65 Borrow, P., Lewicki, H., Hahn, B. H., Shaw, G. M. & Oldstone, M. B. Virus-specific CD8+ cytotoxic T-lymphocyte activity associated with control of viremia in primary human immunodeficiency virus type 1 infection. *Journal of virology* **68**, 6103-6110 (1994).
66 Yu, X. G. *et al.* Consistent patterns in the development and immunodominance of human immunodeficiency virus type 1 (HIV-1)-specific CD8+ T-cell responses following acute HIV-1 infection. *Journal of virology* **76**, 8690-8701 (2002).
67 Wilson, J. D. *et al.* Direct visualization of HIV-1-specific cytotoxic T lymphocytes during primary infection. *Aids* **14**, 225-233 (2000).
68 Jin, X. *et al.* Dramatic rise in plasma viremia after CD8(+) T cell depletion in simian immunodeficiency virus-infected macaques. *The Journal of experimental medicine* **189**, 991-998 (1999).
69 Schmitz, J. E. *et al.* Control of viremia in simian immunodeficiency virus infection by CD8+ lymphocytes. *Science* **283**, 857-860 (1999).
70 Migueles, S. A. *et al.* HLA B*5701 is highly associated with restriction of virus replication in a subgroup of HIV-infected long term nonprogressors. *Proceedings of the National Academy of Sciences of the United States of America* **97**, 2709-2714, doi:10.1073/pnas.050567397 (2000).
71 Frahm, N. *et al.* Control of human immunodeficiency virus replication by cytotoxic T lymphocytes targeting subdominant epitopes. *Nature immunology* **7**, 173-178, doi:10.1038/ni1281 (2006).
72 Honeyborne, I. *et al.* Control of human immunodeficiency virus type 1 is associated with HLA-B*13 and targeting of multiple gag-specific CD8+ T-cell epitopes. *Journal of virology* **81**, 3667-3672, doi:10.1128/JVI.02689-06 (2007).
73 Emu, B. *et al.* HLA class I-restricted T-cell responses may contribute to the control of human immunodeficiency virus infection, but such responses are not always necessary for long-term virus control. *Journal of virology* **82**, 5398-5407, doi:10.1128/JVI.02176-07 (2008).

74 Lambotte, O. *et al.* HIV controllers: a homogeneous group of HIV-1-infected patients with spontaneous control of viral replication. *Clinical infectious diseases : an official publication of the Infectious Diseases Society of America* **41**, 1053-1056, doi:10.1086/433188 (2005).
75 Boaz, M. J., Waters, A., Murad, S., Easterbrook, P. J. & Vyakarnam, A. Presence of HIV-1 Gag-specific IFN-gamma+IL-2+ and CD28+IL-2+ CD4 T cell responses is associated with nonprogression in HIV-1 infection. *Journal of immunology* **169**, 6376-6385 (2002).
76 Almeida, J. R. *et al.* Superior control of HIV-1 replication by CD8+ T cells is reflected by their avidity, polyfunctionality, and clonal turnover. *The Journal of experimental medicine* **204**, 2473-2485, doi:10.1084/jem.20070784 (2007).
77 Migueles, S. A. *et al.* HIV-specific CD8+ T cell proliferation is coupled to perforin expression and is maintained in nonprogressors. *Nature immunology* **3**, 1061-1068, doi:10.1038/ni845 (2002).
78 Saez-Cirion, A. *et al.* HIV controllers exhibit potent CD8 T cell capacity to suppress HIV infection ex vivo and peculiar cytotoxic T lymphocyte activation phenotype. *Proceedings of the National Academy of Sciences of the United States of America* **104**, 6776-6781, doi:10.1073/pnas.0611244104 (2007).
79 Chen, H. *et al.* Differential neutralization of human immunodeficiency virus (HIV) replication in autologous CD4 T cells by HIV-specific cytotoxic T lymphocytes. *Journal of virology* **83**, 3138-3149, doi:10.1128/JVI.02073-08 (2009).
80 Migueles, S. A. *et al.* Lytic granule loading of CD8+ T cells is required for HIV-infected cell elimination associated with immune control. *Immunity* **29**, 1009-1021, doi:10.1016/j.immuni.2008.10.010 (2008).
81 Hersperger, A. R. *et al.* Perforin expression directly ex vivo by HIV-specific CD8 T-cells is a correlate of HIV elite control. *PLoS pathogens* **6**, e1000917, doi:10.1371/journal.ppat.1000917 (2010).
82 Goonetilleke, N. *et al.* The first T cell response to transmitted/founder virus contributes to the control of acute viremia in HIV-1 infection. *The Journal of experimental medicine* **206**, 1253-1272, doi:10.1084/jem.20090365 (2009).
83 Edwards, B. H. *et al.* Magnitude of functional CD8+ T-cell responses to the gag protein of human immunodeficiency virus type 1 correlates inversely with viral load in plasma. *Journal of virology* **76**, 2298-2305 (2002).
84 Kiepiela, P. *et al.* CD8+ T-cell responses to different HIV proteins have discordant associations with viral load. *Nature medicine* **13**, 46-53, doi:10.1038/nm1520 (2007).
85 Schneidewind, A. *et al.* Structural and functional constraints limit options for cytotoxic T-lymphocyte escape in the immunodominant HLA-B27-restricted epitope in human immunodeficiency virus type 1 capsid. *Journal of virology* **82**, 5594-5605, doi:10.1128/JVI.02356-07 (2008).
86 Schneidewind, A. *et al.* Transmission and long-term stability of compensated CD8 escape mutations. *Journal of virology* **83**, 3993-3997, doi:10.1128/JVI.01108-08 (2009).
87 Ferrando-Martinez, S. *et al.* HIV infection-related premature immunosenescence: high rates of immune exhaustion after short time of infection. *Current HIV research* **9**, 289-294 (2011).
88 Mosmann, T. R., Cherwinski, H., Bond, M. W., Giedlin, M. A. & Coffman, R. L. Two types of murine helper T cell clone. I. Definition according to profiles of lymphokine activities and secreted proteins. 1986. *Journal of immunology* **175**, 5-14 (2005).
89 Simon, M. M., Landolfo, S., Diamantstein, T. & Hochgeschwender, U. Antigen- and lectin-sensitized murine cytolytic T lymphocyte-precursors require both interleukin 2 and endogenously produced immune (gamma) interferon for their growth and differentiation into effector cells. *Current topics in microbiology and immunology* **126**, 173-185 (1986).

90 Shedlock, D. J. & Shen, H. Requirement for CD4 T cell help in generating functional CD8 T cell memory. *Science* **300**, 337-339, doi:10.1126/science.1082305 (2003).
91 Sun, J. C. & Bevan, M. J. Defective CD8 T cell memory following acute infection without CD4 T cell help. *Science* **300**, 339-342, doi:10.1126/science.1083317 (2003).
92 Lebman, D. A. & Coffman, R. L. Interleukin 4 causes isotype switching to IgE in T cell-stimulated clonal B cell cultures. *The Journal of experimental medicine* **168**, 853-862 (1988).
93 Veldhoen, M., Hocking, R. J., Atkins, C. J., Locksley, R. M. & Stockinger, B. TGFbeta in the context of an inflammatory cytokine milieu supports de novo differentiation of IL-17-producing T cells. *Immunity* **24**, 179-189, doi:10.1016/j.immuni.2006.01.001 (2006).
94 Khanna, R. *et al.* Class I processing-defective Burkitt's lymphoma cells are recognized efficiently by CD4+ EBV-specific CTLs. *Journal of immunology* **158**, 3619-3625 (1997).
95 Long, H. M. *et al.* CD4+ T-cell responses to Epstein-Barr virus (EBV) latent-cycle antigens and the recognition of EBV-transformed lymphoblastoid cell lines. *Journal of virology* **79**, 4896-4907, doi:10.1128/JVI.79.8.4896-4907.2005 (2005).
96 Soghoian, D. Z. & Streeck, H. Cytolytic CD4(+) T cells in viral immunity. *Expert review of vaccines* **9**, 1453-1463, doi:10.1586/erv.10.132 (2010).
97 Debbabi, H. *et al.* Primary type II alveolar epithelial cells present microbial antigens to antigen-specific CD4+ T cells. *American journal of physiology. Lung cellular and molecular physiology* **289**, L274-279, doi:10.1152/ajplung.00004.2005 (2005).
98 Brien, J. D., Uhrlaub, J. L. & Nikolich-Zugich, J. West Nile virus-specific CD4 T cells exhibit direct antiviral cytokine secretion and cytotoxicity and are sufficient for antiviral protection. *Journal of immunology* **181**, 8568-8575 (2008).
99 Sparks-Thissen, R. L., Braaten, D. C., Kreher, S., Speck, S. H. & Virgin, H. W. t. An optimized CD4 T-cell response can control productive and latent gammaherpesvirus infection. *Journal of virology* **78**, 6827-6835, doi:10.1128/JVI.78.13.6827-6835.2004 (2004).
100 Stuller, K. A., Cush, S. S. & Flano, E. Persistent gamma-herpesvirus infection induces a CD4 T cell response containing functionally distinct effector populations. *Journal of immunology* **184**, 3850-3856, doi:10.4049/jimmunol.0902935 (2010).
101 Munz, C. *et al.* Human CD4(+) T lymphocytes consistently respond to the latent Epstein-Barr virus nuclear antigen EBNA1. *The Journal of experimental medicine* **191**, 1649-1660 (2000).
102 Soghoian, D. Z. *et al.* HIV-specific cytolytic CD4 T cell responses during acute HIV infection predict disease outcome. *Science translational medicine* **4**, 123ra125, doi:10.1126/scitranslmed.3003165 (2012).
103 Ritchie, A. J. *et al.* Differences in HIV-specific T cell responses between HIV-exposed and -unexposed HIV-seronegative individuals. *Journal of virology* **85**, 3507-3516, doi:10.1128/JVI.02444-10 (2011).
104 Lok, J. J. *et al.* Long-term increase in CD4+ T-cell counts during combination antiretroviral therapy for HIV-1 infection. *Aids* **24**, 1867-1876, doi:10.1097/QAD.0b013e32833adbcf (2010).
105 Rehr, M. *et al.* Emergence of polyfunctional CD8+ T cells after prolonged suppression of human immunodeficiency virus replication by antiretroviral therapy. *Journal of virology* **82**, 3391-3404, doi:10.1128/JVI.02383-07 (2008).
106 Guihot, A., Bourgarit, A., Carcelain, G. & Autran, B. Immune reconstitution after a decade of combined antiretroviral therapies for human immunodeficiency virus. *Trends in immunology* **32**, 131-137, doi:10.1016/j.it.2010.12.002 (2011).
107 Guihot, A. *et al.* Immune and virological benefits of 10 years of permanent viral control with antiretroviral therapy. *Aids* **24**, 614-617, doi:10.1097/QAD.0b013e32833556f3 (2010).
108 Mocroft, A. *et al.* The incidence of AIDS-defining illnesses at a current CD4 count >/= 200 cells/muL in the post-combination antiretroviral therapy era. *Clinical infectious diseases : an*

official publication of the Infectious Diseases Society of America **57**, 1038-1047, doi:10.1093/cid/cit423 (2013).
109 Hleyhel, M. *et al.* Risk of AIDS-defining cancers among HIV-1-infected patients in France between 1992 and 2009: results from the FHDH-ANRS CO4 cohort. *Clinical infectious diseases : an official publication of the Infectious Diseases Society of America* **57**, 1638-1647, doi:10.1093/cid/cit497 (2013).
110 Mocroft, A. *et al.* Decline in the AIDS and death rates in the EuroSIDA study: an observational study. *Lancet* **362**, 22-29 (2003).
111 Palella, F. J., Jr. *et al.* Survival benefit of initiating antiretroviral therapy in HIV-infected persons in different CD4+ cell strata. *Annals of internal medicine* **138**, 620-626 (2003).
112 Rodger, A. J. *et al.* Mortality in well controlled HIV in the continuous antiretroviral therapy arms of the SMART and ESPRIT trials compared with the general population. *Aids* **27**, 973-979, doi:10.1097/QAD.0b013e32835cae9c (2013).
113 May, M. T. *et al.* Impact on life expectancy of HIV-1 positive individuals of CD4+ cell count and viral load response to antiretroviral therapy. *Aids* **28**, 1193-1202, doi:10.1097/QAD.0000000000000243 (2014).
114 Taiwo, B. *et al.* Antiretroviral drug resistance in HIV-1-infected patients experiencing persistent low-level viremia during first-line therapy. *The Journal of infectious diseases* **204**, 515-520, doi:10.1093/infdis/jir353 (2011).
115 Vardhanabhuti, S., Taiwo, B., Kuritzkes, D. R., Eron, J. J., Jr. & Bosch, R. J. Phylogenetic evidence of HIV-1 sequence evolution in subjects with persistent low-level viraemia. *Antiviral therapy* **20**, 73-76, doi:10.3851/IMP2772 (2015).
116 Donnell, D. *et al.* Heterosexual HIV-1 transmission after initiation of antiretroviral therapy: a prospective cohort analysis. *Lancet* **375**, 2092-2098, doi:10.1016/S0140-6736(10)60705-2 (2010).
117 Cohen, M. S. *et al.* Prevention of HIV-1 infection with early antiretroviral therapy. *The New England journal of medicine* **365**, 493-505, doi:10.1056/NEJMoa1105243 (2011).
118 Cihlar, T. & Ray, A. S. Nucleoside and nucleotide HIV reverse transcriptase inhibitors: 25 years after zidovudine. *Antiviral research* **85**, 39-58, doi:10.1016/j.antiviral.2009.09.014 (2010).
119 Clavel, F. & Hance, A. J. HIV drug resistance. *The New England journal of medicine* **350**, 1023-1035, doi:10.1056/NEJMra025195 (2004).
120 Sluis-Cremer, N. The emerging profile of cross-resistance among the nonnucleoside HIV-1 reverse transcriptase inhibitors. *Viruses* **6**, 2960-2973, doi:10.3390/v6082960 (2014).
121 Flexner, C. HIV-protease inhibitors. *The New England journal of medicine* **338**, 1281-1292, doi:10.1056/NEJM199804303381808 (1998).
122 Nijhuis, M., van Maarseveen, N. M. & Boucher, C. A. HIV protease resistance and viral fitness. *Current opinion in HIV and AIDS* **2**, 108-115, doi:10.1097/COH.0b013e32801682f6 (2007).
123 Nijhuis, M. *et al.* A novel substrate-based HIV-1 protease inhibitor drug resistance mechanism. *PLoS medicine* **4**, e36, doi:10.1371/journal.pmed.0040036 (2007).
124 Croxtall, J. D. & Keam, S. J. Raltegravir: a review of its use in the management of HIV infection in treatment-experienced patients. *Drugs* **69**, 1059-1075, doi:10.2165/00003495-200969080-00007 (2009).
125 Chirch, L. M., Morrison, S. & Steigbigel, R. T. Treatment of HIV infection with raltegravir. *Expert opinion on pharmacotherapy* **10**, 1203-1211, doi:10.1517/14656560902911488 (2009).
126 Tilton, J. C. & Doms, R. W. Entry inhibitors in the treatment of HIV-1 infection. *Antiviral research* **85**, 91-100, doi:10.1016/j.antiviral.2009.07.022 (2010).
127 Lengauer, T., Sander, O., Sierra, S., Thielen, A. & Kaiser, R. Bioinformatics prediction of HIV coreceptor usage. *Nature biotechnology* **25**, 1407-1410, doi:10.1038/nbt1371 (2007).

128 Este, J. A. & Telenti, A. HIV entry inhibitors. *Lancet* **370**, 81-88, doi:10.1016/S0140-6736(07)61052-6 (2007).
129 Miller, M. D. & Hazuda, D. J. HIV resistance to the fusion inhibitor enfuvirtide: mechanisms and clinical implications. *Drug resistance updates : reviews and commentaries in antimicrobial and anticancer chemotherapy* **7**, 89-95, doi:10.1016/j.drup.2004.03.003 (2004).
130 Kumar, G. N., Rodrigues, A. D., Buko, A. M. & Denissen, J. F. Cytochrome P450-mediated metabolism of the HIV-1 protease inhibitor ritonavir (ABT-538) in human liver microsomes. *The Journal of pharmacology and experimental therapeutics* **277**, 423-431 (1996).
131 Guaraldi, G., Prakash, M., Moecklinghoff, C. & Stellbrink, H. J. Morbidity in older HIV-infected patients: impact of long-term antiretroviral use. *AIDS reviews* **16**, 75-89 (2014).
132 Martinez, E. *et al.* Risk of lipodystrophy in HIV-1-infected patients treated with protease inhibitors: a prospective cohort study. *Lancet* **357**, 592-598, doi:10.1016/S0140-6736(00)04056-3 (2001).
133 Giralt, M. *et al.* HIV-1 infection alters gene expression in adipose tissue, which contributes to HIV- 1/HAART-associated lipodystrophy. *Antiviral therapy* **11**, 729-740 (2006).
134 Capeau, J. *et al.* [Lipodystrophies related to antiretroviral treatment of HIV infection]. *Medecine sciences : M/S* **22**, 531-536, doi:10.1051/medsci/2006225531 (2006).
135 Caron-Debarle, M. *et al.* Adipose tissue as a target of HIV-1 antiretroviral drugs. Potential consequences on metabolic regulations. *Current pharmaceutical design* **16**, 3352-3360 (2010).
136 Lagathu, C. *et al.* Antiretroviral drugs with adverse effects on adipocyte lipid metabolism and survival alter the expression and secretion of proinflammatory cytokines and adiponectin in vitro. *Antiviral therapy* **9**, 911-920 (2004).
137 Guaraldi, G. *et al.* CD8 T-cell activation is associated with lipodystrophy and visceral fat accumulation in antiretroviral therapy-treated virologically suppressed HIV-infected patients. *Journal of acquired immune deficiency syndromes* **64**, 360-366, doi:10.1097/QAI.0000000000000001 (2013).
138 Saves, M. *et al.* Factors related to lipodystrophy and metabolic alterations in patients with human immunodeficiency virus infection receiving highly active antiretroviral therapy. *Clinical infectious diseases : an official publication of the Infectious Diseases Society of America* **34**, 1396-1405, doi:10.1086/339866 (2002).
139 Bard, J. M. *et al.* Association of apolipoproteins C3 and E with metabolic changes in HIV-infected adults treated with a protease-inhibitor-containing antiretroviral therapy. *Antiviral therapy* **11**, 361-370 (2006).
140 Brown, T. T. *et al.* Antiretroviral therapy and the prevalence and incidence of diabetes mellitus in the multicenter AIDS cohort study. *Archives of internal medicine* **165**, 1179-1184, doi:10.1001/archinte.165.10.1179 (2005).
141 Ledergerber, B. *et al.* Factors associated with the incidence of type 2 diabetes mellitus in HIV-infected participants in the Swiss HIV Cohort Study. *Clinical infectious diseases : an official publication of the Infectious Diseases Society of America* **45**, 111-119, doi:10.1086/518619 (2007).
142 De Wit, S. *et al.* Incidence and risk factors for new-onset diabetes in HIV-infected patients: the Data Collection on Adverse Events of Anti-HIV Drugs (D:A:D) study. *Diabetes care* **31**, 1224-1229, doi:10.2337/dc07-2013 (2008).
143 Capeau, J. *et al.* Ten-year diabetes incidence in 1046 HIV-infected patients started on a combination antiretroviral treatment. *Aids* **26**, 303-314, doi:10.1097/QAD.0b013e32834e8776 (2012).
144 Lang, S. *et al.* Increased risk of myocardial infarction in HIV-infected patients in France, relative to the general population. *Aids* **24**, 1228-1230, doi:10.1097/QAD.0b013e328339192f (2010).

145 Mu, H., Chai, H., Lin, P. H., Yao, Q. & Chen, C. Current update on HIV-associated vascular disease and endothelial dysfunction. *World journal of surgery* **31**, 632-643, doi:10.1007/s00268-006-0730-0 (2007).
146 Mondy, K. E. Determinants of endothelial function in human immunodeficiency virus infection: a complex interplay among therapy, disease, and host factors. *Journal of the cardiometabolic syndrome* **3**, 88-92 (2008).
147 Worm, S. W. *et al.* Risk of myocardial infarction in patients with HIV infection exposed to specific individual antiretroviral drugs from the 3 major drug classes: the data collection on adverse events of anti-HIV drugs (D:A:D) study. *The Journal of infectious diseases* **201**, 318-330, doi:10.1086/649897 (2010).
148 Brown, T. T. & Qaqish, R. B. Antiretroviral therapy and the prevalence of osteopenia and osteoporosis: a meta-analytic review. *Aids* **20**, 2165-2174, doi:10.1097/QAD.0b013e32801022eb (2006).
149 Duvivier, C. *et al.* Greater decrease in bone mineral density with protease inhibitor regimens compared with nonnucleoside reverse transcriptase inhibitor regimens in HIV-1 infected naive patients. *Aids* **23**, 817-824, doi:10.1097/QAD.0b013e328328f789 (2009).
150 Assoumou, L. *et al.* Changes in bone mineral density over a 2-year period in HIV-1-infected men under combined antiretroviral therapy with osteopenia. *Aids* **27**, 2425-2430, doi:10.1097/QAD.0b013e32836378c3 (2013).
151 Hansen, A. B. *et al.* Incidence of low and high-energy fractures in persons with and without HIV infection: a Danish population-based cohort study. *Aids* **26**, 285-293, doi:10.1097/QAD.0b013e32834ed8a7 (2012).
152 Bedimo, R., Maalouf, N. M., Zhang, S., Drechsler, H. & Tebas, P. Osteoporotic fracture risk associated with cumulative exposure to tenofovir and other antiretroviral agents. *Aids* **26**, 825-831, doi:10.1097/QAD.0b013e32835192ae (2012).
153 Katlama, C. *et al.* Barriers to a cure for HIV: new ways to target and eradicate HIV-1 reservoirs. *Lancet* **381**, 2109-2117, doi:10.1016/S0140-6736(13)60104-X (2013).
154 Chun, T. W. & Fauci, A. S. HIV reservoirs: pathogenesis and obstacles to viral eradication and cure. *Aids* **26**, 1261-1268, doi:10.1097/QAD.0b013e328353f3f1 (2012).
155 Hatano, H. Immune activation and HIV persistence: considerations for novel therapeutic interventions. *Current opinion in HIV and AIDS* **8**, 211-216, doi:10.1097/COH.0b013e32835f9788 (2013).
156 Wong, J. K. *et al.* Recovery of replication-competent HIV despite prolonged suppression of plasma viremia. *Science* **278**, 1291-1295 (1997).
157 Finzi, D. *et al.* Identification of a reservoir for HIV-1 in patients on highly active antiretroviral therapy. *Science* **278**, 1295-1300 (1997).
158 Chun, T. W. *et al.* Presence of an inducible HIV-1 latent reservoir during highly active antiretroviral therapy. *Proceedings of the National Academy of Sciences of the United States of America* **94**, 13193-13197 (1997).
159 Harrigan, P. R., Whaley, M. & Montaner, J. S. Rate of HIV-1 RNA rebound upon stopping antiretroviral therapy. *Aids* **13**, F59-62 (1999).
160 Davey, R. T., Jr. *et al.* HIV-1 and T cell dynamics after interruption of highly active antiretroviral therapy (HAART) in patients with a history of sustained viral suppression. *Proceedings of the National Academy of Sciences of the United States of America* **96**, 15109-15114 (1999).
161 Garcia, F. *et al.* Dynamics of viral load rebound and immunological changes after stopping effective antiretroviral therapy. *Aids* **13**, F79-86 (1999).

162 Chun, T. W. *et al.* Early establishment of a pool of latently infected, resting CD4(+) T cells during primary HIV-1 infection. *Proceedings of the National Academy of Sciences of the United States of America* **95**, 8869-8873 (1998).
163 Whitney, J. B. *et al.* Rapid seeding of the viral reservoir prior to SIV viraemia in rhesus monkeys. *Nature* **512**, 74-77, doi:10.1038/nature13594 (2014).
164 Passaes, C. P. & Saez-Cirion, A. HIV cure research: advances and prospects. *Virology* **454-455**, 340-352, doi:10.1016/j.virol.2014.02.021 (2014).
165 Siliciano, J. D. *et al.* Stability of the latent reservoir for HIV-1 in patients receiving valproic acid. *The Journal of infectious diseases* **195**, 833-836, doi:10.1086/511823 (2007).
166 Sagot-Lerolle, N. *et al.* Prolonged valproic acid treatment does not reduce the size of latent HIV reservoir. *Aids* **22**, 1125-1129, doi:10.1097/QAD.0b013e3282fd6ddc (2008).
167 Archin, N. M. *et al.* Valproic acid without intensified antiviral therapy has limited impact on persistent HIV infection of resting CD4+ T cells. *Aids* **22**, 1131-1135, doi:10.1097/QAD.0b013e3282fd6df4 (2008).
168 Rasmussen, T. A. *et al.* Comparison of HDAC inhibitors in clinical development: effect on HIV production in latently infected cells and T-cell activation. *Human vaccines & immunotherapeutics* **9**, 993-1001, doi:10.4161/hv.23800 (2013).
169 Hochreiter, J., McCance-Katz, E. F., Lapham, J., Ma, Q. & Morse, G. D. Disulfiram metabolite S-methyl-N,N-diethylthiocarbamate quantitation in human plasma with reverse phase ultra performance liquid chromatography and mass spectrometry. *Journal of chromatography. B, Analytical technologies in the biomedical and life sciences* **897**, 80-84, doi:10.1016/j.jchromb.2012.03.035 (2012).
170 Spivak, A. M. *et al.* A pilot study assessing the safety and latency-reversing activity of disulfiram in HIV-1-infected adults on antiretroviral therapy. *Clinical infectious diseases : an official publication of the Infectious Diseases Society of America* **58**, 883-890, doi:10.1093/cid/cit813 (2014).
171 Doyon, G., Zerbato, J., Mellors, J. W. & Sluis-Cremer, N. Disulfiram reactivates latent HIV-1 expression through depletion of the phosphatase and tensin homolog. *Aids* **27**, F7-F11, doi:10.1097/QAD.0b013e3283570620 (2013).
172 Kulkosky, J. *et al.* Intensification and stimulation therapy for human immunodeficiency virus type 1 reservoirs in infected persons receiving virally suppressive highly active antiretroviral therapy. *The Journal of infectious diseases* **186**, 1403-1411, doi:10.1086/344357 (2002).
173 Scripture-Adams, D. D., Brooks, D. G., Korin, Y. D. & Zack, J. A. Interleukin-7 induces expression of latent human immunodeficiency virus type 1 with minimal effects on T-cell phenotype. *Journal of virology* **76**, 13077-13082 (2002).
174 Wang, F. X. *et al.* IL-7 is a potent and proviral strain-specific inducer of latent HIV-1 cellular reservoirs of infected individuals on virally suppressive HAART. *The Journal of clinical investigation* **115**, 128-137, doi:10.1172/JCI22574 (2005).
175 Dornadula, G. *et al.* Residual HIV-1 RNA in blood plasma of patients taking suppressive highly active antiretroviral therapy. *Jama* **282**, 1627-1632 (1999).
176 Hermankova, M. *et al.* HIV-1 drug resistance profiles in children and adults with viral load of <50 copies/ml receiving combination therapy. *Jama* **286**, 196-207 (2001).
177 Dinoso, J. B. *et al.* Treatment intensification does not reduce residual HIV-1 viremia in patients on highly active antiretroviral therapy. *Proceedings of the National Academy of Sciences of the United States of America* **106**, 9403-9408, doi:10.1073/pnas.0903107106 (2009).
178 Gandhi, R. T. *et al.* The effect of raltegravir intensification on low-level residual viremia in HIV-infected patients on antiretroviral therapy: a randomized controlled trial. *PLoS medicine* **7**, doi:10.1371/journal.pmed.1000321 (2010).

179 Buzon, M. J. *et al.* HIV-1 replication and immune dynamics are affected by raltegravir intensification of HAART-suppressed subjects. *Nature medicine* **16**, 460-465, doi:10.1038/nm.2111 (2010).
180 Llibre, J. M. *et al.* Treatment intensification with raltegravir in subjects with sustained HIV-1 viraemia suppression: a randomized 48-week study. *Antiviral therapy* **17**, 355-364, doi:10.3851/IMP1917 (2012).
181 Migueles, S. A. *et al.* Defective human immunodeficiency virus-specific CD8+ T-cell polyfunctionality, proliferation, and cytotoxicity are not restored by antiretroviral therapy. *Journal of virology* **83**, 11876-11889, doi:10.1128/JVI.01153-09 (2009).
182 Keating, S. M. *et al.* The effect of HIV infection and HAART on inflammatory biomarkers in a population-based cohort of women. *Aids* **25**, 1823-1832, doi:10.1097/QAD.0b013e3283489d1f (2011).
183 French, M. A., King, M. S., Tschampa, J. M., da Silva, B. A. & Landay, A. L. Serum immune activation markers are persistently increased in patients with HIV infection after 6 years of antiretroviral therapy despite suppression of viral replication and reconstitution of CD4+ T cells. *The Journal of infectious diseases* **200**, 1212-1215, doi:10.1086/605890 (2009).
184 Nixon, D. E. & Landay, A. L. Biomarkers of immune dysfunction in HIV. *Current opinion in HIV and AIDS* **5**, 498-503, doi:10.1097/COH.0b013e32833ed6f4 (2010).
185 Mavigner, M. *et al.* HIV-1 residual viremia correlates with persistent T-cell activation in poor immunological responders to combination antiretroviral therapy. *PloS one* **4**, e7658, doi:10.1371/journal.pone.0007658 (2009).
186 Massanella, M. *et al.* Raltegravir intensification shows differing effects on CD8 and CD4 T cells in HIV-infected HAART-suppressed individuals with poor CD4 T-cell recovery. *Aids* **26**, 2285-2293, doi:10.1097/QAD.0b013e328359f20f (2012).
187 Lackner, A. A., Mohan, M. & Veazey, R. S. The gastrointestinal tract and AIDS pathogenesis. *Gastroenterology* **136**, 1965-1978 (2009).
188 Petrara, M. R. *et al.* Epstein-Barr virus load and immune activation in human immunodeficiency virus type 1-infected patients. *Journal of clinical virology : the official publication of the Pan American Society for Clinical Virology* **53**, 195-200, doi:10.1016/j.jcv.2011.12.013 (2012).
189 Wittkop, L. *et al.* Effect of cytomegalovirus-induced immune response, self antigen-induced immune response, and microbial translocation on chronic immune activation in successfully treated HIV type 1-infected patients: the ANRS CO3 Aquitaine Cohort. *The Journal of infectious diseases* **207**, 622-627, doi:10.1093/infdis/jis732 (2013).
190 van Lunzen, J., zur Wiesch, J. S., Schuhmacher, U., Hauber, I. & Hauber, J. in *7th IAS Conference on HIV Pathogenesis, Treatment and Prevention.* Vol. TUPE246 (2013).
191 Persaud, D., Gay, H. & Ziemniak, C. F. e. a. in *20th Conference on Retroviruses and Opportunistic Infections* Vol. Atlanta, GA (2013).
192 Perrin, L. & Telenti, A. HIV treatment failure: testing for HIV resistance in clinical practice. *Science* **280**, 1871-1873 (1998).
193 Ledergerber, B. *et al.* Clinical progression and virological failure on highly active antiretroviral therapy in HIV-1 patients: a prospective cohort study. Swiss HIV Cohort Study. *Lancet* **353**, 863-868 (1999).
194 Graham, D. B. *et al.* Increased thymic output in HIV-negative patients after antiretroviral therapy. *Aids* **19**, 1467-1472 (2005).
195 De Rossi, A. *et al.* Increased thymic output after initiation of antiretroviral therapy in human immunodeficiency virus type 1-infected children in the Paediatric European Network for Treatment of AIDS (PENTA) 5 Trial. *The Journal of infectious diseases* **186**, 312-320, doi:10.1086/341657 (2002).

196 Ometto, L. *et al.* Immune reconstitution in HIV-1-infected children on antiretroviral therapy: role of thymic output and viral fitness. *Aids* **16**, 839-849 (2002).
197 Delmonte, O. M., Bertolotto, G., Ricotti, E. & Tovo, P. A. Immunomodulatory effects of two HIV protease inhibitors, Saquinavir and Ritonavir, on lymphocytes from healthy seronegative individuals. *Immunology letters* **111**, 111-115, doi:10.1016/j.imlet.2007.06.003 (2007).
198 Heagy, W., Crumpacker, C., Lopez, P. A. & Finberg, R. W. Inhibition of immune functions by antiviral drugs. *The Journal of clinical investigation* **87**, 1916-1924, doi:10.1172/JCI115217 (1991).
199 Lu, W. & Andrieu, J. M. HIV protease inhibitors restore impaired T-cell proliferative response in vivo and in vitro: a viral-suppression-independent mechanism. *Blood* **96**, 250-258 (2000).
200 Tovo, P. A. Highly active antiretroviral therapy inhibits cytokine production in HIV-uninfected subjects. *Aids* **14**, 743-744 (2000).
201 Giardino Torchia, M. L. *et al.* Dendritic cells/natural killer cross-talk: a novel target for human immunodeficiency virus type-1 protease inhibitors. *PloS one* **5**, e11052, doi:10.1371/journal.pone.0011052 (2010).
202 Gruber, A., Wheat, J. C., Kuhen, K. L., Looney, D. J. & Wong-Staal, F. Differential effects of HIV-1 protease inhibitors on dendritic cell immunophenotype and function. *The Journal of biological chemistry* **276**, 47840-47843, doi:10.1074/jbc.M105582200 (2001).
203 Whelan, K. T. *et al.* The HIV protease inhibitor indinavir reduces immature dendritic cell transendothelial migration. *European journal of immunology* **33**, 2520-2530, doi:10.1002/eji.200323646 (2003).
204 Moretta, L. *et al.* Effector and regulatory events during natural killer-dendritic cell interactions. *Immunological reviews* **214**, 219-228, doi:10.1111/j.1600-065X.2006.00450.x (2006).
205 Lebbe, C. *et al.* Clinical and biological impact of antiretroviral therapy with protease inhibitors on HIV-related Kaposi's sarcoma. *Aids* **12**, F45-49 (1998).
206 Bower, M. *et al.* Highly active anti-retroviral therapy (HAART) prolongs time to treatment failure in Kaposi's sarcoma. *Aids* **13**, 2105-2111 (1999).
207 Sgadari, C. *et al.* HIV protease inhibitors are potent anti-angiogenic molecules and promote regression of Kaposi sarcoma. *Nature medicine* **8**, 225-232, doi:10.1038/nm0302-225 (2002).
208 Monini, P., Sgadari, C., Toschi, E., Barillari, G. & Ensoli, B. Antitumour effects of antiretroviral therapy. *Nature reviews. Cancer* **4**, 861-875, doi:10.1038/nrc1479 (2004).
209 Pajonk, F., Himmelsbach, J., Riess, K., Sommer, A. & McBride, W. H. The human immunodeficiency virus (HIV)-1 protease inhibitor saquinavir inhibits proteasome function and causes apoptosis and radiosensitization in non-HIV-associated human cancer cells. *Cancer research* **62**, 5230-5235 (2002).
210 Timeus, F. *et al.* The effects of saquinavir on imatinib-resistant chronic myelogenous leukemia cell lines. *Haematologica* **91**, 711-712 (2006).
211 Spugnini, E. P. *et al.* Effects of indinavir in a preliminary phase I study on dogs with stage III slenic hemangiosarcoma. *In vivo* **20**, 125-127 (2006).
212 Laurent, N. *et al.* Effects of the proteasome inhibitor ritonavir on glioma growth in vitro and in vivo. *Molecular cancer therapeutics* **3**, 129-136 (2004).
213 Maggiorella, L. *et al.* Combined radiation sensitizing and anti-angiogenic effects of ionizing radiation and the protease inhibitor ritonavir in a head and neck carcinoma model. *Anticancer research* **25**, 4357-4362 (2005).
214 Brunner, T. B. *et al.* Phase I trial of the human immunodeficiency virus protease inhibitor nelfinavir and chemoradiation for locally advanced pancreatic cancer. *Journal of clinical oncology : official journal of the American Society of Clinical Oncology* **26**, 2699-2706, doi:10.1200/JCO.2007.15.2355 (2008).

215 Blumenthal, G. M. *et al.* A phase I trial of the HIV protease inhibitor nelfinavir in adults with solid tumors. *Oncotarget* **5**, 8161-8172 (2014).
216 Buijsen, J. *et al.* Phase I trial of the combination of the Akt inhibitor nelfinavir and chemoradiation for locally advanced rectal cancer. *Radiotherapy and oncology : journal of the European Society for Therapeutic Radiology and Oncology* **107**, 184-188, doi:10.1016/j.radonc.2013.03.023 (2013).
217 Diez-Rivero, C. M., Lafuente, E. M. & Reche, P. A. Computational analysis and modeling of cleavage by the immunoproteasome and the constitutive proteasome. *BMC bioinformatics* **11**, 479, doi:10.1186/1471-2105-11-479 (2010).
218 Andre, P. *et al.* An inhibitor of HIV-1 protease modulates proteasome activity, antigen presentation, and T cell responses. *Proceedings of the National Academy of Sciences of the United States of America* **95**, 13120-13124 (1998).
219 Gaedicke, S. *et al.* Antitumor effect of the human immunodeficiency virus protease inhibitor ritonavir: induction of tumor-cell apoptosis associated with perturbation of proteasomal proteolysis. *Cancer research* **62**, 6901-6908 (2002).
220 Kelleher, A. D. *et al.* Effects of retroviral protease inhibitors on proteasome function and processing of HIV-derived MHC class I-restricted cytotoxic T lymphocyte epitopes. *AIDS research and human retroviruses* **17**, 1063-1066, doi:10.1089/088922201300343744 (2001).
221 Rock, K. L. *et al.* Inhibitors of the proteasome block the degradation of most cell proteins and the generation of peptides presented on MHC class I molecules. *Cell* **78**, 761-771 (1994).
222 Goldberg, A. L. Protein degradation and protection against misfolded or damaged proteins. *Nature* **426**, 895-899, doi:10.1038/nature02263 (2003).
223 Besche, H. C., Peth, A. & Goldberg, A. L. Getting to first base in proteasome assembly. *Cell* **138**, 25-28, doi:10.1016/j.cell.2009.06.035 (2009).
224 Heinemeyer, W., Fischer, M., Krimmer, T., Stachon, U. & Wolf, D. H. The active sites of the eukaryotic 20 S proteasome and their involvement in subunit precursor processing. *The Journal of biological chemistry* **272**, 25200-25209 (1997).
225 Kisselev, A. F., Akopian, T. N., Woo, K. M. & Goldberg, A. L. The sizes of peptides generated from protein by mammalian 26 and 20 S proteasomes. Implications for understanding the degradative mechanism and antigen presentation. *The Journal of biological chemistry* **274**, 3363-3371 (1999).
226 Groll, M. *et al.* Structure of 20S proteasome from yeast at 2.4 A resolution. *Nature* **386**, 463-471, doi:10.1038/386463a0 (1997).
227 Nussbaum, A. K. *et al.* Cleavage motifs of the yeast 20S proteasome beta subunits deduced from digests of enolase 1. *Proceedings of the National Academy of Sciences of the United States of America* **95**, 12504-12509 (1998).
228 Khan, S. *et al.* Immunoproteasomes largely replace constitutive proteasomes during an antiviral and antibacterial immune response in the liver. *Journal of immunology* **167**, 6859-6868 (2001).
229 Griffin, T. A. *et al.* Immunoproteasome assembly: cooperative incorporation of interferon gamma (IFN-gamma)-inducible subunits. *The Journal of experimental medicine* **187**, 97-104 (1998).
230 Cascio, P., Hilton, C., Kisselev, A. F., Rock, K. L. & Goldberg, A. L. 26S proteasomes and immunoproteasomes produce mainly N-extended versions of an antigenic peptide. *The EMBO journal* **20**, 2357-2366, doi:10.1093/emboj/20.10.2357 (2001).
231 Zanker, D., Waithman, J., Yewdell, J. W. & Chen, W. Mixed proteasomes function to increase viral peptide diversity and broaden antiviral CD8+ T cell responses. *Journal of immunology* **191**, 52-59, doi:10.4049/jimmunol.1300802 (2013).

232 Beninga, J., Rock, K. L. & Goldberg, A. L. Interferon-gamma can stimulate post-proteasomal trimming of the N terminus of an antigenic peptide by inducing leucine aminopeptidase. *The Journal of biological chemistry* **273**, 18734-18742 (1998).
233 Stoltze, L. *et al.* Two new proteases in the MHC class I processing pathway. *Nature immunology* **1**, 413-418, doi:10.1038/80852 (2000).
234 Portaro, F. C. *et al.* Thimet oligopeptidase and the stability of MHC class I epitopes in macrophage cytosol. *Biochemical and biophysical research communications* **255**, 596-601, doi:10.1006/bbrc.1999.0251 (1999).
235 Silva, C. L., Portaro, F. C., Bonato, V. L., de Camargo, A. C. & Ferro, E. S. Thimet oligopeptidase (EC 3.4.24.15), a novel protein on the route of MHC class I antigen presentation. *Biochemical and biophysical research communications* **255**, 591-595, doi:10.1006/bbrc.1999.0250 (1999).
236 York, I. A. *et al.* The cytosolic endopeptidase, thimet oligopeptidase, destroys antigenic peptides and limits the extent of MHC class I antigen presentation. *Immunity* **18**, 429-440 (2003).
237 York, I. A., Bhutani, N., Zendzian, S., Goldberg, A. L. & Rock, K. L. Tripeptidyl peptidase II is the major peptidase needed to trim long antigenic precursors, but is not required for most MHC class I antigen presentation. *Journal of immunology* **177**, 1434-1443 (2006).
238 Seifert, U. *et al.* An essential role for tripeptidyl peptidase in the generation of an MHC class I epitope. *Nature immunology* **4**, 375-379, doi:10.1038/ni905 (2003).
239 Reits, E. *et al.* Peptide diffusion, protection, and degradation in nuclear and cytoplasmic compartments before antigen presentation by MHC class I. *Immunity* **18**, 97-108 (2003).
240 Yewdell, J. W., Reits, E. & Neefjes, J. Making sense of mass destruction: quantitating MHC class I antigen presentation. *Nature reviews. Immunology* **3**, 952-961, doi:10.1038/nri1250 (2003).
241 Lazaro, E. *et al.* Variable HIV peptide stability in human cytosol is critical to epitope presentation and immune escape. *The Journal of clinical investigation* **121**, 2480-2492, doi:10.1172/JCI44932 (2011).
242 Zhang, S. C. *et al.* Aminopeptidase substrate preference affects HIV epitope presentation and predicts immune escape patterns in HIV-infected individuals. *Journal of immunology* **188**, 5924-5934, doi:10.4049/jimmunol.1200219 (2012).
243 Le Gall, S., Stamegna, P. & Walker, B. D. Portable flanking sequences modulate CTL epitope processing. *The Journal of clinical investigation* **117**, 3563-3575, doi:10.1172/JCI32047 (2007).
244 Kunisawa, J. & Shastri, N. The group II chaperonin TRiC protects proteolytic intermediates from degradation in the MHC class I antigen processing pathway. *Molecular cell* **12**, 565-576 (2003).
245 Kunisawa, J. & Shastri, N. Hsp90alpha chaperones large C-terminally extended proteolytic intermediates in the MHC class I antigen processing pathway. *Immunity* **24**, 523-534, doi:10.1016/j.immuni.2006.03.015 (2006).
246 Lauvau, G. *et al.* Human transporters associated with antigen processing (TAPs) select epitope precursor peptides for processing in the endoplasmic reticulum and presentation to T cells. *The Journal of experimental medicine* **190**, 1227-1240 (1999).
247 Serwold, T., Gaw, S. & Shastri, N. ER aminopeptidases generate a unique pool of peptides for MHC class I molecules. *Nature immunology* **2**, 644-651, doi:10.1038/89800 (2001).
248 Brouwenstijn, N., Serwold, T. & Shastri, N. MHC class I molecules can direct proteolytic cleavage of antigenic precursors in the endoplasmic reticulum. *Immunity* **15**, 95-104 (2001).
249 Saric, T. *et al.* An IFN-gamma-induced aminopeptidase in the ER, ERAP1, trims precursors to MHC class I-presented peptides. *Nature immunology* **3**, 1169-1176, doi:10.1038/ni859 (2002).
250 Serwold, T., Gonzalez, F., Kim, J., Jacob, R. & Shastri, N. ERAAP customizes peptides for MHC class I molecules in the endoplasmic reticulum. *Nature* **419**, 480-483, doi:10.1038/nature01074 (2002).

251 York, I. A. *et al.* The ER aminopeptidase ERAP1 enhances or limits antigen presentation by trimming epitopes to 8-9 residues. *Nature immunology* **3**, 1177-1184, doi:10.1038/ni860 (2002).
252 Saveanu, L. *et al.* Concerted peptide trimming by human ERAP1 and ERAP2 aminopeptidase complexes in the endoplasmic reticulum. *Nature immunology* **6**, 689-697, doi:10.1038/ni1208 (2005).
253 Kanaseki, T., Blanchard, N., Hammer, G. E., Gonzalez, F. & Shastri, N. ERAAP synergizes with MHC class I molecules to make the final cut in the antigenic peptide precursors in the endoplasmic reticulum. *Immunity* **25**, 795-806, doi:10.1016/j.immuni.2006.09.012 (2006).
254 Blanchard, N. *et al.* Endoplasmic reticulum aminopeptidase associated with antigen processing defines the composition and structure of MHC class I peptide repertoire in normal and virus-infected cells. *Journal of immunology* **184**, 3033-3042, doi:10.4049/jimmunol.0903712 (2010).
255 Bansal, A. *et al.* CD8 T cell response and evolutionary pressure to HIV-1 cryptic epitopes derived from antisense transcription. *The Journal of experimental medicine* **207**, 51-59, doi:10.1084/jem.20092060 (2010).
256 Berger, C. T. *et al.* Viral adaptation to immune selection pressure by HLA class I-restricted CTL responses targeting epitopes in HIV frameshift sequences. *The Journal of experimental medicine* **207**, 61-75, doi:10.1084/jem.20091808 (2010).
257 van Baalen, C. A. *et al.* Impact of antigen expression kinetics on the effectiveness of HIV-specific cytotoxic T lymphocytes. *European journal of immunology* **32**, 2644-2652, doi:10.1002/1521-4141(200209)32:9<2644::AID-IMMU2644>3.0.CO;2-R (2002).
258 Mo, A. X., van Lelyveld, S. F., Craiu, A. & Rock, K. L. Sequences that flank subdominant and cryptic epitopes influence the proteolytic generation of MHC class I-presented peptides. *Journal of immunology* **164**, 4003-4010 (2000).
259 Cardinaud, S. *et al.* CTL escape mediated by proteasomal destruction of an HIV-1 cryptic epitope. *PLoS pathogens* **7**, e1002049, doi:10.1371/journal.ppat.1002049 (2011).
260 Amigorena, S. & Savina, A. Intracellular mechanisms of antigen cross presentation in dendritic cells. *Current opinion in immunology* **22**, 109-117, doi:10.1016/j.coi.2010.01.022 (2010).
261 Kovacsovics-Bankowski, M. & Rock, K. L. A phagosome-to-cytosol pathway for exogenous antigens presented on MHC class I molecules. *Science* **267**, 243-246 (1995).
262 Burgdorf, S., Scholz, C., Kautz, A., Tampe, R. & Kurts, C. Spatial and mechanistic separation of cross-presentation and endogenous antigen presentation. *Nature immunology* **9**, 558-566, doi:10.1038/ni.1601 (2008).
263 Bertholet, S. *et al.* Leishmania antigens are presented to CD8+ T cells by a transporter associated with antigen processing-independent pathway in vitro and in vivo. *Journal of immunology* **177**, 3525-3533 (2006).
264 Shen, L., Sigal, L. J., Boes, M. & Rock, K. L. Important role of cathepsin S in generating peptides for TAP-independent MHC class I crosspresentation in vivo. *Immunity* **21**, 155-165, doi:10.1016/j.immuni.2004.07.004 (2004).
265 Joffre, O. P., Segura, E., Savina, A. & Amigorena, S. Cross-presentation by dendritic cells. *Nature reviews. Immunology* **12**, 557-569, doi:10.1038/nri3254 (2012).
266 Cresswell, P., Ackerman, A. L., Giodini, A., Peaper, D. R. & Wearsch, P. A. Mechanisms of MHC class I-restricted antigen processing and cross-presentation. *Immunological reviews* **207**, 145-157, doi:10.1111/j.0105-2896.2005.00316.x (2005).
267 Honey, K. & Rudensky, A. Y. Lysosomal cysteine proteases regulate antigen presentation. *Nature reviews. Immunology* **3**, 472-482, doi:10.1038/nri1110 (2003).
268 Delamarre, L., Pack, M., Chang, H., Mellman, I. & Trombetta, E. S. Differential lysosomal proteolysis in antigen-presenting cells determines antigen fate. *Science* **307**, 1630-1634, doi:10.1126/science.1108003 (2005).

269 Dinter, J. *et al.* Variable processing and cross-presentation of HIV by dendritic cells and macrophages shapes CTL immunodominance and immune escape. *PLoS pathogens* **11**, e1004725, doi:10.1371/journal.ppat.1004725 (2015).
270 Accapezzato, D. *et al.* Chloroquine enhances human CD8+ T cell responses against soluble antigens in vivo. *The Journal of experimental medicine* **202**, 817-828, doi:10.1084/jem.20051106 (2005).
271 Belizaire, R. & Unanue, E. R. Targeting proteins to distinct subcellular compartments reveals unique requirements for MHC class I and II presentation. *Proceedings of the National Academy of Sciences of the United States of America* **106**, 17463-17468, doi:10.1073/pnas.0908583106 (2009).
272 Savina, A. *et al.* NOX2 controls phagosomal pH to regulate antigen processing during crosspresentation by dendritic cells. *Cell* **126**, 205-218, doi:10.1016/j.cell.2006.05.035 (2006).
273 Mantegazza, A. R. *et al.* NADPH oxidase controls phagosomal pH and antigen cross-presentation in human dendritic cells. *Blood* **112**, 4712-4722, doi:10.1182/blood-2008-01-134791 (2008).
274 Rodriguez, A., Regnault, A., Kleijmeer, M., Ricciardi-Castagnoli, P. & Amigorena, S. Selective transport of internalized antigens to the cytosol for MHC class I presentation in dendritic cells. *Nature cell biology* **1**, 362-368, doi:10.1038/14058 (1999).
275 York, I. A., Brehm, M. A., Zendzian, S., Towne, C. F. & Rock, K. L. Endoplasmic reticulum aminopeptidase 1 (ERAP1) trims MHC class I-presented peptides in vivo and plays an important role in immunodominance. *Proceedings of the National Academy of Sciences of the United States of America* **103**, 9202-9207, doi:10.1073/pnas.0603095103 (2006).
276 Courtete, J. *et al.* Suppression of cervical carcinoma cell growth by intracytoplasmic codelivery of anti-oncoprotein E6 antibody and small interfering RNA. *Molecular cancer therapeutics* **6**, 1728-1735, doi:10.1158/1535-7163.MCT-06-0808 (2007).
277 Desplancq, D. *et al.* Single-chain Fv fragment antibodies selected from an intrabody library as effective mono- or bivalent reagents for in vitro protein detection. *Journal of immunological methods* **369**, 42-50, doi:10.1016/j.jim.2011.04.001 (2011).
278 Freund, G. *et al.* Targeting endogenous nuclear antigens by electrotransfer of monoclonal antibodies in living cells. *mAbs* **5**, 518-522, doi:10.4161/mabs.25084 (2013).
279 Freund, G. *et al.* Generation of an intrabody-based reagent suitable for imaging endogenous proliferating cell nuclear antigen in living cancer cells. *Journal of molecular recognition : JMR* **27**, 549-558, doi:10.1002/jmr.2378 (2014).
280 Lagrange, M. *et al.* Intracellular scFvs against the viral E6 oncoprotein provoke apoptosis in human papillomavirus-positive cancer cells. *Biochemical and biophysical research communications* **361**, 487-492, doi:10.1016/j.bbrc.2007.07.040 (2007).
281 Schmidtke, G. *et al.* How an inhibitor of the HIV-I protease modulates proteasome activity. *The Journal of biological chemistry* **274**, 35734-35740 (1999).
282 Sato, A., Asano, T., Ito, K. & Asano, T. Ritonavir interacts with bortezomib to enhance protein ubiquitination and histone acetylation synergistically in renal cancer cells. *Urology* **79**, 966 e913-921, doi:10.1016/j.urology.2011.11.033 (2012).
283 Ruschak, A. M. & Kay, L. E. Proteasome allostery as a population shift between interchanging conformers. *Proceedings of the National Academy of Sciences of the United States of America* **109**, E3454-3462, doi:10.1073/pnas.1213640109 (2012).
284 Jankowska, E. *et al.* Potential allosteric modulators of the proteasome activity. *Biopolymers* **93**, 481-495, doi:10.1002/bip.21381 (2010).
285 Kisselev, A. F., Akopian, T. N., Castillo, V. & Goldberg, A. L. Proteasome active sites allosterically regulate each other, suggesting a cyclical bite-chew mechanism for protein breakdown. *Molecular cell* **4**, 395-402 (1999).

286 Novinec, M. *et al.* A novel allosteric mechanism in the cysteine peptidase cathepsin K discovered by computational methods. *Nature communications* **5**, 3287, doi:10.1038/ncomms4287 (2014).
287 Caglic, D., Pungercar, J. R., Pejler, G., Turk, V. & Turk, B. Glycosaminoglycans facilitate procathepsin B activation through disruption of propeptide-mature enzyme interactions. *The Journal of biological chemistry* **282**, 33076-33085, doi:10.1074/jbc.M705761200 (2007).
288 Vasiljeva, O., Dolinar, M., Pungercar, J. R., Turk, V. & Turk, B. Recombinant human procathepsin S is capable of autocatalytic processing at neutral pH in the presence of glycosaminoglycans. *FEBS letters* **579**, 1285-1290, doi:10.1016/j.febslet.2004.12.093 (2005).
289 Carr, A. *et al.* A syndrome of peripheral lipodystrophy, hyperlipidaemia and insulin resistance in patients receiving HIV protease inhibitors. *Aids* **12**, F51-58 (1998).
290 Boesecke, C. & Cooper, D. A. Toxicity of HIV protease inhibitors: clinical considerations. *Current opinion in HIV and AIDS* **3**, 653-659, doi:10.1097/COH.0b013e328312c392 (2008).
291 Spector, A. A. HIV protease inhibitors and hyperlipidemia: a fatty acid connection. *Arteriosclerosis, thrombosis, and vascular biology* **26**, 7-9, doi:10.1161/01.ATV.0000198749.28422.29 (2006).
292 Anuurad, E., Bremer, A. & Berglund, L. HIV protease inhibitors and obesity. *Current opinion in endocrinology, diabetes, and obesity* **17**, 478-485, doi:10.1097/MED.0b013e32833dde87 (2010).
293 Waring, J. F. *et al.* Identification of proteasome gene regulation in a rat model for HIV protease inhibitor-induced hyperlipidemia. *Archives of toxicology* **84**, 263-270, doi:10.1007/s00204-010-0527-7 (2010).
294 Lum, P. Y. *et al.* Gene expression profiling of rat liver reveals a mechanistic basis for ritonavir-induced hyperlipidemia. *Genomics* **90**, 464-473, doi:10.1016/j.ygeno.2007.06.004 (2007).
295 Meiners, S. *et al.* Inhibition of proteasome activity induces concerted expression of proteasome genes and de novo formation of Mammalian proteasomes. *The Journal of biological chemistry* **278**, 21517-21525, doi:10.1074/jbc.M301032200 (2003).
296 Riddle, T. M., Kuhel, D. G., Woollett, L. A., Fichtenbaum, C. J. & Hui, D. Y. HIV protease inhibitor induces fatty acid and sterol biosynthesis in liver and adipose tissues due to the accumulation of activated sterol regulatory element-binding proteins in the nucleus. *The Journal of biological chemistry* **276**, 37514-37519, doi:10.1074/jbc.M104557200 (2001).
297 Kramer, W. *et al.* Aminopeptidase N (CD13) is a molecular target of the cholesterol absorption inhibitor ezetimibe in the enterocyte brush border membrane. *The Journal of biological chemistry* **280**, 1306-1320, doi:10.1074/jbc.M406309200 (2005).
298 Levy, E. *et al.* Intestinal cholesterol transport proteins: an update and beyond. *Current opinion in lipidology* **18**, 310-318, doi:10.1097/MOL.0b013e32813fa2e2 (2007).
299 Yeh, T. Y., Sbodio, J. I., Tsun, Z. Y., Luo, B. & Chi, N. W. Insulin-stimulated exocytosis of GLUT4 is enhanced by IRAP and its partner tankyrase. *The Biochemical journal* **402**, 279-290, doi:10.1042/BJ20060793 (2007).
300 Menzel, K. *et al.* Cathepsins B, L and D in inflammatory bowel disease macrophages and potential therapeutic effects of cathepsin inhibition in vivo. *Clinical and experimental immunology* **146**, 169-180, doi:10.1111/j.1365-2249.2006.03188.x (2006).
301 Kovsan, J., Ben-Romano, R., Souza, S. C., Greenberg, A. S. & Rudich, A. Regulation of adipocyte lipolysis by degradation of the perilipin protein: nelfinavir enhances lysosome-mediated perilipin proteolysis. *The Journal of biological chemistry* **282**, 21704-21711, doi:10.1074/jbc.M702223200 (2007).
302 Saftig, P. *et al.* Impaired osteoclastic bone resorption leads to osteopetrosis in cathepsin-K-deficient mice. *Proceedings of the National Academy of Sciences of the United States of America* **95**, 13453-13458 (1998).

303 Bromme, D., Okamoto, K., Wang, B. B. & Biroc, S. Human cathepsin O2, a matrix protein-degrading cysteine protease expressed in osteoclasts. Functional expression of human cathepsin O2 in Spodoptera frugiperda and characterization of the enzyme. *The Journal of biological chemistry* **271**, 2126-2132 (1996).
304 Perisic Nanut, M., Sabotic, J., Jewett, A. & Kos, J. Cysteine cathepsins as regulators of the cytotoxicity of NK and T cells. *Frontiers in immunology* **5**, 616, doi:10.3389/fimmu.2014.00616 (2014).
305 Kos, J. *et al.* Cathepsin S in tumours, regional lymph nodes and sera of patients with lung cancer: relation to prognosis. *British journal of cancer* **85**, 1193-1200, doi:10.1054/bjoc.2001.2057 (2001).
306 Flannery, T. *et al.* The clinical significance of cathepsin S expression in human astrocytomas. *The American journal of pathology* **163**, 175-182, doi:10.1016/S0002-9440(10)63641-3 (2003).
307 Hou, W. S. *et al.* Comparison of cathepsins K and S expression within the rheumatoid and osteoarthritic synovium. *Arthritis and rheumatism* **46**, 663-674, doi:10.1002/art.10114 (2002).
308 Sukhova, G. K. *et al.* Deficiency of cathepsin S reduces atherosclerosis in LDL receptor-deficient mice. *The Journal of clinical investigation* **111**, 897-906, doi:10.1172/JCI14915 (2003).
309 Fang, J., Shi, G. P. & Vaghy, P. L. Identification of the increased expression of monocyte chemoattractant protein-1, cathepsin S, UPIX-1, and other genes in dystrophin-deficient mouse muscles by suppression subtractive hybridization. *Journal of cellular biochemistry* **79**, 164-172 (2000).
310 Kourjian, G. *et al.* Sequence-specific alterations of epitope production by HIV protease inhibitors. *Journal of immunology* **192**, 3496-3506, doi:10.4049/jimmunol.1302805 (2014).
311 Plastaras, J. P. *et al.* Validation and toxicity of PI3K/Akt pathway inhibition by HIV protease inhibitors in humans. *Cancer biology & therapy* **7**, 628-635 (2008).
312 El-Benna, J., Dang, P. M., Gougerot-Pocidalo, M. A., Marie, J. C. & Braut-Boucher, F. p47phox, the phagocyte NADPH oxidase/NOX2 organizer: structure, phosphorylation and implication in diseases. *Experimental & molecular medicine* **41**, 217-225, doi:10.3858/emm.2009.41.4.058 (2009).
313 Babior, B. M. Oxidants from phagocytes: agents of defense and destruction. *Blood* **64**, 959-966 (1984).
314 Segal, A. W. How neutrophils kill microbes. *Annual review of immunology* **23**, 197-223, doi:10.1146/annurev.immunol.23.021704.115653 (2005).
315 Hampton, M. B., Kettle, A. J. & Winterbourn, C. C. Inside the neutrophil phagosome: oxidants, myeloperoxidase, and bacterial killing. *Blood* **92**, 3007-3017 (1998).
316 Nathan, C. Neutrophils and immunity: challenges and opportunities. *Nature reviews. Immunology* **6**, 173-182, doi:10.1038/nri1785 (2006).
317 Meischl, C. & Roos, D. The molecular basis of chronic granulomatous disease. *Springer seminars in immunopathology* **19**, 417-434 (1998).
318 Kannengiesser, C. *et al.* Molecular epidemiology of chronic granulomatous disease in a series of 80 kindreds: identification of 31 novel mutations. *Human mutation* **29**, E132-149, doi:10.1002/humu.20820 (2008).
319 Thornberry, N. A. *et al.* A combinatorial approach defines specificities of members of the caspase family and granzyme B. Functional relationships established for key mediators of apoptosis. *The Journal of biological chemistry* **272**, 17907-17911 (1997).
320 Lazaro, E. *et al.* Differential HIV epitope processing in monocytes and CD4 T cells affects cytotoxic T lymphocyte recognition. *The Journal of infectious diseases* **200**, 236-243, doi:10.1086/599837 (2009).

321 Dinter, J. *et al.* Different antigen-processing activities in dendritic cells, macrophages, and monocytes lead to uneven production of HIV epitopes and affect CTL recognition. *Journal of immunology* **193**, 4322-4334, doi:10.4049/jimmunol.1400491 (2014).
322 Turk, V. *et al.* Cysteine cathepsins: from structure, function and regulation to new frontiers. *Biochimica et biophysica acta* **1824**, 68-88, doi:10.1016/j.bbapap.2011.10.002 (2012).
323 Feeney, M. E. *et al.* HIV-1 viral escape in infancy followed by emergence of a variant-specific CTL response. *Journal of immunology* **174**, 7524-7530 (2005).
324 Allen, T. M. *et al.* Selective escape from CD8+ T-cell responses represents a major driving force of human immunodeficiency virus type 1 (HIV-1) sequence diversity and reveals constraints on HIV-1 evolution. *Journal of virology* **79**, 13239-13249, doi:10.1128/JVI.79.21.13239-13249.2005 (2005).
325 O'Connell, K. A., Hegarty, R. W., Siliciano, R. F. & Blankson, J. N. Viral suppression of multiple escape mutants by de novo CD8(+) T cell responses in a human immunodeficiency virus-1 infected elite suppressor. *Retrovirology* **8**, 63, doi:10.1186/1742-4690-8-63 (2011).
326 Turnbull, E. L. *et al.* Kinetics of expansion of epitope-specific T cell responses during primary HIV-1 infection. *Journal of immunology* **182**, 7131-7145, doi:10.4049/jimmunol.0803658 (2009).
327 Liu, M. K. *et al.* Vertical T cell immunodominance and epitope entropy determine HIV-1 escape. *The Journal of clinical investigation* **123**, 380-393, doi:10.1172/JCI65330 (2013).
328 Borrow, P. *et al.* Antiviral pressure exerted by HIV-1-specific cytotoxic T lymphocytes (CTLs) during primary infection demonstrated by rapid selection of CTL escape virus. *Nature medicine* **3**, 205-211 (1997).
329 Nowak, M. A. *et al.* Antigenic oscillations and shifting immunodominance in HIV-1 infections. *Nature* **375**, 606-611, doi:10.1038/375606a0 (1995).
330 Archin, N. M. *et al.* Administration of vorinostat disrupts HIV-1 latency in patients on antiretroviral therapy. *Nature* **487**, 482-485, doi:10.1038/nature11286 (2012).
331 Siliciano, J. D. & Siliciano, R. F. HIV-1 eradication strategies: design and assessment. *Current opinion in HIV and AIDS* **8**, 318-325, doi:10.1097/COH.0b013e328361eaca (2013).
332 Deng, K. *et al.* Broad CTL response is required to clear latent HIV-1 due to dominance of escape mutations. *Nature* **517**, 381-385, doi:10.1038/nature14053 (2015).
333 Jalali, Z. & Rockstroh, J. K. Antiviral drugs and the treatment of hepatitis C. *Current HIV/AIDS reports* **9**, 132-138, doi:10.1007/s11904-012-0111-2 (2012).
334 Naidoo, K., Baxter, C. & Abdool Karim, S. S. When to start antiretroviral therapy during tuberculosis treatment? *Current opinion in infectious diseases* **26**, 35-42, doi:10.1097/QCO.0b013e32835ba8f9 (2013).
335 Walker, N. F., Meintjes, G. & Wilkinson, R. J. HIV-1 and the immune response to TB. *Future virology* **8**, 57-80, doi:10.2217/fvl.12.123 (2013).
336 Bono, C. *et al.* The human immunodeficiency virus-1 protease inhibitor nelfinavir impairs proteasome activity and inhibits the proliferation of multiple myeloma cells in vitro and in vivo. *Haematologica* **97**, 1101-1109, doi:10.3324/haematol.2011.049981 (2012).
337 Kawabata, S. *et al.* Synergistic effects of nelfinavir and bortezomib on proteotoxic death of NSCLC and multiple myeloma cells. *Cell death & disease* **3**, e353, doi:10.1038/cddis.2012.87 (2012).
338 Kraus, M. *et al.* Ritonavir induces endoplasmic reticulum stress and sensitizes sarcoma cells toward bortezomib-induced apoptosis. *Molecular cancer therapeutics* **7**, 1940-1948, doi:10.1158/1535-7163.MCT-07-2375 (2008).
339 Sgadari, C., Monini, P., Barillari, G. & Ensoli, B. Use of HIV protease inhibitors to block Kaposi's sarcoma and tumour growth. *The Lancet. Oncology* **4**, 537-547 (2003).

340 Zeng, J. *et al.* Nelfinavir induces radiation sensitization in pituitary adenoma cells. *Cancer biology & therapy* **12**, 657-663 (2011).
341 Kimple, R. J. *et al.* Radiosensitization of epidermal growth factor receptor/HER2-positive pancreatic cancer is mediated by inhibition of Akt independent of ras mutational status. *Clinical cancer research : an official journal of the American Association for Cancer Research* **16**, 912-923, doi:10.1158/1078-0432.CCR-09-1324 (2010).

Annexes

HIV PIs plasma and intracellular concentration

A real-time killing assay to follow viral epitope presentation to CD8 T cells. *Pauline Gourdain, Julie Boucau, Georgio Kourjian, Nicole Lai, Ellen Duong, and Sylvie Le Gall. J Immunol Methods 398-399:60-7 (2013)*

Mechanisms of HIV Protein Degradation into Épitopes: Implications for Vaccine Design. *Marijana Rucevic, Julie Boucau, Jens Dinter, Georgio Kourjian and Sylvie Le Gall. Viruses 6, 3271-3292; doi:10.3390 (2014)*

Variable Processing and Cross-presentation of HIV by Dendritic Cells and Macrophages Shapes CTL Immunodominance and Immune Escape. *Jens Dinter, Ellen Duong, Nicole Y. Lai, Matthew J. Berberich, Georgio Kourjian, Edith Bracho-Sanchez, Duong Chu, Hang Su, Shao Chong Zhang and Sylvie Le Gall. PLOS Pathogens doi: 10.1371(2015)*

Identification of naturally processed HIV peptides from HIV-infected cells reveals nested and cell-specific peptides and novel T cell immune responses. *Marijana Rucevic, Georgio Kourjian, Julie Boucau, Wilfredo Garcia Bertran, Matthew Berberich, Bruce D. Walker and Sylvie Le Gall. In preparation (2015)*

HIV PIs plasma and intracellular concentration

	Average Cmax	Average Cmin	Highest C	Average Ratio Intra/Plasma	concentration used	Ref
Saquinavir	6.71	0.72	18.5	2.5	5 and 10	(1-6)
Nelfinavir	6.03	1.99	9.4	4.25	5 and 10	(1, 6-8)
Ritonavir	15.5	4.2	20.5	2-3	5 and 10	(1, 9)
Kaletra						
Lopinavir	11	3.45	15.2	1.2	5 and 10	(6, 10-12)
Ritonavir	1.9	0.2	2.2	4.6	1 and 2	
Indinavir	12.6	0.25	16.6	1.2	5 and 10	(1, 6)
Atazanavir	5.75	1	6.2	4	5 and 10	(13-15)
Darunavir	7.5	2.1	9.6	4	5 and 10	(16)

Highest C: Highest concentration; Intra/Plasma: ration intracellular concentration / Plasma concentration; concentration used: lower value in live cells, higher value in cell extracts. Concentration (μM)

1. Acosta, E. P., T. N. Kakuda, R. C. Brundage, P. L. Anderson, and C. V. Fletcher. 2000. Pharmacodynamics of human immunodeficiency virus type 1 protease inhibitors. *Clinical infectious diseases : an official publication of the Infectious Diseases Society of America* 30 Suppl 2: S151-159.
2. van Heeswijk, R. P., A. I. Veldkamp, J. W. Mulder, P. L. Meenhorst, J. M. Lange, J. H. Beijnen, and R. M. Hoetelmans. 2000. Once-daily dosing of saquinavir and low-dose ritonavir in HIV-1-infected individuals: a pharmacokinetic pilot study. *Aids* 14: F103-110.
3. Veldkamp, A. I., R. P. van Heeswijk, J. W. Mulder, P. L. Meenhorst, G. Schreij, S. van der Geest, J. M. Lange, J. H. Beijnen, and R. M. Hoetelmans. 2001. Steady-state pharmacokinetics of twice-daily dosing of saquinavir plus ritonavir in HIV-1-infected individuals. *Journal of acquired immune deficiency syndromes* 27: 344-349.
4. Cardiello, P. G., T. Monhaphol, A. Mahanontharit, R. P. van Heeswijk, D. Burger, A. Hill, K. Ruxrungtham, J. M. Lange, D. A. Cooper, and P. Phanuphak. 2003. Pharmacokinetics of once-daily saquinavir hard-gelatin capsules and saquinavir soft-gelatin capsules boosted with ritonavir in HIV-1-infected subjects. *Journal of acquired immune deficiency syndromes* 32: 375-379.
5. Pai, M. P., C. A. Schriever, M. Diaz-Linares, R. M. Novak, and K. A. Rodvold. 2004. Sex-related differences in the pharmacokinetics of once-daily saquinavir soft-gelatin capsules boosted with

low-dose ritonavir in patients infected with human immunodeficiency virus type 1. *Pharmacotherapy* 24: 592-599.
6. Colombo, S., A. Telenti, T. Buclin, H. Furrer, B. L. Lee, J. Biollaz, L. A. Decosterd, and H. I. V. C. S. Swiss. 2006. Are plasma levels valid surrogates for cellular concentrations of antiretroviral drugs in HIV-infected patients? *Therapeutic drug monitoring* 28: 332-338.
7. Pai, V. B., and M. C. Nahata. 1999. Nelfinavir mesylate: a protease inhibitor. *The Annals of pharmacotherapy* 33: 325-339.
8. Hennessy, M., S. Clarke, J. P. Spiers, D. Kelleher, F. Mulcahy, P. Hoggard, D. Back, and M. Barry. 2004. Intracellular accumulation of nelfinavir and its relationship to P-glycoprotein expression and function in HIV-infected patients. *Antiviral therapy* 9: 115-122.
9. Akeb, F., B. Ferrua, C. Creminon, C. Roptin, J. Grassi, M. C. Nevers, R. Guedj, R. Garraffo, and D. Duval. 2002. Quantification of plasma and intracellular levels of the HIV protease inhibitor ritonavir by competitive ELISA. *Journal of immunological methods* 263: 1-9.
10. Hsu, A., J. Isaacson, S. Brun, B. Bernstein, W. Lam, R. Bertz, C. Foit, K. Rynkiewicz, B. Richards, M. King, R. Rode, D. J. Kempf, G. R. Granneman, and E. Sun. 2003. Pharmacokinetic-pharmacodynamic analysis of lopinavir-ritonavir in combination with efavirenz and two nucleoside reverse transcriptase inhibitors in extensively pretreated human immunodeficiency virus-infected patients. *Antimicrobial agents and chemotherapy* 47: 350-359.
11. Breilh, D., I. Pellegrin, A. Rouzes, K. Berthoin, F. Xuereb, H. Budzinski, M. Munck, H. J. Fleury, M. C. Saux, and J. L. Pellegrin. 2004. Virological, intracellular and plasma pharmacological parameters predicting response to lopinavir/ritonavir (KALEPHAR study). *Aids* 18: 1305-1310.
12. Crommentuyn, K. M., J. W. Mulder, A. T. Mairuhu, E. C. van Gorp, P. L. Meenhorst, A. D. Huitema, and J. H. Beijnen. 2004. The plasma and intracellular steady-state pharmacokinetics of lopinavir/ritonavir in HIV-1-infected patients. *Antiviral therapy* 9: 779-785.
13. Dumond, J. B., J. L. Adams, H. M. Prince, R. L. Kendrick, R. Wang, S. H. Jennings, S. Malone, N. White, C. Sykes, A. H. Corbett, K. B. Patterson, A. Forrest, and A. D. Kashuba. 2013. Pharmacokinetics of two common antiretroviral regimens in older HIV-infected patients: a pilot study. *HIV medicine* 14: 401-409.
14. Bertz, R. J., A. Persson, E. Chung, L. Zhu, J. Zhang, D. McGrath, and D. Grasela. 2013. Pharmacokinetics and pharmacodynamics of atazanavir-containing antiretroviral regimens, with or without ritonavir, in patients who are HIV-positive and treatment-naive. *Pharmacotherapy* 33: 284-294.
15. Roucairol, C., S. Azoulay, M. C. Nevers, C. Creminon, T. Lavrut, R. Garraffo, J. Grassi, A. Burger, and D. Duval. 2007. Quantitative immunoassay to measure plasma and intracellular atazanavir levels: analysis of drug accumulation in cultured T cells. *Antimicrobial agents and chemotherapy* 51: 405-411.
16. Jackson, A., V. Watson, D. Back, S. Khoo, N. Liptrott, D. Egan, K. Gedela, C. Higgs, R. Abbas, B. Gazzard, and M. Boffito. 2011. Plasma and intracellular pharmacokinetics of darunavir/ritonavir once daily and raltegravir once and twice daily in HIV-infected individuals. *Journal of acquired immune deficiency syndromes* 58: 450-457.

Journal of Immunological Methods 398–399 (2013) 60–67

Contents lists available at ScienceDirect

Journal of Immunological Methods

journal homepage: www.elsevier.com/locate/jim

Research paper

A real-time killing assay to follow viral epitope presentation to CD8 T cells

Pauline Gourdain, Julie Boucau, Georgio Kourjian, Nicole Y. Lai, Ellen Duong, Sylvie Le Gall *

Ragon Institute of MGH, MIT and Harvard, Massachusetts General Hospital, Harvard Medical School, Cambridge, MA, USA

ARTICLE INFO

Article history:
Received 23 May 2013
Accepted 13 September 2013
Available online 20 September 2013

Keywords:
HIV
Antigen processing
CD8 T cells
Real-time killing assay
Cytotoxicity
Kinetics

ABSTRACT

The ability of cytotoxic T lymphocytes (CTL) to clear virus-infected cells requires the presentation of viral peptides intracellularly processed and displayed by major histocompatibility complex class I. Assays to measure CTL-mediated killing often use peptides exogenously added onto target cells – which does not account for epitope processing – or follow killing of infected cells at a single time point. In this study we established a real-time fluorogenic cytotoxic assay that measures the release of the Glucose-6-phosphate-dehydrogenase by dying target cells every 5 min after addition of CTL. It has comparable sensitivity to ^{51}chromium-based killing assay with the additional advantage of incorporating the kinetics of epitope presentation. We showed that HIV infection of immortalized or primary CD4 T cells leads to asynchronous killing by two CTL clones specific for epitopes located in different proteins. Real-time monitoring of killing of virus-infected cells will enable identification of immune responses efficiently preventing virus dissemination.

1. Introduction

Cytotoxic T lymphocytes (CTL) are one of the key components of host defense against viral infection or tumor cell elimination. Virus-specific CTL responses are elicited in most viral infections, including influenza, HIV, EBV, CMV and HCV (Bangham, 2009). HIV-specific CTL play a critical role in containing HIV viremia in acute infection or in situation of spontaneous control (Hersperger et al., 2011). However in chronic infections such as HIV and HCV the virus is not cleared despite the presence of CTL responses (Migueles and Connors, 2001; Rowland-Jones et al., 2001). The identification of criteria defining protective immune responses is paramount to the design of vaccine immunogens (Burton et al., 2012). Several parameters including peptide sequence and avidity for MHC and T cell receptor (TCR), proliferative capacity, production of cytokines and cytolytic granule release contribute to the antiviral capacity of the CTL responses (Almeida et al., 2007; Migueles et al., 2008; Hersperger et al., 2010; Ndhlovu et al., 2013). However one parameter often disregarded in the identification of efficacious immune responses is the timing of epitope presentation.

The killing of an infected cell by epitope-specific T cells is the culminating event of a multistep process. MHC-I epitopes displayed in the surface of cells come from the degradation of proteins in a multistep pathway involving peptidases located in the cytosol, in the endoplasmic reticulum, and for exogenous antigens peptidases from the endo-lysosomal pathway (Neefjes et al., 2011). The presentation of MHC-I-epitope is a prerequisite to the interaction between target and effector cells, activation of T cells, release of cytolytic granules content by T cells, and eventually disintegration of the target cell.

Multiple assays have been developed to assess killing of target cells or activation of effector T cells at a given time point following infection (Shacklett, 2002; Lemonnier, 2013). Radioactive isotope ^{51}chromium (^{51}Cr) or tritium (^{3}H) killing

Abbreviations: CFSE, carboxyfluorescein succinimidyl ester; MTG, MitoTrackerGreen; CAM, calceinacetoxymethylester; 7-AAD, 7-amino-actinomycin D; G6PDH, glucose 6-phosphate dehydrogenase.

* Corresponding author at: Ragon Institute of MGH, MIT and Harvard, Massachusetts General Hospital, Harvard Medical School, 400 Technology Square, Cambridge, MA 02139, USA. Tel.: +1 857 268 7010; fax: +1 857 268 7142.
E-mail address: sylvie_legall@hms.harvard.edu (S. Le Gall).

0022-1759/$ – see front matter © 2013 Elsevier B.V. All rights reserved.
http://dx.doi.org/10.1016/j.jim.2013.09.009

assays are the traditional methods to assess virus-specific T cell-mediated cytotoxicity (Brunner et al., 1968; Usharauli et al., 2006). They are based on generating infected target cell populations and labeling them with ^{51}Cr or ^{3}H. The addition of virus-specific T cells leads to killing of target cells and release of radioactivity into the culture supernatant. Quantification of ^{51}Cr- or ^{3}H-release provides a measure of the specificity and the cytotoxic capacity of T cells in the effector cell population at a single time point typically measured several hours after addition of CTL.

Several non-radioactive techniques have been developed to assess the killing of target cells (Cholujova et al., 2008) or apoptosis in various culture conditions (McMillian et al., 2002). Dyes to label target cells include carboxyfluorescein succinimidyl ester (CFSE) (Wierda et al., 1989), MitoTrackerGreen (MTG), calceinacetoxymethylester (CAM), Vybrant DiO (DiO), 7-amino-actinomycin D (7-AAD) (Lecoeur et al., 2001; Sheehy et al., 2001) or caspase-3 substrates (Liu et al., 2002; He et al., 2005). They measure cell apoptosis (7-AAD; caspase-3 substrates), disintegration of dying cells after recognition by T cells (release of CFSE or MTG), the proportion of live/dead cells with two substrates such as CFSE/PKH26 (Lee-MacAry et al., 2001; Sheehy et al., 2001), or track surviving cells (CAM; (Roden et al., 1999)). All these dyes are intracellular markers which may leak out of the cells and can be toxic to primary cells such as dendritic cells. Extracellular substrates cleaved by enzymes released by dying cells such as resazurin cleaved by glucose 6-phosphate dehydrogenase (G6PDH) have been used to measure apoptosis and drug-induced cytotoxicity but not to follow T cell-mediated lysis of target cells (Batchelor and Zhou, 2004).

Indirect assays to assess recognition of target cells by effector T cells measure CD8 T cell activation by measuring the production of cytokines such as interferon gamma or Interleukin 2 (Miyahira et al., 1995; Maino and Picker, 1998; Mwau et al., 2002; Janetzki et al., 2005; Nomura et al., 2008), the release of cytolytic granules through exposure of CD107a (Betts et al., 2003) or cytotoxic molecules (perforin and granzymes) (Snyder et al., 2003; Snyder-Cappione et al., 2006; Hersperger et al., 2010). However these parameters do not address whether killing and clearance of infected cells occurred, a critical issue in chronic infections such as HIV and HCV where T cells can be partly functionally impaired (Hersperger et al., 2011).

Despite their advantages, all these approaches provide limited information about the timing of presentation of an epitope to its cognate CTL, a factor critical to ensure efficient clearance of infected cells — that is independent of the antiviral function of T cells. Here we present a new non-radioactive cytotoxic assay with a low toxicity and a low cell number requirement that allows us to sensitively measure the killing of target cells in real-time after addition of CTL, and to compare the kinetics of presentation of endogenously processed HIV epitopes to HIV-specific CTL.

2. Material and methods

2.1. Study participants

HIV-negative and HIV-infected donors were recruited at Massachusetts General Hospital (MGH) in Boston. Partners Human Research Committee (Boston, MA) approved the use of anonymous buffy coats under protocol 2005P001218, the use of samples from HIV-negative coded donors under protocol 2010P002121 and the use of coded HIV-infected samples under protocols 2010P002463 and 2003P001894. All participants provided written informed consent for participation in the study.

2.2. Peptides

Highly purified peptides (>98% pure) were purchased from MGH peptide core facility.

2.3. Cell culture

EBV-immortalized B cells were maintained in RPMI 10% FCS. KF11-, TW10-, ATK9- and RK9-specific CTL clones were isolated by limiting dilution and maintained in the presence of 50 U/ml IL-2 (R10-IL2) using the CD3-specific mAb 12 F6 and irradiated PBMC as stimulus for T cell proliferation (Le Gall et al., 2007).

2.4. Cell sorting

CD4 T cells were enriched from freshly isolated peripheral blood mononuclear cells (PBMCs) by magnetic immunodepletion of cells expressing CD8, CD14, CD16, CD19, CD20, CD36, CD56, CD66b, CD123, TCRγ/δ, glycophorin A and dextran-coated magnetic particles, according to the manufacturer's instructions (StemCell). The percentage of CD4 T cells assessed by flow cytometry was >90%. PHA-stimulated CD4 T cells were obtained by incubating CD4 T cells at 1×10^6/ml in R10-IL2 with 0.25 μg/ml PHA for 4–6 days.

2.5. HIV infection

VSV-G-pseudotyped viral stocks were prepared by co-transfection of 293 T cells with NL4-3 proviral DNA (or with a GFP-encoding provirus) along with a CMV-VSV-G plasmid and titrated as previously described (Miura et al., 2009). B cells or PHA-activated CD4 T cells were harvested and incubated at 2×10^6/well in R10 in 24-well plates. VSV-G-pseudotyped virus was added at a concentration of 100 ng p24 per well for 5 h. Cells were washed twice and plated again. Every other day until day 10, cells were monitored for infection rate and used as targets in real-time or ^{51}Cr killing assays.

2.6. Flow cytometry

Cells were washed and incubated with CD4-PE and HLA-DR-APC antibody (pre-titrated volume, BD Pharmingen). Cells were then permeabilized with the Cytofix/Cytoperm Plus kit (BD Biosciences) for 20 min following manufacturer's instructions and stained for intracellular p24 with p24-FITC antibody (pre-titrated volume, Santa Cruz Biotech) for 30 min. Cells were fixed and acquired on a two-laser Calibur flow cytometer using CellQuestPro software (BD Biosciences) and data were analyzed using FlowJo software (TreeStar).

2.7. Real-time fluorogenic killing assay

Target cells (B cells or PHA-activated CD4 T cells) were harvested, suspended in fresh medium (Complete RPMI without serum, R^+) and plated at 20×10^3 cells/75 μl per well in dark 96-well plates. Peptides were added in 75 μl of RPMI without serum (R^+) at different concentrations (0.4 μg/ml; 0.04 μg/ml; and 0.004 μg/ml). Plates were incubated at 37 °C, 5% CO_2 for 20 min. Plates were washed once with 150 μl of RPMI 10% serum (R10) per well and spun 30 s, 2500 rpm. 225 μl of media was aspirated at the lowest speed with an automatic multichannel pipette. Plates were washed for the second time with 225 μl of R10 per well and spun 30 s at 2500 rpm. 225 μl of media was aspirated at the lowest speed with an automatic multichannel pipette. A third wash was performed before CTL were added at 40×10^3 cells/75 μl per well in R10 serum. 50 μl of resazurin/reaction mixture was added to each well (Vibrant Cytotoxicity Assay Kit Molecular Probes; (Batchelor and Zhou, 2004)). For a positive control, 5 μl of 100X Triton cell lysis buffer was added. Wells were mixed with the automatic multichannel pipette and fluorescence emission (Ex: 530–560/Em: 580–600) was recorded every 5 min for 4 h on a Victor3 plate reader (PerkinElmer). Spontaneous fluorescence is defined as fluorescence emission by uninfected B cells and CTL without exogenously added peptide. Maximum fluorescence is defined as fluorescence emission by B cells mixed with CTL and cell lysis buffer.

Specific fluorescence was calculated as [(fluorescence in the presence of target cells and CTL − spontaneous fluorescence) / (maximum fluorescence − spontaneous fluorescence)] × 100. Target cells with or without peptides were incubated with substrate in order to check the basal level of G6PDH released by targets (fluorescence levels below to spontaneous release).

2.8. ^{51}Cr-based killing Assay

^{51}Cr-labeled B cells were pulsed with different peptide doses (0.4 μg/ml, 0.04 μg/ml or 0.004 μg/ml of the optimal peptide and 0.4 μg/ml of the mutated one) diluted in R^+ for 30 min at 37 °C. KF11-specific, TW10-specific, RK9-specific, or ATK9-specific CTL clones were added at a 4:1 ratio and incubated for 4 h with target cells. Radioactivity was measured in 30 μl of culture supernatant. Cell lysis was calculated as [(^{51}Cr release due to peptide − spontaneous release) / (total release − spontaneous release)] × 100 as in (Le Gall et al., 2007).

2.9. Statistical analysis

Maximum slope and area under curve (AUC) were calculated with Microsoft Excel. Data were analyzed using GraphPad Prism software (version 5).

3. Results

3.1. A fluorogenic assay to measure real-time CTL-mediated killing of target cells

We aimed to design a killing assay that allows us to follow the lysis of target cells after addition of CTL in real-time. We adapted a fluorogenic assay measuring the activity of glucose 6-phosphate dehydrogenase (G6PDH) during apoptosis and drug-induced cytotoxicity (Batchelor and Zhou, 2004), an enzyme released by dying cells (Zhang et al., 2000). The membrane-impermeable substrate is added in the culture medium — which avoids intracellular toxicity and leakage observed with intracellular substrates. The release of G6PDH by dying cells leads to the cleavage of a G6PDH-specific fluorogenic substrate and fluorescence emission (Fig. 1A). To measure CTL-mediated cell killing HLA-$B57^+$ B cells were pulsed with variable amounts of cognate peptide (HLA-B57-restricted KF11, KAFSPEVIPMF, aa 30–40 in Gag p24) or with a mutated KF11 peptide (KF11-K89 KAFSPEVIKKF) of low functional avidity (i.e. low binding affinity for HLA-B57 and/or TCR of CD8 T cells) (Lazaro et al., 2011). Spontaneous release of G6PDH was measured with B cells and CTL without peptides (or with irrelevant peptide) and maximum release was measured with B cells and CTL mixed with Triton lysis buffer. Fluorescence emission was measured every 5 min from the moment CTL (or detergent) were mixed with target cells. Fluorescence emission increased over time and with the amount of KF11 peptide used to pulse target cells (Fig. 1B). At each reading time point we calculated a specific fluorescence – equivalent to a specific lysis % – as [(fluorescence in the presence of peptide-pulsed cells − spontaneous fluorescence) / (maximum fluorescence − spontaneous fluorescence)] × 100 (Fig. 1C). In the presence of KF11-pulsed B cells lysis was detectable as early as 1 h after addition of CTL and increased over time. The lysis % was proportional to the amount of KF11 peptide used to pulse cells. In the presence of a mutated peptide KF11-K89 lysis remained low (Fig. 1C). To validate the assay we performed in parallel a fluorogenic and a ^{51}Cr-based killing assay on HLA-$A11^+$ B cells pulsed with increasing amounts of HLA-A11-restricted B cell line and HLA-A11-restricted ATK9 peptide (AIFQSSMTK, aa 158–166 in reverse transcriptase of HIV-1 polymerase (Walker et al., 1989)). The specific lysis % measured at 4 h after addition of the CTL similarly increased with the amount of peptides in both assays (Fig. 1D). We expanded the comparison of the two killing assays to two target cell lines, 2 CTL clones and 6 different peptide concentrations ranging from 0 to 0.2 μg/ml: HLA-$B57^+$ B cells pulsed with KF11 or HLA-$A3^+A11^+$ B cells pulsed with or A11-ATK9 peptide. Lysis % measured in parallel by real-time fluorogenic or ^{51}Cr-based assays for each peptide-clone combination were compared 4 h after addition of CTL clones. We found a significant correlation between the lysis % obtained with the two different assays ($p < 0.0001$ $r = 0.55$ Spearman test; Fig. 1E), indicating that target cell lysis as measured by real-time killing assay accurately corresponded to the one measured by classical ^{51}Cr release assay with the advantage of following target cell lysis in real-time.

3.2. Real-time detection of epitopes presented by HIV-infected cells to virus-specific CTL

We aimed to assess whether the assay is sensitive enough to measure the killing of HIV-infected cells, where viral antigens are endogenously processed and presented at the cell surface rather than exogenously pulsed onto cells (Fig. 2). HLA-$B57^+$ B cells were incubated for 5 h with VSV-G-pseudotyped HIV and then extensively washed. Cells were

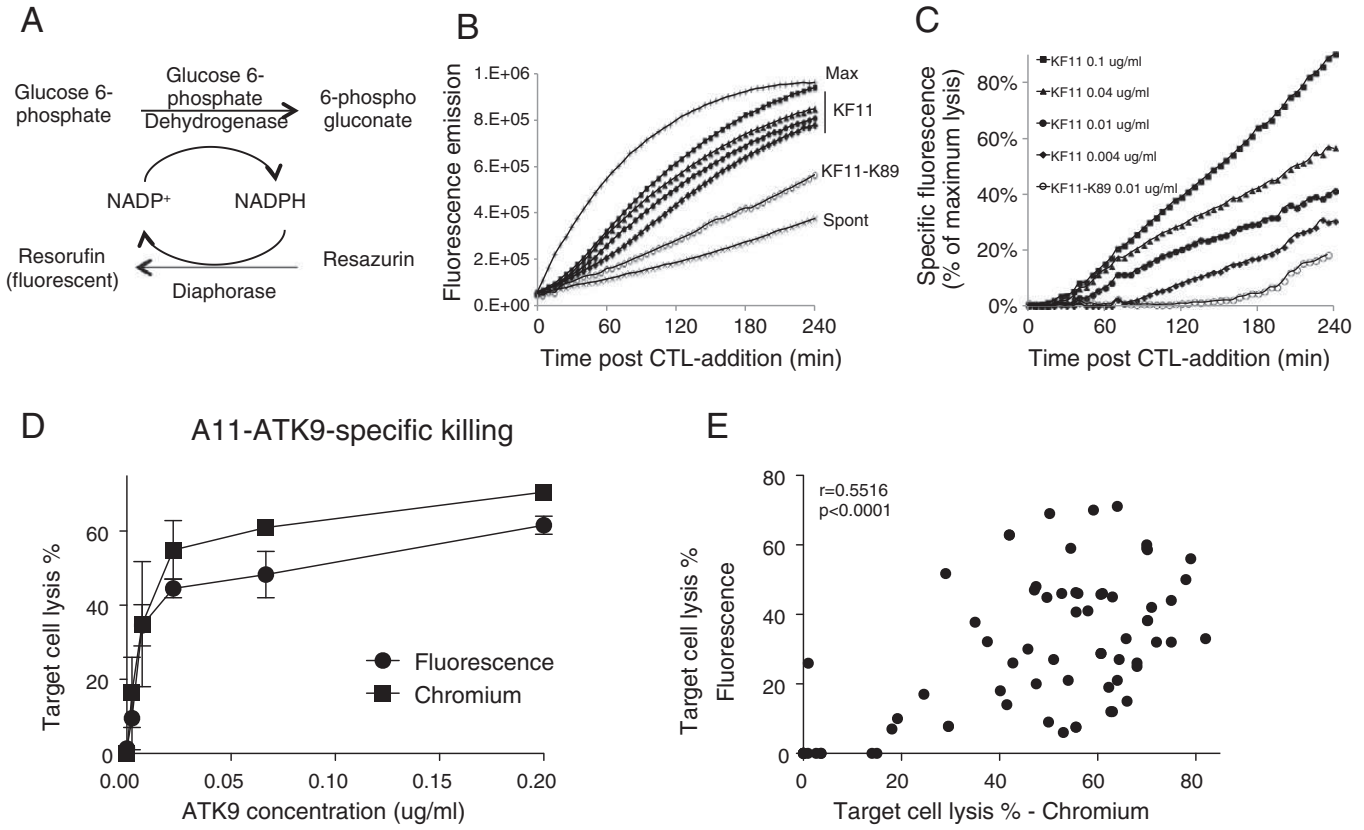

Fig. 1. A fluorogenic assay to measure real-time CTL-mediated cell killing. A. Principle of the coupled enzymatic assay for detection of glucose 6-phosphate dehydrogenase activity. Oxidation of glucose 6-phosphate by glucose 6-phosphate dehydrogenase results in the generation of NADPH, which in turn leads to the reduction of resazurin by diaphorase to yield fluorescent resorufin (Batchelor and Zhou, 2004). B. HLA-B57$^+$ B cells were incubated with increasing amounts of B57-restricted KF11 optimal peptide (0.1 μg/ml black squares; 0.04 μg/ml black triangles; 0.01 μg/ml black circles; 0.004 μg/ml black diamonds) or a mutated version of KF11 KF11-K89 (open circles) poorly recognized by KF11-specific CTL clones. Spontaneous cleavage of substrate (Spont; X) was calculated at each time point as the fluorescence released by B cell + KF11-specific CTL point without peptide. Maximum (Max; +) is calculated as the fluorescence released by B cell in the presence of KF11-specific CTL and Triton 0.5%. Fluorescence emission was measured every 5 min for 4 h from the time the CTL were added to target cells. Autofluorescence of substrate in the presence of PBS is subtracted at each time point. C. Specific fluorescence in the presence of increasing amount of KF11 or KF11-89 is measured at each point as [(Fluorescence − Spont) / (Max − Spont)] × 100. D. ^{51}Cr-labeled or unlabeled HLA-B57$^+$ B cells were incubated with increasing amounts of KF11 peptide and used as targets in a ^{51}Cr-based or fluorogenic killing assay with KF11-specific CTL (E:T 4:1). Lysis percentage of target cells by Cr-release assay (black squares) or fluorescence assay (black circles) was measured after a 4-hour incubation. E. The comparison of killing of target cells pulsed with increasing amounts of peptides was expanded to 4 different CTL clones (A11-ATK9, A03-RK9, B57-KF11, and B57-TW10). Correlation calculated with Spearman test.

collected at 10 h, 24 h, and 48 h after infection and used as targets in a real-time killing assay with CTL specific for two HLA-B57-restricted p24 epitopes KF11 and TW10 (epitope TSTLQEQIGW, aa 108–117 in Gag p24) (Llano et al., 2009). As shown in Fig. 2A, the percentage of target cell lysis increased with time starting at 10% after 10 h post infection until 50–60% after 48 h. These results indicate that the presence of KF11 and TW10 epitopes displayed with MHC-I at the surface of B cell increased during the first 48 h of infection. As a positive control, target cells loaded with 0.4 μg/ml of KF11 or TW10 peptide were evenly lysed at 60–70% at each time point. By comparing the lysis of HIV-infected B cells with that of B cells pulsed with various amounts of optimal epitopes KF11 or TW10 as in (Le Gall et al., 2007), we estimated that the antigenic peptide equivalent displayed at the surface of B cells between 10 and 48 h after infection increased from 0.16 to 27 nM for KF11, and 3.4 and from 86 nM for TW10. We compared the killing of target B cells at 10 to 48 h post-infection with the corresponding percentage of infected B cells determined by intracellular p24 staining. Infection was measured by flow cytometry after intracellular staining of B cells with a p24 antibody and ranged in average between 3 and 43% depending on the time point. For both KF11- and TW10-specific CTL clones (Fig. 2B), we found a strong association between lysis % and % of p24-positive cells ($p < 0.0001$ $r = 0.857$, $p < 0.0001$ $r = 0.901$ Spearman test, respectively Fig. 2B), indicating that target cell lysis as measured by real-time killing assay reflected the percentage of HIV-infected cells processing and presenting HIV epitopes. In addition, HLA-B57$^+$ or HLA-A03$^+$11$^+$ B cell lines were infected with a HIV-derived lentiviral vector expressing GFP and pseudotyped with VSV-G. Infection rates were measured by GFP expression and ranged between 6 and 62%. HLA-B57$^+$ B cells were used as targets with KF11- and TW10-specific CTL, HLA-A03$^+$A11$^+$ B cell lines were used as targets with p17 A03-RK9 (RLRPGGKKK, aa 20–28 in p17 Gag (Harrer et al., 1996; Yu et al., 2002)) and A11-ATK9 specific CTL. The killing of two different target cell lines by four different clones correlates with the % of GFP-expressing cells ($R = 0.6716$; $p = 0.0003$), indicating that the real-time CTL killing assay allows the detection of a wide range of infected cells presenting various amounts of HIV epitopes.

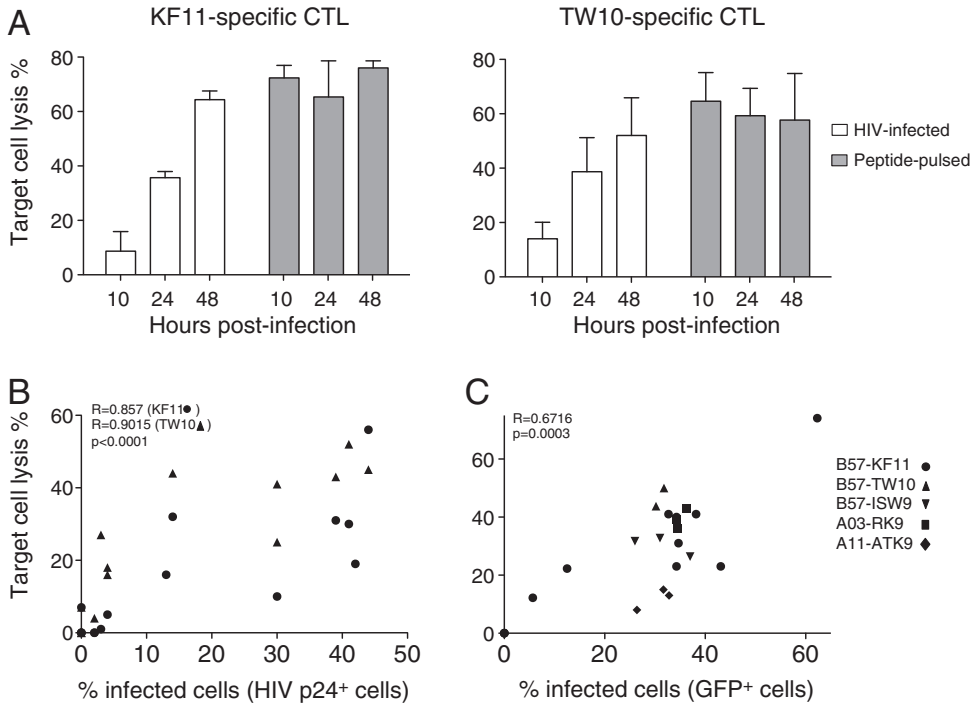

Fig. 2. Detection of HIV-infected cells by real-time killing assay. A. HLA-B57$^+$ B cells were infected with VSV-G-pseudotyped HIV. Lysis of HIV-infected (white bars) or peptide-pulsed (gray bars) target cells by HLA-B57-restricted Gag KF11-specific (left) or TW10-specific (right) CTL was monitored at 10, 24 or 48 h post-infection. Lysis % corresponds to a 4-hour time point after addition of CTL. B. Correlation between target cell lysis by KF11- (black circles) or TW10-specific (black triangles) CTL clones and % infected cells of measured by p24-specific intracellular staining. C. HLA-B57 or HLA-A03/11 B cells were infected with a VSV-G pseudotyped lentiviral vector expressing GFP. Correlation between HLA-B57 or HLA-A03/11 target cells lysis by HLA-B57-restricted ISW9- (black inverted triangles), KF11- or TW10-specific CTL clones or by A3-RK9- (black squares) or A11-ATK9-specific (black diamonds) respectively and % of infected cells monitored by GFP staining. Correlation by Spearman test.

3.3. Monitoring differential epitope presentation by HIV-infected cells

We then assessed whether the real-time killing assay was adequate to compare the kinetics of presentation of several HIV epitopes during HIV infection (Fig. 3). In order to specifically compare epitope presentation and killing by different CTL clones without confounding factors we chose epitopes for which the functional avidity of the epitopes for MHC-I and the TCR of CTL was equivalent. Building on previous measurements done by ^{51}Cr-release assay (Le Gall et al., 2007; Zhang et al., 2012) we compared the fluorescence-based killing of B cells expressing HLA-B57 and/or HLA-A11 pulsed with increasing amounts of peptides 4 h after addition of CTL (Fig. 3A). Similar lysis % of target cells by the two clones were observed at various peptide concentrations, showing similar functional avidity of the two clones. We then compared the endogenous presentation of HLA-B57-restricted KF11 epitope located in Gag p24 and a HLA-A03/11-restricted ATK9 epitope from reverse transcriptase, a protein expressed later in the viral cycle. HLA-B57$^+$A11$^+$ B cells were infected with VSV-G-pseudotyped HIV-1. Infection rate with this VSV-G non-replicative virus ranged between 10–75% between days 1 to 4 and diminished after 4 days as non-infected cells grew faster. Lysis of target cells 3 days post-infection in one representative experiment was monitored over 4 h after the addition of KF11- and ATK9-specific CTL (Fig. 3B). It showed that killing of infected cells by KF11-specific CTL started earlier after addition of CTL and reached higher specific lysis compared to ATK9 (32% vs 9%). Considering that the 2 epitopes have similar functional avidity this difference in lysis is likely due to differences in the amount of KF11 and ATK9 peptides displayed by HIV-infected cells. Target cell lysis at 4 h after CTL addition was monitored at day 2, 3, 4, 5, 7 and 10 post-infection (Fig. 3C). The killing of HIV-infected B cells by KF11-specific CTL occurred as early as day 2 whereas killing by ATK9-specific CTL began at day 3. Alternatively HLA-B57$^+$A11$^+$ primary CD4 T cells stimulated with PHA were infected with replicative HIV-1 NL4-3. Killing of CD4 T cells by epitope-specific CTL was monitored during 4 h at day 2, 3, 4, 5, 7 and 10 post-infection. Similarly to the kinetics of killing of HIV-infected B cells, the killing of HIV-infected CD4 T cells by ATK9-specific CTL was delayed (day 4) compared to killing by KF11-specific CTL (day 2). These results suggest that delayed and lower expression of Pol compared to Gag and/or less efficient processing of this RT epitope leads to a lesser epitope presentation and delayed killing of HIV-infected CD4 T cells by the ATK9-specific CTL. In conclusion, the real-time killing assay allows us to indirectly evaluate the amount of viral epitope presented by infected cells and to identify viral epitopes detectable by CTL early in the course of infection.

4. Discussion

CD8 T cells play a major role in the clearance of many viral infections and constitute a critical arm of immune responses elicited by vaccines. It is therefore important to develop

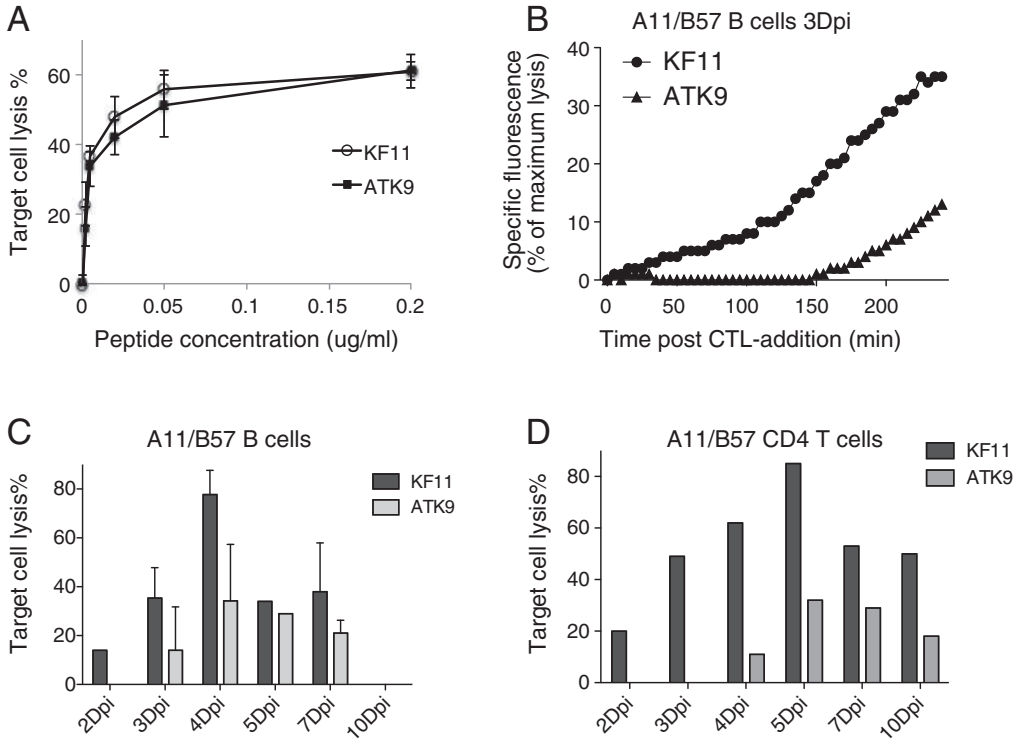

Fig. 3. Real-time epitope presentation by HIV-infected cells to CTL. A. HLA-A11$^+$B57$^+$ B cells were pulsed with increasing amounts of B57-restricted KF11 or A11-restricted ATK9 and used as targets in a fluorescence killing assay with KF11-specific (open circles) or ATK9-specific (black squares) CTL. Average of 3 experiments. B. HLA-A11$^+$B57$^+$ B cells were infected with VSV-G pseudotyped HIV. At 3 days post-infection cells were used as targets with KF11- (black circles) or ATK9-specific CTL (black triangles). Specific fluorescence was measured every 5 min for 4 h after addition of epitope-specific CTL. C. Lysis of infected B cells by KF11-specific (dark gray) or ATK9-specific (light gray) CTL was measured 2 to 10 days post-infection. Average of 4 experiments. D. HLA-A11$^+$B57$^+$ PHA-activated primary CD4 T cells were infected with replicative HIV-1 NL4-3 and lysis of infected cells by KF11-specific (dark gray) or ATK9-specific (light grey) was measured 2 to 10 days post-infection. Lysis % in panels C and D correspond to the 4-hour time point after addition of CTL.

assays identifying immune responses able to efficiently kill virus-infected cells. The efficiency of killing of infected cells is defined not only by the intrinsic capacity of T cells to secrete cytokines and granzymes, but also by their capacity to rapidly recognize their targets. CTL-mediated killing of infected cells requires the degradation of a pathogen protein into epitopes, loading onto MHC-I and display of the epitope by MHC-I at the cell surface in sufficient amount to trigger activation of CTL. This sequence of events is dynamic, yet current killing assays do not permit multiple measurements after infection as they typically monitor a single time point.

Here we developed a fluorogenic killing assay to monitor in real-time the killing of HIV-infected cells by CTL. The assay makes use of an extracellular G6PDH-specific substrate — that limits toxicity and leakage and allows us to follow target cell lysis every 5 min or as frequently as needed after addition of CTL. It allowed parallel detection of the killing of immortalized or primary target cells by several epitope-specific T cell clones. This assay gives similar lysis % to classical ^{51}Cr-release assay, uses fewer cells, is throughput and sensitive enough to detect cells pulsed with low concentration peptides, as well as HIV-infected cells displaying peptides endogenously processed during infection. Although HIV infection was the focus of this study, this assay could be used with any primary cells infected with any virus or viral vector and to measure the killing mediated by various immune cells with cytolytic capacities such as CD8 T cells, cytolytic CD4 T cells or NK cells.

A major application of this assay is to be able to monitor epitope presentation after viral infection. We can compare the presentation of epitopes from viral proteins expressed at various stages of the viral life cycle or compare the presentation of epitopes within a given protein. We showed in this study that the killing of HIV-infected B cell lines as well as the killing of HIV-infected primary CD4 T cells by CTL recognizing a Pol epitope ATK9 is delayed compared to that triggered by a Gag-specific CTL (KF11) despite equivalent functional avidity of the two clones. This delay in recognition of infected cells could be due to the 20-fold higher amount of Gag compared to Pol in HIV virions. Pol is synthesized as part of a Gag–Pol polyprotein by a ribosome frameshift near the 3' end of Gag and requires further cleavage of Gag–Pol by HIV protease. This process results in lower and later production of Pol compared to Gag (Jacks et al., 1988; Louis et al., 1994) and may lead to a lower and delayed presentation of the Pol epitope to epitope-specific CTL. Another difference in Gag and Pol epitope presentation could stem from differences in the efficiency and timing of epitope production. We previously showed that the endogenous expression of Gag p17 protein with a C-terminal tag containing a fragment of Pol including ATK9 leads to 4-fold less killing (measured by ^{51}Cr release assay) by Pol ATK9-specific CTL than by the Gag-specific RK9 CTL, demonstrating that even a synchronized expression of Gag–Pol did not erase the difference in CTL killing efficiency (Le Gall et al., 2007). In support of this difference in epitope presentation we demonstrated that the

cytosolic degradation of Gag p17 RK9-contaning peptides leads to earlier and higher production of epitope RK9 than that of Pol ATK9-containing peptide (Le Gall et al., 2007). We showed that differences in HIV epitope production and presentation are driven by motifs within (Lazaro et al., 2011) and outside (Draenert et al., 2004; Zhang et al., 2012) of the viral epitope and will affect recognition by CTL ((Lazaro et al., 2011) and additional unpublished data). Altogether these results suggest that differences in the timing and amount of epitopes produced inside infected cells and the timing of their display at the cell surface is defined by the efficiency of epitope processing as much as by the kinetics and level of expression of viral proteins during the virus life cycle.

5. Conclusion

We developed a throughput real-time CTL killing assay that integrates kinetics of viral life cycle, efficiency of degradation of viral proteins into epitopes and timing of presentation of viral epitopes to monitor killing of virus-infected cells by various virus-specific CD8 T cells (and potentially by any other immune cells with cytolytic function). This assay, adaptable to any virus infection or target cells, will allow to easily identify immune responses able to recognize infected cells early and efficiently — which is integral to preventing viral spread and therefore of high interest for vaccine design.

Acknowledgments

This study was supported by grants A1084753 and A1084106 from NIAID.

References

Almeida, J.R., Price, D.A., Papagno, L., Arkoub, Z.A., Sauce, D., Bornstein, E., Asher, T.E., Samri, A., Schnuriger, A., Theodorou, I., Costagliola, D., Rouzioux, C., Agut, H., Marcelin, A.G., Douek, D., Autran, B., Appay, V., 2007. Superior control of HIV-1 replication by CD8+ T cells is reflected by their avidity, polyfunctionality, and clonal turnover. J. Exp. Med. 204, 2473.

Bangham, C.R., 2009. CTL quality and the control of human retroviral infections. Eur. J. Immunol. 39, 1700.

Batchelor, R.H., Zhou, M., 2004. Use of cellular glucose-6-phosphate dehydrogenase for cell quantitation: applications in cytotoxicity and apoptosis assays. Anal. Biochem. 329, 35.

Betts, M.R., Brenchley, J.M., Price, D.A., De Rosa, S.C., Douek, D.C., Roederer, M., Koup, R.A., 2003. Sensitive and viable identification of antigen-specific CD8+ T cells by a flow cytometric assay for degranulation. J. Immunol. Methods 281, 65.

Brunner, K.T., Mauel, J., Cerottini, J.C., Chapuis, B., 1968. Quantitative assay of the lytic action of immune lymphoid cells on 51-Cr-labelled allogeneic target cells in vitro; inhibition by isoantibody and by drugs. Immunology 14, 181.

Burton, D.R., Ahmed, R., Barouch, D.H., Butera, S.T., Crotty, S., Godzik, A., Kaufmann, D.E., McElrath, M.J., Nussenzweig, M.C., Pulendran, B., Scanlan, C.N., Schief, W.R., Silvestri, G., Streeck, H., Walker, B.D., Walker, L.M., Ward, A.B., Wilson, I.A., Wyatt, R., 2012. A blueprint for HIV vaccine discovery. Cell Host Microbe 12, 396.

Cholujova, D., Jakubikova, J., Kubes, M., Arendacka, B., Sapak, M., Ihnatko, R., Sedlak, J., 2008. Comparative study of four fluorescent probes for evaluation of natural killer cell cytotoxicity assays. Immunobiology 213, 629.

Draenert, R., Le Gall, S., Pfafferott, K.J., Leslie, A.J., Chetty, P., Brander, C., Holmes, E.C., Chang, S.C., Feeney, M.E., Addo, M.M., Ruiz, L., Ramduth, D., Jeena, P., Altfeld, M., Thomas, S., Tang, Y., Verrill, C.L., Dixon, C., Prado, J.G., Kiepiela, P., Martinez-Picado, J., Walker, B.D., Goulder, P.J., 2004. Immune selection for altered antigen processing leads to cytotoxic T lymphocyte escape in chronic HIV-1 infection. J. Exp. Med. 199, 905.

Harrer, T., Harrer, E., Kalams, S.A., Barbosa, P., Trocha, A., Johnson, R.P., Elbeik, T., Feinberg, M.B., Buchbinder, S.P., Walker, B.D., 1996. Cytotoxic T lymphocytes in asymptomatic long-term nonprogressing HIV-1 infection. breadth and specificity of the response and relation to in vivo viral quasispecies in a person with prolonged infection and low viral load. J. Immunol. 156, 2616.

He, L., Hakimi, J., Salha, D., Miron, I., Dunn, P., Radvanyi, L., 2005. A sensitive flow cytometry-based cytotoxic T-lymphocyte assay through detection of cleaved caspase 3 in target cells. J. Immunol. Methods 304, 43.

Hersperger, A.R., Pereyra, F., Nason, M., Demers, K., Sheth, P., Shin, L.Y., Kovacs, C.M., Rodriguez, B., Sieg, S.F., Teixeira-Johnson, L., Gudonis, D., Goepfert, P.A., Lederman, M.M., Frank, I., Makedonas, G., Kaul, R., Walker, B.D., Betts, M.R., 2010. Perforin expression directly ex vivo by HIV-specific CD8 T-cells is a correlate of HIV elite control. PLoS Pathog. 6, e1000917.

Hersperger, A.R., Migueles, S.A., Betts, M.R., Connors, M., 2011. Qualitative features of the HIV-specific CD8+ T-cell response associated with immunologic control. Curr. Opin. HIV AIDS 6, 169.

Jacks, T., Power, M.D., Masiarz, F.R., Luciw, P.A., Barr, P.J., Varmus, H.E., 1988. Characterization of ribosomal frameshifting in HIV-1 gag-pol expression. Nature 331, 280.

Janetzki, S., Cox, J.H., Oden, N., Ferrari, G., 2005. Standardization and validation issues of the ELISPOT assay. Methods Mol. Biol. 302, 51.

Lazaro, E., Kadie, C., Stamegna, P., Zhang, S.C., Gourdain, P., Lai, N.Y., Zhang, M., Martinez, S.A., Heckerman, D., Le Gall, S., 2011. Variable HIV peptide stability in human cytosol is critical to epitope presentation and immune escape. J. Clin. Invest. 121, 2480.

Le Gall, S., Stamegna, P., Walker, B.D., 2007. Portable flanking sequences modulate CTL epitope processing. J. Clin. Invest. 117, 3563.

Lecoeur, H., Fevrier, M., Garcia, S., Riviere, Y., Gougeon, M.L., 2001. A novel flow cytometric assay for quantitation and multiparametric characterization of cell-mediated cytotoxicity. J. Immunol. Methods 253, 177.

Lee-MacAry, A.E., Ross, E.L., Davies, D., Laylor, R., Honeychurch, J., Glennie, M.J., Snary, D., Wilkinson, R.W., 2001. Development of a novel flow cytometric cell-mediated cytotoxicity assay using the fluorophores PKH-26 and TO-PRO-3 iodide. J. Immunol. Methods 252, 83.

Lemonnier, F.A., 2013. Evaluating CD8(+) T cell responses in vitro. Methods Mol. Biol. 960, 261.

Liu, L., Chahroudi, A., Silvestri, G., Wernett, M.E., Kaiser, W.J., Safrit, J.T., Komoriya, A., Altman, J.D., Packard, B.Z., Feinberg, M.B., 2002. Visualization and quantification of T cell-mediated cytotoxicity using cell-permeable fluorogenic caspase substrates. Nat. Med. 8, 185.

Llano, A., F.N., Brander, C., 2009. How to optimally define optimal cytotoxic T lymphocyte epitopes in HIV infection? HIV Molecular Immunology, p. 3.

Louis, J.M., Nashed, N.T., Parris, K.D., Kimmel, A.R., Jerina, D.M., 1994. Kinetics and mechanism of autoprocessing of human immunodeficiency virus type 1 protease from an analog of the Gag-Pol polyprotein. Proc. Natl. Acad. Sci. U. S. A. 91, 7970.

Maino, V.C., Picker, L.J., 1998. Identification of functional subsets by flow cytometry: intracellular detection of cytokine expression. Cytometry 34, 207.

McMillian, M.K., Li, L., Parker, J.B., Patel, L., Zhong, Z., Gunnett, J.W., Powers, W.J., Johnson, M.D., 2002. An improved resazurin-based cytotoxicity assay for hepatic cells. Cell Biol. Toxicol. 18, 157.

Migueles, S.A., Connors, M., 2001. Frequency and function of HIV-specific CD8(+) T cells. Immunol. Lett. 79, 141.

Migueles, S.A., Osborne, C.M., Royce, C., Compton, A.A., Joshi, R.P., Weeks, K.A., Rood, J.E., Berkley, A.M., Sacha, J.B., Cogliano-Shutta, N.A., Lloyd, M., Roby, G., Kwan, R., McLaughlin, M., Stallings, S., Rehm, C., O'Shea, M.A., Mican, J., Packard, B.Z., Komoriya, A., Palmer, S., Wiegand, A.P., Maldarelli, F., Coffin, J.M., Mellors, J.W., Hallahan, C.W., Follman, D.A., Connors, M., 2008. Lytic granule loading of CD8+ T cells is required for HIV-infected cell elimination associated with immune control. Immunity 29, 1009.

Miura, T., Brockman, M.A., Schneidewind, A., Lobritz, M., Pereyra, F., Rathod, A., Block, B.L., Brumme, Z.L., Brumme, C.J., Baker, B., Rothchild, A.C., Li, B., Trocha, A., Cutrell, E., Frahm, N., Brander, C., Toth, I., Arts, E.J., Allen, T.M., Walker, B.D., 2009. HLA-B57/B*5801 human immunodeficiency virus type 1 elite controllers select for rare gag variants associated with reduced viral replication capacity and strong cytotoxic T-lymphocyte [corrected] recognition. J. Virol. 83, 2743.

Miyahira, Y., Murata, K., Rodriguez, D., Rodriguez, J.R., Esteban, M., Rodrigues, M.M., Zavala, F., 1995. Quantification of antigen specific CD8+ T cells using an ELISPOT assay. J. Immunol. Methods 181, 45.

Mwau, M., McMichael, A.J., Hanke, T., 2002. Design and validation of an enzyme-linked immunospot assay for use in clinical trials of candidate HIV vaccines. AIDS Res. Hum. Retroviruses 18, 611.

Ndhlovu, Z.M., Chibnik, L.B., Proudfoot, J., Vine, S., McMullen, A., Cesa, K., Porichis, F., Jones, R.B., Alvino, D.M., Hart, M.G., Stampouloglou, E., Piechocka-Trocha, A., Kadie, C., Pereyra, F., Heckerman, D., De Jager, P.L.,

Walker, B.D., Kaufmann, D.E., 2013. High-dimensional immunomonitoring models of HIV-1-specific CD8 T-cell responses accurately identify subjects achieving spontaneous viral control. Blood 121, 801.
Neefjes, J., Jongsma, M.L., Paul, P., Bakke, O., 2011. Towards a systems understanding of MHC class I and MHC class II antigen presentation. Nat. Rev. Immunol. 11 (12), 823.
Nomura, L., Maino, V.C., Maecker, H.T., 2008. Standardization and optimization of multiparameter intracellular cytokine staining. Cytometry A 73, 984.
Roden, M.M., Lee, K.H., Panelli, M.C., Marincola, F.M., 1999. A novel cytolysis assay using fluorescent labeling and quantitative fluorescent scanning technology. J. Immunol. Methods 226, 29.
Rowland-Jones, S.L., Pinheiro, S., Kaul, R., Hansasuta, P., Gillespie, G., Dong, T., Plummer, F.A., Bwayo, J.B., Fidler, S., Weber, J., McMichael, A., Appay, V., 2001. How important is the 'quality' of the cytotoxic T lymphocyte (CTL) response in protection against HIV infection? Immunol. Lett. 79, 15.
Shacklett, B.L., 2002. Beyond ^{51}Cr release: New methods for assessing HIV-1-specific CD8 + T cell responses in peripheral blood and mucosal tissues. Clin. Exp. Immunol. 130, 172.
Sheehy, M.E., McDermott, A.B., Furlan, S.N., Klenerman, P., Nixon, D.F., 2001. A novel technique for the fluorometric assessment of T lymphocyte antigen specific lysis. J. Immunol. Methods 249, 99.
Snyder, J.E., Bowers, W.J., Livingstone, A.M., Lee, F.E., Federoff, H.J., Mosmann, T.R., 2003. Measuring the frequency of mouse and human cytotoxic T cells by the Lysispot assay: independent regulation of cytokine secretion and short-term killing. Nat. Med. 9, 231.
Snyder-Cappione, J.E., Divekar, A.A., Maupin, G.M., Jin, X., Demeter, L.M., Mosmann, T.R., 2006. HIV-specific cytotoxic cell frequencies measured directly ex vivo by the Lysispot assay can be higher or lower than the frequencies of IFN-gamma-secreting cells: anti-HIV cytotoxicity is not generally impaired relative to other chronic virus responses. J. Immunol. 176, 2662.
Usharauli, D., Perez-Diez, A., Matzinger, P., 2006. The JAM Test and its daughter P-JAM: simple tests of DNA fragmentation to measure cell death and stasis. Nat. Protoc. 1, 672.
Walker, B.D., Flexner, C., Birch-Limberger, K., Fisher, L., Paradis, T.J., Aldovini, A., Young, R., Moos, B., Scholey, R.T., 1989. Long-term culture and fine specificity of human cytotoxic T-lymphocyte clones reactive with human immunodeficiency virus type 1. Proc. Natl. Acad. Sci. U. S. A. 86, 9514.
Wierda, W.G., Mehr, D.S., Kim, Y.B., 1989. Comparison of fluorochrome-labeled and 51Cr-labeled targets for natural killer cytotoxicity assay. J. Immunol. Methods 122, 15.
Yu, X.G., Addo, M.M., Rosenberg, E.S., Rodriguez, W.R., Lee, P.K., Fitzpatrick, C.A., Johnston, M.N., Strick, D., Goulder, P.J., Walker, B.D., Altfeld, M., 2002. Consistent patterns in the development and immunodominance of human immunodeficiency virus type 1 (HIV-1)-specific CD8 + T-cell responses following acute HIV-1 infection. J. Virol. 76, 8690.
Zhang, Z., Apse, K., Pang, J., Stanton, R.C., 2000. High glucose inhibits glucose-6-phosphate dehydrogenase via cAMP in aortic endothelial cells. J. Biol. Chem. 275, 40042.
Zhang, S.C., Martin, E., Shimada, M., Godfrey, S.B., Fricke, J., Locastro, S., Lai, N.Y., Liebesny, P., Carlson, J.M., Brumme, C.J., Ogbechie, O.A., Chen, H., Walker, B.D., Brumme, Z.L., Kavanagh, D.G., Le Gall, S., 2012. Aminopeptidase substrate preference affects HIV epitope presentation and predicts immune escape patterns in HIV-infected individuals. J. Immunol. 188, 5924.

Viruses **2014**, *6*, 3271-3292; doi:10.3390/v6083271

OPEN ACCESS

viruses

ISSN 1999-4915

www.mdpi.com/journal/viruses

Review

Mechanisms of HIV Protein Degradation into Epitopes: Implications for Vaccine Design

Marijana Rucevic †, Julie Boucau †, Jens Dinter †, Georgio Kourjian † and Sylvie Le Gall *

Ragon Institute of MGH, MIT and Harvard, Massachusetts General Hospital and Harvard Medical School, Cambridge, MA 02139, USA;
E-Mails: Rucevic.Marijana@mgh.harvard.edu (M.R.); jnoucau@mgh.harvard.edu (J.B.); jdinter@mgh.harvard.edu (J.D.); gkourjian@mgh.harvard.edu (G.K.)

† These authors contributed equally to this work.

* Author to whom correspondence should be addressed; E-Mail: sylvie_legall@hms.harvard.edu; Tel.: +1-857-268-7010.

Received: 11 June 2014; in revised form: 6 August 2014 / Accepted: 11 August 2014 / Published: 21 August 2014

Abstract: The degradation of HIV-derived proteins into epitopes displayed by MHC-I or MHC-II are the first events leading to the priming of HIV-specific immune responses and to the recognition of infected cells. Despite a wealth of information about peptidases involved in protein degradation, our knowledge of epitope presentation during HIV infection remains limited. Here we review current data on HIV protein degradation linking epitope production and immunodominance, viral evolution and impaired epitope presentation. We propose that an in-depth understanding of HIV antigen processing and presentation in relevant primary cells could be exploited to identify signatures leading to efficient or inefficient epitope presentation in HIV proteomes, and to improve the design of immunogens eliciting immune responses efficiently recognizing all infected cells.

Keywords: HIV; antigen processing; protein degradation; proteasome; aminopeptidase; peptidase; immunogen; vaccine vector; dendritic cells; T cells; viral evolution

1. Antigen Processing Pathways

Protein degradation by the antigen processing machinery is a continuous process regulating all cellular functions by defining the lifespan of all proteins, discarding misfolded proteins, recycling amino acids to make new proteins, and initiating immune monitoring [1].

Proteins and misfolded or incomplete translation products such as defective ribosomal products [2] are degraded by proteasomes, the most ubiquitous cellular proteases. Proteasomes are made of 4 rings, 2 outer rings of 7 distinct alpha subunits and 2 inner rings of 7 distinct beta subunits, including 3 catalytic subunits cleaving after hydrophobic, acidic or basic residues respectively, allowing for the cleavage of all substrates [3,4]. The 20S core proteasomes can be fitted with regulatory lids leading to the assembly of 26S proteasomes. The 19S lid interacts with E3 ubiquitin ligases and polyubiquitinated substrates and contributes to unfolding substrates before degradation and opening of the proteasome chamber. Whereas 26S proteasomes degrade mostly polyubiquitinated substrates, 20S proteasomes and proteasomes capped with regulatory PA28/11S lids are able to degrade non-polyubiquitinated substrates. Besides constitutive proteasomes expressed in all cell types, immunoproteasomes are present in lymphoid tissues and can be induced in other cell types upon infection or cytokine exposure [5]. Interferon gamma induces the expression of catalytic immunosubunits and PA28 lids leading to the assembly of 20S and 26S immunoproteasomes [6]. All proteasomes degrade proteins into fragments ranging from a few residues up to 32 aa long, including epitopes, peptides containing epitopes (epitope precursors) and also amino acids to be recycled for protein synthesis [7]. Although peptides generated by various types of proteasomes overlap, they may also create unique peptides [7,8]. Immunoproteasomes tend to produce longer peptides ending with C-terminal hydrophobic residues, the most frequent C-terminal anchor for most MHC-I isotypes, and may favor the production of epitopes [9]. The presence of both proteasomes and immunoproteasomes in the same cell is associated with a greater variety of peptides available for presentation [10]. Degradation products from the proteasome can be further degraded by proteasomes as well as other cytosolic peptidases including endopeptidases TPPII [11,12], thimet oligopeptidases (TOP) [13–15], leucine aminopeptidase (LAP) [11,12], puromycin sensitive aminopeptidase (PSA) [16], bleomycin sensitive hydrolase (BH) [17], insulin degrading enzyme [18] or nardilysin [19]. Each peptidase has specificities in terms of substrate length and residues but they are not always well defined. The contribution of post-proteasomal peptidases is variable according to epitopes [18,19], sometimes controversial [20–22], and the order in which they cleave substrates is rarely defined [23,24]. Cytosolic peptidases cannot unfold proteins and therefore degrade post-proteasomal degradation products. Post-proteasomal peptidases such as TOP can produce epitopes from longer precursors or destroy peptides, thus contributing to defining sequences and the amount of peptides available for presentation to T cells [15,25]. Cytosolic peptides of mostly 8–16 aa long with adequate anchor residues for the transporter associated to antigen processing (TAP) [26] are translocated into the endoplasmic reticulum (ER) where peptides can be trimmed by ER-resident aminopeptidases ERAP1 [21,27–29] and ERAP2 [30] before loading onto MHC-I. Exogenous antigens such as proteins, dead cells, antibodies-coated viruses can be endocytosed or phagocytosed and degraded by various cathepsins [31,32], proteases and IRAP [33] in endosomes and lysosomes. Some degradation peptides can be transferred back in the cytosol or ER for further trimming and cross-presentation by MHC-I. In cells expressing MHC-II a specific lysosomal compartment called MIIC enables loading of peptides

onto MHC-II molecules after removal of the invariant chain [34]. Although MHC-II epitope processing is mostly accomplished by endolysosomal proteases, proteasomes may be involved in the production of MHC-II epitopes of endogenous origin. The distinction between endogenous and exogenous processing pathways is becoming more tenuous as many combinations of peptidases and compartments may be involved in the presentation or cross-presentation of peptides [35]. Additionally, the variable intracellular stability of peptides prior to loading onto MHC-I alters the amount of peptides available for MHC-I presentation [36,37]. Altogether the location, trafficking path and the presence or absence of cleavable motifs by various peptidases will shape the degradation patterns of proteins [38].

2. Degradation of HIV Proteins into Epitopes

Despite rather extensive knowledge of protein degradation pathways and high-throughput methods to sequence HIV in large cohorts of patients, our capacity to rapidly identify or predict T cell epitopes in pathogen-derived proteins after infection or vaccination is still cumbersome, mostly relying on screening of T cell responses by Elispot using PBMCs from infected persons. The identification of potential anchor residues for various MHC-I isotypes in HIV sequences shows that there are more putative epitopes than actual immune responses, suggesting limitations in either production of peptides, their presentation by MHC or available TCR repertoire. We still do not know which HIV peptides are actually processed and presented by HIV-infected cells. These studies are still technically difficult due to the high number of infected cells required for peptide extraction. The first evidence of presentation of HIV peptides by HIV-infected cell lines came through acid elution and HPLC purification of peptide fractions reactive against HIV-specific CD8 T cells [39]. A second study using HIV-infected cells secreting soluble HLA (to enhance the amount of HLA collected and sensitivity of the assay) identified by mass spectrometry numerous self-derived peptides eluted off soluble HLA molecules, and showed changes in the amount or identity of self-derived peptides. It did not lead to the identification of HIV peptides, possibly due to HIV peptide presentation being below the threshold of detection by mass spectrometers [40]. Another study identified HIV-derived MHC-II peptides presented by DC endocytosing p24 coupled to anti-DEC205 antibody [41]. Increased sensitivity of new mass spectrometers and various improvements in assays and mass spectrometry data analysis software will probably lead to the identification of a landscape of HIV and self-derived epitopes presented by HIV-infected cells in a near future. However, MHC-bound peptides from HIV-infected cells will always be limited by the combination of HLA of the donor and the technological limit of detection of peptides. It is necessary to better understand how HIV proteins are degraded into peptides in cells to evaluate the capacity of proteins (or immunogens) to generate peptides compatible with loading onto MHC-I or MHC-II, and the impact of cell type or infection on HIV epitope presentation. In addition to epitopes encoded by the conventional reading frames of HIV genes several groups identified cryptic epitopes derived from the degradation of HIV translation products derived from alternate reading frames of HIV shifted by 1, 2 or 3 bases during translation [42]. Cryptic epitopes elicited CTL responses and immune pressure leading to HLA-restricted intraepitopic mutations [43,44], including some impairing processing [45]. Whether these immune responses contribute to reducing viral load in natural infection or should be included in vaccine immunogens is still unknown.

This new category of HIV-derived epitopes highlights our limited knowledge of the source of HIV epitopes and peptides presented by HIV-infected cells.

To study epitope production and presentation several experimental systems have been developed. The use of HIV-infected cells as targets for assays measuring HIV-specific T cell functions (killing, proliferation, cytokine production) measures both endogenous processing and presentation of epitopes and variability of MHC-peptide-TCR, and is limited by the availability of HIV-specific T cell clones. *In vitro* degradation of HIV proteins by purified proteasomes [46–48], ERAP1 [49,50] or by specific purified cathepsins [51] enables detailed studies of degradation patterns and cleavage preferences by specific peptidases. *In vitro* proteasomal degradation of Nef showed production of numerous peptides in epitope-rich areas of Nef enriched in hydrophobic residues [46]. Degradation of HIV p24 or p17 by proteasomes and ERAP1 also led to the efficient production of peptides containing immunodominant epitopes [49,50]. Degradation of HIV Env by purified cathepsins showed efficient production of epitopes (compared to proteasomal degradation) that may contribute to elicitation of CD4 T cell responses [51]. Single peptidase degradation facilitates the assessment of mutations on the production of epitope precursors or epitopes at a specific step of antigen processing [50,52]. However since protein degradation is a continuum involving multiple proteases (or several variants of proteasome species such as 20S/26S in the same cell), this approach may not permit the investigation of the complete processing of an epitope. Additionally, peptidases are often purified from cell lines that may not always be the most relevant to HIV infection. The use of intracellular compartments for protein degradation (cytosol, endosomes, lysosomes) allows us to account for all peptidases present in a given compartment and a given cell type or infection (although we cannot completely rule out that the preparation of subcellular fractions by damaging the normal structure of compartments may have some impact on protein degradation kinetics or patterns). The degradation of HIV proteins or long peptides in cytosolic extracts of primary cells showed that the kinetics of epitopes is variable even among overlapping epitopes [53,54], and that the efficiency of production of epitopes (timing and amount) is defined by motifs located within and outside epitopes [47,49,53,55,56], and the intracellular stability of peptides before loading onto MHC [36].

HIV virions enter cells by fusion at the plasma membrane and by endocytosis or antibody-mediated phagocytosis for immune complexes. Vaccines such as viral vectors or nanoparticles decorated with peptides or proteins enter dendritic cells by endocytosis. Degradation of HIV Envelope after deglycolysation showed poor proteasomal degradation and efficient degradation by cathepsins, in accordance with intrinsic differences in antigen degradation according to peptidases' substrate preferences [51]. Side-by-side degradations of HIV proteins in cytosolic and endolysosomal extracts from primary cells showed that some MHC-I epitopes are similarly processed in the two pathways while others are better processed in one of them [57]. These results suggest that the mode of entry of HIV virions or immunogens, in addition to the subset of target cells, will affect production and presentation of HIV epitopes as shown in non-HIV models [58,59].

A corollary to studies on efficiency of epitope production is to better understand mechanisms leading to impaired epitope presentation in the context of viral evolution. HLA-restricted mutations occur frequently in HIV-infected individuals during acute and chronic infection [60–65]. Some of these mutations are induced by immune pressure to avoid epitope presentation or correspond to mutations restoring viral fitness [66–73]. Many HLA-restricted mutations within epitopes impair binding to MHC-I

or to the TCR of CD8 T cells [67,74,75]. Mutations outside epitopes may affect the trimming of extended peptides into epitopes or change the degradation of long peptides by proteasomes [45,76–80]. Two recent studies identified motifs corresponding to antigen processing mutations at the population level by defining residues that can or cannot be cleaved by families of peptidases or group of peptidases in a subcellular compartment. One study identified residues that can be variably cleaved or not cleaved by aminopeptidases (some of which had been previously identified [81,82]), and demonstrated that the presence of poorly or non cleavable motifs introduced near an HIV epitope reduced or abolished epitope production *in vitro* and presentation to T cells [55]. In a population of over 1000 HIV-infected persons, N-flanking mutations evolved mostly toward poorly cleavable residues, showing that antigen processing mutations are frequent and can be predicted [55]. In another study that defined motifs linked to intracellular peptide stability or instability, a number of intraepitopic HLA-restricted mutations identified in a large population of HIV-infected persons (21 out of 25 mutants tested so far) led to decreased cytosolic stability and decreased the amount of peptide presented to CTL [36]. Thus, HIV has developed many ways to block epitope presentation through peptide destruction or through impaired trimming of long peptides into peptides better suited for MHC-I binding [83], leading to suboptimal presentation of peptides to CD8 T cells and impaired clearance of infected cells.

The accumulation of data on protein degradation by purified proteasomes led to the development of prediction tools such as NetChOP or PaProC to define potential cleavage sites in proteins of interest [84–87]. Although they do not account for the impact of infection or specifics of proteasomes in relevant primary cells they are valuable tools to identify potential proteasomal cleavage sites in an antigen. Improvements to these predictors for epitope processing came by incorporating binding of proteasomal degradation peptides to TAP for translocation into the ER, and more recently by combining proteasomal degradation, TAP binding and ERAP1 trimming to identify putative epitopes or the potential impact of HLA-restricted mutations on epitope processing [50,52,88]. A prediction tool for cytosolic peptide stability [36], which incorporates degradation by various PBMC cytosolic peptidases, could be included as an additional factor influencing the amount of peptides available for presentation. Our even more limited knowledge of MHC-II HIV epitope production and the loose and promiscuous binding of peptides to MHC-II renders the prediction of MHC-II epitopes more difficult. Considering the importance of CD4 T helper responses to elicit sustainable CD8 T cell responses, and the intriguing elicitation of MHC-II-restricted CD8 T cells responses after vaccination with an attenuated CMV vector expressing SIV proteins [89], predictors for MHC-II epitope processing will be necessary; so far only a few predictors of peptide binding to a few MHC-II alleles are available [90–92]. The current datasets available on protein degradation are still insufficient to build a complete predictor recapitulating protein degradation and epitope presentation by MHC-I or MHC-II alleles.

3. Antigen Processing in the Context of HIV Infection

HIV infection induces massive changes of cellular metabolism [93] and creates unique conditions for antigen processing and presentation in term of targeted cell subsets and conditions for protein degradation. Whether HIV epitope production in HIV infection or during preventive vaccination of healthy donors, or therapeutic vaccination of HIV-infected persons leads to the production of similar epitopes and priming of protective immune responses is not known.

HIV infects CD4 T cells, monocytes, macrophages and dendritic cells but we do not know if they similarly process and present HIV epitopes during infection. Whereas all cells contain proteasomes and post-proteasomal peptidases, their levels of expression and hydrolytic activities in primary cell subsets from a given individual are poorly defined. We showed that primary CD4 T cells present lower proteasomal and aminopeptidase activities than monocytes isolated from the same donor [54]. These differences affected the rate of degradation of long HIV peptides into epitopes, the kinetics of epitope production and the amount of epitopes and extended epitopes produced. *In vitro* degradation of HIV p24 by purified proteasomes from mature DC or activated CD4 T cells showed differences in the degradation patterns of p24 and production of HIV epitopes, supporting intrinsic differences in the hydrolytic activities of peptidases from different cell subsets [48]. HIV can enter cells by fusion at the plasma membrane or by endocytosis. The proportion of the two entry modes in various cell types is not well defined, not exclusive and may affect the degradation of incoming virions in infected cells. However, we are still lacking direct identification and comparison of HIV peptides presented by all HIV-infectable cell subsets and how potential differences may affect the timing and recognition of infected target cells by HIV-specific T cells.

HIV infection profoundly affects the transcriptional programs of cells [93] and triggers a cytokine storm including production of interferon alpha, gamma and interleukins. Interferon gamma induces the expression of catalytic immunosubunits of proteasomes toward immunoproteasomes and increases the expression of several aminopeptidases (LAP, ERAP1), TAP and MHC molecules [94,95]. TNF or LPS can also induce the formation of immunoproteasomes, but the impact of other cytokines or combination of cytokines and chemokines on the antigen processing machinery is not well defined [96]. Cytokines, virus or TLR ligands such as LPS or HIV RNA binding TLR7/8 trigger maturation of dendritic cells and macrophages. Maturation of dendritic cells reduces their antigen processing activities and modifies epitope presentation as shown previously indirectly through epitope-specific T cell activation assays in various infection models [97–101].

HIV Protease inhibitors (PI) are designed to block HIV protease catalytic sites to prevent HIV maturation into fully infectious particles. First generation PIs such as Saquinavir and Ritonavir present some cross-reactivity with proteasome catalytic sites and alter proteasome activity *in vivo* in mice as well as in human cells *in vitro* and LCMV-specific T cell responses in treated mice [102–106]. A recent study showed that HIV PIs affected not only proteasome but also aminopeptidase activities in various ways according to drug and concentration in human PBMC. HIV PIs modified HIV peptide degradation and epitope production, both in *in vitro* degradation assays in extracts treated with PIs, and in HIV-infected cells endogenously processing and presenting HIV peptides to HIV-specific T cells [107].

Besides these external stimuli, HIV infection itself affects antigen processing. In cells isolated from HIV-infected donors CD4 T cells present lower activities than monocytes as seen in cells isolated from healthy donors. Peptidase activities in cells from HIV-infected donors were heterogeneous with a trend toward decrease in CD4 T cells and increase in monocytes compared to healthy donors [54]. The very low number of circulating HIV-infected cells and variable cellular activation levels in patients may contribute to the heterogeneity of antigen processing activities measured in patients' PBMC. *In vitro* HIV infection alters antigen processing activities in monocyte-derived macrophages [108,109]. Interestingly, the entry mode of HIV (infection or receptor-mediated endocytosis of naked virus or AT-2 inactivated virus, complement-mediated opsonization particles) variably affects peptidase activities

and subsequently epitope presentation to T cells, at least in *in vitro* studies [109–111]. *In vitro* studies revealed that uptake of HIV Tat altered epitope processing activities and viral epitope presentation but the impact on the processing of HIV is not known [112]. However, uptake of HIV proteins, antiretrovirals or cytokine-induced modifications may alter antigen processing in neighboring uninfected cells in HIV-infected persons.

4. Exploiting Assays and Knowledge of HIV Antigen Processing and Processing for Improved Vaccine Design

A commonly accepted approach to HIV vaccine design (including prophylactic vaccines protecting from infection or therapeutic vaccines clearing or controlling established infection) would combine a potent antibody response to prevent establishment of infection and sustainable T cell responses to control viral replication [113]. Challenges faced by vaccinologists include the genetic diversity of HIV, our lack of understanding of protective immunity (since there is no case of natural clearance of HIV infection), the establishment of viral reservoirs that cannot be eliminated with antiretroviral therapy, and our inability to induce B cells making specific neutralizing antibodies [114]. Current areas of focus in vaccine development examined in *in vitro* studies, preclinical animal studies and clinical trials include designing and testing various types of immunogens (proteins, peptides, nucleic acids) [115], viral vectors (non-replicative or attenuated persistent) [116,117], vectorless system (nanoparticles carrying immunogen) [118], and adjuvants [119]. Since current clinical trials and vaccines eliciting antibodies are addressed elsewhere in this journal issue this review will focus on important notions to consider in the design of vaccines eliciting T cell immunity.

HIV infection leads to a predictable hierarchy of T cell responses with narrow immunodominance of one or several T cell responses for each HLA type [64,120]. Immunodominance of T cell responses is defined as the most frequent T cell immune responses (or T cell responses eliciting the highest production of interferon gamma) in a population sharing a given HLA [121,122]. Since HIV is not cleared by immune responses elicited during infection, a vaccine leading to the same immunodominance patterns as natural HIV infection will probably not be successful at preventing or clearing HIV infection. Two indirect lines of evidence support the need of breaking natural immunodominance during vaccination. First the Merck STEP clinical trial based on an adenovirus 5 vector expressing full HIV proteins elicited T cell immune responses in vaccinees similar to those elicited during natural HIV infection. However these responses failed to protect vaccinees from HIV infection or to reduce viral load in those who became infected [123]. Secondly an attenuated Rhesus CMV vector expressing complete SIV proteins (*i.e.*, live persistent virus with attenuated capacity to replicate) led to clearance of high or low dose SIV infection in 50% of Rhesus macaques up to 3 years after infection. The attenuated vector led to broad CD4 and CD8 T cell responses with an effector phenotype that were detected both in blood and lymph nodes of vaccinated monkeys [124–126]. Intriguingly, most SIV-specific CD8 T cell responses elicited by the vaccine recognized MHC-II-restricted epitopes [89]. The mechanisms leading to elicitation of unconventional immune responses in all vaccinated Monkeys, their potential role in the clearance of infection in 50% of monkeys are still unknown. Finally the presence of dominant immune responses with limited antiviral capacity and the association between subdominant immune responses and lower viral load in HIV-infected persons [127] support the hypothesis that breaking natural

immunodominance may enhance the efficacy of HIV vaccines [128]. As both attenuated CMV vectors and adenoviral vectors expressed complete SIV or HIV proteins, breaking immunodominance could be accomplished through the use of specific viral vectors. However a better understanding of the effect of vectors on epitope presentation and priming is required. Factors shaping immunodominance in various viral infections include—alone or in combination—kinetics of processing and presentation of epitopes, affinity for HLA or the TCR and the TCR repertoire [49,53,129–132]. The identification and fine mapping of HIV-specific naïve and memory CD4 T cell helper responses in unexposed donors showed that 83% of epitopes share homologies with microbial organisms (which may have primed these preexisting HIV-specific responses). These intriguing results suggest that the immune repertoire prior to HIV infection may contribute to shaping immunodominance of HIV immune responses during infection [133].

Breaking immunodominance could be accomplished through different approaches. Eliminating known immunodominant epitopes through deletions or mutations preventing presentation [134], or limiting the immunogen to portions of HIV proteins assembled in a chimeric protein [135] broke natural immunodominance and led to different hierarchies of immune responses after vaccination. These immunogens did not prevent establishment of infection but offered partial protection after challenge with a Vaccinia virus-derived vector expressing HIV in a mouse model [134]. Another approach to modify immunogens, successfully used to shift immunodominance in other viral infections in mice is to introduce mutations in region flanking epitopes so as to increase the production of some epitopes and decrease the production of others [136–141]. The introduction of cleavable or poorly cleavable motifs around HIV epitopes increased or decreased epitope processing by 10- to 100-fold and could be used to optimize epitope presentation [47,53]. In the absence of better understanding of protective immune responses the benefit of these approaches is still limited but they provide ways to test and modify epitope production and presentation and to refine the design of vaccine immunogen before *in vivo* validation.

The high variability of HIV in the infected population and across clades may require either the design of vaccines specific for clades or to focus the immune responses on the most conserved areas of the virus [115]. The emergence of escape mutations in acute HIV infection is largely predictable for many HLA which can be exploited in vaccine strategies. If vaccines elicit immune responses not only against consensus HIV sequences but also against frequent HLA-restricted mutants this will create additional pressure on the virus that will be forced to evolve toward variants with low replicative capacity. Mosaic immunogens made of a combination of distinct immunogens containing either HIV consensus sequences of Gag, Pol, Env (mosaic 1) or sequences carrying increasing number of frequent mutations (mosaic 2 or 3) have been computationally engineered and inserted into adenoviral vectors [142]. These mosaic vectors used in prime boost combinations elicited SIV-specific CD4 and CD8 T cell and antibody responses, and significantly reduced the per-exposure risk of acquisition of SIV [143]. Whether mutations introduced in mosaic 2 may alter immunogen degradation and lead to the presentation of new epitopes is not known but may broaden immune responses after vaccination. The opposite and complementary approach to the mosaic is the design of immunogens limited to the most conserved areas of several HIV proteins and when needed the most frequent variant of the sequence so as to cover >98% of HIV sequences [135,144,145]. Conserved sequences constitute vulnerable areas of the virus that can be identified in a linear fashion by sequence comparison in cohorts of HIV-infected persons [146], or as

sectors of HIV proteins that coevolve at multiple sites under a given HLA pressure [73,147]. Peptides corresponding to conserved areas can be assembled in a chimeric protein by addition of linkers that do not create new epitopes based on the presence of potential anchors but introduce efficient cleavage sites for liberation of HIV fragments. These immunogens used in DNA prime/boost vaccination elicited CD4, CD8 T cell and antibodies responses in mice and Macaques and will eventually be tested in clinical trials [148,149]. Alternatively, peptides from conserved areas of HIV proteins may be used in peptide-based vaccines where peptides and adjuvants are electroporated [150] or carried to lymph nodes by nanoparticles [151]. In addition to conserved and variable areas of HIV proteins, cryptic epitopes generated from alternate reading frames could potentially be included in HIV immunogens, provided that immune responses against these epitopes are shown to contribute to reducing viral load.

The choice of vectors and adjuvants and the specific subset of dendritic cells endocytosing the vaccine and could also alter conditions in which the peptides are processed [119,152–154]. Adjuvants such as CpG, TLR ligands will trigger changes in hydrolytic activities of endolysosomal peptidases, epitope production and presentation, and possibly affect priming of immune responses [155–157]. Virus-derived vectors such as adenovirus or CMV could elicit or recall T cell immunity against these viruses and may alter the overall hierarchy of immune responses against the immunogen after vaccination. Replication-competent viruses used as persistent vectors might interact with the antigen processing machinery and possibly affect production of epitopes. The elicitation of MHC-II-restricted CD8 T cell responses by attenuated CMV vectors expressing SIV antigens in vaccinated monkeys sheds light on our limited understanding of conditions established by vectors for priming of immune responses but open new avenues to manipulate immunodominance and immunity during vaccination [158].

Therapeutic vaccines aiming at clearing or substantially reducing HIV infection is urgently needed to replace lifelong treatment of the HIV-infected population. One approach consists in combining reactivation of HIV provirus with drugs such as HDAC inhibitors with vaccines boosting HIV immune responses in HIV-infected persons receiving ART [159,160]. Latent infection of CD4 T cells, provirus reactivation and ART might create unique conditions for the processing and presentation of HIV epitopes. Defining epitopes presented in the context of latency (if any) and of reactivation will be necessary to better define epitopes and corresponding immune responses that should be boosted by therapeutic vaccines.

Further studies are needed to identify protective immune responses for prophylactic and therapeutic vaccines, specifically with regards to epitope specificity covering various HLA, ratio or phenotypes of CD4 and CD8 T cell responses, and how to specifically induce them during vaccination. Guiding principles such as encompassing viral diversity or focusing on conserved areas, adequate matching epitope presentation between infected cells and DC receiving vaccines are defined, and multiple tools to study epitope production and immune responses are available. Regardless of the vector or adjuvants used for vaccination, the HIV immunogen will have to be processed in professional antigen presenting cells for the priming of immune responses. It is necessary to ensure that—in the context established by the specific vaccination strategies discussed above—this HIV immunogen will be properly degraded into MHC-I and MHC-II epitopes corresponding to sustainable protective immune responses able to recognize infected cells. Assays to follow protein degradation into epitopes and motifs to optimize epitope provide a way to test epitope production from vaccine immunogens before larger studies in

animal models and clinical trials, and guidelines to the design of immunogens leading to optimized epitope presentation.

Acknowledgments

The authors acknowledge financial support from NIAID R01 A1084753, R01 A1084106 and R01 AI112493 and thank Matthew Berberich for critical reading the manuscript. Jens Dinter is a Ph.D. student supported by a fellowship from the Ernst-Schering-Foundation.

Conflicts of Interest

The authors declare no conflict of interest.

References

1. Blum, J.S.; Wearsch, P.A.; Cresswell, P. Pathways of antigen processing. *Annu. Rev. Immunol.* **2013**, *31*, 443–473.
2. Yewdell, J.W. Plumbing the sources of endogenous MHC class I peptide ligands. *Curr. Opin. Immunol.* **2007**, *19*, 79–86.
3. Besche, H.C.; Peth, A.; Goldberg, A.L. Getting to first base in proteasome assembly. *Cell* **2009**, *138*, 25–28.
4. Kisselev, A.F.; Callard, A.; Goldberg, A.L. Importance of the different proteolytic sites of the proteasome and the efficacy of inhibitors varies with the protein substrate. *J. Biol. Chem.* **2006**, *281*, 8582–8590.
5. Khan, S.; van den Broek, M.; Schwarz, K.; de Giuli, R.; Diener, P.A.; Groettrup, M. Immunoproteasomes largely replace constitutive proteasomes during an antiviral and antibacterial immune response in the liver. *J. Immunol.* **2001**, *167*, 6859–6868.
6. Griffin, T.A.; Nandi, D.; Cruz, M.; Fehling, H.J.; Kaer, L.V.; Monaco, J.J.; Colbert, R.A. Immunoproteasome assembly: Cooperative incorporation of interferon gamma (IFN-gamma)-inducible subunits. *J. Exp. Med.* **1998**, *187*, 97–104.
7. Kisselev, A.; Akopian, T.; Woo, K.M.; Goldberg, A.L. The sizes of peptides generated from protein by mammalian 26 and 20 S proteasomes. Implications for understanding the degradative mechanism and antigen presentation. *J. Biol. Chem.* **1999**, *274*, 3363–3371.
8. Emmerich, N.P.; Nussbaum, A.K.; Stevanovic, S.; Priemer, M.; Toes, R.E.; Rammensee, H.G.; Schild, H. The human 26 S and 20S proteasomes generate overlapping but different sets of peptide fragments from a model protein substrate. *J. Biol. Chem.* **2000**, *275*, 21140–21148.
9. Cascio, P.; Hilton, C.; Kisselev, A.F.; Rock, K.L.; Goldberg, A. 26S proteasomes and immunoproteasomes produce mainly N-extended versions of an antigenic peptide. *EMBO J.* **2001**, *20*, 2357–2366.
10. Zanker, D.; Waithman, J.; Yewdell, J.W.; Chen, W. Mixed proteasomes function to increase viral peptide diversity and broaden antiviral CD8+ T cell responses. *J. Immunol.* **2013**, *191*, 52–59.
11. Kawahara, M.; York, I.A.; Hearn, A.; Farfan, D.; Rock, K.L. Analysis of the role of tripeptidyl peptidase II in MHC class I antigen presentation *in vivo*. *J. Immunol.* **2009**, *183*, 6069–6077.

12. Seifer, U.; Maranon, C.; Shmueli, A.; Desoutter, J.F.; Wesoloski, L.; Janek, K.; Henklein, P.; Diescher, S.; Andrieu, M.; de la Salle, H.; *et al.* An essential role for tripeptidyl peptidase in the generation of an MHC class I epitope. *Nat. Immunol.* **2003**, *4*, 375–379.
13. Saric, T.; Beninga, J.; Graef, C.I.; Akopian, T.; Rock, K.L.; Goldberg, A.L. Major histocompatibility complex class I-presented antigenic peptides are degraded in cytosolic extracts primarily by thimet oligopeptidase. *J. Biol. Chem.* **2001**, *276*, 36474–36481.
14. Saric, T.; Graef, C.I.; Goldberg, A.L. Pathway for degradation of peptides generated by proteasomes: A key role for thimet oligopeptidase and other metallopeptidases. *J. Biol. Chem.* **2004**, *279*, 46723–46732.
15. York, I.A.; Mo, A.X.Y.; Lemerise, K.; Zeng, W.; Shen, Y.; Abraham, C.R.; Saric, T.; Goldberg, A.; Rock, K.L. The cytosolic endopeptidase, thimet oligopeptidase, destroys antigenic peptides and limits the extent of MHC class I antigen presentation. *Immunity* **2003**, *18*, 429–440.
16. Towne, C.F.; York, I.A.; Neijssen, J.; Karow, M.L.; Murphy, A.J.; Valenzuela, D.M.; Yancopoulos, G.D.; Neefjes, J.J.; Rock, K.L. Puromycin-sensitive aminopeptidase limits MHC class I presentation in dendritic cells but does not affect CD8 T cell responses during viral infections. *J. Immunol.* **2008**, *180*, 1704–1712.
17. Towne, C.F.; York, I.A.; Watkin, L.B.; Lazo, J.S.; Rock, K.L. Analysis of the role of bleomycin hydrolase in antigen presentation and the generation of CD8 T cell responses. *J. Immunol*. **2007**, *178*, 6923–6930.
18. Parmentier, N.; Stroobant, V.; Colau, D.; de Diesbach, P.; Morel, S.; Chapiro, J.; van Endert, P.; van den Eynde, B.J. Production of an antigenic peptide by insulin-degrading enzyme. *Nat. Immunol.* **2010**, *11*, 449–454.
19. Kessler, J.H.; Khan, S.; Seifert, U.; le Gall, S.; Chow, K.M.; Paschen, A.; Bres-Vloemans, S.A.; de Ru, A.; van Montfoort, N.; Franken, K.L.; *et al.* Antigen processing by nardilysin and thimet oligopeptidase generates cytotoxic T cell epitopes. *Nat. Immunol.* **2011**, *12*, 45–53.
20. York, I.A.; Bhutani, N.; Zendzian, S.; Goldberg, A.L.; Rock, K.L. Tripeptidyl Peptidase II Is the Major Peptidase Needed to Trim Long Antigenic Precursors, but Is Not Required for Most MHC Class I Antigen Presentation. *J. Immunol.* **2006**, *177*, 1434–1443.
21. York, I.A.; Chang, S.C.; Saric, T.; Keys, J.A.; Favreau, J.M.; Goldberg, A.; Rock, K.L. The ER aminopeptidase ERAPI enhances or limits antigen presentation by trimming epitopes to 8–9 residues. Nat. Immunol. **2002**, *3*, 1177–1184.
22. Reits, E.; Neijssen, J.; Herberts, C.; Benckhuijsen, W.; Janssen, L.; Drijfhout, J.W.; Neefjes, J. A major role for TPPII in trimming proteasomal degradation products for MHC class I antigen presentation. *Immunity* **2004**, *20*, 495–506.
23. Rock, K.L.; York, I.A.; Goldberg, A.L. Post-proteasomal antigen processing for major histocompatibility complex class I presentation. *Nat. Immunol.* **2004**, *5*, 670–677.
24. Saveanu, L.; Carroll, O.; Hassainya, Y.; van Endert, P. Complexity, contradictions, and conundrums: Studying post-proteasomal proteolysis in HLA class I antigen presentation. *Immunol. Rev.* **2005**, *207*, 42–59.
25. Portaro, F.C.; Gomes, M.D.; Cabrera, A.; Fernandes, B.L.; Silva, C.L.; Ferro, E.S.; Juliano, L.; de Camargo, A.C. Thimet oligopeptidase and the stability of MHC class I epitopes in macrophage cytosol. *Biochem. Biophys. Res. Commun.* **1999**, *255*, 596–601.

26. Lauvau, G.; Kakimi, K.; Niedermann, G.; Ostankovitch, M.; Yotnda, P.; Firat, H.; Chisari, F.V.; van Endert, P.M. Human transporters associated with antigen processing (TAPs) select epitope precursor peptides for processing in the endoplasmic reticulum and presentation to T cells. *J. Exp. Med.* **1999**, *190*, 1227–1240.
27. Serwold, T.; Gaw, S.; Shastri, N. ER aminopeptidases generate a unique pool of peptides for MHC class I molecules. *Nat. Immunol.* **2001**, *2*, 644–651.
28. Serwold, T.; Gonzalez, F.; Kim, J.; Jacob, R.; Shastri, N. ERAAP customizes peptides for MHC class I molecules in the endoplasmic reticulum. *Nature* **2002**, *419*, 480–483.
29. Kanaseki, T.; Blanchard, N.; Hammer, G.E.; Gonzalez, F.; Shastri, N. ERAAP synergizes with MHC class I molecules to make the final cut in the antigenic peptide precursors in the endoplasmic reticulum. *Immunity* **2006**, *25*, 795–806.
30. Saveanu, L.; Carroll, O.; Lindo, V.; Del Val, M.; Lopez, D.; Lepelletier, Y.; Greer, F.; Schomburg, L.; Fruci, D.; Niedermann, G.; *et al.* Concerted peptide trimming by human ERAP1 and ERAP2 aminopeptidase complexes in the endoplasmic reticulum. *Nat. Immunol.* **2005**, *6*, 689–697.
31. Beers, C.; Burich, A.; Kleijmeer, M.J.; Griffith, J.M.; Wong, P.; Rudensky, A.Y. Cathepsin S controls MHC class II-mediated antigen presentation by epithelial cells *in vivo*. *J. Immunol.* **2005**, *174*, 1205–1212.
32. Riese, R.J.; Mitchell, R.N.; Villadangos, J.A.; Shi, G.P.; Palmer, J.T.; Karp, E.R.; de Sanctis, G.T.; Ploegh, H.L.; Chapman, H.A. Cathepsin S activity regulates antigen presentation and immunity. *J. Clin. Investig.* **1998**, *101*, 2351–2363.
33. Saveanu, L.; Carroll, O.; Weimershaus, M.; Guermonprez, P.; Firat, E.; Lindo, V.; Greer, F.; Davoust, J.; Kratzer, R.; Keller, S.R.; *et al.* IRAP identifies an endosomal compartment required for MHC class I cross-presentation. *Science* **2009**, *325*, 213–217.
34. Watts, C. The endosome-lysosome pathway and information generation in the immune system. *Biochim. Biophys. Acta* **2012**, *1824*, 14–21.
35. Segura, E.; Villadangos, J.A. A modular and combinatorial view of the antigen cross-presentation pathway in dendritic cells. *Traffic* **2011**, *12*, 1677–1685.
36. Lazaro, E.; Kadie, C.; Stamegna, P.; Zhang, S.C.; Gourdain, P.; Lai, N.Y.; Zhang, M.; Martinez, S.M.; Heckerman, D.; le Gall, S. Variable HIV peptide stability in human cytosol is critical to epitope presentation and immune escape. *J. Clin. Investig.* **2011**, *121*, 2480–2492.
37. Herberts, C.A.; Neijssen, J.J.; de Haan, J.; Janssen, L.; Drijfhout, J.W.; Reits, E.A.; Neefjes, J.J. Cutting edge: HLA-B27 acquires many N-terminal dibasic peptides: Coupling cytosolic peptide stability to antigen presentation. *J. Immunol.* **2006**, *176*, 2697–2701.
38. Schnurr, M.; Chen, Q.; Shin, A.; Chen, W.; Toy, T.; Jenderek, C.; Green, S.; Miloradovic, L.; Drane, D.; Davis, I.D.; *et al.* Tumor antigen processing and presentation depend critically on dendritic cell type and the mode of antigen delivery. *Blood* **2005**, *105*, 2465–2472.
39. Tsomides, T.J.; Aldovini, A.; Johnson, R.P.; Walker, B.D.; Young, R.A.; Eisen, H.N. Naturally processed viral peptides recognized by cytotoxic T lymphocytes on cells chronically infected by human immunodeficiency virus type 1. *J. Exp. Med.* **1994**, *180*, 1283–1293.

40. Hickman, H.D.; Luis, A.D.; Bardet, W.; Buchli, R.; Battson, C.L.; Shearer, M.H.; Jackson, K.W.; Kennedy, R.C.; Hildebrand, W.H. Cutting edge: Class I presentation of host peptides following HIV infection. *J. Immunol.* **2003**, *171*, 22–26.
41. Bozzacco, L.; Yu, H.; Dengjel, J.; Trumpfheller, C.; Zebroski, H.A., 3rd; Zhang, N.; Kuttner, V.; Ueberheide, B.M.; Deng, H.; Chait, B.T.; *et al.* Strategy for identifying dendritic cell-processed CD4+ T cell epitopes from the HIV gag p24 protein. *PLoS One* **2012**, *7*, e41897.
42. Cardinaud, S.; Moris, A.; Fevrier, M.; Rohrlich, P.S.; Weiss, L.; Langlade-Demoyen, P.; Lemonnier, F.A.; Schwartz, O.; Habel, A. Identification of cryptic MHC I-restricted epitopes encoded by HIV-1 alternative reading frames. *J. Exp. Med.* **2004**, *199*, 1053–1063.
43. Bansal, A.; Carlson, J.; Yan, J.; Akinsiku, O.T.; Schaefer, M.; Sabbaj, S.; Bet, A.; Levy, D.N.; Heath, S.; Tang, J.; *et al.* CD8 T cell response and evolutionary pressure to HIV-1 cryptic epitopes derived from antisense transcription. *J. Exp. Med.* **2010**, *207*, 51–59.
44. Berger, C.T.; Carlson, J.M.; Brumme, C.J.; Hartman, K.L.; Brumme, Z.L.; Henry, L.M.; Rosato, P.C.; Piechocka-Trocha, A.; Brockman, M.A.; Harrigan, P.R.; *et al.* Viral adaptation to immune selection pressure by HLA class I-restricted CTL responses targeting epitopes in HIV frameshift sequences. *J. Exp. Med.* **2010**, *207*, 61–75.
45. Cardinaud, S.; Consiglieri, G.; Bouziat, R.; Urrutia, A.; Graff-Dubois, S.; Fourati, S.; Malet, I.; Guergnon, J.; Guihot, A.; Katlama, C.; *et al.* CTL escape mediated by proteasomal destruction of an HIV-1 cryptic epitope. *PLoS Pathog.* **2011**, *7*, e1002049.
46. Lucchiari-Hartz, M.; Lindo, V.; Hitziger, N.; Gaedicke, S.; Saveanu, L.; van Endert, P.M.; Greer, F.; Eichmann, K.; Niederman, G. Differential proteasomal processing of hydrophobic and hydrophilic protein regions: Contribution to cytotoxic T lymphocyte epitope clustering in HIV-1-Nef. *Proc. Natl. Acad. Sci. USA* **2003**, *100*, 7755–7760.
47. Steers, N.J.; Currier, J.R.; Jobe, O.; Tovanabutra, S.; Ratto-Kim, S.; Marovich, M.A.; Kim, J.H.; Michael, N.L.; Alving, C.R.; Rao, M. Designing the epitope flanking regions for optimal generation of CTL epitopes. *Vaccine* **2014**, *32*, 3509–3516.
48. Steers, N.J.; Currier, J.R.; Kijak, G.H.; di Targiani, R.C.; Saxena, A.; Marovich, M.A.; Kim, J.H.; Michael, N.L.; Alving, C.R.; Rao, M. Cell type-specific proteasomal processing of HIV-1 Gag-p24 results in an altered epitope repertoire. *J. Virol.* **2011**, *85*, 1541–1553.
49. Tenzer, S.; Wee, E.; Burgevin, A.; Stewart-Jones, G.; Friis, L.; Lamberth, K.; Chang, C.H.; Harndahl, M.; Weimershaus, M.; Gerstoft, J.; *et al.* Antigen processing influences HIV-specific cytotoxic T lymphocyte immunodominance. *Nat. Immunol.* **2009**, *10*, 636–646.
50. Tenzer, S.; Crawford, H.; Pymm, P.; Gifford, R.; Sreenu, V.B.; Weimershaus, M.; de Oliveira, T.; Burgevin, A.; Gerstoft, J.; Akkad, N.; *et al.* HIV-1 Adaptation to Antigen Processing Results in Population-Level Immune Evasion and Affects Subtype Diversification. *Cell Rep.* **2014**, *7*, 448–463.
51. Steers, N.J.; Ratto-Kim, S.; de Souza, M.S.; Currier, J.R.; Kim, J.H.; Michael, N.L.; Alving, C.R.; Rao, M. HIV-1 envelope resistance to proteasomal cleavage: Implications for vaccine induced immune responses. *PLoS One* **2012**, *7*, e42579.

52. Tenzer, S.; Peters, B.; Bulik, S.; Schoor, O.; Lemmel, C.; Schatz, M.M.; Kloetzel, P.M.; Rammensee, H.G.; Schild, H.; Holzhutter, H.G. Modeling the MHC class I pathway by combining predictions of proteasomal cleavage, TAP transport and MHC class I binding. *Cell Mol. Life Sci.* **2005**, *62*, 1025–1037.
53. Le Gall, S.; Stamegna, P.; Walker, B.D. Portable flanking sequences modulate CTL epitope processing. *J. Clin. Investig.* **2007**, *117*, 3563–3575.
54. Lazaro, E.; Godfrey, S.B.; Stamegna, P.; Ogbechie, T.; Kerrigan, C.; Zhang, M.; Walker, B.D.; le Gall, S. Differential HIV epitope processing in monocytes and CD4 T cells affects cytotoxic T lymphocyte recognition. *J. Infect. Dis.* **2009**, *200*, 236–243.
55. Zhang, S.C.; Martin, E.; Shimada, M.; Godfrey, S.B.; Fricke, J.; Locastro, S.; Lai, N.Y.; Liebesny, P.; Carlson, J.M.; Brumme, C.J.; *et al.* Aminopeptidase Substrate Preference Affects HIV Epitope Presentation and Predicts Immune Escape Patterns in HIV-Infected Individuals. *J. Immunol.* **2012**, *188*, 5924–5934.
56. Draenert, R.; Brander, C.; Yu, X.G.; Altfeld, M.; Verrill, C.L.; Feeney, M.E.; Walker, B.D.; Goulder, P.J. Impact of intrapeptide epitope location on CD8 T cell recognition: Implications for design of overlapping peptide panels. *Aids* **2004**, *18*, 871–876.
57. Vaithilingam, A.; Lai, N.Y.; Duong, E.; Boucau, J.; Xu, Y.; Shimada, M.; Gandhi, M.; le Gall, S. A simple methodology to assess endolysosomal protease activity involved in antigen processing in human primary cells. *BMC Cell Biol.* **2013**, *14*, 35.
58. Chatterjee, B.; Smed-Sorensen, A.; Cohn, L.; Chalouni, C.; Vandlen, R.; Lee, B.C.; Widger, J.; Keler, T.; Delamarre, L.; Mellman, I. Internalization and endosomal degradation of receptor-bound antigens regulate the efficiency of cross presentation by human dendritic cells. *Blood* **2012**, *120*, 2011–2020.
59. Cohn, L.; Chatterjee, B.; Esselborn, F.; Smed-Sorensen, A.; Nakamura, N.; Chalouni, C.; Lee, B.C.; Vandlen, R.; Keler, T.; Lauer, P.; *et al.* Antigen delivery to early endosomes eliminates the superiority of human blood BDCA3+ dendritic cells at cross presentation. *J. Exp. Med.* **2013**, *210*, 1049–1063.
60. Kawashima, Y.; Pfafferott, K.; Frater, J.; Matthews, P.; Payne, R.; Addo, M.; Gatanaga, H.; Fujiwara, M.; Hachiya, A.; Koizumi, H.; *et al.* Adaptation of HIV-1 to human leukocyte antigen class I. *Nature* **2009**, *458*, 641–645.
61. Bartha, I.; Carlson, J.M.; Brumme, C.J.; McLaren, P.J.; Brumme, Z.L.; John, M.; Haas, D.W.; Martinez-Picado, J.; Dalmau, J.; Lopez-Galindez, C.; *et al.* A genome-to-genome analysis of associations between human genetic variation, HIV-1 sequence diversity, and viral control. *Elife* **2013**, *2*, e01123.
62. Karlsson, A.C.; Iversen, A.K.; Chapman, J.M.; de Oliviera, T.; Spotts, G.; McMichael, A.J.; Davenport, M.P.; Hecht, F.M.; Nixon, D.F. Sequential broadening of CTL responses in early HIV-1 infection is associated with viral escape. *PLoS One* **2007**, *2*, e225.
63. Allen, T.M.; Altfeld, M.; Geer, S.C.; Kalife, E.T.; Moore, C.; O'Sullivan K.M.; Desouza, I.; Feeney, M.E.; Eldridge, R.L.; Maier, E.L.; *et al.* Selective escape from CD8+ T-cell responses represents a major driving force of human immunodeficiency virus type 1 (HIV-1) sequence diversity and reveals constraints on HIV-1 evolution. *J. Virol.* **2005**, *79*, 13239–13249.

64. Kiepiela, P.; Leslie, A.J.; Honeyborne, I.; Ramduth, D.; Thobakgale, C.; Chetty, S.; Rathnavalu, P.; Moore, C.; Pfafferott, K.J.; Hilton, L.; *et al.* Dominant influence of HLA-B in mediating the potential co-evolution of HIV and HLA. *Nature* **2004**, *432*, 769–775.
65. Boutwell, C.L.; Rolland, M.M.; Herbeck, J.T.; Mullins, J.I.; Allen, T.M. Viral evolution and escape during acute HIV-1 infection. *J. Infect. Dis.* **2010**, *202*, S309–S314.
66. Goulder, P.J.; Watkins, D.I. HIV and SIV CTL escape: Implications for vaccine design. *Nat. Rev. Immunol.* **2004**, *4*, 630–640.
67. Leslie, A.J.; Pfafferott, K.J.; Chetty, P.; Draenert, R.; Addo, M.M.; Feeney, M.; Tang, Y.; Holmes, E.C.; Allen, T.; Prado, J.G.; *et al.* HIV evolution: CTL escape mutation and reversion after transmission. *Nat. Med.* **2004**, *10*, 282–289.
68. Kelleher, A.D.; Long, C.; Hiolmes, E.C.; Allen, R.L.; Wilson, J.; Conlon, C.; Workman, C.; Shaunak, S.; Olson, K.; Goulder, P.J.; *et al.* Clustered mutations in HIV-1 gag are consistently required for escape from HLA-B27-restricted cytotoxic T lymphocyte responses. *J. Exp. Med.* **2001**, *193*, 375–386.
69. Brockman, M.A.; Schneidewind, A.; Lahaie, M.; Schmidt, A.; Miura, T.; Desouza, I.; Ryvkin, F.; Derdeyn, C.A.; Allen, S.; Hunter, E.; *et al.* Escape and compensation from early HLA-B57-mediated cytotoxic T-lymphocyte pressure on human immunodeficiency virus type 1 Gag alter capsid interactions with cyclophilin A. *J. Virol.* **2007**, *81*, 12608–12618.
70. Crawford, H.; Prado, J.G.; Leslie, A.; Hue, S.; Honeyborne, I.; Reddy, S.; van der Stok, M.; Mncube, Z.; Brander, C.; Rousseau, C.; *et al.* Compensatory mutation partially restores fitness and delays reversion of escape mutation within the immunodominant HLA-B*5703-restricted Gag epitope in chronic human immunodeficiency virus type 1 infection. *J. Virol.* **2007**, *81*, 8346–8351.
71. Goepfert, P.A.; Lumm, W.; Farmer, P.; Matthews, P.; Prendergast, A.; Carlson, J.M.; Derdeyn, C.A.; Tang, J.; Kaslow, R.A.; Bansal, A.; *et al.* Transmission of HIV-1 Gag immune escape mutations is associated with reduced viral load in linked recipients. *J. Exp. Med.* **2008**, *205*, 1009–1017.
72. Troyer, R.M.; McNevin, J.; Liu, Y.; Zhang, S.C.; Krizan, R.W.; Abraha, A.; Tebit, D.M.; Zhao, H.; Avila, S.; Lobritz, M.A.; *et al.* Variable fitness impact of HIV-1 escape mutations to cytotoxic T lymphocyte (CTL) response. *PLoS Pathog.* **2009**, *5*, e1000365.
73. Rolland, M.; Carlson, J.M.; Manocheewa, S.; Swain, J.V.; Lanxon-Cookson, E.; Deng, W.; Rousseau, C.M.; Raugi, D.N.; Learn, G.H.; Maust, B.S.; *et al.* Amino-acid co-variation in HIV-1 Gag subtype C: HLA-mediated selection pressure and compensatory dynamics. *PLoS One* **2010**, *5*, doi:10.1371/journal.pone.0012463.
74. Iversen, A.K.; Stewart-Jones, G.; Learn, G.H.; Christie, N.; Sylvester-Hviid, C.; Armitage, A.E.; Kaul, R.; Beattie, T.; Lee, J.K.; Li, Y.; *et al.* Conflicting selective forces affect T cell receptor contacts in an immunodominant human immunodeficiency virus epitope. *Nat. Immunol.* **2006**, *7*, 179–189.
75. Jones, N.A.; Wei, X.; Flower, D.R.; Wong, M.; Michor, F.; Saag, M.S.; Hahn, B.H.; Nowak, M.A.; Shaw, G.M.; Borrow, P. Determinants of human immunodeficiency virus type 1 escape from the primary CD8+ cytotoxic T lymphocyte response. *J. Exp. Med.* **2004**, *200*, 1243–1256.

76. Allen, T.M.; Altfeld, M.; Yu, X.G.; O'Sullivan, K.M.; Lichterfeld, M.; le Gall, S.; John, M.; Mothe, B.R.; Lee, P.K.; Kalife, E.T.; *et al.* Selection, transmission, and reversion of an antigen-processing cytotoxic T-lymphocyte escape mutation in human immunodeficiency virus type 1 infection. *J. Virol.* **2004**, *78*, 7069–7078.
77. Draenert, R.; le Gall, S.; Pfafferott, K.J.; Alasdair, L.J.; Chetty, P.; Brander, C.; Holmes, E.C.; Chang, S.C.; Feeney, M.E.; Addo, M.M.; *et al.* Immune selection for altered antigen processing leads to cytotoxic T lymphocyte escape in chronic HIV-1 infection. *J. Exp. Med.* **2004**, *199*, 905–915.
78. Kimura, Y.; Gushima, T.; Rawale, S.; Kaumaya, P.; Walker, C.M. Escape mutations alter proteasome processing of major histocompatibility complex class I-restricted epitopes in persistent hepatitis C virus infection. *J. Virol.* **2005**, *79*, 4870–4876.
79. Yokomaku, Y.; Miura, H.; Tomiyama, H.; Kawana-Tachikawa, A.; Takiguchi, M.; Kojima, A.; Nagai, Y.; Iwamoto, A.; Matsuda, Z.; Ariyoshi, K. Impaired processing and presentation of cytotoxic-T-lymphocyte (CTL) epitopes are major escape mechanisms from CTL immune pressure in human immunodeficiency virus type 1 infection. *J. Virol.* **2004**, *78*, 1324–1332.
80. Milicic, A.; Price, D.A.; Zimbwa, P.; Booth, B.L.; Brown, H.L.; Easterbrook, P.J.; Olsen, K.; Robinson, N.; Gileadi, U.; Sewell, A.K.; *et al.* CD8+ T cell epitope-flanking mutations disrupt proteasomal processing of HIV-1 Nef. *J. Immunol.* **2005**, *175*, 4618–4626.
81. Hearn, A.; York, I.A.; Bishop, C.; Rock, K.L. Characterizing the specificity and cooperation of aminopeptidases in the cytosol and endoplasmic reticulum during MHC class I antigen presentation. *J. Immunol.* **2010**, *184*, 4725–4732.
82. Schatz, M.M.; Peters, B.; Akkad, N.; Ullrich, N.; Martinez, A.N.; Carroll, O.; Bulik, S.; Rammensee, H.G.; van Endert, P.; Holzhutter, H.G.; *et al.* Characterizing the N-terminal processing motif of MHC class I ligands. *J. Immunol.* **2008**, *180*, 3210–3217.
83. Le Gall, S. MHC-I-restricted HIV epitope processing, immune control and immunogen design. *HIV Ther. Future Med.* **2010**, *4*, 101–117.
84. Hakenberg, J.; Nussbaum, A.K.; Schild, H.; Rammensee, H.G.; Kuttler, C.; Holzhutter, H.G.; Kloetzel, P.M.; Kaufmann, S.H.; Mollenkopf, H.J. MAPPP: MHC class I antigenic peptide processing prediction. *Appl. Bioinform.* **2003**, *2*, 155–158.
85. Saxova, P.; Buus, S.; Brunak, S.; Kesmir, C. Predicting proteasomal cleavage sites: A comparison of available methods. *Int. Immunol.* **2003**, *15*, 781–787.
86. Nussbaum, A.K.; Kuttler, C.; Hadeler, K.P.; Rammensee, H.G.; Schild, H. PAProC: A prediction algorithm for proteasomal cleavages available on the WWW. *Immunogenetics* **2001**, *53*, 87–94.
87. Kuttler, C.; Nussbaum, A.K.; Dick, T.P.; Rammensee, H.G.; Schild, H.; Hadeler, K.P. An algorithm for the prediction of proteasomal cleavages. *J. Mol. Biol.* **2000**, *298*, 417–429.
88. Sette, A.; Newman, M.; Livingston, B.; McKinney, D.; Sidney, J.; Ishioka, G.; Tangri, S.; Alexander, J.; Fikes, J.; Chesnut, R. Optimizing vaccine design for cellular processing, MHC binding and TCR recognition. *Tissue Antigens* **2002**, *59*, 443–451.
89. Hansen, S.G.; Sacha, J.B.; Hughes, C.M.; Ford, J.C.; Burwitz, B.J.; Scholz, I.; Gilbride, R.M.; Lewis, M.S.; Gilliam, A.N.; Ventura, A.B.; *et al.* Cytomegalovirus vectors violate CD8+ T cell epitope recognition paradigms. *Science* **2013**, *340*, 1237874.

90. Nielsen, M.; Lund, O.; Buus, S.; Lundegaard, C. MHC class II epitope predictive algorithms. *Immunology* **2010**, *130*, 319–328.
91. Nielsen, M.; Lundegaard, C.; Lund, O. Prediction of MHC class II binding affinity using SMM-align, a novel stabilization matrix alignment method. *BMC Bioinform.* **2007**, *8*, 238.
92. Jorgensen, K.W.; Buus, S.; Nielsen, M. Structural properties of MHC class II ligands, implications for the prediction of MHC class II epitopes. *PLoS One* **2010**, *5*, e15877.
93. Mohammadi, P.; Desfarges, S.; Bartha, I.; Joos, B.; Zangger, N.; Munoz, M.; Gunthard, H.F.; Beerenwinkel, N.; Telenti, A.; Ciuffi, A. 24 hours in the life of HIV-1 in a T cell line. *PLoS Pathog.* **2013**, *9*, e1003161.
94. Beninga, J.; Rock, K.L.; Goldberg, A. Interferon-gamma can stimulate post-proteasomal trimming of the N terminus of an antigenic peptide by inducing leucine aminopeptidase. *J. Biol. Chem.* **1998**, *273*, 18734–18742.
95. Reis, J.; Guan, X.Q.; Kisselev, A.F.; Papasian, C.J.; Qureshi, A.A.; Morrison, D.C.; van Way, C.W., 3rd; Vogel, S.N.; Qureshi, N. LPS-induced formation of immunoproteasomes: TNF-alpha and nitric oxide production are regulated by altered composition of proteasome-active sites. *Cell Biochem. Biophys.* **2011**, *60*, 77–88.
96. Link, C.; Gavioli, R.; Ebensen, T.; Canella, A.; Reinhard, E.; Guzman, C.A. The Toll-like receptor ligand MALP-2 stimulates dendritic cell maturation and modulates proteasome composition and activity. *Eur. J. Immunol.* **2004**, *34*, 899–907.
97. Delamarre, L.; Holcombe, H.; Mellman, I. Presentation of exogenous antigens on major histocompatibility complex (MHC) class I and MHC class II molecules is differentially regulated during dendritic cell maturation. *J. Exp. Med.* **2003**, *198*, 111–122.
98. Crespo, M.I.; Zacca, E.R.; Nunez, N.G.; Ranocchia, R.P.; Maccioni, M.; Maletto, B.A.; Pistoresi-Palencia, M.C.; Moron, G. TLR7 triggering with polyuridylic acid promotes cross-presentation in CD8alpha+ conventional dendritic cells by enhancing antigen preservation and MHC class I antigen permanence on the dendritic cell surface. *J. Immunol.* **2013**, *190*, 948–960.
99. Gil-Torregrosa, B.C.; Lennon-Dumenil, A.M.; Kessler, B.; Guermonprez, P.; Ploegh, H.L.; Fruci, D.; van Endert, P.; Amigorena, S. Control of cross-presentation during dendritic cell maturation. *Eur. J. Immunol.* **2004**, *34*, 398–407.
100. Macagno, A.; Gilliet, M.; Sallusto, F.; Lanzavecchia, A.; Nestle, F.O.; Groettrup, M. Dendritic cells up-regulate immunoproteasomes and the proteasome regulator PA28 during maturation. *Eur. J. Immunol.* **1999**, *29*, 4037–4042.
101. Basler, M.; Youhnovski, N.; van Den Broek, M.; Przybylski, M.; Groettrup, M. Immunoproteasomes down-regulate presentation of a subdominant T cell epitope from lymphocytic choriomeningitis virus. *J. Immunol.* **2004**, *173*, 3925–3934.
102. Piccinini, M.; Mostert, M.; Rinaudo, M.T. Proteasomes as drug targets. *Curr. Drug Targets* **2003**, *4*, 657–671.
103. Piccinini, M.; Rinaudo, M.T.; Anselmino, A.; Buccinna, B.; Ramondetti, C.; Dematteis, A.; Ricotti, E.; Palmisano, L.; Mostert, M.; Tovo, P.A. The HIV protease inhibitors nelfinavir and saquinavir, but not a variety of HIV reverse transcriptase inhibitors, adversely affect human proteasome function. *Antivir. Ther.* **2005**, *10*, 215–223.

104. Piccinini, M.; Rinaudo, M.T.; Chiapello, N.; Ricotti, E.; Baldovino, S.; Mostert, M.; Tovo, P.A. The human 26S proteasome is a target of antiretroviral agents. *Aids* **2002**, *16*, 693–700.
105. Andre, P.; Groettrup, M.; Klenerman, P.; de Giuli, R.; Booth, B.L., Jr.; Cerundolo, V.; Bonneville, M.; Jotereau, F.; Zinkernagel, R.M.; Lotteau, V. An inhibitor of HIV-1 protease modulates proteasome activity, antigen presentation, and T cell responses. *Proc. Natl. Acad. Sci. USA* **1998**, *95*, 13120–13124.
106. Schmidtke, G.; Holzhutter, H.G.; Bogyo, M.; Kairies, N.; Groll, M.; de Giuli, R.; Emch, S.; Groettrup, M. How an inhibitor of the HIV-I protease modulates proteasome activity. *J. Biol. Chem.* **1999**, *274*, 35734–35740.
107. Kourjian, G.; Xu, Y.; Mondesire-Crump, I.; Shimada, M.; Gourdain, P.; le Gall, S. Sequence-Specific Alterations of Epitope Production by HIV Protease Inhibitors. *J. Immunol.* **2014**, *192*, 3496–3506.
108. Haorah, J.; Heilman, D.; Diekmann, C.; Osna, N.; Donohue, T.M., Jr.; Ghorpade, A.; Persidsky, Y. Alcohol and HIV decrease proteasome and immunoproteasome function in macrophages: Implications for impaired immune function during disease. *Cell Immunol.* **2004**, *229*, 139–148.
109. Tjomsland, V.; Ellegard, R.; Burgener, A.; Mogk, K.; Che, K.F.; Westmacott, G.; Hinkula, J.; Lifson, J.D.; Larsson, M. Complement opsonization of HIV-1 results in a different intracellular processing pattern and enhanced MHC class I presentation by dendritic cells. *Eur. J. Immunol.* **2013**, *43*, 1470–1483.
110. Larsson, M.; Fonteneau, J.F.; Lirvall, M.; Haslett, P.; Lifson, J.D.; Bhardwaj, N. Activation of HIV-1 specific CD4 and CD8 T cells by human dendritic cells: Roles for cross-presentation and non-infectious HIV-1 virus. *Aids* **2002**, *16*, 1319–1329.
111. Fonteneau, J.F.; Kavanagh, D.G.; Lirvall, M.; Sanders, C.; Cover, T.L.; Bhardwaj, N.; Larsson, M. Characterization of the MHC class I cross-presentation pathway for cell-associated antigens by human dendritic cells. *Blood* **2003**, *102*, 4448–4455.
112. Gavioli, R.; Gallerani, E.; Fortini, C.; Fabris, M.; Bottoni, A.; Canella, A.; Bonaccorsi, A.; Marastoni, M.; Micheletti, F.; Cafaro, A.; *et al.* HIV-1 tat protein modulates the generation of cytotoxic T cell epitopes by modifying proteasome composition and enzymatic activity. *J. Immunol.* **2004**, *173*, 3838–3843.
113. Burton, D.R.; Ahmed, R.; Barouch, D.H.; Butera, S.T.; Crotty, S.; Godzik, A.; Kaufmann, D.E.; McElrath, M.J.; Nussenzweig, M.C.; Pulendran, B.; *et al.* A Blueprint for HIV Vaccine Discovery. *Cell Host Microbe* **2012**, *12*, 396–407.
114. Picker, L.J.; Hansen, S.G.; Lifson, J.D. New paradigms for HIV/AIDS vaccine development. *Annu. Rev. Med.* **2012**, *63*, 95–111.
115. Stephenson, K.E.; Barouch, D.H. A global approach to HIV-1 vaccine development. *Immunol. Rev.* **2013**, *254*, 295–304.
116. Johnson, J.A.; Barouch, D.H.; Baden, L.R. Nonreplicating vectors in HIV vaccines. *Curr. Opin. HIV AIDS* **2013**, *8*, 412–420.
117. Parks, C.L.; Picker, L.J.; King, C.R. Development of replication-competent viral vectors for HIV vaccine delivery. *Curr. Opin. HIV AIDS* **2013**, *8*, 402–411.
118. Irvine, D.J.; Swartz, M.A.; Szeto, G.L. Engineering synthetic vaccines using cues from natural immunity. *Nat. Mater.* **2013**, *12*, 978–990.

119. Moody, M.A. Modulation of HIV-1 immunity by adjuvants. *Curr. Opin. HIV AIDS* **2014**, *9*, 242–249.
120. Altfeld, M.; Kalife, E.T.; Qi, Y.; Streeck, H.; Lichterfeld, M.; Johnston, M.N.; Burgett, N.; Swart, M.E.; Yang, A.; Alter, G.; *et al.* HLA class I alleles that contribute strongly to the initial CD8+ T cell responses against HIV-1 are associated with delayed progression to AIDS. *PLoS Med.* **2006**, *3*, 1851–1863.
121. Lichterfeld, M.; Yu, X.G.; le Gall, S.; Altfeld, M. Immunodominance of HIV-1-specific CD8(+) T-cell responses in acute HIV-1 infection: At the crossroads of viral and host genetics. *Trends Immunol.* **2005**, *26*, 166–171.
122. Yewdell, J.W. Confronting complexity: Real-world immunodominance in antiviral CD8+ T cell responses. *Immunity* **2006**, *25*, 533–543.
123. Hanke, T. STEP trial and HIV-1 vaccines inducing T-cell responses. *Expert Rev. Vaccines* **2008**, *7*, 303–309.
124. Hansen, S.G.; Ford, J.C.; Lewis, M.S.; Ventura, A.B.; Hughes, C.M.; Coyne-Johnson, L.; Whizin, N.; Oswald, K.; Shoemaker, R.; Swanson, T.; *et al.* Profound early control of highly pathogenic SIV by an effector memory T-cell vaccine. *Nature* **2011**, *473*, 523–527.
125. Hansen, S.G.; Piatak, M., Jr.; Ventura, A.B.; Hughes, C.M.; Gilbride, R.M.; Ford, J.C.; Oswald, K.; Shoemaker, R.; Li, Y.; Lewis, M.S.; *et al.* Immune clearance of highly pathogenic SIV infection. *Nature* **2013**, *502*, 100–104.
126. Hansen, S.G.; Vieville, C.; Whizin, N.; Coyne-Johnson, L.; Siess, D.C.; Drummond, D.D.; Legasse, A.W.; Axthelm, M.K.; Oswald, K.; Trubey, C.M.; *et al.* Effector memory T cell responses are associated with protection of rhesus monkeys from mucosal simian immunodeficiency virus challenge. *Nat. Med.* **2009**, *15*, 293–299.
127. Frahm, N.; Kiepiela, P.; Adams, S.; Linde, C.H.; Hewitt, H.S.; Sango, K.; Feeney, M.E.; Addo, M.M.; Lichterfeld, M.; Lahaie, M.P.; *et al.* Control of human immunodeficiency virus replication by cytotoxic T lymphocytes targeting subdominant epitopes. *Nat. Immunol.* **2006**, *7*, 173–178.
128. Hertz, T.; Ahmed, H.; Friedrich, D.P.; Casimiro, D.R.; Self, S.G.; Corey, L.; McElrath, M.J.; Buchbinder, S.; Horton, H.; Frahm, N.; *et al.* HIV-1 vaccine-induced T-cell responses cluster in epitope hotspots that differ from those induced in natural infection with HIV-1. *PLoS Pathog.* **2013**, *9*, e1003404.
129. Chen, W.; Anton, L.C.; Bennink, J.R.; Yewdell, J.W. Dissecting the multifactorial causes of immunodominance in class I-restricted T cell responses to viruses. *Immunity* **2000**, *12*, 83–93.
130. Deng, Y.; Yewdell, J.W.; Eisenlohr, L.C.; Bennink, J.R. MHC affinity, peptide liberation, T cell repertoire, and immunodominance all contribute to the paucity of MHC class I-restricted peptides recognized by antiviral CTL. *J. Immunol.* **1997**, *158*, 1507–1515.
131. Mullbacher, A.; Lobigs, M.; Yewdell, J.W.; Bennink, J.R.; Tha Hla, R.; Blanden, R.V. High peptide affinity for MHC class I does not correlate with immunodominance. *Scand. J. Immunol.* **1999**, *50*, 420–426.
132. Chen, W.; Norburry, C.C.; Cho, Y.; Yewdell, J.W.; Bennink, J.R. Immunoproteasomes shape immunodominance hierarchies of antiviral CD8(+) T cells at the levels of T cell repertoire and presentation of viral antigens. *J. Exp. Med.* **2001**, *193*, 1319–1326.

133. Campion, S.L.; Brodie, T.M.; Fischer, W.; Korber, B.T.; Rossetti, A.; Goonetilleke, N.; McMichael, A.J.; Sallusto, F. Proteome-wide analysis of HIV-specific naive and memory CD4+ T cells in unexposed blood donors. *J. Exp. Med.* **2014**, *211*, 1273–1280.
134. Im, E.J.; Hong, J.P.; Roshorm, Y.; Bridgeman, A.; Letourneau, S.; Liljestrom, P.; Potash, M.J.; Volsky, D.J.; McMichael, A.J.; Hanke, T. Protective efficacy of serially up-ranked subdominant CD8+ T cell epitopes against virus challenges. *PLoS Pathog.* **2011**, *7*, e1002041.
135. Borthwick, N.; Ahmed, T.; Ondondo, B.; Hayes, P.; Rose, A.; Ebrahimsa, U.; Hayton, E.J.; Black, A.; Bridgeman, A.; Rosario, M.; *et al.* Vaccine-elicited human T cells recognizing conserved protein regions inhibit HIV-1. *Mol. Ther.* **2014**, *22*, 464–475.
136. Johnstone, C.; de Leon, P.; Medina, F.; Melero, J.A.; Garcia-Barreno, B.; del Val, M. Shifting immunodominance pattern of two cytotoxic T-lymphocyte epitopes in the F glycoprotein of the Long strain of respiratory syncytial virus. *J. Gen. Virol.* **2004**, *85*, 3229–3238.
137. Beekman, N.J.; van Veelen, P.A.; van Hall, T.; Neisig, A.; Sijts, A.J.; Camps, M.; Kloetzel, P.M.; Neefjes, J.; Melief, C.J.; Ossendrop, F. Abrogation of CTL epitope processing by single amino acid substitution flanking the C-terminal proteasome cleavage site. *J. Immunol.* **2000**, *164*, 1898–1905.
138. Bergmann, C.C.; Yao, Q.; Ho, C.K.; Buckwold, S.L. Flanking residues alter antigenicity and immunogenicity of multi-unit CTL epitopes. *J. Immunol.* **1996**, *157*, 3242–3249.
139. Eisenlohr, L.C.; Yewdell, J.W.; Bennink, J.R. Flanking sequences influence the presentation of an endogenously synthesized peptide to cytotoxic T lymphocytes. *J. Exp. Med.* **1992**, *175*, 481–487.
140. Holland, C.J.; Cole, D.K.; Godkin, A. Re-Directing CD4(+) T Cell Responses with the Flanking Residues of MHC Class II-Bound Peptides: The Core is Not Enough. *Front. Immunol.* **2013**, *4*, 172.
141. Yellen-Shaw, A.J.; Wherry, E.J.; Dubois, G.C.; Eisenlohr, L.C. Point mutation flanking a CTL epitope ablates *in vitro* and *in vivo* recognition of a full-length viral protein. *J. Immunol.* **1997**, *158*, 3227–3234.
142. Fischer, W.; Perkins, S.; Theiler, J.; Bhattacharya, T.; Yusim, K.; Funkhouser, R.; Kuiken, C.; Haynes, B.; Letvin, N.L.; Walker, B.D.; *et al.* Polyvalent vaccines for optimal coverage of potential T-cell epitopes in global HIV-1 variants. *Nat. Med.* **2007**, *13*, 100–106.
143. Barouch, D.H.; Stephenson, K.E.; Borducchi, E.N.; Smith, K.; Stanley, K.; McNally, A.G.; Liu, J.; Abbink, P.; Maxfield, L.F.; Seaman, M.S.; *et al.* Protective efficacy of a global HIV-1 mosaic vaccine against heterologous SHIV challenges in rhesus monkeys. *Cell* **2013**, *155*, 531–539.
144. Nickle, D.C.; Rolland, M.; Jensen, M.A.; Pond, S.L.; Deng, W.; Seligman, M.; Heckerman, D.; Mullins, J.I.; Jojic, N. Coping with viral diversity in HIV vaccine design. *PLoS Comput. Biol.* **2007**, *3*, e75.
145. Rolland, M.; Manocheewa, S.; Swain, J.V.; Lanxon-Cookson, E.C.; Kim, M.; Westfall, D.H.; Larsen, B.B.; Gilbert, P.B.; Mullins, J.I. HIV-1 conserved-element vaccines: Relationship between sequence conservation and replicative capacity. *J. Virol.* **2013**, *87*, 5461–5467.
146. Rolland, M.; Nickle, D.C.; Mullins, J.I. HIV-1 group M conserved elements vaccine. *PLoS Pathog.* **2007**, *3*, e157.
147. Dahirel, V.; Shekhar, K.; Pereyra, F.; Miura, T.; Artyomov, M.; Talsania, S.; Allen, T.M.; Altfeld, M.; Carrington, M.; Irvine, D.J.; *et al.* Coordinate linkage of HIV evolution reveals regions of immunological vulnerability. *Proc. Natl. Acad. Sci. USA* **2011**, *108*, 11530–11535.

148. Kulkarni, V.; Rosati, M.; Valentin, A.; Ganneru, B.; Singh, A.K.; Yan, J.; Rolland, M.; Alicea, C.; Beach, R.K.; Zhang, G.M.; *et al.* HIV-1 p24(gag) derived conserved element DNA vaccine increases the breadth of immune response in mice. *PLoS One* **2013**, *8*, e60245.
149. Kulkarni, V.; Valentin, A.; Rosati, M.; Alicea, C.; Singh, A.K.; Jalah, R.; Broderick, K.E.; Sardesai, N.Y.; Le Gall, S.; Mothe, B.; *et al.* Altered response hierarchy and increased T-cell breadth upon HIV-1 conserved element DNA vaccination in macaques. *PLoS One* **2014**, *9*, e86254.
150. Rosario, M.; Borthwick, N.; Stewart-Jones, G.B.; Mbewe-Mvula, A.; Bridgeman, A.; Colloca, S.; Montefiori, D.; McMichael, A.J.; Nicosia, A.; Drijfhout, J.W.; *et al.* Prime-boost regimens with adjuvanted synthetic long peptides elicit T cells and antibodies to conserved regions of HIV-1 in macaques. *Aids* **2012**, *26*, 275–284.
151. DeMuth, P.C.; Li, A.V.; Abbink, P.; Liu, J.; Li, H.; Stanley, K.A.; Smith, K.M.; Lavine, C.L.; Seaman, M.S.; Kramer, J.A.; *et al.* Vaccine delivery with microneedle skin patches in nonhuman primates. *Nat. Biotechnol.* **2013**, *31*, 1082–1085.
152. Duthie, M.S.; Windish, H.P.; Fox, C.B.; Reed, S.G. Use of defined TLR ligands as adjuvants within human vaccines. *Immunol. Rev.* **2011**, *239*, 178–196.
153. Tan, T.G.; Mui, E.; Cong, H.; Witola, W.H.; Montpetit, A.; Muench, S.P.; Sidney, J.; Alexander, J.; Sette, A.; Grigg, M.E.; *et al.* Identification of T. gondii epitopes, adjuvants, and host genetic factors that influence protection of mice and humans. *Vaccine* **2010**, *28*, 3977–3989.
154. Zhu, Q.; Egelston, C.; Gagnon, S.; Sui, Y.; Belyakov, I.M.; Klinman, D.M.; Berzofsky, J.A. Using 3 TLR ligands as a combination adjuvant induces qualitative changes in T cell responses needed for antiviral protection in mice. *J. Clin. Investig.* **2010**, *120*, 607–616.
155. Park, H.; Adamson, L.; Ha, T.; Mullen, K.; Hagen, S.I.; Nogueron, A.; Sylwester, A.W.; Axthelm, M.K.; Legasse, A.; Piatak, M., Jr.; *et al.* Polyinosinic-polycytidylic acid is the most effective TLR adjuvant for SIV Gag protein-induced T cell responses in nonhuman primates. *J. Immunol.* **2013**, *190*, 4103–4115.
156. Lore, K.; Betts, M.R.; Brenchley, J.M.; Kuruppu, J.; Khojasteh, S.; Perfetto, S.; Roederer, M.; Seder, R.A.; Koup, R.A. Toll-like receptor ligands modulate dendritic cells to augment cytomegalovirus- and HIV-1-specific T cell responses. *J. Immunol.* **2003**, *171*, 4320–4328.
157. Wille-Reece, U.; Flynn, B.J.; Lore, K.; Koup, R.A.; Kedl, R.M.; Mattapallil, J.J.; Weiss, W.R.; Roederer, M.; Seder, R.A. HIV Gag protein conjugated to a Toll-like receptor 7/8 agonist improves the magnitude and quality of Th1 and CD8+ T cell responses in nonhuman primates. *Proc. Natl. Acad. Sci. USA* **2005**, *102*, 15190–15194.
158. Goonetilleke, N.; McMichael, A.J. Immunology. Antigen processing takes a new direction. *Science* **2013**, *340*, 937–938.
159. Archin, N.M.; Margolis, D.M. Emerging strategies to deplete the HIV reservoir. *Curr. Opin. Infect. Dis.* **2014**, *27*, 29–35.

160. Deeks, S.G.; Autran, B.; Berkhout, B.; Benkirane, M.; Cairns, S.; Chomont, N.; Chun, T.W.; Churchill, M.; Mascio, M.D.; Katlama, C.; *et al.* Towards an HIV cure: A global scientific strategy. *Nat. Rev. Immunol.* **2012**, *12*, 607–614.

PLOS | PATHOGENS

RESEARCH ARTICLE

Variable Processing and Cross-presentation of HIV by Dendritic Cells and Macrophages Shapes CTL Immunodominance and Immune Escape

Jens Dinter, Ellen Duong, Nicole Y. Lai, Matthew J. Berberich, Georgio Kourjian, Edith Bracho-Sanchez, Duong Chu, Hang Su, Shao Chong Zhang, Sylvie Le Gall*

Ragon Institute of MGH, MIT and Harvard, Massachusetts General Hospital, Harvard Medical School, Cambridge, Massachusetts, United States of America

* sylvie_legall@hms.harvard.edu

Citation: Dinter J, Duong E, Lai NY, Berberich MJ, Kourjian G, Bracho-Sanchez E, et al. (2015) Variable Processing and Cross-presentation of HIV by Dendritic Cells and Macrophages Shapes CTL Immunodominance and Immune Escape. PLoS Pathog 11(3): e1004725. doi:10.1371/journal.ppat.1004725

Editor: David T. Evans, University of Wisconsin, UNITED STATES

Received: November 2, 2014

Accepted: February 3, 2015

Published: March 17, 2015

Data Availability Statement: All relevant data are within the paper and its Supporting Information files.

Funding: The project was funded by grants R01 AI084753 and R01 AI084106 from NIAID to SLG. JD is funded in part by a Ph.D. training fellowship from the Ernst Schering Foundation. The funders had no role in study design, data collection and analysis, decision to publish, or preparation of the manuscript.

Competing Interests: The authors have declared that no competing interests exist.

Abstract

Dendritic cells (DCs) and macrophages (Møs) internalize and process exogenous HIV-derived antigens for cross-presentation by MHC-I to cytotoxic $CD8^+$ T cells (CTL). However, how degradation patterns of HIV antigens in the cross-presentation pathways affect immunodominance and immune escape is poorly defined. Here, we studied the processing and cross-presentation of dominant and subdominant HIV-1 Gag-derived epitopes and HLA-restricted mutants by monocyte-derived DCs and Møs. The cross-presentation of HIV proteins by both DCs and Møs led to higher CTL responses specific for immunodominant epitopes. The low CTL responses to subdominant epitopes were increased by pretreatment of target cells with peptidase inhibitors, suggestive of higher intracellular degradation of the corresponding peptides. Using DC and Mø cell extracts as a source of cytosolic, endosomal or lysosomal proteases to degrade long HIV peptides, we identified by mass spectrometry cell-specific and compartment-specific degradation patterns, which favored the production of peptides containing immunodominant epitopes in all compartments. The intracellular stability of optimal HIV-1 epitopes prior to loading onto MHC was highly variable and sequence-dependent in all compartments, and followed CTL hierarchy with immunodominant epitopes presenting higher stability rates. Common HLA-associated mutations in a dominant epitope appearing during acute HIV infection modified the degradation patterns of long HIV peptides, reduced intracellular stability and epitope production in cross-presentation-competent cell compartments, showing that impaired epitope production in the cross-presentation pathway contributes to immune escape. These findings highlight the contribution of degradation patterns in the cross-presentation pathway to HIV immunodominance and provide the first demonstration of immune escape affecting epitope cross-presentation.

Author Summary

Pathogens such as HIV can enter cells by fusion at the plasma membrane for delivery in the cytosol, or by internalization in endolysosomal vesicles. Pathogens can be degraded in these various compartments into peptides (epitopes) displayed at the cell surface by MHC-I. The presentation of pathogen-derived peptides triggers the activation of T cell immune responses and the clearance of infected cells. How the diversity of compartments in which HIV traffics combined with the diversity of HIV sequences affects the degradation of HIV and the recognition of infected cells by immune cells is not understood. We compared the degradation of HIV proteins in subcellular compartments of dendritic cells and macrophages, two cell types targeted by HIV and the subsequent presentation of epitopes to T cells. We show variable degradation patterns of HIV according to compartments, and the preferential production and superior intracellular stability of immunodominant epitopes corresponding to stronger T cell responses. Frequent mutations in immunodominant epitopes during acute infection resulted in decreased production and intracellular stability of these epitopes. Together these results demonstrate the importance of protein degradation patterns in shaping immunodominant epitopes and the contribution of impaired epitope production in all cellular compartments to immune escape during HIV infection.

Introduction

Cytotoxic $CD8^+$ T cell (CTL) responses play an important role in the outcome of viral infections. CTL responses elicited during HIV or HCV infection follow a predictable immunodominance hierarchy, whereby immunodominant T cell responses are defined by a higher frequency in a population sharing a HLA, or by a higher magnitude of interferon-gamma production in an individual [1]. The acute phase of HIV infection is characterized by narrow immunodominance patterns [2,3], and immune pressure leading to frequent escape mutations in immunodominant epitopes changes the T cell response hierarchy during disease progression [4–9]. Since immunodominance established during HIV infection or reproduced by some HIV vaccines does not clear or prevent infection, breaking immunodominance hierarchies to induce the presentation of broader subdominant but protective epitopes provides an interesting alternative for vaccine design.

Immunodominance is shaped by multiple factors [10], including binding affinity to MHC or the TCR [11,12], frequency of $CD8^+$ T cell precursors and the TCR repertoire [13], kinetics of expression and amount of viral proteins [14], and efficiency of antigen processing [15–17]. How degradation patterns during cross-presentation of antigens, specifically in the case of highly variable pathogens like HIV, may shape immunodominance and viral evolution is not well understood. Antigen presenting cells (APC) such as DCs and Møs cross-present antigens from various sources, such as cell-associated antigens [18–21], viral particles [22–24], or viral proteins [25,26] for priming or activation of T cell responses. Internalized antigens first undergo proteolytic processing by cathepsins in endocytic compartments [27] where they can be loaded onto MHC I or MHC II molecules for presentation to $CD8^+$ or $CD4^+$ T cells [28], or eventually escape into the cytosol [29] for additional degradation [30,31], translocation in the ER and cross-presentation by MHC I.

The cell type and the trafficking of antigens have a crucial impact on their processing, as different proteases in each compartment can produce or destroy epitopes, thus shaping the surface peptidome [25,32,33]. Different cell types express individual patterns of proteases, which affect

epitope processing as we previously showed for the degradation of several HIV epitopes by cytosolic peptidases [34,35]. In a given cell type, the degradation of proteins in the cytosol and in the ER [34–36] contribute to defining the timing and amount of peptides available for presentation, and have been shown to preferentially produce multiple epitopes corresponding to immunodominant responses in HIV [16,17] and HCV infection [15]. Moreover, differences in degradation patterns of HIV peptides in cytosolic, endosomal or lysosomal cell extracts isolated from human PBMCs [37,38] further highlight the critical role of antigen trafficking on epitope processing. Mutations within and outside epitopes alter degradation patterns by proteasomes and aminopeptidases in the cytosol or in the ER, reduce epitope presentation and lead to immune escape [39–42]. Nothing is known about the impact of these mutations on the degradation patterns during cross-presentation despite its potential impact for T cell priming and activation.

The aim of this study was to systematically examine the processing and cross-presentation of dominant and subdominant HIV Gag-derived epitopes and of natural mutants of an immunodominant epitope by monocyte-derived DCs and Møs. We showed a preferential production and a superior intracellular stability of peptides containing immunodominant epitopes in cytosol and endolysosomes. Moreover, we showed that frequent HLA-restricted mutations in an immunodominant peptide associated with shifts in immunodominance patterns, modified the degradation patterns of HIV fragments in endolysosomes and reduced epitope stability and production in the cross-presentation pathway. These results highlight the contribution of degradation patterns in the cross-presentation pathways of APC to immunodominance and immune escape in HIV infection.

Materials and Methods

Ethics statement

Cells were isolated from HLA-typed blood donors or anonymous buffy coats after written informed consent and approval by the Partners Human Research Committee under protocol 2005P001218 (Boston, USA).

Cell culture

Human peripheral blood mononuclear cells (PBMCs) were isolated by Ficoll-Hypaque (Sigma-Aldrich) density centrifugation. Monocytes were enriched using CD14+ magnetic isolation kits (StemCell) and differentiated into DCs and Møs during a 6-day culture. DCs were cultured in AIM-V media with 1% human serum AB (Gemini Bio-Products) supplemented with 20ng/mL IL-4 and 10ng/mL GM-CSF (CellGenix). On days 2 and 4, fresh IL-4 and GM-CSF were added. Møs were cultured in ultra low attachment plates (Corning) in AIM-V media with 10% human serum AB. Where indicated, maturation of DCs and Møs was induced by TLR ligand stimulation with 2μg/mL LPS, 1μg/mL CL097, or 1μg/mL R848 (Invivogen) for 2 days [35]. Epitope-specific CTL clones were maintained in the presence of 50U/mL IL-2, using 0.1μg/mL CD3-specific mAb 12F6, and irradiated feeder cells as stimulus for T cell proliferation.

ELISPOT cross-presentation assay

Immature DCs and Møs were exposed to recombinant HIV-1 p24-protein, HIV-1 p55-protein or control protein (Protein Sciences Corporation, USA) for 1hr at 37°C. Where indicated, cells were pre-incubated for 45 minutes with inhibitors for proteasome (10μM MG132 (Enzo Life Sciences)) or cysteine proteases (5μM E64 (Sigma-Aldrich)). Cells pulsed with equivalent molar concentrations of the optimal epitopes were used as controls for antigen presentation and CTL clone specificity. DCs and Møs were thoroughly washed and cultured overnight with

epitope-specific CTL clones at a 2:1 effector-to-target ratio in 96-well plates (Millipore) coated with anti-IFN-γ mAb 1-D1K (Mabtech). ELISPOT plates were washed and developed as described previously [43].

P24 uptake assay

DCs or Møs ($1x10^6$ cells/mL) were exposed to the following protease inhibitors for 45 minutes: 10μM MG132, 5μM E64, 10μM cathepsin S inhibitor Z-FL-COCHO, 10μM leupeptin (Enzo Life Sciences), 120μM bestatin (Sigma-Aldrich), before incubation with different concentrations of recombinant HIV-1 p24-protein for 1hr at 37°C or 4°C. Samples were thoroughly washed in ice-cold PBS and immediately treated with 3mg/mL pronase E (Sigma-Aldrich) in AIM-V media without serum for 10 minutes on ice. Cells were washed, lysed in 0.5% Triton X-100 containing lysis buffer and the amount of p24 protein in cell lysates was measured using a standard HIV-1 p24 antigen ELISA (Perkin Elmer).

Fluorescent measurement of proteolytic activities in live cells and cell extracts

Whole cell extracts from DCs and Møs were prepared by 0.125% digitonin permeabilization in ice-cold lysis buffer (50mM HEPES, 50mM potassium acetate, 5mM $MgCl_2$, 1mM DTT, 1mM ATP, 0.5mM EDTA, 10% Glycerol, pH 7.4), followed by 17,762 rcf centrifugation at 4°C for 15 minutes to remove cell debris as previously done [17,35,44]. The proteolytic activities of cathepsin S (cell, 50μM; extracts, 10μM Z-VVR-AMC), omni cathepsins (cell, 50μM; extracts, 50μM Z-FR-AMC), cathepsin D&E (extracts, 10μM Mca-GKPILFFRLK-Dnp, Enzo Life Sciences), and cathepsin B (extracts, 50μM Z-RR-AMC, Bachem) were measured by cleavage of peptide-specific fluorogenic substrates. Incubation with the relevant inhibitor of cathepsin S (10μM ZFL-COCHOO, Calbiochem), cathepsin B (10μM Z-RLVazaglyIV-OMe, Bachem), omnicathepsins (50μM E64), and cathepsin D&E (100μM Pepstatin A, Enzo Life Sciences) confirmed the specificity of reactions. For cells, $2x10^4$ DCs or Møs in PBS/0.0025% digitonin were used to measure the proteolytic activities. For cell extracts, equivalent amounts as determined by total protein concentration were used in reaction buffer (50mM sodium chloride, 50mM potassium phosphate, 2mM DTT, 2mM EDTA; pH 7.4, pH5.5 or pH4.0, respectively). The rate of fluorescence emission, which is proportional to the proteolytic activity, was measured every 5 minutes at 37°C in a Victor-3 Plate Reader (Perkin Elmer) [34,35].

In vitro peptide degradation assay

2nmol of >98% pure peptides (Bio-Synthesis, USA) were digested with 15μg of whole cell extracts, normalized to actin levels, at 37°C in 50μL of degradation buffer (50mM Tris-HCl, 137mM potassium acetate, 1mM $MgCl_2$, and 1mM ATP, pH7.4, pH5.5, or pH4.0) [37,45]. At various time points the reaction was stopped with 2.5μL of 100% formic acid (FA) and peptide fragments were purified by 5% trichloroacetic acid precipitation.

Mass spectrometry analysis

Peptides in the digestion mix were identified by in house mass spectrometry. Equal amounts of peptide degradation samples were injected into a Nano-HPLC (Eksigent) and online nanosprayed into an Orbitrap mass spectrometer (LTQ Orbitrap Discovery, Thermo) with a flow rate of 400nL/min. A Nano cHiPLC trap column (200μm x 0.5mm ChromXP c18-CL 5μm 120Å; Eksigent) was used to remove salts in the sample buffer. Peptides were separated in a Nano cHiPLC column (75μm x 15cm ChromXP c18-CL 5μm 300Å; Eksigent) over a gradient

of 2% to 40% buffer B (buffer A: 0.1% FA in water; buffer B: 0.1% FA in acetonitrile) and mass spectra were recorded in the range of 370 to 2000Daltons. In tandem MS/MS mode, the eight most intense peaks were selected with a window of 1Da and fragmented. The collision gas was helium, and the collision voltage was 35V. Masses in the mass spectra were searched against source peptide databases with Proteome Discoverer (Thermo Scientific). The integrated area under a peptide peak is proportional to its abundance. Each sample was run on the mass spectrometer at least twice.

Intracellular stability of optimal epitopes

One nmol of highly purified peptide was degraded in 15μg of whole cell extracts at 37°C in degradation buffer at pH7.4 or pH4.0 [37]. Aliquots were taken at 0, 10, 30, and 60 minutes, and the reaction was stopped with 2.5μL of 100% TFA. The remaining peptide at each time point was quantified by reversed-phase HPLC (RP-HPLC; Waters). 100% represents the amount of peptide detected at time point 0 calculated as the area under the peptide peak. A stability rate of each peptide was calculated by a nonlinear regression (one-phase exponential decay) of the degradation profile obtained over a 60-minute incubation [35,44]. Peptides incubated in buffer without cell extracts were used as controls.

Statistical analysis

Spearman's rank correlation coefficient was used to examine bivariate associations. The Kruskal-Wallis test was used to compare measurements between groups. In figures, p-value criteria are assigned as * $p<0.05$, ** $p<0.01$ and *** $p<0.001$. Statistical analyses were conducted using GraphPad Prism (GraphPad Prism Software, USA).

Results

Cross-presentation of the immunodominant HLA-B57-restricted Gag p24 TW10 and KF11 epitopes is more efficient than that of subdominant ISW9 epitope

We analyzed the cross-presentation of the three optimally defined HLA-B57 restricted HIV epitopes originating from HIV-1 p24 protein by immature monocyte-derived DCs and Møs: subdominant B57-ISW9 (ISPRTLNAW, aa 15–23 in Gag p24), dominant B57-KF11 (KAFSPEVIPMF, aa 30–40 in Gag p24), and dominant B57-TW10 (TSTLQEQIGW, aa 108–117 in Gag p24) [46,47]. B57-ISW9-specific CTL responses to cross-presenting DCs were 28-fold and 94-fold lower compared with B57-KF11 and B57-TW10-specific responses, respectively (Fig. 1A, left panel). Similar results were observed with cross-presenting Møs, with 47-fold lower B57-ISW9-specific CTL responses compared with B57-KF11 and B57-TW10-specific CTL responses (Fig. 1A, right panel). DCs and Møs pulsed with increasing amounts of synthetic ISW9 or TW10 peptides similarly activated epitope-specific CTLs (Fig. 1B). Since a previous study showed comparable affinities of ISW9, KF11 and TW10 peptides for HLA-B57 [48], our results suggest that differences in CTL responses to cross-presenting DCs and Møs are not due to differences in peptide avidity among the clones, but likely to differential epitope production. To ensure that epitopes cross-presented by DCs and Møs were endogenously processed, we measured the intracellular concentrations of HIV-1 p24 protein after uptake at 37°C or 4°C. In both cell subsets the intracellular concentration of HIV p24 increased with the amount of p24 used for uptake at 37°C whereas the uptake at 4°C was minimal (Fig. 1C). Immature Møs showed at least 5-fold lower intracellular p24 concentrations than DCs, which may indicate a faster degradation of internalized protein by Møs [49]. Moreover, B57-KF11-specific CTL

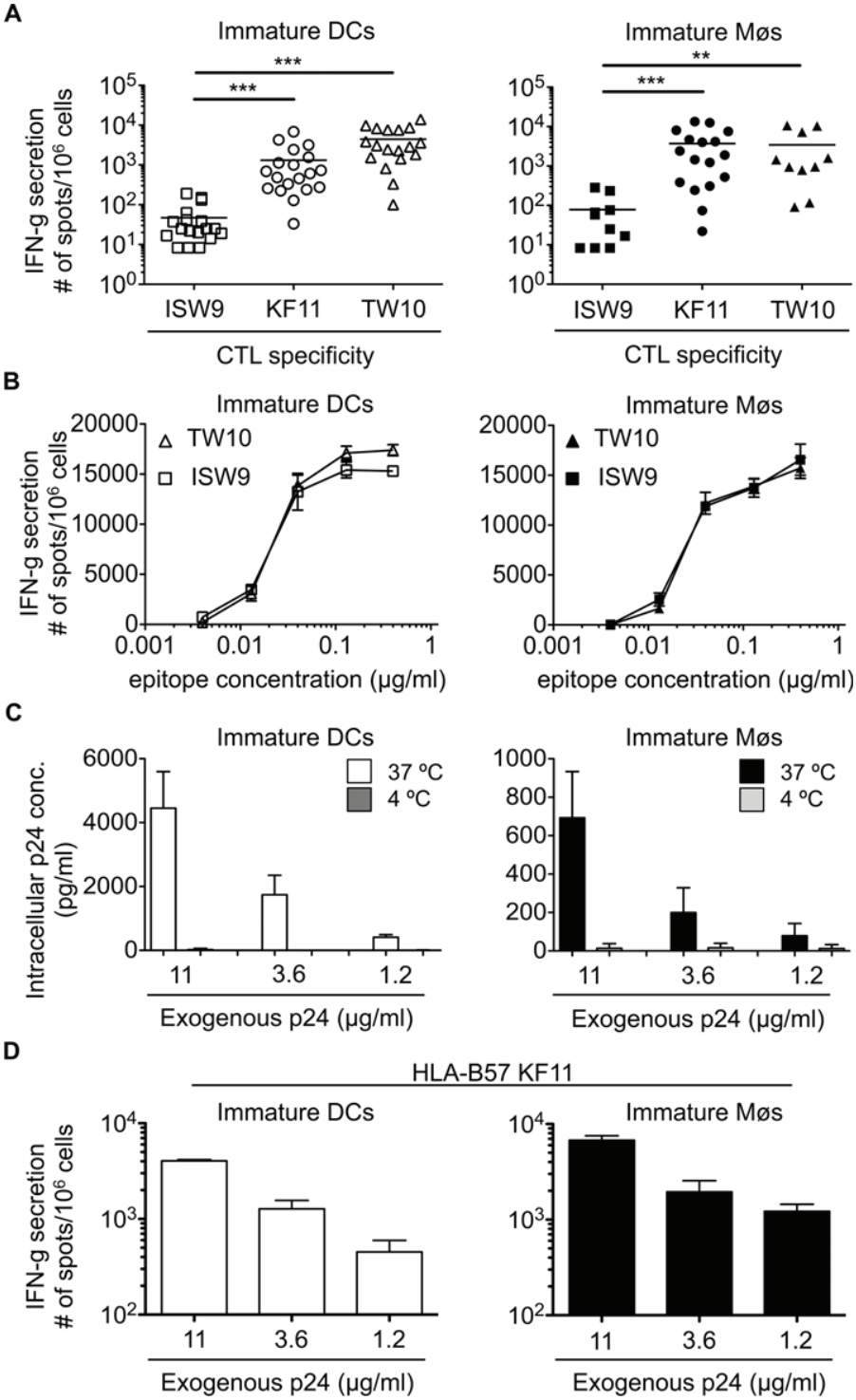

Fig 1. The immunodominant HLA-B57-restricted TW10 and KF11 epitopes are more efficiently cross-presented than subdominant ISW9 epitope. A. Immature DCs (open symbols) and Møs (solid symbols) were incubated with recombinant HIV-1 p24 protein and used as antigen presenting cells in an overnight IFN-gamma ELISPOT assay with HLA-B57 ISW9-specific (□), KF11-specific (○), and TW10-specific (Δ) CTL clones as effector cells. CTL responses in form of spot forming cells are shown for n≥10 donors. B. CTL responses to immature DCs (open symbols) and Møs (solid symbols) pulsed with different concentrations of

optimal epitope B57-ISW9 (□) or B57-TW10 (Δ) were measured in an overnight IFN-gamma ELISPOT assay. Data are representative of two independent experiments with different donors. Due to the limited number of DCs and Møs generated from HLA-B57$^+$ donors, the titration of epitopes was only done for B57-ISW9 and B57-TW10. C. Immature DCs (open bars) and immature Møs (solid bars) were pre-treated with a cocktail of protease inhibitors to reduce intracellular degradation before addition of different concentrations of recombinant HIV-1 p24 protein at 37°C or 4°C. Internalized p24 protein was determined by a standard p24 ELISA assay using whole cell extracts from lysed DCs and Møs. Results are from three independent experiments with different donors and show mean ± SD. D. Immature DCs (open bars) or immature Møs (solid bars) were incubated with different concentrations of recombinant HIV-1 p24 protein and used as antigen presenting cells to B57-KF11-specific CTLs. Responses in form of spot forming cells are shown. Data are representative of two independent experiments with different donors.

doi:10.1371/journal.ppat.1004725.g001

responses increased with the amount of exogenous p24 protein added to cells, in accordance with higher amount of intracellular p24 leading to higher amount of peptide presentation (Fig. 1D). Together, these data show that the higher CTL responses against dominant TW10 and KF11 epitopes after uptake of p24 by DCs and Møs are due to cross-presentation of higher amounts of both peptides compared with subdominant ISW9.

Protease activities in cross-presentation competent cell compartments differently affect processing of HIV-1 epitopes in DCs and Møs

We aimed to identify factors contributing to the production or destruction of the three epitopes in each cell type. Incubation of immature DCs with proteasome inhibitor MG132 resulted in a 43-fold and 4-fold increased presentation of B57-ISW9 and B57-KF11 epitopes, respectively, suggesting that proteasomal degradation of epitope-containing peptides limited the amount of ISW9 and KF11 available for presentation (Fig. 2A). In contrast, inhibition of cysteine proteases by E64 had no effect on the cross-presentation of both epitopes, indicating that fragments escape early into the cytosol before trafficking to compartments with high cysteine protease activity. B57-TW10-specific CTL responses to cross-presenting immature DCs decreased approximately 3-fold upon inhibition of proteasomes, suggesting that proteasomal processing is required for efficient presentation of TW10. In contrast to DCs, the cross-presentation of B57-ISW9 by immature Møs was not affected upon inhibition of proteasomes, suggesting that the cross-presentation of ISW9 in Møs is proteasome-independent (Fig. 2B). B57-KF11 and B57-TW10 CTL responses decreased 2- and 3-fold respectively upon proteasome inhibition with MG132 or epoxomicin in Møs, suggesting that the processing of both epitopes requires proteasome processing in Møs. Inhibition of cysteine proteases in Møs did not affect the cross-presentation of ISW9, KF11 and TW10. Together, these results indicate that cross-presentation of HIV-1 p24 involves distinct proteases in DCs and Møs, which can be essential or detrimental for the processing of epitopes.

The immunodominant epitopes B57-KF11 and B57-TW10 are more efficiently produced in cytosolic and endolysosomal extracts than subdominant epitope B57-ISW9

Exogenous antigens internalized by DCs and Møs first encounter several proteases in endo- and lysosomes [27], before presentation or additional degradation in the cytosol. In line with previous studies we observed lower omnicathepsin and cathepsin S activities in DCs compared with Møs [49], which further decreased upon maturation of DCs as shown by an inverse correlation between both activities and the % of mature DCs (S1A Fig). To assess how degradation of HIV peptides along the cross-presentation pathway of immature and TLR ligand-stimulated DCs and Møs may contribute to shaping immunodominance patterns, we used a previously

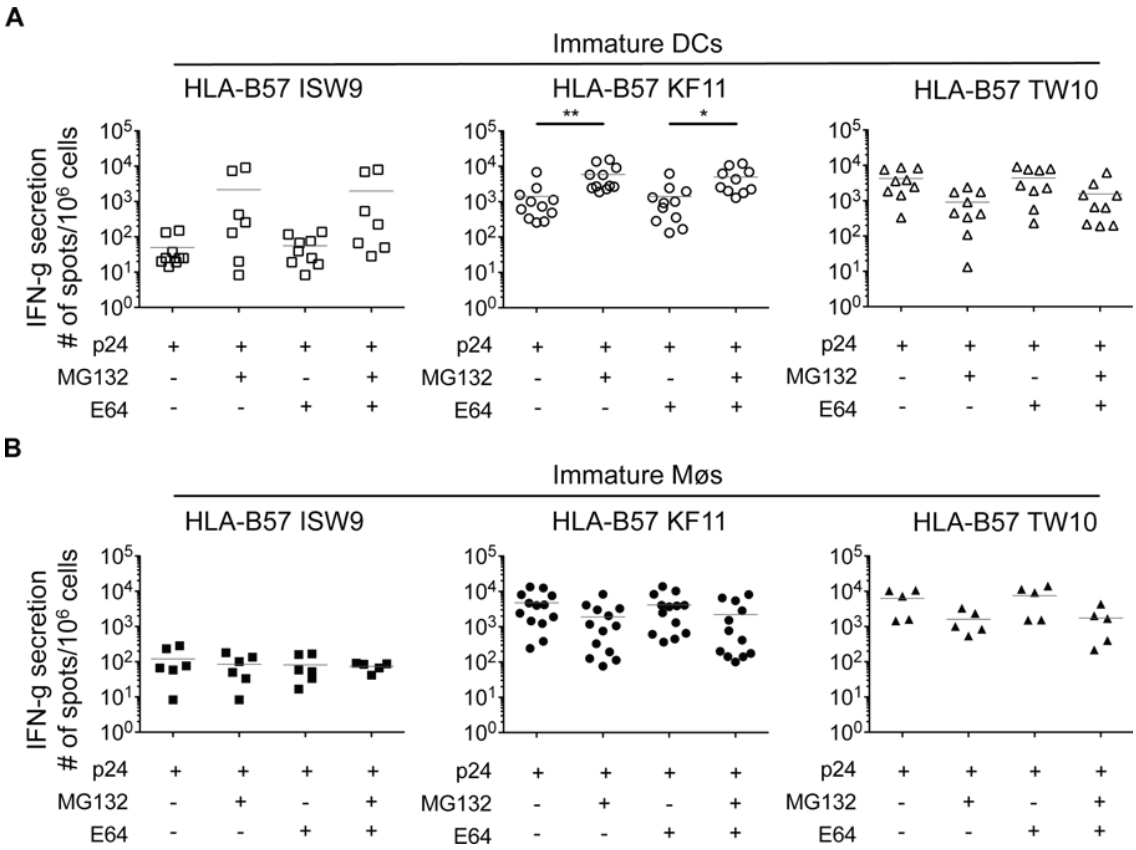

Fig 2. Inhibition of proteasomes increases B57-KF11 and B57-ISW9 epitope cross-presentation by DCs but not Møs (A) Immature DCs (open symbols) and (B) immature Møs (solid symbols) were pretreated with proteasome inhibitor (MG132) or a broad inhibitor of cysteine proteases (E64) before addition of recombinant HIV-1 p24 protein. CTL responses to HLA-B57 ISW9-specific (□), KF11-specific (○), and TW10-specific (Δ) were measured as described in Fig. 1. Similarly, incubation of DCs with epoxomicin, a selective chymotrytpic proteasome inhibitor, increased HLA-B57-KF11-specific CTL responses by 11-fold. Results are from n≥5 donors.

doi:10.1371/journal.ppat.1004725.g002

developed degradation assay recapitulating degradation in the cross-presentation compartments [37]. This assay allows the simultaneous analysis of degradation products by cytosolic, endosomal and lysosomal peptidases from the same cells using mass spectrometry. Omni-cathepsin and cathepsin S activities measured in live intact cells correlated to their matching cell extracts, as previously demonstrated for cytosolic proteases [35] (S1B Fig) and could be activated at different pH values, in accordance with differential cathepsin activation in endosomes and lysosomes (S1C Fig) [37].

Degradation of a synthetic 35-mer peptide containing the epitopes B57-ISW9 and B57-KF11 (MVHQAISPRTLNAWVKVVEEKAFSPEVIPMFAALS, aa 10–44 in Gag p24) [34,35,37] showed the production of peptides of variable lengths at different pH values over time (S2 Fig). To assess and compare the production of peptides in each cell subset and cell compartment, we used the area under each peptide peak identified by mass spectrometry, which we previously showed to be proportional to the amount of the corresponding peptide [35,50]. Peptides were grouped according to their lengths or epitope content, and the contribution of each category of peptides to the total degradation products was calculated for each time point. Degradation at pH4.0 in cell extracts from immature DCs yielded shorter fragments compared with degradation at pH7.4, with majority of fragments being 8–12 and 13–18 aa long and contributing to

45% and 51% of total peptide intensity at 120 minutes, respectively (Fig. 3A, upper left panel). The degradation of fragments containing both epitopes ($ISW9^+/KF11^+$) resulted in the preferential production of B57-KF11 epitope-containing fragments ($ISW9^-/KF11^+$), and only small amounts of B57-ISW9 epitope-containing fragments ($ISW9^+/KF11^-$) in extracts of immature DCs at all pH values tested (Fig. 3B, upper left panel). KF11- and ISW9-containing fragments were produced more efficiently at pH7.4 than at pH5.5 and pH4.0, indicating a higher presentation in the direct presentation pathway, or if epitope precursors escape from endolysosomes. Similar results were observed for immature Møs (Fig. 3A/B, lower left panel), in line with comparable cytosolic and endocytic hydrolytic activities in immature DCs and Møs [35]. Degradation of the 35-mer in extracts from DCs and Møs matured with LPS yielded similar degradation patterns with fragments of comparable lengths and higher amounts of fragments containing immunodominant epitope B57-KF11 (Fig. 3A/B, right panel).

We further analyzed the cleavage patterns by measuring the relative amount of fragments with a specific N terminus or C terminus (Fig. 3C, upper or lower graph of each panel). After 30 minutes of degradation at pH7.4 several minor cleavage sites produced ISW9- and KF11-containing fragments, whereas at pH5.5 and pH4.0 the generation of fragments with a Tryptophan at the N terminus destroyed ISW9 and fragments with a Methionine and Proline at the C terminus destroyed KF11. Further trimming resulted in the appearance of new N- and C-terminal cleavage sites, which still preserved KF11-containing peptides at pH7.4, whereas at pH5.5 and pH4.0 both epitopes were further destroyed. These data indicate that this p24 35-mer is sensitive to degradation in all three cell compartments in DCs and Møs, and favors the production of dominant epitope KF11 over that of subdominant ISW9, in line with the more efficient cross-presentation of KF11 and the rescue of ISW9 in the presence of protease inhibitors.

Moreover, we analyzed the production of 16 well described HIV $CD8^+$ and $CD4^+$ T cell epitopes [46] and epitope precursors, defined as N-terminal extended epitopes, located in this 35-mer (S3A–S3B Fig). Peptides were produced in extracts of both cell subsets at all pH values tested (B57-KF11, B15-HL9, A25-QW11, B57-FF9, B57-KP9), preferentially produced at pH7.4 (B57-ISW9, A02-TV9), or at pH5.5 and pH4.0 (B45-VI11, B15-VF9, B44-EV9) or not produced at any time (B07-SV9). These results highlight a variable production or degradation of epitopes in different cell compartments, which may affect their capacity to activate $CD8^+$ or $CD4^+$ T cells during infection or cross-presentation.

We next extended the analysis to another HIV-1 Gag p24-derived peptide containing the epitope B57-TW10 (GSDIAGTTSTLQEQIGWMTNNPPIPVGGEIY, aa 101–131 in Gag p24), dominant in HIV acute infection (Fig. 4). In contrast to p24 35-mer, the majority of degradation products identified after 10 to 120 minutes in extracts from immature DCs and Møs at pH7.4, pH5.5 and pH4.0 represented the original fragment or long fragments of mostly >26aa (Fig. 4A), containing the TW10 epitope with N- and C-terminal extensions (Fig. 4B). Similarly, degradation in extracts from mature DCs and Møs showed comparable kinetics of degradation and resulted in the production of fragments with similar lengths. Accordingly the few cleavage sites identified after 30 or 120 minutes were mostly located outside B57-TW10 at all three pH values, protecting the antigenic peptide from degradation, in line with the highly efficient cross-presentation of B57-TW10 (S4 Fig).

The relative resistance of the B57-TW10-containing fragment to intracellular degradation contrasted with the rapid degradation of the p24 fragment containing B57-ISW9 and B57-KF11 which may contribute to a higher amount of TW10-containing peptide available for presentation by direct or cross-presentation, thus contributing to the dominance of TW10-specific CTL responses during acute HIV infection.

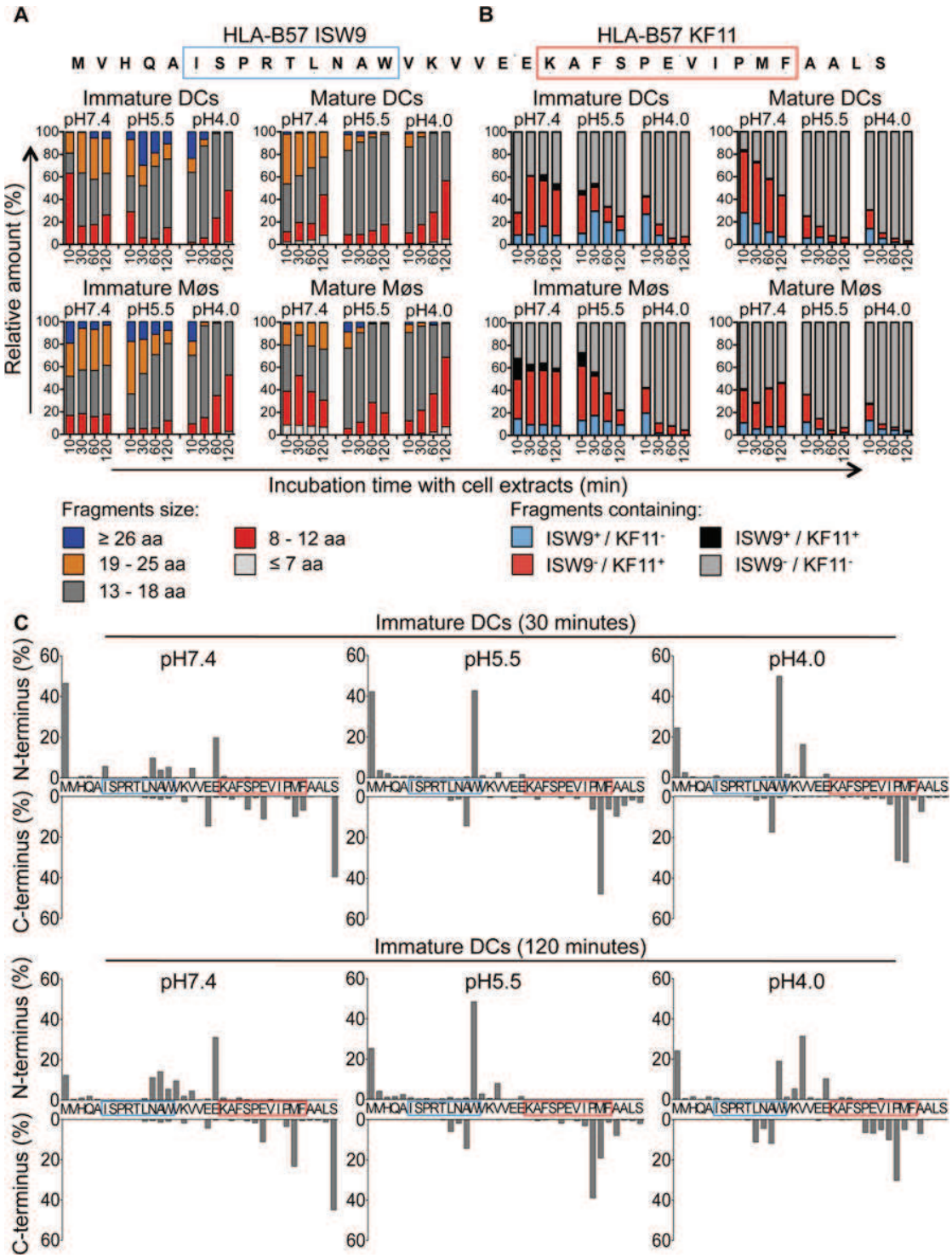

Fig 3. The immunodominant epitope B57-KF11 is more efficiently produced in cross-presentation-competent compartments than subdominant epitope B57-ISW9. A. Two nmol of p24–35mer (MVHQAISPRTLNAWVKVVEEKAFSPEVIPMFAALS, aa 10–44 in Gag p24) were degraded in 15μg of whole cell extracts from immature and mature DCs and Møs for 10, 30, 60, and 120 minutes in degradation buffer at pH7.4, pH5.5 or pH4.0. Degradation products identified by mass spectrometry were grouped according to their lengths of fragments: equal or longer than 26 aa (blue), 19–25 aa (orange), 13–18 aa (gray), 8–12 aa (red), and fragments equal or shorter than 7 aa (light gray). The peak area of each identified peptide was calculated with Proteome Discoverer and the contribution of each category of peptides to the total intensity of all degradation products is shown at each time point. B. All degradation

products of p24–35mer were identified as described in (A). Peptides were grouped into fragments containing B57-ISW9 and B57-KF11 epitopes (black), containing only B57-KF11 epitope (red), containing only B57-ISW9 epitope (blue), or neither epitope (gray), respectively. C. Cleavage patterns of p24–35mer incubated with whole cell extracts from immature DCs for 30 minutes (upper panel) or 120 minutes (lower panel) at pH7.4, pH5.5, and pH4.0 are shown as the contribution of each cleavage site, presented as cleavage N-terminal or C-terminal to a specific amino acid, to the total intensity of all degradation products. For (A-C) data are representative of three independent experiments with three different donors.

doi:10.1371/journal.ppat.1004725.g003

Limited degradation of RK9-containing fragments results in efficient cross-presentation of the immunodominant HLA-A03 RK9 epitope by DCs and Møs

We next analyzed the cross-presentation of another immunodominant epitope located in a different HIV-1 protein and restricted by a different HLA allele. The A03-RK9 epitope (RLRPGGKKK, aa 20–28 in Gag p17) is efficiently produced in the endogenous processing pathway for presentation to A03-RK9-specific CTLs [17,44]. Immature DCs and Møs, incubated with recombinant HIV-1 p55 protein elicited A03-RK9-specific CTL responses as strong as cells exogenously pulsed with 1.2 ug/ml RK9 (Fig. 5A-B). RK9 cross-presentation was not affected by inhibition of proteasome or cysteine proteases, in line with the limited sensitivity of proteasome and cathepsin-mediated degradation resulting in high amounts of peptide for maximum T cell stimulation (Fig. 5A). The incubation of DCs or Møs with different concentrations

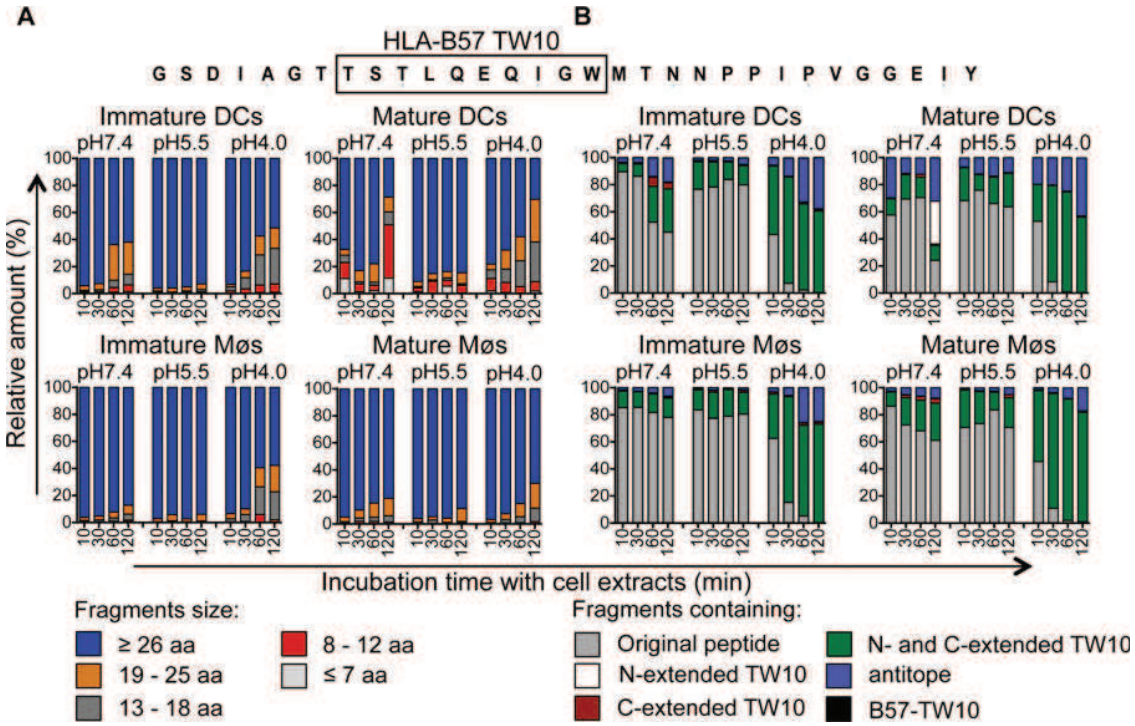

Fig 4. Slow degradation of TW10-containing peptides results in high amounts of B57-TW10 available for cross-presentation. A. Two nmol of p24–31mer (GSDIAGTTSTLQEQIGWMTNNPPIPVGGEIY, aa 101–131 in Gag p24) were degraded in 15μg of whole cell extracts from immature and mature DCs and Møs for 10, 30, 60, and 120 minutes in degradation buffer at pH7.4, pH5.5 or pH4.0. Degradation products identified by mass spectrometry were grouped according to their lengths of fragments as described in Fig. 3. The contribution of each category of peptides to the total intensity of all degradation products is shown at each time point. B. All degradation products of p24–31mer were grouped into fragments containing B57-TW10 (black), B57-TW10 epitope with N-terminal extensions (white), B57-TW10 epitope with C-terminal extensions (red), B57-TW10 epitope with N- and C-terminal extensions (green), antitopes defined as fragments lacking B57-TW10 (blue), or the original peptide (gray), respectively. The contribution of each category of peptides to the total intensity of all degradation products is shown at each time point.

doi:10.1371/journal.ppat.1004725.g004

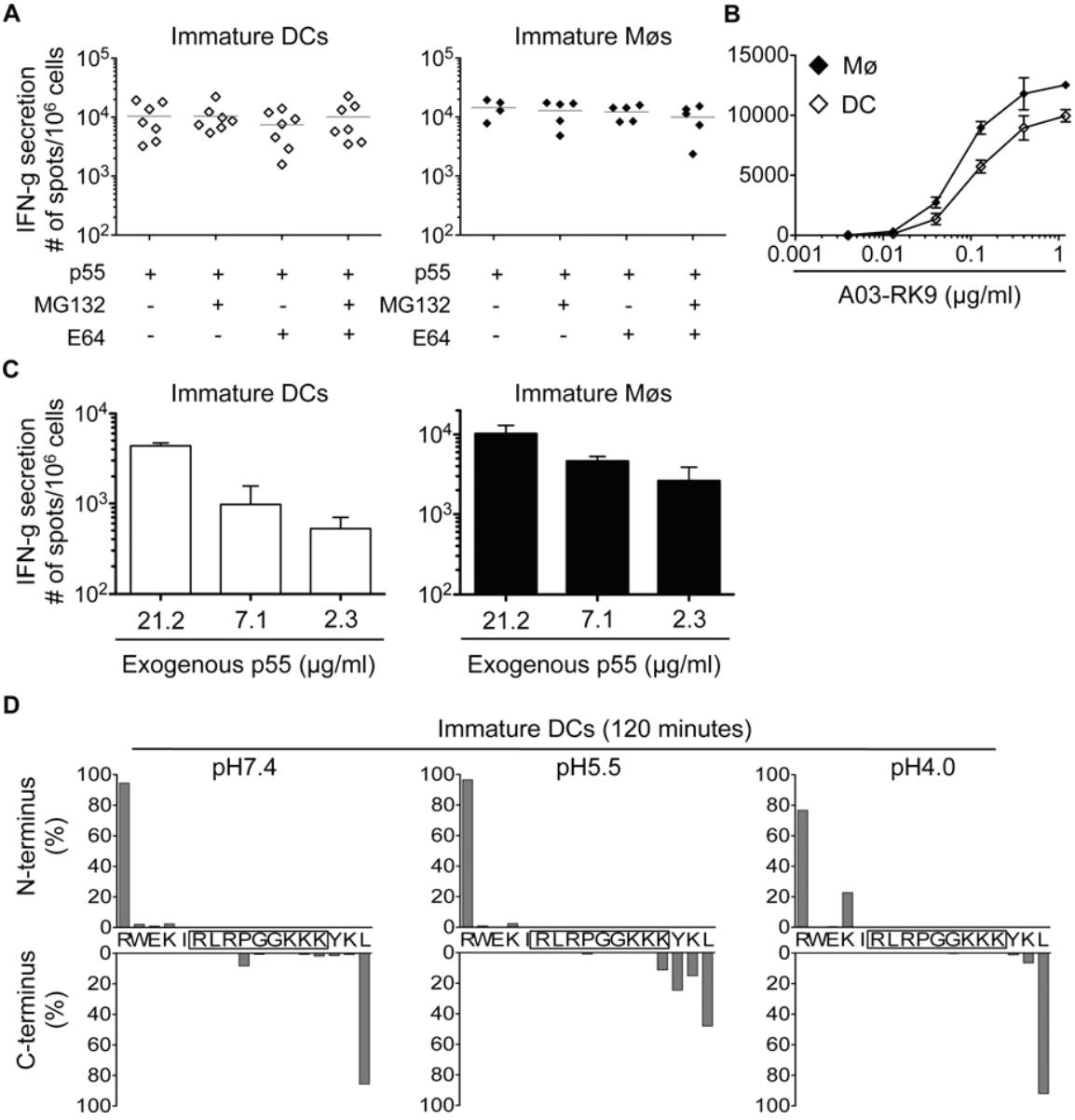

Fig 5. Limited degradation of RK9-containing fragments results in cross-presentation of high amounts of HLA-A03 RK9 epitope. A. Immature DCs (◇) or Møs (◆) were incubated with recombinant HIV-1 p55 protein and used as antigen presenting cells in an overnight IFN-gamma ELISPOT assay with HLA-A03 RK9-specific CTLs as effector cells. CTL responses in form of spot forming cells are shown for n≥5 donors. B. CTL responses to immature DCs (◇) and immature Møs (◆) pulsed with different concentrations of optimal epitope A03-RK9 were measured as described before. C. Immature DCs (open bars) or Møs (solid bars) were incubated with different concentrations of recombinant HIV-1 p55 protein and used as antigen presenting cells in an overnight IFN-gamma ELISPOT assay with HLA-A03 RK9-specific CTLs as effector cells. CTL responses in form of spot forming cells are shown. D. Cleavage patterns of p17–17mer incubated with whole cell extracts from immature DCs for 120 minutes at pH7.4, pH5.5, and pH4.0 are shown as the contribution of each cleavage site, presented as cleavage N-terminal or C-terminal to a specific amino acid, to the total intensity of all degradation products. For (B-D) data are representative of two independent experiments with different donors.

doi:10.1371/journal.ppat.1004725.g005

of p55 protein resulted in concentration-dependent A03-RK9-specific CTL responses (Fig. 5C). In vitro degradation of HIV-1 p17-derived peptide containing the A03-RK9 epitope (RWEKIRLRPGGKKKYKL, aa 15–31 in p17) showed minimal degradation of A03-RK9 at all pH values tested (Fig. 5D). These data indicate that the limited degradation of this peptide may

result in more fragments available for cross-presentation compared with B57-ISW9 and B57-KF11 epitopes, thus contributing to immunodominance of RK9-specific CTL responses.

Intracellular epitope stability of HIV-1 epitopes in cytosolic and lysosomal cell extracts follows CTL responses hierarchy

The variable stability of epitopes in cytosolic extracts of PBMCs contributes to the amount of peptide available for presentation to T cells [44,50,51]. We hypothesize that peptide stability in cytosol and endolysosomes of DCs and Møs may contribute to the relative efficiency of cross-presentation of immunodominant epitopes. We first measured the stability of A03-RK9, a dominant epitope in the acute phase, and B57-KF11, a dominant epitope in the chronic phase, in whole cell extracts of immature DCs and Møs at pH7.4 and pH4.0. In cell extracts of immature DCs, the B57-KF11 epitope was 10-fold faster degraded at pH4.0 than at pH7.4 (half-lives of 1.9 minutes versus 20 minutes) whereas the A03-RK9 epitope was 20-fold faster degraded at pH7.4 than at pH4.0 (half-lives of 61 minutes versus 1223 minutes) (Fig. 6A, left panel). Similar results were observed in cell extracts from immature Møs (Fig. 6A, right panel). We next compared the intracellular stability of seven well-defined dominant and subdominant MHC I epitopes located in HIV Gag p24, Gag p17 and RT, and examined whether their stability corresponded to immunodominance patterns observed in HIV infection. To rank epitopes we calculated a stability rate as done before [44,50]. In cell extracts of immature DCs at pH7.4 the dominant epitopes A03-RK9 and B57-TW10 showed approximately 5-fold and 4-fold higher stability rates compared with the subdominant epitopes B57-ISW9 and A11-ATK9 (AIFQSSMTK, aa 158–166 in RT), respectively (Fig. 6B, upper left panel). At pH4.0 we detected dramatically reduced stability rates for B57-ISW9, B57-KF11, B57-FF9, and A11-ATK9, indicating a more rapid proteolysis by proteases located in endo- and lysosomes. However, the observed stability rates of all epitopes formed the same hierarchy as seen at pH7.4. Similar results were observed in cell extracts of immature Møs (Fig. 6B, lower left panel). Moreover, the subdominant A03-KK9 epitope overlapping with the dominant A03-RK9 epitope had a 3-fold lower stability rate in both cell subsets at pH4.0, whereas the dominant and overlapping epitopes B57-KF11 (KAFSPEVIPMF, aa 30–40 in Gag p24) and B57-FF9 (FSPEVIPMF, aa 32–40 in Gag p24) [52] had comparable stability rates. In line with our previous study [35], the cytosolic stability rate of all epitopes was not affected upon maturation of DCs and Møs with LPS (Fig. 6B, upper and lower right panel). Together, these results show that the intracellular stability of optimal HIV epitopes is highly variable in DCs and Møs and in different cell compartments, but follows similar hierarchies and may contribute to differences seen in cross-presentation and immunodominance patterns observed in HIV infection.

Frequent escape mutations in an immunodominant epitope reduce epitope production and peptide stability in the cross-presentation pathway

Immune pressure exerted by T cell immune responses leads to predictable mutations within and outside epitopes altering viral fitness, epitope processing and presentation [44]. In HLA-B57^{+} patients the TW10 epitope rapidly mutates at residues 3 and 9 during acute infection [53,54], and the dominant TW10 CTL response wanes while KF11-specific CTL responses become dominant [2,55]. To assess the impact of escape mutations on degradation patterns in the cross-presentation pathway, peptides containing the TW10 epitope or its naturally occurring variants TW10 T3N or TW10 T3N/G9A were degraded in whole cell extracts from immature DCs and Møs at pH7.4 and pH4.0 for 10, 30 and 60 minutes. Degradation of the two variants at pH7.4 showed comparable kinetics of disappearance of the original peptides

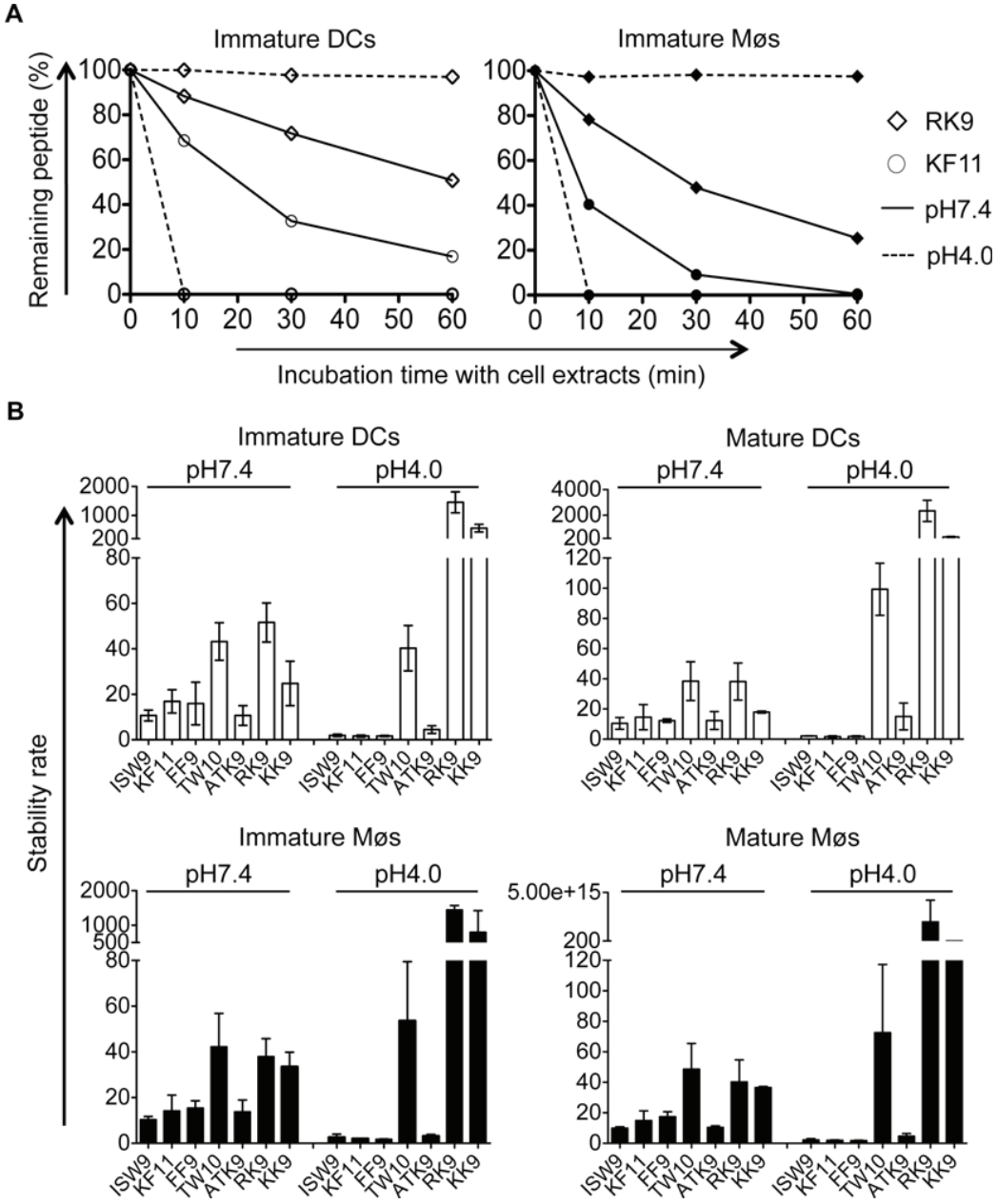

Fig 6. The intracellular stability of HIV-1 epitopes in the cytosol and lysosomes follows CTL responses hierarchy. A. One nmol of highly purified HLA-B57-restricted KF11 (○) and HLA-A03-restricted RK9 (◇) were degraded in 15μg of immature DC or Mø extracts (open or solid symbols, respectively) in degradation buffer at pH7.4 (solid line) or pH4.0 (dashed line). Degradation products were analyzed by RP-HPLC after 10, 30, and 60 minutes. 100% represents the amount of peptide detected at time 0, calculated as the surface area under the peptide peak. B. The stability rate of optimal epitopes B57-ISW9, B57-KF11, B57-FF9, B57-TW10, A11-ATK9, A03-RK9, and A03-KK9 at pH7.4 and pH4.0 was calculated by a nonlinear regression (one-phase exponential decay) of the degradation profile obtained over a 60-minute incubation in extracts of immature and mature DCs (upper panel) and Møs (lower panel). Bars represent the mean ± SD of three independent experiments for each epitope with extracts from different healthy donors.

doi:10.1371/journal.ppat.1004725.g006

(64–67% of original peptides left), whereas the WT showed faster degradation with 23% of the original peptide left after 60 minutes (Fig. 7A). However, both mutants generated less N- and C-extended TW10-containing peptides than the WT at pH7.4 (23% TW10 T3N variant, 19% TW10 T3N/G9A variant vs. 45% TW10 WT at 60 minutes). Degradation at pH4.0

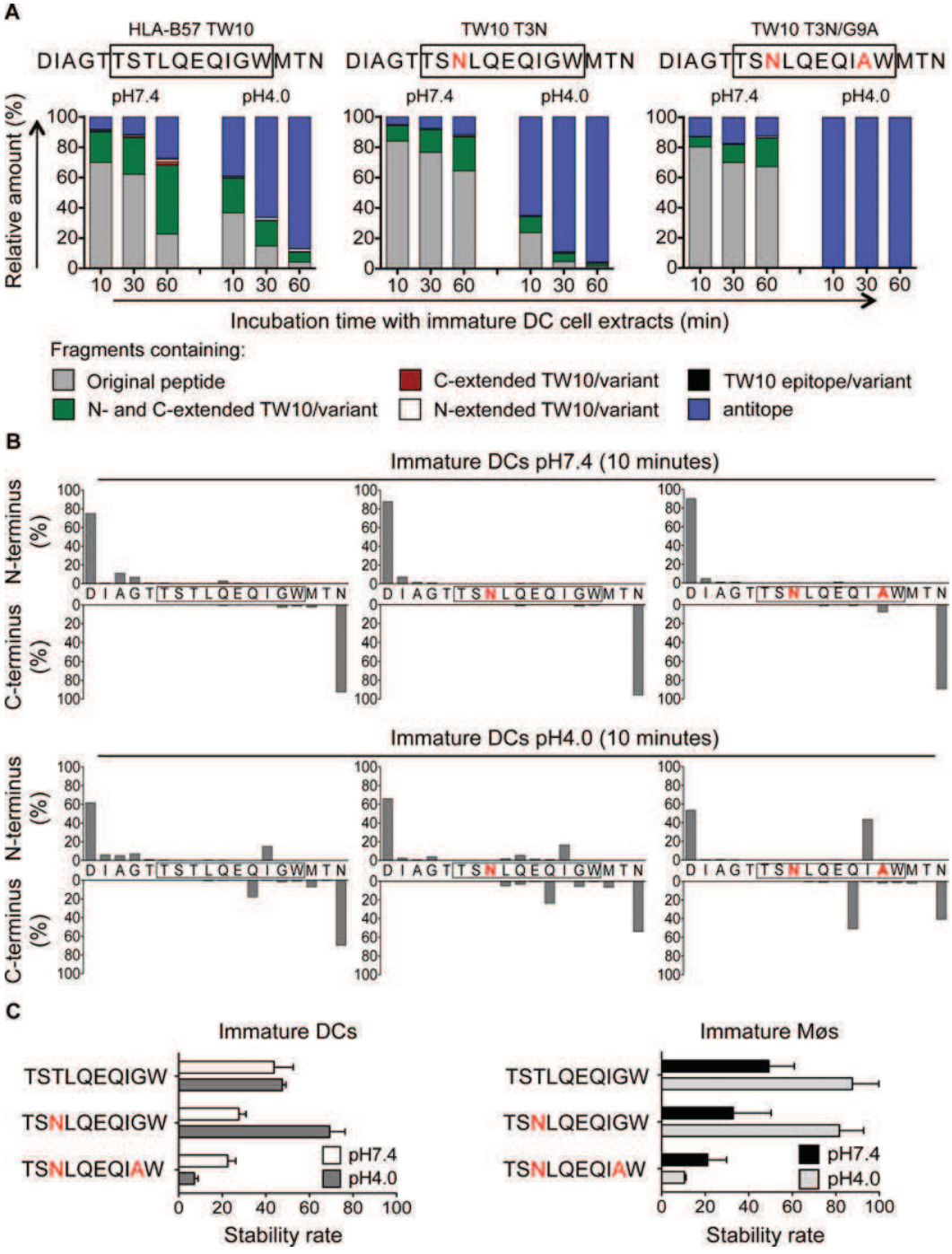

Fig 7. Escape mutations in immunodominant epitopes reduce epitope production and stability in the cross-presentation-competent cell compartments. A. Two nmol of 5-TW10–3 (DIAGTTSTLQEQIGWMTN, aa 103–120 in Gag p24), 5-TW10–3 T3N (DIAGTTSNLQEQIGWMTN), and 5-TW10–3 T3N/G9A (DIAGTTSNLQEQIAWMTN) were degraded in 15μg of whole cell extracts from immature DCs for 10, 30 or 60 minutes in degradation buffer at pH7.4 and pH4.0. Degradation products identified by mass spectrometry were grouped into fragments containing the optimal epitope TW10 or its mutant (black), the epitope/mutant with N-terminal extensions (white), the epitope/mutant with C-terminal extensions (red), the epitope/mutant with N- and C-terminal extensions (green), antitopes defined as fragments lacking part of the epitope/mutant (blue), or the original peptide (gray), respectively. The contribution of each category of peptides to the total intensity of all degradation products is shown at each time point. B. Cleavage patterns of 5-TW10–3, 5-TW10–3 T3N, and 5-TW10–3 T3N/G9A incubated with whole cell extracts from immature DCs for 10 minutes at pH7.4 (upper panel) or at pH4.0 (lower panel) are shown as the contribution of each cleavage site, presented as cleavage N-terminal or C-terminal to a specific amino acid, to the total intensity of all degradation products. For (A-B) data are representative of two independent experiments with different donors. C. One nmol of highly purified HLA-B57-

restricted TW10, TW10-T3N or TW10-T3N/G9A mutants were degraded in 15μg of immature DCs or Møs extracts (right and left panel) in degradation buffer at pH7.4 or pH4.0. A stability rate was calculated as described before. Bars represent the mean ± SD of three independent experiments for each epitope with extracts from different healthy donors.

doi:10.1371/journal.ppat.1004725.g007

demonstrated a very fast kinetic of degradation of the T3N/G9A peptide, and generation of a majority of fragments lacking part of the epitope (antitopes) (39% TW10 WT, 65% T3N variant, and 99% T3N/G9A variant of antitopes produced after 10 minutes). The analysis of the N- and C-terminal cleavage sites showed that TW10 WT and TW10 T3N sequences were spared from degradation at pH7.4, whereas a cleavage site between Tryptophane and Alanine partly destroyed the TW10 T3N/G9A variant within 10 minutes of degradation (Fig. 7B, upper panel). At pH4.0, in line with the faster degradation of the long peptides into antitopes, two major cleavage sites produced short antitopes with an Isoleucine at the N-terminus or a Glutamine at the C-terminus that partly destroyed TW10 WT, and more extensively TW10 T3N/G9A. These cleavage sites were 2.8-fold and 2.6-fold more pronounced in the TW10 T3N/G9A variant compared with the TW10 WT and the TW10 T3N variant (Fig. 7B, lower panel). We compared the cytosolic and lysosomal stability of TW10 epitope and its variants in DCs and Møs (Fig. 7C). Similar intracellular stabilities were observed for B57-TW10 and TW10 T3N in each compartment whereas the stability of TW10 T3N/G9A was reduced by 7- to 8-fold in both compartments. These results demonstrate that the low intracellular stability of TW10 T3N/G9A variant contribute to reducing the epitope presentation in both direct and cross-presentation pathways, in line with our previous findings in cells infected with virus containing TW10 WT or variants [44]. This represents the first demonstration of an escape mutation affecting the cross-presentation of an HIV epitope.

Discussion

This study shows how degradation patterns in the cross-presentation pathway of APCs favor the production of immunodominant HIV epitopes and provides the first demonstration of antigen processing mutations affecting the cross-presentation of HIV epitopes by APCs to CTLs.

The production and presentation of HIV epitopes are affected by both the cell subsets and the cellular compartments in which antigen traffics [34–36,38]. Differences in the processing of epitopes between monocyte-derived DCs and Møs include the involvement of distinct sets of peptidases in the production or destruction of epitopes, and in the trafficking of degradation products. While proteasomes were involved in the degradation of B57-ISW9-containing fragments in DCs, its processing in Møs was proteasome-independent, suggesting possible differences in the trafficking of epitope-containing fragments and the involvement of proteases located in different subcellular compartments [33,56–58]. The degradation of peptides by specific proteases and the translocation across different cell compartments has been demonstrated to depend on the size of fragments [59,60], which may contribute to the observed differences in cross-presentation of B57-ISW9 and B57-KF11 by DCs and Møs upon proteasome inhibition. The formation of specific peptide pools [61] or DC-specific antigen storage compartments [62] may permit the fast cross-presentation of HIV peptides by DCs and Møs but this remains to be demonstrated. In addition, cell-specific peptidases such as a serine protease uniquely expressed in monocytes [63], may lead to cell-specific processing of epitopes and may contribute to the differential priming of immune responses by different tissue DC subsets observed in vivo [64–66]. However, further transcriptomics, proteomics [67] and functional analyses are needed to identify additional cell subset-specific peptidases that may shape epitope presentation by various APC subsets.

A major difference between DCs and Møs contributing to the ability of DCs for cross-priming is their capacity to tightly control endolysosomal pH at higher values than in Møs [68,69], which leads to lower cathepsin activities and slower degradation rates of proteins [49]. However lower peptidase activities are not always corresponding to better epitope production, as we identified epitopes processed in higher amount in Møs or in monocytes than in DCs [35]. Although technically still challenging it will be essential to determine the relative amount of peptides required for priming or activation of T cell responses by DCs or other infectable cell subsets, and how this will affect the capacity of T cells to recognize infected targets and clear infection.

The level of peptidase activities in a given cell type and compartment, and the sensitivity of a given antigenic sequence to degradation in this compartment shapes the amount of epitope available for presentation [70]. In the cytosol the degradation profiles of proteins into epitopes [17,42] and the intrinsic stability of HIV peptides before loading onto MHC [35,44,51] determine the timing and amount of peptide available for presentation and are defined by specific motifs. It is likely that these steps in the endolysosomal pathway will be driven by motifs that still remain to be identified.

A direct consequence of this sequence- and compartment-dependent degradation of proteins is the impact of HLA-restricted mutations on HIV epitope processing and cross-presentation. Immune pressure selects variants impairing viral fitness and/or epitope presentation, reducing binding to MHC or to the TCR [71]. Flanking mutations have been shown to prevent the processing of epitopes [16,40,42,72] and intraepitopic mutations can destroy epitopes [44,73,74], which demonstrates the adaptation of HIV to antigen processing in the cytosol. This study provides the first demonstration that a frequently detected HLA-restricted mutation during acute infection affects the cross- and direct presentation of an epitope in DCs and Møs. While the WT epitope B57-TW10, dominant in the acute phase, is efficiently processed and highly stable in endo-lysosomes and the cytosol of DCs and Møs its mutant is degraded faster than WT. The lower amount of epitope available for presentation may lead to less epitope presented to T cells and therefore results most likely in subdominant responses, which coincides with a shift in immunodominance toward B57-KF11 in HLA-B57 persons during chronic HIV infection [2,55].

A vaccine eliciting the same immunodominance patterns as natural infection cannot be successful at preventing or clearing HIV infection. Breaking natural immunodominance and targeting immune responses towards protective epitopes [55] is required in the design of a T cell arm of vaccine strategies [75,76]. The combination of sequence alterations to modulate epitope production and intracellular peptide stability and to break natural immunodominance, the use of adjuvants modulating epitope processing as well as the targeting of immunogens to specific cell compartments offers ways to modulate epitope presentation to induce protective immunity in HIV infection and beyond.

Supporting Information

S1 Fig. Lysosomal activities in DC and Mø cell extracts reflect activities in live cells. A. Omnicathepsin and cathepsin S activities in immature and TLR-matured DCs were plotted against the percentage of CD86+ CD83+ DCs for each experiment. Surface expression was analyzed by flow cytometry. Comparison by Spearman test is indicated. n≥26 measurements. B. Omnicathepsin and cathepsin S hydrolytic activities measured in live intact immature or mature DCs (◇) and Møs (◆) were plotted against their activities in corresponding cell extracts at pH4.0. A partial correlation on Spearman ranked data was performed to control for cell type-dependent effects. n≥30 measurements. C. Cathepsin D, cathepsin S, cathepsin B, and omni cathepsin activities (combined cathepsin S, L, B activities) were measured with specific

fluorogenic substrates in whole cell extracts of immature DCs at pH4.0, pH5.5, and pH7.4, respectively. Mean ± SD is shown for n≥5 independent donors.
(TIF)

S2 Fig. Degradation of a HIV-1 p24 35mer in DC cell extracts at pH4.0, pH5.5 and pH7.4. Peptides containing the epitopes B57-ISW9 and B57-KF11 (black bars), B57-ISW9 epitope (blue bars), B57-KF11 epitope (red bars) or lacking both epitopes (gray bars) were identified by mass spectrometry. Optimal B57-ISW9 (blue star) and B57-KF11 (red star) are indicated. Data represent one of three independent experiments from different donors.
(TIF)

S3 Fig. Variable production of 16 HIV-1 epitopes in cytosolic and endo-lysosomal extracts of DCs and Møs. A. The map shows the location of 12 MHC-I epitopes (black arrows) and 4 MHC-II epitopes (gray arrows) within the sequence of Gag p24–35mer (aa 10–44). B. Summary of the relative amount of optimal epitopes and corresponding N-terminal extensions detected by mass spectrometry after 10, 30, 60, and 120 minutes degradation in extracts of immature DCs, mature DCs, immature Møs, mature Møs at pH7.4, pH5.5 and pH4.0. Epitope precursors, defined as peptides with the correct C-terminus and extended by up to three residues at the N-terminus, could be further trimmed in the ER. Numbers represent contribution of optimals and N-extended optimals to the total intensity of all degradation products at each time point. The presence of optimal epitopes is indicated (*). Data represent one of three mass spectrometry analyses from independent experiments.
(TIF)

S4 Fig. Limited degradation of TW10-containing fragments in cross-presentation-competent compartments of immature DCs. Cleavage patterns of p24–31mer (aa 101–131 in Gag p24) incubated with whole cell extracts from immature DCs for 30 minutes (left panel) or 120 minutes (right panel) at pH7.4, pH5.5, and pH4.0 are shown as the contribution of each cleavage site, presented as cleavage N-terminal or C-terminal to a specific amino acid, to the total intensity of all degradation products. Data are representative of three independent experiments with three different donors.
(TIF)

Acknowledgments

The authors would like to thank Dr. Bruce Walker and Pauline Gourdain for stimulating discussions about this manuscript, Tom Zhu and Yang Xu for technical assistance.

Author Contributions

Conceived and designed the experiments: JD SLG SCZ. Performed the experiments: JD ED NYL EBS DC MJB. Analyzed the data: JD ED NYL MJB GK SLG. Contributed reagents/materials/analysis tools: HS GK. Wrote the paper: JL SLG NYL ED.

References

1. Yewdell JW Confronting complexity: real-world immunodominance in antiviral CD8+ T cell responses. Immunity. 2006; 25: 533–543. PMID: 17046682
2. Altfeld M, Kalife ET, Qi Y, Streeck H, Lichterfeld M, Johnston MN, et al. HLA Alleles Associated with Delayed Progression to AIDS Contribute Strongly to the Initial CD8(+) T Cell Response against HIV-1. PLoS Med. 2006; 3: e403. PMID: 17076553

3. Turnbull EL, Wong M, Wang S, Wei X, Jones NA, Conrod KE, et al. Kinetics of expansion of epitope-specific T cell responses during primary HIV-1 infection. J Immunol. 2009; 182: 7131–7145. doi: 10.4049/jimmunol.0803658 PMID: 19454710

4. Borrow P, Lewicki H, Wei X, Horwitz MS, Peffer N, Meyers H, et al. Antiviral pressure exerted by HIV-1-specific cytotoxic T lymphocytes (CTLs) during primary infection demonstrated by rapid selection of CTL escape virus. Nat Med. 1997; 3: 205–211. PMID: 9018240

5. Allen TM, Altfeld M, Geer SC, Kalife ET, Moore C, O'Sullivan K M, et al. Selective escape from CD8+ T-cell responses represents a major driving force of human immunodeficiency virus type 1 (HIV-1) sequence diversity and reveals constraints on HIV-1 evolution. J Virol. 2005; 79: 13239–13249. PMID: 16227247

6. Kawashima Y, Pfafferott K, Frater J, Matthews P, Payne R, Addo M, et al. Adaptation of HIV-1 to human leukocyte antigen class I. Nature. 2009; 458: 641–645. doi: 10.1038/nature07746 PMID: 19242411

7. Liu MK, Hawkins N, Ritchie AJ, Ganusov VV, Whale V, Brackenridge S, et al. Vertical T cell immunodominance and epitope entropy determine HIV-1 escape. J Clin Invest. 2013; 123: 380–393. doi: 10.1172/JCI65330 PMID: 23221345

8. Oxenius A, Price DA, Trkola A, Edwards C, Gostick E, Zhang HT, et al. Loss of viral control in early HIV-1 infection is temporally associated with sequential escape from CD8+ T cell responses and decrease in HIV-1-specific CD4+ and CD8+ T cell frequencies. J Infect Dis. 2004; 190: 713–721. PMID: 15272399

9. Troyer RM, McNevin J, Liu Y, Zhang SC, Krizan RW, Abraha A, et al. Variable fitness impact of HIV-1 escape mutations to cytotoxic T lymphocyte (CTL) response. PLoS Pathog. 2009; 5: e1000365. doi: 10.1371/journal.ppat.1000365 PMID: 19343217

10. Chen W, Anton LC, Bennink JR, Yewdell JW Dissecting the multifactorial causes of immunodominance in class I-restricted T cell responses to viruses. Immunity. 2000; 12: 83–93. PMID: 10661408

11. Bihl F, Frahm N, Di Giammarino L, Sidney J, John M, Yusim K, et al. Impact of HLA-B alleles, epitope binding affinity, functional avidity, and viral coinfection on the immunodominance of virus-specific CTL responses. J Immunol. 2006; 176: 4094–4101. PMID: 16547245

12. Osuna CE, Gonzalez AM, Chang HH, Hung AS, Ehlinger E, Anasti K, et al. TCR affinity associated with functional differences between dominant and subdominant SIV epitope-specific CD8+ T cells in Mamu-A*01+ rhesus monkeys. PLoS Pathog. 2014; 10: e1004069. doi: 10.1371/journal.ppat.1004069 PMID: 24743648

13. Schmidt J, Neumann-Haefelin C, Altay T, Gostick E, Price DA, Lohmann V, et al. Immunodominance of HLA-A2-restricted hepatitis C virus-specific CD8+ T cell responses is linked to naive-precursor frequency. J Virol. 2011; 85: 5232–5236. doi: 10.1128/JVI.00093-11 PMID: 21367907

14. Probst HC, Tschannen K, Gallimore A, Martinic M, Basler M, Dumrese T, et al. Immunodominance of an antiviral cytotoxic T cell response is shaped by the kinetics of viral protein expression. J Immunol. 2003; 171: 5415–5422. PMID: 14607945

15. Schmidt J, Iversen AK, Tenzer S, Gostick E, Price DA, Lohmann V, et al. Rapid antigen processing and presentation of a protective and immunodominant HLA-B*27-restricted hepatitis C virus-specific CD8+ T-cell epitope. PLoS Pathog. 2012; 8: e1003042. doi: 10.1371/journal.ppat.1003042 PMID: 23209413

16. Tenzer S, Wee E, Burgevin A, Stewart-Jones G, Friis L, Lamberth K, et al. Antigen processing influences HIV-specific cytotoxic T lymphocyte immunodominance. Nat Immunol. 2009; 10: 636–646. doi: 10.1038/ni.1728 PMID: 19412183

17. Le Gall S, Stamegna P, Walker BD Portable flanking sequences modulate CTL epitope processing. J Clin Invest. 2007; 117: 3563–3575. PMID: 17975674

18. Asano K, Nabeyama A, Miyake Y, Qiu CH, Kurita A, Tomura M, et al. CD169-positive macrophages dominate antitumor immunity by crosspresenting dead cell-associated antigens. Immunity. 2011; 34: 85–95. doi: 10.1016/j.immuni.2010.12.011 PMID: 21194983

19. Fonteneau JF, Kavanagh DG, Lirvall M, Sanders C, Cover TL, Bhardwaj N, et al. Characterization of the MHC class I cross-presentation pathway for cell-associated antigens by human dendritic cells. Blood. 2003; 102: 4448–4455. PMID: 12933572

20. Larsson M, Fonteneau JF, Lirvall M, Haslett P, Lifson JD, Bhardwaj N Activation of HIV-1 specific CD4 and CD8 T cells by human dendritic cells: roles for cross-presentation and non-infectious HIV-1 virus. AIDS. 2002; 16: 1319–1329. PMID: 12131208

21. Maranon C, Desoutter JF, Hoeffel G, Cohen W, Hanau D, Hosmalin A Dendritic cells cross-present HIV antigens from live as well as apoptotic infected CD4+ T lymphocytes. Proc Natl Acad Sci U S A. 2004; 101: 6092–6097. PMID: 15079077

22. Buseyne F, Le Gall S, Boccaccio C, Abastado JP, Lifson JD, Arthur LO, et al. MHC-I-restricted presentation of HIV-1 virion antigens without viral replication. Nat Med. 2001; 7: 344–349. PMID: 11231634

23. Sabado RL, Babcock E, Kavanagh DG, Tjomsland V, Walker BD, Lifson JD, et al. Pathways utilized by dendritic cells for binding, uptake, processing and presentation of antigens derived from HIV-1. Eur J Immunol. 2007; 37: 1752–1763. PMID: 17534864

24. Tjomsland V, Ellegard R, Burgener A, Mogk K, Che KF, Westmacott G, et al. Complement opsonization of HIV-1 results in a different intracellular processing pattern and enhanced MHC class I presentation by dendritic cells. Eur J Immunol. 2013; 43: 1470–1483. doi: 10.1002/eji.201242935 PMID: 23526630

25. Belizaire R, Unanue ER Targeting proteins to distinct subcellular compartments reveals unique requirements for MHC class I and II presentation. Proc Natl Acad Sci U S A. 2009; 106: 17463–17468. doi: 10.1073/pnas.0908583106 PMID: 19805168

26. Huang XL, Fan Z, Zheng L, Borowski L, Li H, Thomas EK, et al. Priming of human immunodeficiency virus type 1 (HIV-1)-specific CD8+ T cell responses by dendritic cells loaded with HIV-1 proteins. J Infect Dis. 2003; 187: 315–319. PMID: 12552458

27. Colbert JD, Matthews SP, Miller G, Watts C Diverse regulatory roles for lysosomal proteases in the immune response. Eur J Immunol. 2009; 39: 2955–2965. doi: 10.1002/eji.200939650 PMID: 19637232

28. Shen L, Sigal LJ, Boes M, Rock KL Important role of cathepsin S in generating peptides for TAP-independent MHC class I crosspresentation in vivo. Immunity. 2004; 21: 155–165. PMID: 15308097

29. Fonteneau JF, Gilliet M, Larsson M, Dasilva I, Munz C, Liu YJ, et al. Activation of influenza virus-specific CD4+ and CD8+ T cells: a new role for plasmacytoid dendritic cells in adaptive immunity. Blood. 2003; 101: 3520–3526. PMID: 12511409

30. Lucchiari-Hartz M, van Endert PM, Lauvau G, Maier R, Meyerhans A, Mann D, et al. Cytotoxic T lymphocyte epitopes of HIV-1 Nef: Generation of multiple definitive major histocompatibility complex class I ligands by proteasomes. J Exp Med. 2000; 191: 239–252. PMID: 10637269

31. Geier E, Pfeifer G, Wilm M, Lucchiari-Hartz M, Baumeister W, Eichmann K, et al. A giant protease with potential to substitute for some functions of the proteasome. Science. 1999; 283: 978–981. PMID: 9974389

32. Lutz MB, Rovere P, Kleijmeer MJ, Rescigno M, Assmann CU, Oorschot VM, et al. Intracellular routes and selective retention of antigens in mildly acidic cathepsin D/lysosome-associated membrane protein-1/MHC class II-positive vesicles in immature dendritic cells. J Immunol. 1997; 159: 3707–3716. PMID: 9378956

33. Kamphorst AO, Guermonprez P, Dudziak D, Nussenzweig MC Route of antigen uptake differentially impacts presentation by dendritic cells and activated monocytes. J Immunol. 2010; 185: 3426–3435. doi: 10.4049/jimmunol.1001205 PMID: 20729332

34. Lazaro E, Godfrey SB, Stamegna P, Ogbechie T, Kerrigan C, Zhang M, et al. Differential HIV epitope processing in monocytes and CD4 T cells affects cytotoxic T lymphocyte recognition. J Infect Dis. 2009; 200: 236–243. doi: 10.1086/599837 PMID: 19505257

35. Dinter J, Gourdain P, Lai NY, Duong E, Bracho-Sanchez E, Rucevic M, et al. Different Antigen-Processing Activities in Dendritic Cells, Macrophages, and Monocytes Lead to Uneven Production of HIV Epitopes and Affect CTL Recognition. J Immunol. 2014.

36. Steers NJ, Currier JR, Kijak GH, di Targiani RC, Saxena A, Marovich MA, et al. Cell type-specific proteasomal processing of HIV-1 Gag-p24 results in an altered epitope repertoire. J Virol. 2011; 85: 1541–1553. doi: 10.1128/JVI.01790-10 PMID: 21106750

37. Vaithilingam A, Lai NY, Duong E, Boucau J, Xu Y, Shimada M, et al. A simple methodology to assess endolysosomal protease activity involved in antigen processing in human primary cells. BMC Cell Biol. 2013; 14: 35. doi: 10.1186/1471-2121-14-35 PMID: 23937268

38. Steers NJ, Ratto-Kim S, de Souza MS, Currier JR, Kim JH, Michael NL, et al. HIV-1 envelope resistance to proteasomal cleavage: implications for vaccine induced immune responses. PLoS One. 2012; 7: e42579. doi: 10.1371/journal.pone.0042579 PMID: 22880042

39. Allen TM, Altfeld M, Yu XG, O'Sullivan KM, Lichterfeld M, Le Gall S, et al. Selection, transmission, and reversion of an antigen-processing cytotoxic T-lymphocyte escape mutation in human immunodeficiency virus type 1 infection. J Virol. 2004; 78: 7069–7078. PMID: 15194783

40. Draenert R, Le Gall S, Pfafferott KJ, Leslie AJ, Chetty P, Brander C, et al. Immune selection for altered antigen processing leads to cytotoxic T lymphocyte escape in chronic HIV-1 infection. J Exp Med. 2004; 199: 905–915. PMID: 15067030

41. Yokomaku Y, Miura H, Tomiyama H, Kawana-Tachikawa A, Takiguchi M, Kojima A, et al. Impaired processing and presentation of cytotoxic-T-lymphocyte (CTL) epitopes are major escape mechanisms from CTL immune pressure in human immunodeficiency virus type 1 infection. J Virol. 2004; 78: 1324–1332. PMID: 14722287

42. Zhang SC, Martin E, Shimada M, Godfrey SB, Fricke J, Locastro S, et al. Aminopeptidase substrate preference affects HIV epitope presentation and predicts immune escape patterns in HIV-infected individuals. J Immunol. 2012; 188: 5924–5934. doi: 10.4049/jimmunol.1200219 PMID: 22586036

43. Streeck H, Frahm N, Walker BD The role of IFN-gamma Elispot assay in HIV vaccine research. Nat Protoc. 2009; 4: 461–469. doi: 10.1038/nprot.2009.7 PMID: 19282851

44. Lazaro E, Kadie C, Stamegna P, Zhang SC, Gourdain P, Lai NY, et al. Variable HIV peptide stability in human cytosol is critical to epitope presentation and immune escape. J Clin Invest. 2011; 121: 2480–2492. doi: 10.1172/JCI44932 PMID: 21555856

45. Trombetta ES, Ebersold M, Garrett W, Pypaert M, Mellman I Activation of lysosomal function during dendritic cell maturation. Science. 2003; 299: 1400–1403. PMID: 12610307

46. Yusim K, Korber BTM, Brander C, Barouch D, de Boer R, Haynes BF, et al. HIV Molecular Immunology 2013. Los Alamos National Laboratory, Theoretical Biology and Biophysics, Los Alamos, New Mexico. 2013.

47. Goulder PJ, Bunce M, Krausa P, McIntyre K, Crowley S, Morgan B, et al. Novel, cross-restricted, conserved, and immunodominant cytotoxic T lymphocyte epitopes in slow progressors in HIV type 1 infection. AIDS Res Hum Retroviruses. 1996; 12: 1691–1698. PMID: 8959245

48. Friedrich D, Jalbert E, Dinges WL, Sidney J, Sette A, Huang Y, et al. Vaccine-induced HIV-specific CD8+ T cells utilize preferential HLA alleles and target-specific regions of HIV-1. J Acquir Immune Defic Syndr. 2011; 58: 248–252. doi: 10.1097/QAI.0b013e318228f992 PMID: 21709567

49. Delamarre L, Pack M, Chang H, Mellman I, Trombetta ES Differential lysosomal proteolysis in antigen-presenting cells determines antigen fate. Science. 2005; 307: 1630–1634. PMID: 15761154

50. Kourjian G, Xu Y, Mondesire-Crump I, Shimada M, Gourdain P, Le Gall S Sequence-specific alterations of epitope production by HIV protease inhibitors. J Immunol. 2014; 192: 3496–3506. doi: 10.4049/jimmunol.1302805 PMID: 24616479

51. Herberts CA, Neijssen JJ, de Haan J, Janssen L, Drijfhout JW, Reits EA, et al. Cutting edge: HLA-B27 acquires many N-terminal dibasic peptides: coupling cytosolic peptide stability to antigen presentation. J Immunol. 2006; 176: 2697–2701. PMID: 16493024

52. Frahm N, Adams S, Kiepiela P, Linde CH, Hewitt HS, Lichterfeld M, et al. HLA-B63 presents HLA-B57/B58-restricted cytotoxic T-lymphocyte epitopes and is associated with low human immunodeficiency virus load. J Virol. 2005; 79: 10218–10225. PMID: 16051815

53. Brockman MA, Schneidewind A, Lahaie M, Schmidt A, Miura T, Desouza I, et al. Escape and compensation from early HLA-B57-mediated cytotoxic T-lymphocyte pressure on human immunodeficiency virus type 1 Gag alter capsid interactions with cyclophilin A. J Virol. 2007; 81: 12608–12618. PMID: 17728232

54. Miura T, Brockman MA, Schneidewind A, Lobritz M, Pereyra F, Rathod A, et al. HLA-B57/B*5801 human immunodeficiency virus type 1 elite controllers select for rare gag variants associated with reduced viral replication capacity and strong cytotoxic T-lymphocyte [corrected] recognition. J Virol. 2009; 83: 2743–2755. doi: 10.1128/JVI.02265-08 PMID: 19116253

55. Pereyra F, Heckerman D, Carlson JM, Kadie C, Soghoian DZ, Karel D, et al. HIV control is mediated in part by CD8+ T-cell targeting of specific epitopes. J Virol. 2014.

56. Luckey CJ, King GM, Marto JA, Venketeswaran S, Maier BF, Crotzer VL, et al. Proteasomes can either generate or destroy MHC class I epitopes: evidence for nonproteasomal epitope generation in the cytosol. J Immunol. 1998; 161: 112–121. PMID: 9647214

57. Lopez D, Del Val M Selective involvement of proteasomes and cysteine proteases in MHC class I antigen presentation. J Immunol. 1997; 159: 5769–5772. PMID: 9550370

58. Burster T, Beck A, Tolosa E, Schnorrer P, Weissert R, Reich M, et al. Differential processing of autoantigens in lysosomes from human monocyte-derived and peripheral blood dendritic cells. J Immunol. 2005; 175: 5940–5949. PMID: 16237087

59. Yang B, Hahn YS, Hahn CS, Braciale TJ The requirement for proteasome activity class I major histocompatibility complex antigen presentation is dictated by the length of preprocessed antigen. J Exp Med. 1996; 183: 1545–1552. PMID: 8666912

60. Rodriguez A, Regnault A, Kleijmeer M, Ricciardi-Castagnoli P, Amigorena S Selective transport of internalized antigens to the cytosol for MHC class I presentation in dendritic cells. Nat Cell Biol. 1999; 1: 362–368. PMID: 10559964

61. Lev A, Takeda K, Zanker D, Maynard JC, Dimberu P, Waffarn E, et al. The exception that reinforces the rule: crosspriming by cytosolic peptides that escape degradation. Immunity. 2008; 28: 787–798. doi: 10.1016/j.immuni.2008.04.015 PMID: 18549799

62. van Montfoort N, Camps MG, Khan S, Filippov DV, Weterings JJ, Griffith JM, et al. Antigen storage compartments in mature dendritic cells facilitate prolonged cytotoxic T lymphocyte cross-priming

capacity. Proc Natl Acad Sci U S A. 2009; 106: 6730–6735. doi: 10.1073/pnas.0900969106 PMID: 19346487

63. Chateau MT, Robert-Hebmann V, Devaux C, Lazaro JB, Canard B, Coux O Human monocytes possess a serine protease activity capable of degrading HIV-1 reverse transcriptase in vitro. Biochem Biophys Res Commun. 2001; 285: 863–872. PMID: 11467830

64. Dudziak D, Kamphorst AO, Heidkamp GF, Buchholz VR, Trumpfheller C, Yamazaki S, et al. Differential antigen processing by dendritic cell subsets in vivo. Science. 2007; 315: 107–111. PMID: 17204652

65. Idoyaga J, Lubkin A, Fiorese C, Lahoud MH, Caminschi I, Huang Y, et al. Comparable T helper 1 (Th1) and CD8 T-cell immunity by targeting HIV gag p24 to CD8 dendritic cells within antibodies to Langerin, DEC205, and Clec9A. Proc Natl Acad Sci U S A. 2011; 108: 2384–2389. doi: 10.1073/pnas.1019547108 PMID: 21262813

66. Igyarto BZ, Haley K, Ortner D, Bobr A, Gerami-Nejad M, Edelson BT, et al. Skin-resident murine dendritic cell subsets promote distinct and opposing antigen-specific T helper cell responses. Immunity. 2011; 35: 260–272. doi: 10.1016/j.immuni.2011.06.005 PMID: 21782478

67. Duclos S, Clavarino G, Rousserie G, Goyette G, Boulais J, Camossetto V, et al. The endosomal proteome of macrophage and dendritic cells. Proteomics. 2011; 11: 854–864. doi: 10.1002/pmic.201000577 PMID: 21280226

68. Savina A, Jancic C, Hugues S, Guermonprez P, Vargas P, Moura IC, et al. NOX2 controls phagosomal pH to regulate antigen processing during crosspresentation by dendritic cells. Cell. 2006; 126: 205–218. PMID: 16839887

69. Mantegazza AR, Savina A, Vermeulen M, Perez L, Geffner J, Hermine O, et al. NADPH oxidase controls phagosomal pH and antigen cross-presentation in human dendritic cells. Blood. 2008; 112: 4712–4722. doi: 10.1182/blood-2008-01-134791 PMID: 18682599

70. Rucevic M, Boucau J, Dinter J, Kourjian G, Le Gall S Mechanisms of HIV protein degradation into epitopes: implications for vaccine design. Viruses. 2014; 6: 3271–3292. doi: 10.3390/v6083271 PMID: 25196483

71. Goulder PJ, Watkins DI HIV and SIV CTL escape: implications for vaccine design. Nat Rev Immunol. 2004; 4: 630–640. PMID: 15286729

72. Ranasinghe SR, Kramer HB, Wright C, Kessler BM, di Gleria K, Zhang Y, et al. The antiviral efficacy of HIV-specific CD8(+) T-cells to a conserved epitope is heavily dependent on the infecting HIV-1 isolate. PLoS Pathog. 2011; 7: e1001341. doi: 10.1371/journal.ppat.1001341 PMID: 21589893

73. Tanuma J, Fujiwara M, Teruya K, Matsuoka S, Yamanaka H, Gatanaga H, et al. HLA-A*2402-restricted HIV-1-specific cytotoxic T lymphocytes and escape mutation after ART with structured treatment interruptions. Microbes Infect. 2008; 10: 689–698. doi: 10.1016/j.micinf.2008.03.007 PMID: 18462973

74. Ammaranond P, van Bockel DJ, Petoumenos K, McMurchie M, Finlayson R, Middleton MG, et al. HIV immune escape at an immunodominant epitope in HLA-B*27-positive individuals predicts viral load outcome. J Immunol. 2011; 186: 479–488. doi: 10.4049/jimmunol.0903227 PMID: 21115730

75. Burton DR, Ahmed R, Barouch DH, Butera ST, Crotty S, Godzik A, et al. A Blueprint for HIV Vaccine Discovery. Cell Host Microbe. 2012; 12: 396–407. doi: 10.1016/j.chom.2012.09.008 PMID: 23084910

76. Stephenson KE, Barouch DH A global approach to HIV-1 vaccine development. Immunol Rev. 2013; 254: 295–304. doi: 10.1111/imr.12073 PMID: 23772627